Fabian Tobias Mayer

NTNU
Norwegian University of
Science and Technology

Development of a Measuring System to Detect Loads Acting Between the Binding and the Roller Ski

Fabian Tobias Mayer B.Sc.

Development of a Measuring System to Detect Loads Acting Between the Binding and the Roller Ski

Master Thesis in Mechanical Engineering

Norwegian University of Science and Technology

Faculty of Engineering Science and Technology

Department Engineering Design and Materials

NTNU
Norwegian University of
Science and Technology

Abstract

Existing roller ski measuring systems are capable to detect forces between a roller ski and the binding. However, none of them is capable to detect torques. Comprehensive load data is needed for the analysis and improvement of the cross-country skiing technique as well as it is essential for roller ski and binding manufacturers. Currently, no specific standard is available for the dimensioning and testing of roller ski bindings.

With use of cross inventions, a solution was found how to determine spatial forces and torques between a roller ski and the binding without changing their setup and disturbing the performance of the athlete as little as possible. The system can be used for almost all situations during in-situ testing on the road. For the development of the measuring system the SPALTEN methodology by Albers et al. was employed in combination with a set-based approach to achieve an optimal solution.

Strain gauge rosettes mounted at the beam of a commercially available roller ski are used to measure the strain induced by the multiaxial stress state. A lightweight solution based on low cost components was developed for the acquisition of the strain signal. With the recorded strain data, the principal stresses and their directions are calculated. Consecutively, the spatial forces and torques are deduced.

NTNU - NORWEGIAN UNIVERSITY
OF SCIENCE AND TECHNOLOGY
DEPARTMENT OF ENGINEERING DESIGN
AND MATERIALS

MASTER THESIS SPRING 2016
FOR
STUD.TECHN. Fabian Mayer

Development of a Measuring System to Detect Loads Acting Between the Binding and the Roller Ski

Utvikling av et målesystem for bestemmelse av krefter mellom binding og rulleski

Rottefella is a well-known Norwegian-based company that designs, develops and supplies ski bindings for the world market. Rottefella is looking into improving their innovation capabilities by increasing their knowledge on forces that the roller ski binding systems are exposed to under different circumstances.

Rollersafe is a Norwegian-based company that is known for designing and supplying innovative roller skis with advanced, integrated brake systems. The company is in the process of designing a new weight-optimal roller ski in carbon fibers, and needs to gain new insights into service and ultimate force paths to be used as input to the design process.

Both companies are seeking a system to collect load data under regular (service) conditions and 'peak load events' when used by active and pro skiers. The data recorded by the system will be used to design better roller ski bindings, and to establish more relevant laboratory test set-ups for verification of capabilities of future design solutions. The data will additionally be used as input to the design of a weight-optimized roller ski made out of carbon fiber.

The overall objective of this thesis is to develop an accurate measuring system for in-situ measurements of the force components acting between the binding and the roller ski. The main tasks associated with this thesis include the following:

- To review the current state-of-the-art (literature) associated with relevant in-situ measuring systems in order to identify potential cross-over innovation opportunities and gaps;

- To establish a list of requirements, including 'must haves', 'should haves' and 'could haves'. In this connection, the candidate shall interview 'customers' (Rottefella and Rollersafe) and potential users of the system;

- To evaluate and prioritize the different requirements based on the time and resources available for implementation of the different requirements in the actual system design;

- To establish different designs of the measuring system based on the requirements and systematically reduce the number of alternatives to a single final concept for verification using e.g. a Pugh matrix;

- To implement the system into a commercially available production roller-ski – binding system and build a functional prototype for validation;

- Prior to in-situ testing, to establish and conduct a test to determine the capability of the system in recording forces (in all 6 degrees of freedom), including its sensitivity to variability due to noise and different factors (control parameters);

- To use the system to record in-situ field data to demonstrate proof-of-concept;

- To write and structure the thesis;

- If the results are successful and time permits, the candidate shall develop a text that can be published in an academic/scientific journal based on the main findings made in the study.

Formal requirements:

Three weeks after start of the thesis work, an A3 sheet illustrating the work is to be handed in. A template for this presentation is available on the IPM's web site under the menu "Masteroppgave" (https://www.ntnu.edu/web/ipm/master-thesis). This sheet should be updated one week before the master's thesis is submitted.

Risk assessment of experimental activities shall always be performed. Experimental work defined in the problem description shall be planed and risk assessed up-front and within 3 weeks after receiving the problem text. Any specific experimental activities which are not properly covered by the general risk assessment shall be particularly assessed before performing the experimental work. Risk assessments should be signed by the supervisor and copies shall be included in the appendix of the thesis.

The thesis should include the signed problem text, and be written as a research report with summary both in English and Norwegian, conclusion, literature references, table of contents, etc. During preparation of the text, the candidate should make efforts to create a well arranged and well written report. To ease the evaluation of the thesis, it is important to cross-reference text, tables and figures. For evaluation of the work a thorough discussion of results is appreciated.

The thesis shall be submitted electronically via DAIM, NTNU's system for Digital Archiving and Submission of Master's theses.

The contact persons are: Harald Vestøl, Øyvar Svendsen (Rottefella), Atle Stubberud (Rollersafe), professor Sven Matthiesen and Tim Bruchmüller (supervisors at Karlruhe Institute of Technology).

Torgeir Welo
Head of Division

Torgeir Welo
Professor/Supervisor

NTNU
Norges teknisk-
naturvitenskapelige universitet
Institutt for produktutvikling
og materialer

Statement of Authorship

I hereby confirm that I have written the enclosed master thesis by myself. I have not used sources and means other than declared in the text. Everything that was taken directly or indirectly from the literature is marked in the text.

Trondheim, 10 Oct 2016

Fabian Tobias Mayer

Acknowledgement

Table of Contents

                         Fabian Tobias Mayer B.Sc.

List of Figures

List of Tables

Fabian Tobias Mayer B.Sc.

1 Introduction

This master thesis covers the methodical development of a measuring system, which is capable to determine loads between a roller ski and the attached binding. A setup which is able to detect spatial forces and torques was demanded. The measuring system will be used for in situ testing on the road. In order to register reliable values, the system of the roller ski and the binding should be changed as little as possible and the athlete should not be disturbed in his performance.

Cross-country skiing athletes train on roller skis during the summer [1]. This is due to the fact that there are only a very few tracks on which cross-country skiing can be done all year long. Similar to the two different types of skis for classic skiing and skate skiing during winter there are two different types of roller skis. As depicted in Figure 1-1, a roller ski consists of two wheels which are connected by a beam on which the binding is mounted. For the classic technique the rear wheel is a ratchet wheel in order to enable propulsion during a diagonal-stride. Common cross-country skiing boots can be used with the binding.

Figure 1-1: RollerSafe roller ski with a Rottefella binding and cross a country-skiing boot

The measuring system needed to be implemented for roller skis and bindings of the project partners RollerSafe and Rottefella. The roller ski depicted in Figure 1-1 is the skate model branded by RollerSafe. RollerSafe produces roller skis with disk brakes which the athlete can control remotely

with a trigger at the handle of the skiing pole [2]. Rottefella is the leading manufacturer for cross-country skiing bindings and produces special bindings for roller skiing [3]. Such a binding is mounted on the roller ski shown in Figure 1-1. Both companies are seeking a measuring system for in situ testing to collect load data under regular conditions and for peak load events. The data which will be recorded are planned to be used for the optimisation of their products and to develop realistic laboratory tests for their roller ski bindings.

Many different measuring systems for skis and roller skis can be found in the literature. The most commonly used measuring system was designed at the University of Jyväskylä and was introduced by Ohtonen [4] in 2010. Most of the measuring systems found in the literature are used to investigate the performance of the athlete and to improve the skiing technique. Therefore, it was sufficient to determine spatial forces as most of the propulsion is generated by forces. None of the existing systems for skis and roller skis is able to determine spatial torques. For the companies Rottefella and RollerSafe it is crucial to know which torques their products need to withstand. Unexpected torques can lead to malfunctioning like forces do. Additionally to the product dimensioning aspect, the detection of forces and torques will bring new knowledge for the understanding and improvement of the skiing technique.

Another mayor issue of this thesis was the development a suitable data logger with low cost components. Modules from the Hottinger Baldwin Messtechnik GmbH and the National Instruments Corporation could not be used as they exceeded the budget of the project by far.

The thesis was undertaken at the Norwegian University of Science and Technology (NTNU) in Trondheim in cooperation with the two companies RollerSafe AS and Rottefella AS. Fabian Tobias Mayer wrote this master thesis during an ERASMUS exchange semester at the NTNU. The supervisor at the NTNU was Professor Torgeir Welo of the Department of Engineering Design and Materials. Professor Dr.-Ing. Sven Matthiesen of the Institute of Product Engineering supervised the thesis at the home university, the Karlsruhe Institute of Technology (KIT).

2 State of the Art

Force and torque measuring systems from various application areas were investigated in order to determine the state of the art. Firstly, general fundamentals which apply to all force and torque measuring systems were researched. The common setup of load measuring systems, sensors which are used to measure force and torque and the calibration of the systems were regarded. Furthermore, measuring systems which are utilised to determine loads during cross-country skiing and roller skiing were considered. In order to enable cross inventions, load measuring systems from other fields were researched and analysed. Moreover, information on instruments for data acquisition was gathered. In the subsequent chapters more detailed information on these topics is given.

Numerous measuring systems used on cross-country skis and roller skis are described which are able to measure spatial forces. The forces the athlete applies to the ski or roller ski are measured in order to analyse the skiing technique or to determine the physical effort. However, there is no nordic skiing system which is able to measure torques acting between a binding and the roller ski.

On the other hand, numerous solutions to measure force and torque were found considering the fields of tool engineering, sports equipment, medical engineering and automotive engineering. There are even multi-component dynamometers, which are able to measure force and torque in multiple dimensions within one measuring device.

For the existing ski and roller ski measuring systems it was sufficient to measure the loads which are applied by the athlete, as they were used to analyse the technique or the physical effort of the athlete. The frequency of the loads caused by influences from the surrounding like skiing over a crack in the road at high speed is significantly higher than the frequency caused by the athlete. In order to enable the measurement of the absolute maximum forces, a much higher sampling frequency of existing roller ski measuring systems is needed.

Regarding the components which were used for the existing measuring systems, there was a considerable budget available. The measuring system of this project needs to be implemented with a budget which is significantly lower.

In summary this project aims to find out, how to measure spatial forces and torques on a roller ski. Furthermore, the sampling frequency of the measuring system should be significantly higher than the one of the existing ski and roller ski measuring systems. Moreover, the solution should be implemented with a budget lower than the one of existing roller ski measuring system.

2.1 Fundamentals of Load Measuring Systems

The principles how to measure forces and torques were investigated. Knowledge on the setup of load measuring systems was acquired. Furthermore, sensors which are needed for the setup of force and torque measuring systems were researched and the calibration of such measuring systems was investigated. If not mentioned the following sub chapters is based on the *Guide to the Measurement of Force* of the Weight and Force Measurement Panel [5].

2.1.1 Basic Setup of Load Measuring Systems

Load measuring systems usually consist of a measuring chain which comprises transducers, instrumentation and an indicator as depicted in Figure 2-1 [6]. The transducer converts the physical input signal of the measuring system into a measurable output signal which can be a voltage, current or charge. In some cases, there might be a chain of transducers transforming the input signal in several steps [7]. For instance, a strain gauge load cell consists of an elastic element which transforms the applied force into strain. The strain is converted to a change in resistance by a strain gauge resistor. The output of the transducer is transferred to the instrumentation, which comprises signal conditioners, a microcontroller and memory. Signal conditioners process the output signal of the transducers in order to enable processing of the signal with a micro controller, which records it in the memory. Data acquisition is especially needed in case of rapidly changing forces. Besides signal conditioning and data acquisition the instrumentation is needed to power the transducers in case of passive sensing elements. Active sensing elements like piezoelectric crystal force transducers are not powered by the instrumentation. The processed output signal of the instrumentation system is shown to the user on an indicator. If the indicated values are not forces, calculations need to be done. For signals, which are not changing too fast, storage is not necessarily needed and the measured values can be transferred from the signal conditioning unit to the indicator directly [6].
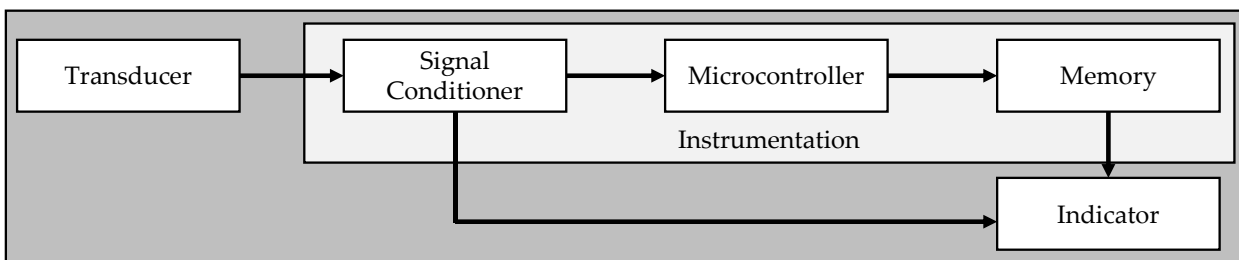
Figure 2-1: Common measuring chain, adapted from [5], [6]

Measuring range, the number of loading points, the direction of the forces, the duration and rate of the forces need to be considered to choose a suitable measuring system. For the suitable choice of the instrumentation the sampling frequency, the amount of data to be collected and the indicator need to be taken into account.

2.1.2 Load Sensors

Loads can be measured utilizing direct or indirect comparing methods. Direct methods compare an unknown force with the gravitational force and indirect methods employ a sensor which is calibrated with a mass of known weight [8]. Typical indirect measuring methods are acceleration measurement, deformation measurement of elastic elements, hydraulic pressure measurement and force balance methods [8]. For the listed methods different transducers are needed which are described in the *Handbook of Force Transducers* by Ştefănescu [9]. He summarises existing force transducers for industrial use and for research. Resistive, inductive, capacitive, piezoelectric, electromagnetic, electrodynamic, magneto elastic, galvano-magnetic, vibrating-wire, resonator, acoustic and gyroscopic force transducers are described. Furthermore, the acting forces can be detected by several force balance methods. Sensors and transducers which might be used for this project were investigated. The basic facts on strain gauge load cells, force sensing resistors, piezo electric transducers, capacitive transducers and accelerometers are present in the next sections.

Strain Gauge Load Cells are the most commonly used sensors to measure loads and therefore easily available [9]. The load cells consist of an elastic element and several strain gauges placed on the element. The strain gauges detect the elongation of the elastic element. If there are local strains the resistance of the strain gauges changes. Strain gauges basically consist of a length of conducting material, which might be considered as a wire. In case the wire is stretched the diameter decreases and the electrical resistance increases. The force acting on the elastic element can be determined with the help of the measured strain, the material properties and the geometry of the elastic element. In order to detect the force accurately a linear stress-strain relationship of the elastic element is needed. Foil strain gauges, semiconductor strain gauges, thin-film strain gauges and wire strain gauges are available. Foil strain gauges, illustrated in Figure 2-2, are the most commonly used. They consist of a measuring pattern made of metal foil placed on backing material made of polyamide or epoxy [5].
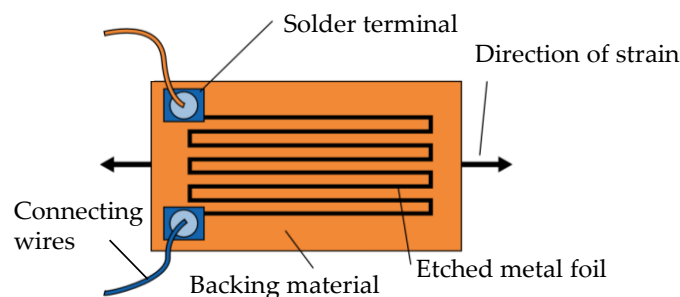
Figure 2-2: Strain gauge with connecting wires, adapted from [10]

The change of resistance of the strain gauges can be determined utilising a Wheatstone bridge configuration. Either the absolute value of the resistance or the change of the resistance can be determined. For measurements with strain gauges the relative change of resistance compared to the initial resistance is relevant. The functional principle and the formulae, which are explained hereafter are based on the *Handbook of Force Transducers* of Ştefănescu [9]. The Wheatstone bridge, depicted in Figure 2-3, has four legs on which the resistors R_1, R_2, R_3 and R_4 are mounted. The circuit is powered with the constant voltage U_0 between point A and C. The balance of the bridge is determined by measuring the voltage U_M between B and D. Dependent on the resistances the voltage is divided on the two sides of the bridge. The measured voltage is represented by equation (2-1).

$$U_M = U_0 \left(\frac{R_1}{R_1 + R_2} - \frac{R_4}{R_3 + R_4} \right)$$

(2-1)

For the resistance of the resistors there is an initial balance condition. The product of the resistors from opposing arms illustrated in Figure 2-3 needs to be equal before a load is applied to the strain gauge resistors.

$$R_1 \, R_3 = R_2 \, R_4$$

(2-2)

Effects, which are caused by two opposite arms of the bridge, are added and the effects of two adjacent arms of the bridge are subtracted.
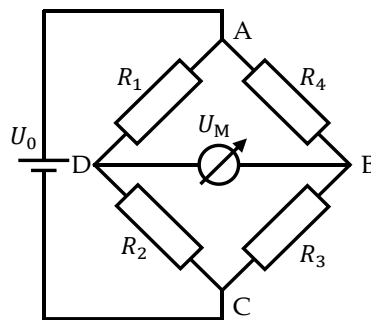
Figure 2-3: Wheatstone bridge, adapted from [6]

Not all of the four resistors necessarily need to be strain gauges. They can be constant resistors. The explanation how to use the strain gauges is based on the *Einführung in die Dehnmessunggsstreifentechnik* by Kabelitz [11]. For a quarter bridge depicted in Figure 2-4 a) only one strain gauge is used. For small strains the nonlinearity of the setup is negligible. However, for large strain there is an error higher than 2%. b) shows a half bridge with two strain gauges. The gauges can either be aligned with the direction of the strain or the transducers might be arranged perpendicular to each other. Perpendicular sensors might be used to compensate transverse strain. Furthermore, it is possible to compensate errors caused by temperature changes. Utilising four strain gauges results in a full bridge depicted in Figure 2-4 c). Similar to the half bridge the sensors can be parallel or perpendicularly aligned to each other. Compared to half

bridges, forces in other directions than the demanded one are compensated in a full bridge configuration.
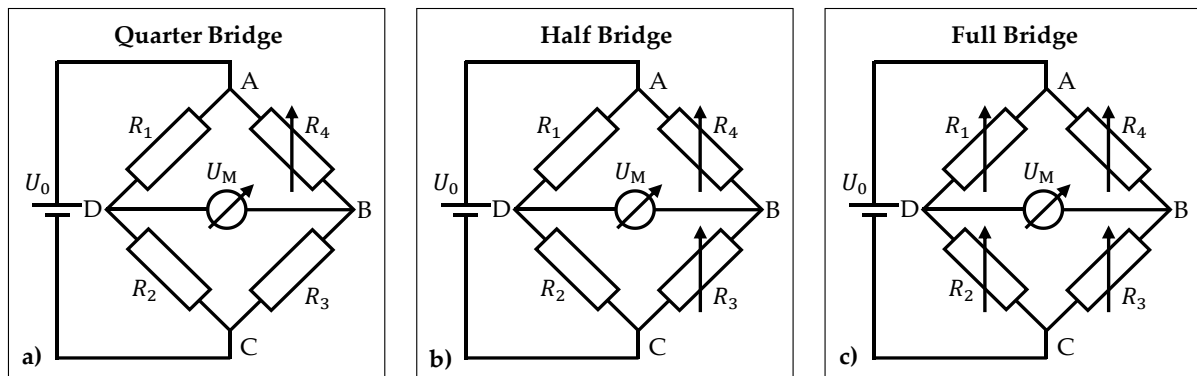
Figure 2-4: Wheatstone bridge configurations with strain gauges: a) Quarter bridge, c) Half bridge and d) Full bridge, adapted from [6]

The strain gauges need to be properly aligned with the strain field, because they should only detect strains along a certain axis. For different load cases different setups of the strain gauges are needed. In Figure 2-5 the position and alignment of the strain gauges in a full bridge configuration is shown for forces and torques. Furthermore, it is depicted how forces might be compensated.
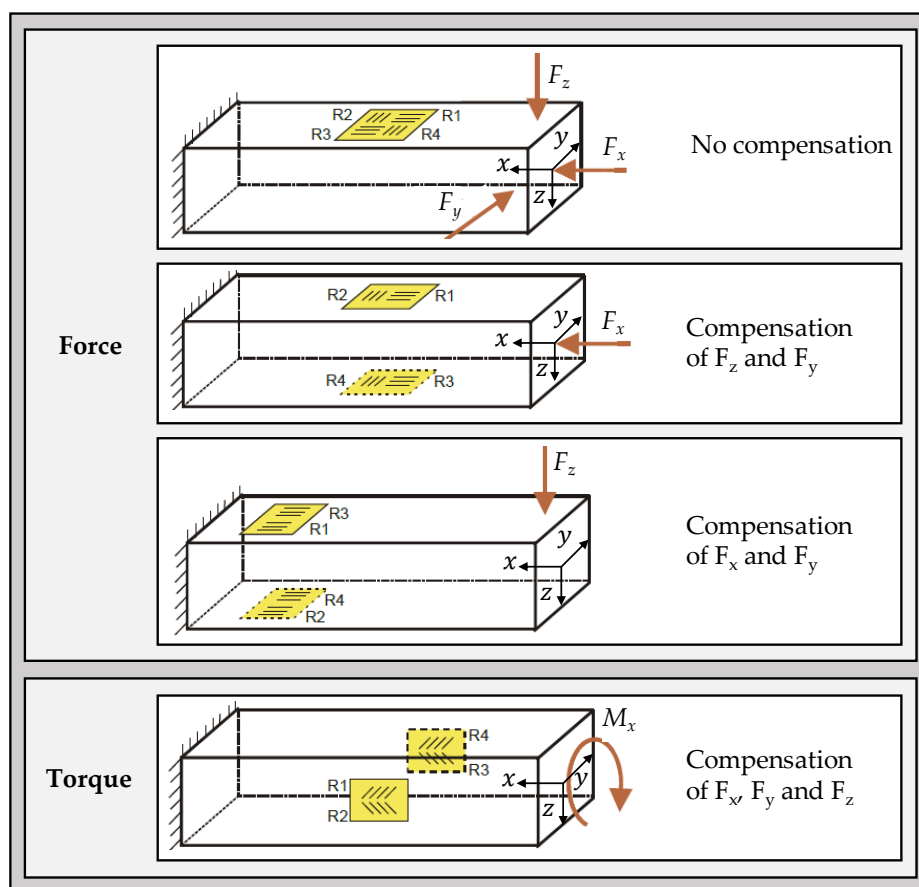
Figure 2-5: Position and alignment of strain gauges in a full bridge configuration for different load cases, adapted from [11]

In case of a multiaxial stress state strain gauge rosettes are utilised to determine the loads. For biaxial stress states with a known principal stress direction a rosette with two strain gauges can be used. The strain gauges need to be aligned with the principal stress directions. If the principal stress directions are unknown or change their direction rosettes with three strain gauges are needed. The principal stresses and their directions are calculated from the alignment of the strain gauges and the measured strains. The explanation how to use to rosettes is based on *Smart Materials* by Hoffmann [6].

The deflection of the elastic element might be determined with other transducers than strain gauges. Linear variable differential transducers make use of the change of the alternating current caused by the displacement of the magnetic core in a customised transformer. Optical strain gauges consist of an optical fibre transporting monochromatic light. The strain is determined by measuring the phase difference of two beams of light.

For some applications it might be suitable to utilise load cells. A strain gauge load cell comprises one or multiple elastic elements equipped with strain gauges. Hollow load cells are typically set under the screw head to measure screw forces [12].

Force Sensing Resistors consist of conductive pushers, a conductive elastomer and a conductive plate. The explanations of the force sensing resistors are based on the *Handbook of Force Transducers* by Ştefănescu [9]. Increasing the applied force, the contact area between the pusher and the elastomer increases. Additionally, the distance between the pusher and the conductive plate decreases. This results in a change of the electrical resistance. In Figure 2-6 the setup of the force sensing resistor and the relation between force and resistance is depicted. The transducer saturates with increasing force and the resistance does not change any more when a certain level of force reached.
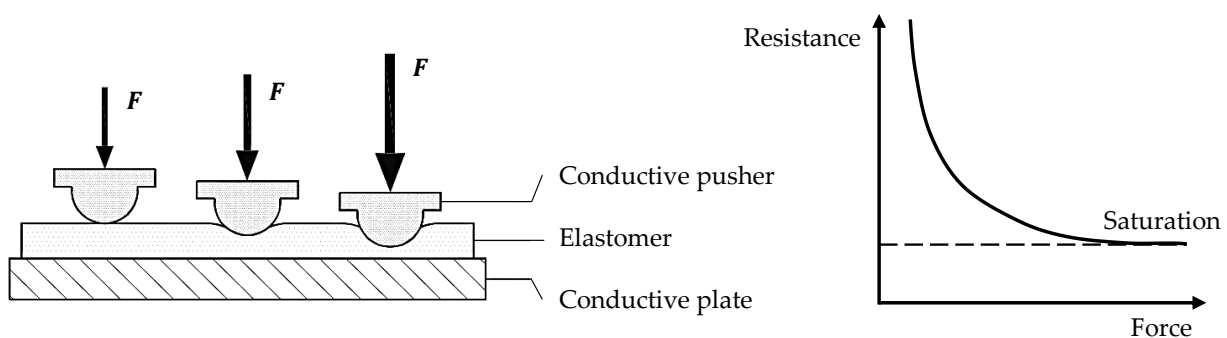
Figure 2-6: Setup of force sensing resistors and their force-resistance dependancy, adapted from [9]

Piezoelectric Crystal Force Transducers are based on the piezoelectric principle. The crystalline material of the transducer converts mechanical stress to electric charge. Dynamic oscillating forces can be measured precisely by piezo electric transducers. However, the transducers are not suitable to detect static forces as charge is generated only by changing forces. For static forces there is a strong signal drift caused by charge leakage. A measure of discharge is the discharge

time constant which is defined as the time until the sensor discharged to 37% of the original charge value. This time constant might be a few seconds or up to 2000 seconds [12]. The discharge time constant is the product of the resistance and the capacity of the circuitry which ahead the amplifier of the sensor. The exponential charge leakage is displayed in Figure 2-7. Piezo electric sensors are available with or without built-in circuitry. In case of sensors without a built-in circuit an external amplifier is needed. High impedance cables are required for the interface between sensor and amplifier. The explanations on the piezoelectric crystal force transducers are based on the *Sensor Technology Handbook* by Wilson [12].

In order to ensure linearity piezoelectric sensors are pre-tensioned with bolts. A preloaded sensor is able to detect tensile and compressive forces. Multi-component piezoelectric force transducers consist of three piezoelectric crystal rings. The orientation of the crystal on the rings is in x-, y- and z-direction which enables the detection of spatial forces.

Percentage of the initial charge

$$q = Qe^{-\frac{t}{RC}}$$

q instantaneous charge
Q initial quantity of charge
R resistance ahead amplifier
C total capacitance ahead to amplifier
t time elapsed

Discharge time constant (RC)
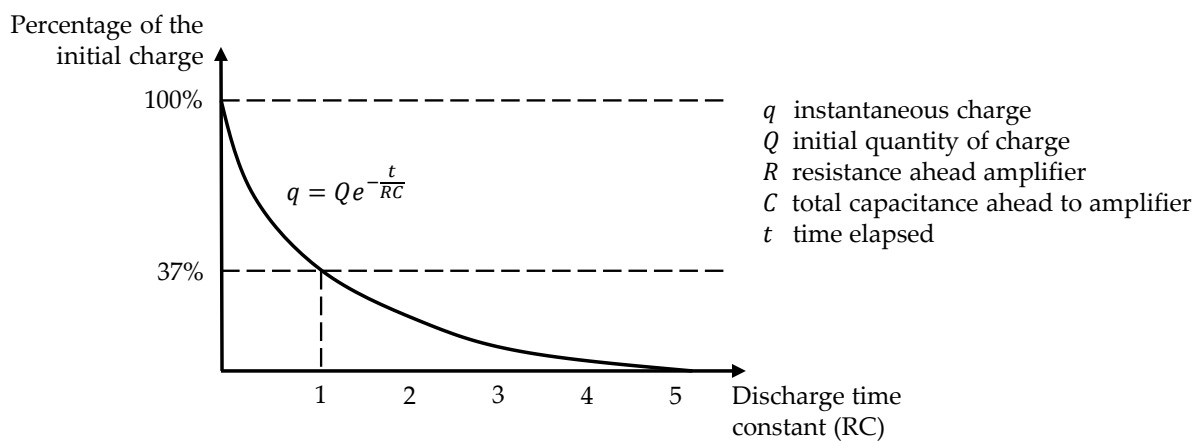
Figure 2-7: Charge leakage of piezoelectric transducers, adapted from [12]

Capacitive transducers comprise a flat, cylindrical or spherical capacitors. Capacitive plate transducers are most common. The capacitor consists of two electrodes and an elastic dielectric element as depicted in Figure 2-8. Elastic elements like disc springs with a linear elastic behaviour in combination with air as dielectric might be used. When a force is applied on the transducer the elastic element is compressed. With increasing load, the distance between the electrodes is decreasing which causes a rise of the capacitance. The change in capacitance is converted into a signal utilizing a relaxation oscillator The dielectric in the gap between the sensors is most likely air. Capacitive transducers are sensitive to dirt because the unwanted particles change the properties of the dielectric [12]. Therefore, the transducers will not function accurately in a dirty environment [12]. If not other was mentioned the information on the capacitive transducers is based on the *Handbook of Force Transducers* by Ştefănescu [9].
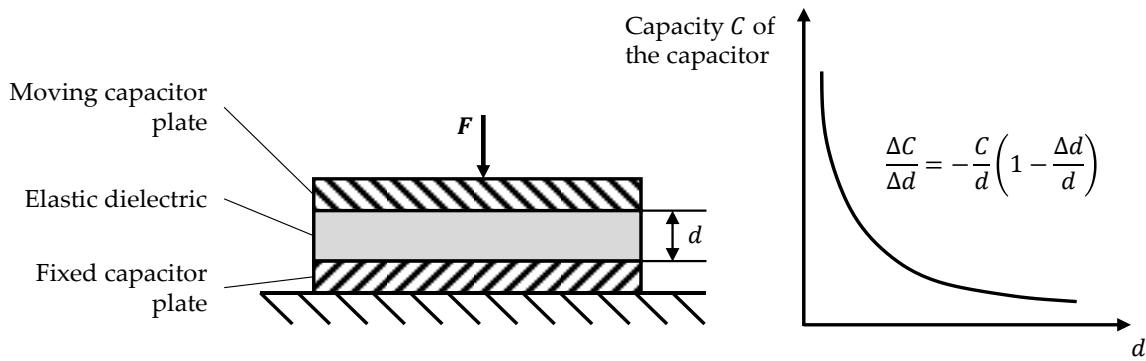
Figure 2-8: Capacitive force transducer and correlation between the plate distance and the capacity, adapted from [9]

Accelerometers are used to measure forces based on the force equilibrium. If the forces, which are acting on a body, are not in equilibrium there is a resulting force which causes acceleration. By measuring the acceleration, it is possible to calculate the force which is accelerating the body. Accelerometers consist of a mass which is displaced relatively to its housing by acceleration. The displacement is detected with piezoelectric or capacitive transducers.

In summary, depending on the measuring setup sensors with different properties are needed. The probably most important properties are the measuring range and the typical uncertainty. For the previously introduced sensors those properties are listed in Table 2-1.

Sensor Type	Measuring Range	Typical Uncertainty
Foil strain gauges	5 N to 50 MN	0.02 % to 1 %
Force sensing resistor	1 N to 100 N	2 % to 5 %
Piezoelectric crystal transducers	1.5 mN to 120 MN	0.3 % to 1 %
Capacitive transducers	10 pN to 0.5 N	0.2 % to 0.5 %
Accelerometers	0.25 N to 20 N	0.0001 %

Table 2-1: Summary of the properties of relevant sensors, based on [5], [13], [9]

2.1.3 Calibration of Load Measuring Systems

Calibration is conducted for all measuring systems after their production. Without a check the accuracy of the system cannot be relied on. Furthermore, calibration data is needed for the initial adjustment of some measuring systems. In addition to the initial calibration, there might be the need of calibration during the lifetime of the measuring system. Degradation of the measuring equipment causes inaccuracies, which need to be readjusted by calibration. Calibration during lifetime can be conducted continuously with additional sensors installed on the system or periodically with external sensors. How frequently calibration is necessary depends on the environment of the measuring system and its usage. Moreover, the calibration can be done for the trans-

ducers or the whole measuring system. In some cases, it might be useful to calibrate in the surrounding where the measuring system is used as temperature and humidity might have an effect on the accuracy of the system.

Depending on the kind of measurement there might be the need of static or dynamic calibration. Static calibration is conducted by applying a static load on the measuring system in order to generate the calibration function. However, dynamic forces are used for a dynamic calibration. For instance, piezoelectric force transducers require dynamic calibration.

The whole range of the measuring system, which is planned to be used, should be calibrated. In case of spatial forces only one axis at a time is calibrated. Cross talk effects need to be considered as calibration of one axis can interfere with the calibration of the other axes.

2.2 Load Measuring Systems for Skis and Roller Skis

Measuring systems for skis and roller skis described in the literature were realised in order to analyse the skiing technique and the physical performance of the athlete. Komi [14] was the first who used a measuring system to analyse and to improve cross-country skiing technique. In the literature systems for classic skiing were spotted which are able to detect forces in the skiing direction and in the vertical direction. For skate skiing systems were utilised, which were able to identify the forces perpendicular to the skiing direction as well. The existing measuring systems might be divided in three groups: Systems which comprise external force plates, systems with force sensors on the ski or roller ski and insoles, which detect the applied pressure.

Force Plates placed under a prepared ski track or under the belt of a treadmill measure ground reaction forces. Ground reaction forces are caused by the athlete who generates forward movement with the skis, the roller skis and the poles. Measurement of those forces enables an indirect detection of the forces the athlete is applying. Kehler et al. [15] used a force plate under the belt of a treadmill to determine the forces during classic roller skiing. They were able to measure vertical forces F_z and horizontal forces F_x in the skiing direction. Komi [14] and Vähäsöyprinki et al. [16] used the same setup for classic skiing on snow. Covering a force plate with snow and preparing it as a ski track enabled the detection of vertical forces F_z and horizontal forces in the skiing direction F_x. Leppävuori et al. [17] improved the system of Komi [14] to facilitate the analysis of skate skiing. The enhanced force plate was able to detect forces in all three directions. All systems were based on strain gauges which measured the deflection of the plates to determine the forces.

Force Sensors on the ski or roller ski determine the forces the athlete applies. For this purpose, sensors are introduced between binding and ski or roller ski. Alternatively, the sensors might be placed on the beam of the roller ski or the wheel bracket to measure their deflection.

Street and Frederick [18] placed piezoelectric transducers between the beam of the roller ski and the binding plate. Two vertical transducers at different positions measured vertical forces F_z whereas two horizontal sensors perpendicular to the skiing direction detected shear forces F_y.

Ainegren et al. [19] and Babiel [20] investigated a plate which is mounted between the binding and the roller ski. In contrast to Street and Frederick [18] they used strain gauges to measure all components of forces F_x, F_y and F_z. Babiel [20] utilised four strain gauges to measure vertical forces F_z, two strain gauges to measure forces F_y perpendicular to the skiing direction and one strain gauge to measure forces F_x in skiing direction. The Neuromuscular Research Centre, University of Jyväskylä in Finland, developed a similar system which, can be mounted on a common NIS plate [21]. The NIS plate is the interface on skis and roller skis on which a Rottefella binding is mounted. The measuring system consists of a front plate and a back plate. For the purpose of reducing cross talk between the sensors forces at each ski are measured in two directions only [22]. In Figure 2-11 the distribution of the force detection on the two bindings is shown. Nevertheless, forces in all three directions can be detected for each side by interchanging the roller skis. This system is used by Linnamo et al. [23], Ohtonen et al. [21] [22] [4] and Pohjola [24].
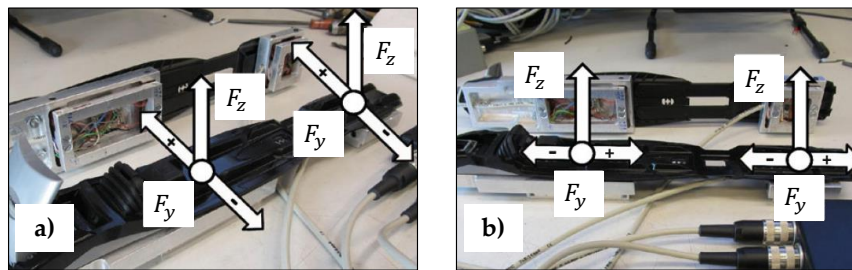
Figure 2-9: Distribution of the force sensors on two bindings a) and b) at the measuring system of the University of Jyväskylä [21]

Pierce et al. [25] implanted beam load cells directly into the surface of the ski instead of using an external force plate. Beam load cells use strain gauges to detect the deflection of the beam. Sensors were placed under the heel and forefoot of the athlete to measure the vertical forces F_z. In front of the binding a sensor measured the horizontal force F_x. Contrary to the previous system Friedrichs and Berger [26] did not use strain gauges on the force plates placed between binding and ski. They registered the forces acting during slalom skiing with force sensing resistors. The force plate depicted in Figure 2-10 consists of four resistive areas. If forces are applied on the measuring plate the resistant layer is compressed, which causes a decrease of the layer's resistance. The torques M_x and M_y are detected evaluating the change of the resistance.
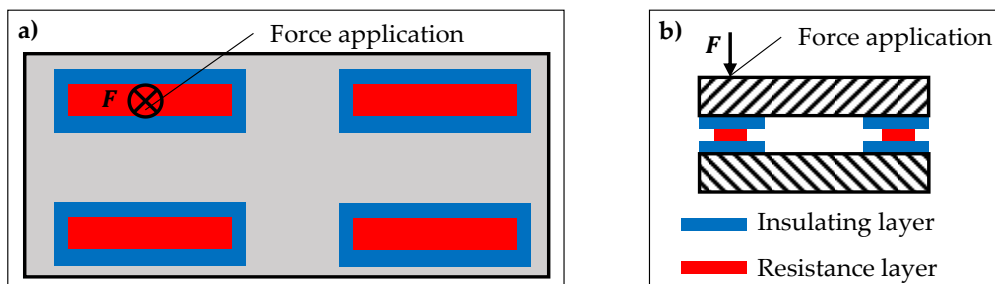
Figure 2-10: Measuring plate for slalom skiing by Friedrichs and Berger: a) Top view, b) Sectional view, adapted from [26]

Hoset et al. [27] were able to measure vertical forces F_z on the roller ski by detecting the deflection of the beam of the roller ski with strain gauges. In order to determine the direction of the force in a ground based coordinate system, the orientation of the roller ski was tracked. Three markers at the roller ski, tracked by a Qualisys Pro Reflex system, allowed to calculate the orientation.

In contrast to measure the deflection of the roller ski beam Bellizzi et al. [28] measured the deflection of the brackets holding the wheels of the roller ski. Placing the strain gauges as shown in Figure 2-11, it was possible to determine horizontal forces F_x and vertical forces F_z.
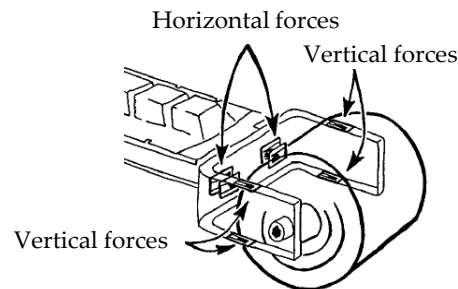
Figure 2-11: Positions of the strain gauges at the setup of Bellizzi et al., adapted from [28]

Insoles Measuring the Pressure under the athlete's feet are meant to evaluate the vertical forces F_z the athlete applies on the ski. Based on evenly distributed capacitive sensors the pressure insole is able to determine the forces perpendicular to the insole. Lindinger et al. [29] and Göpfert et al. [30] used pressure insoles to analyse classic skiing, whereas Stöggl et al. [31] and Stöggl et al. [32] used the system to analyse skate skiing.

2.3   Load Measuring Systems from Other Fields

Measuring systems from other fields than skiing and roller skiing were considered in order to foster cross inventions. This was necessary as a system needed to be developed which does not exist in the field of skiing and roller skiing yet. Systems which are able to detect one or more force and torque components were found. Moreover, information was gathered on multi-component dynamometers which are able to measure forces and torques within one sensor.

2.3.1   Force Measuring Systems from Other Fields

Force measuring systems from the fields of weighting, sports equipment and manufacturing machines were investigated. The measuring systems were classified whether they are able to determine one, two or three force components. Furthermore, the systems were sorted by the kind of sensor they employ. Systems with strain gauges, piezoelectric transducers, force sensing resistors or accelerometers were found.

Strain Gauges were used by Berli, Bönzli [33] and Caya et al. [34] to determine a singel force component. For a weighing application Berli, Bönzli [33] mounted strain gauges on a flexible beam. One end of the beam was fixed to the ground and the force caused by the weight acted on the other end. Due to the applied load the beam bent, which caused a change in resistance of the

strain gauges mounted on the rod. The change in resistance was converted into a load value by using the strain gauges in a Wheatstone full bridge configuration.

Caya et al. [34] made use of a similar technique to measure the force transmitted by the hands of the cyclist to the brake hood. As shown in Figure 2-12 b) a hollow aluminum cylinder equiped with strain gauges was mounted to the handlebar. The cover placed on the cylinder introduced the forces applied by the cyclist to the end of the cylinder. Measuring the deflection of the cylinder it was possible to determine the applied force.
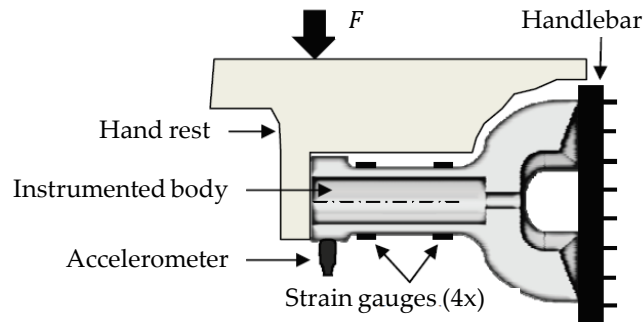
Figure 2-12: Force measuring bicycle handle to detect one force component, adapted from [34]

Parida et al. [35] used strain gauges in combination with octagonal rings to measure two force components during friction stir welding. The welding plate was mounted on four octagonal rings which were equipped with strain gauges. Forces which were acting on the welding plate deformed the octagonal rings underneath. With the strain gauges at the positions 1 to 12 depicted in Figure 2-13 a) it was possible to measure the deflection of the octagonal rings. The strain gauges 1, 2, 3 and 4 are used to detect horizontal forces. Vertical forces are detected by the strain gauges 5, 6, 7, 8, 9, 10, 11 and 12. With the alignment of the octagonal rings A, B, C and D depicted in Figure 2-13 b) it was possible to measure two force components. For the detection of horizontal forces which are parallel to the welding plate, the octagonal rings A and C are used. Vertical forces were detected by all of the four octagonal rings. The change of the strain gauges' resistance was determined using a Wheatstone bridge configuration.
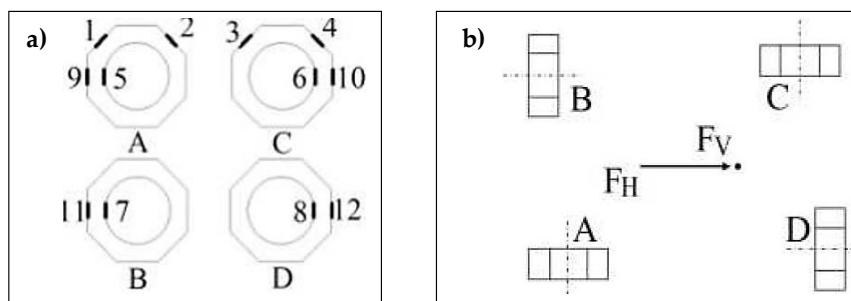
Figure 2-13: Strain gauge based measuring system for stir welding to detect two force components: a) Position of the strain gauges on the octagonal rings, b) Position and orientation of the octagonal rings on the welding plate, adapted from [35]

Spatial forces were detected with strain gauges by Zhao et al. [36], Dai et al. [37], Entacher et al. [38] and Kitayama et al. [39]. Zhao et al. [36] measured spatial cutting forces during lathing in real time with a tool holder comprising octagonal rings. The of the tool holder they used is displayed in Figure 2-14 a). Two octagonal rings were oriented perpendicular to each other to enable measuring of spatial forces. Twelve strain gauge sensors were used in three Wheatstone full bridges.

Dai et al. [37] measured the locomotion forces of geckos on different surfaces. The goal of the project was to determine the interaction of the gecko's feet and the surface. In order to measure the force applied by the gecko, 16 sensors were used which is capable to detect spatial forces. The force sensors shown in Figure 2-14 b) consisted of a T-shaped aluminium profile on which a load carrier were mounted. Strain gauges were placed on the profile to measure the deflection caused by the applied force. For the purpose of detecting the change of the strain gauges' resistance a Wheatstone bridge configuration was used.

Entacher et al. [38] designed a measuring system to detect spatial cutter forces of a tunnel drilling machine. By measuring bolt forces, they managed to measure the forces without changing the cutter. Load washers, which comprise strain gauge full bridges, were mounted beneath the screw head and additional strain gauges were placed in the screw. By measuring the bolt elongation, the bolt force could be calculated and the forces on the cutter were deduced. In order to calculate spatial forces, three equipped bolts were needed and a fourth bolt was used to quantify errors. The position of the bolts within the cutter is shown in Figure 2-14 c).
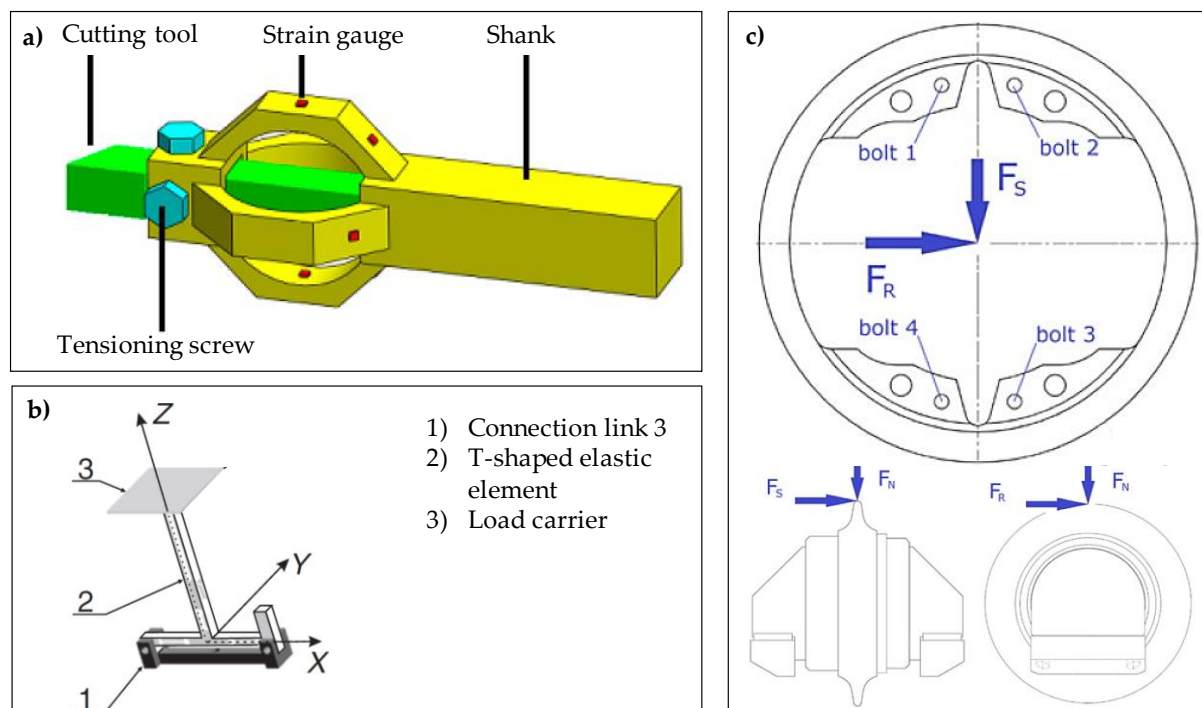
Figure 2-14: Strain gauge based measuring systems to detect spatial forces: a) Cutting force measuring system [36], b) Gecko locomotion force measuring system [37], c) Cutting force measuring system for tunnel drilling [38]

Piezoelectric Transducers were used by Degenstein and Winner [40] to measure clamping forces during the braking process. In order to measure the force between brake pad and disc, piezoelectric sensors were mounted on the friction material. Figure 2-15 shows the integration of the transducers in the brake and where they were mounted on the friction material. Piezoelectric transducers were used, because of their high stiffness which corresponds to the stiffness of the brake pads.
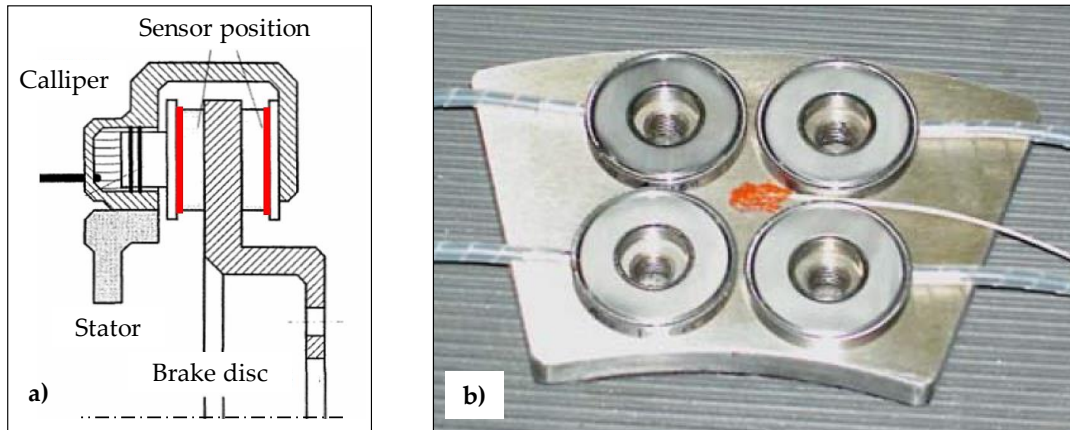
Figure 2-15: Piezoelectric transducer based brake force measuring system to detect one force component: a) Integration of the sensors in the brake [40], b) Position of the sensors on the friction material [40]

Force Sensing Resistors, which measure one force component were integrated in an ankle foot orthosis by Hamid et al. [41]. The sensor output was used to control the actuator movement of the orthosis. Flexible force sensing resistors were placed under the heel area and the big toe. Applying pressure the resistance of the sensors decreased.

Accelerometers were utilised to measure forces by Wei et al. [42] and Braghin et al. [43]. An indirect method to measure the wheel rail force of trains was developed by Wei et al. [42]. Accelerometers and displacement sensors, which were positioned according to Figure 2-16, were used. Vertical forces were determined by measuring the vertical acceleration of the wheel set and its displacement. Knowing the mass of the wheel set and the properties of the spring and damper, it was possible to calculate the vertical forces. For the lateral forces the horizontal properties of the spring and damper were considered.
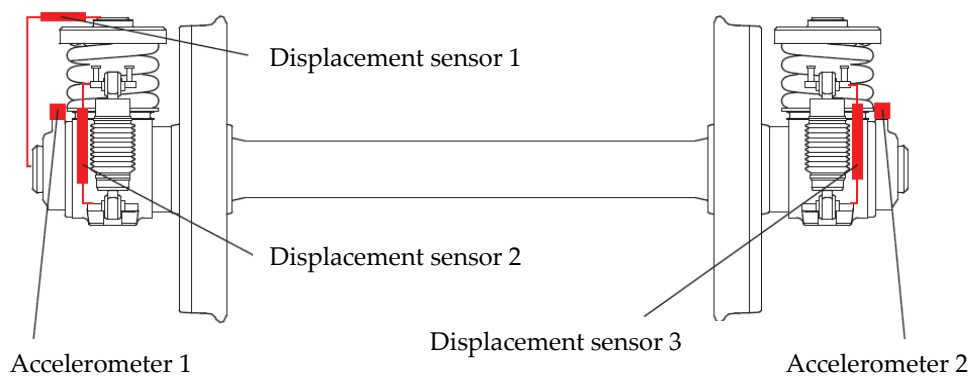
Figure 2-16: Instrumented wheel set to determine wheel rail forces of a train, [42]

Braghin et al. [43] placed accelerometers inside the tyre of a car. The tyres are the only parts of the car which are in contact with the road. Therefore, the purpose was to get as much information as possible from this point by measuring the wheel contact forces. A three axial micro electromechanical accelerometer was used to measure the acceleration to determine spatial forces.

2.3.2 Torque Measuring Systems from Other Fields

Torque is either measured on static elements or on dynamic elements like a turning axle. The explanations how to measure dynamic torques is based on *Ways to Measure the Force Acting on a Rotating Shaft* published by Honeywell [44]. For dynamic measurement contact and non-contact methods are applied. Contact methods use strain gauges to measure the strain oriented 45° to the torque axis and transfer the data via conductive slip rings. Non-contact methods measure the twisting of the shaft using optical or electromagnetic sensors. As shown in Figure 2-17 the sensor detects the twist of the shaft caused by the applied torque. For the unloaded shaft the measuring points are aligned with each other. If there is a torque the shaft is twisted, which causes an offset of the measuring points. Due to the twist, the measuring points pass the sensors at different moments. The time offset of the sensors can be transformed to a torque value. For instance, dynamic measuring systems are used in power steering applications [45].
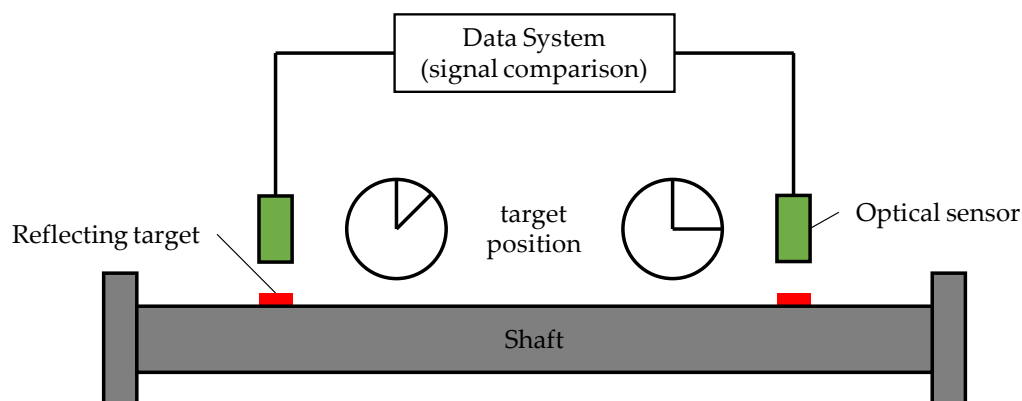
Figure 2-17: Dynamic torque measuring system with optical sensors, adapted from [44]

For the detection of the torques between binding and roller ski static torque measuring systems are needed. Existing measuring systems from the field of tool engineering and sports equipment were investigated. All of the detected measuring systems are based on elastic elements and strain gauges. Similar to the force sensor strain gauges were utilised to measure the deformation of the elastic element which is caused by the applied load.

One torque component is measured by tech wrenches which are used to tighten screws with a certain torque. Huneycutt [46] introduced a tech wrench which emulated a mechanical klick wrench giving feedback when a desired torque is applied. Furthermore, the applied torque is shown on a display. In order to measure the torque acting on the tightened screw there are strain gauges on the lever of the wrench measuring the bending. Due to calibration of the wrench the torque values are related to the measured deformation.

The power meter introduced by SRM [47] depicted in Figure 2-18 utilises four bending beams to determine the torque. The beams are the only connection between bicycle crank and gear set. With 16 strain gauges in full bridge configuration the deflection of the beams is determined. The power can be calculated knowing the cadence and the torque applied by the athlete on the drive train.
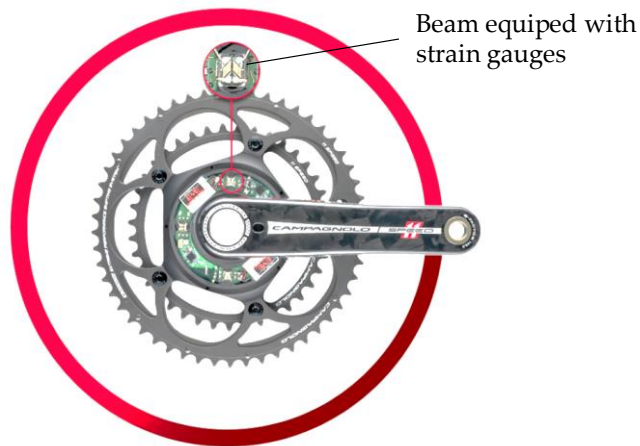
Figure 2-18: SRM power meter which detects one torque component, adapted from [47]

One torque component can be measured with strain gauges oriented 45° to the axis of the torque. Yoxall and Rowson [48] used that principle to determine the opening forces subjects are able to apply to a vacuum lug closure. Strain gauge sensors were mounted in 45° orientation on a shaft which was the only connection between the glass and a lid of the vacuum lug closure. Zhu et al. mounted strain gauges on the shaft of a valve in a 45° angle to determine the start-stop torque of the valve [49].

2.3.3   Multicomponent Dynamometers from Other Fields

Multicomponent dynamometers which are used to measure spatial torques and forces within one sensor were found in the fields of coordinate measuring, wheel force detection and cutting force measurement. The measuring systems comprise strain gauges or piezoelectric transducers.

Strain Gauges were used by Liang et al. [50] to measure spatial forces and two torque components. Their measuring system was integrated in the probing system of a coordinate measuring machine. The probing system depicted in Figure 2-19 a) is utilised for the inspection and calibration of coordinate measuring machines. The sensors were used to determine the contact point of the measuring tip on the probing geometry. The strain was measured on two connected Y-type cross beams, illustrated in Figure 2-19 a), to detect the forces and torques. The position of the strain gauges is depicted in Figure 2-19 b). The upper Y-type beam was utilised to detect torques. Torques along the x-axis cause the beams to bend along the x-axis and the strain gauges R13, R14, R15 and R16 were utilised for the detection. For torques around the y-axis the strain gauges R17, R18, R19 and R20 were used. The lower Y-type beam detected spatial forces. Forces in direction

of the x-axis cause bending of the beams along the y-axis and these forces were detected by the strain gauges R1, R2, R3 and R4. Forces aligned with the y-axis caused bending along the x-axis. Strain gauges R5, R6, R7 and R8 determined the forces in the y-direction. In case of forces aligned with the z-axis all three beams are bent and the output of all strain gauges of the lower Y-type beam was considered.
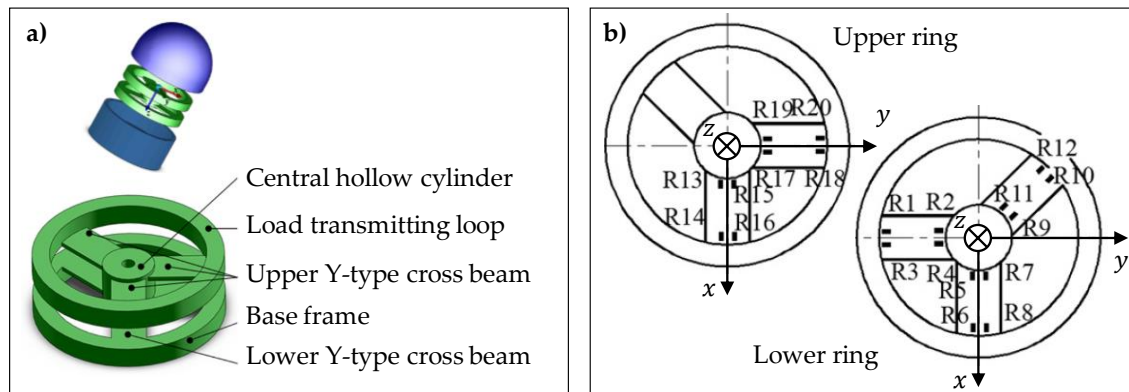
Figure 2-19: Probing system for a coordinate measuring machine: a) The setup of the used Y-type elastic elements [50], b) Strain gauge positions on the Y-type elastic elements [50]

Spatial forces and torques were measured by the multicomponent dynamometer introduced by Feng et al. [51]. The multicomponent dynamometer was mounted on the wheel of a car to measure its acceleration. The system comprised an inner ring fixed to the wheel of a car and a bigger outer ring connected to the inner ring by eight beams. The beams equipped with strain gauges are depicted in Figure 2-20. Forces in x-direction caused pressure in beam C and tension in beam G. The according forces were measured using the strain gauges R5, R6, R13 and R14. Forces in z-direction were determined similarly considering beam A and E. Forces in y-direction deformed all eight beams and the forces were measured utilizing strain gauge R17, R18, R19, R20, R21, R22, R23 and R24. Torques which were aligned with the x-axis induced bending deformation of beam A and E. In this case the strain gauges R17, R21, R25 and R29 were made use of. For torques around the z-axis the beams C and G including the sensors R19, R23, R27 and R31 were regarded. Torques in y-direction applied on all of the eight beams and the bending is measured with R1, R2, R5, R6, R9, R10, R13 and R14 [52]. A similar measuring system to detect loads during chipping is introduced by ATI Industrial Automation.
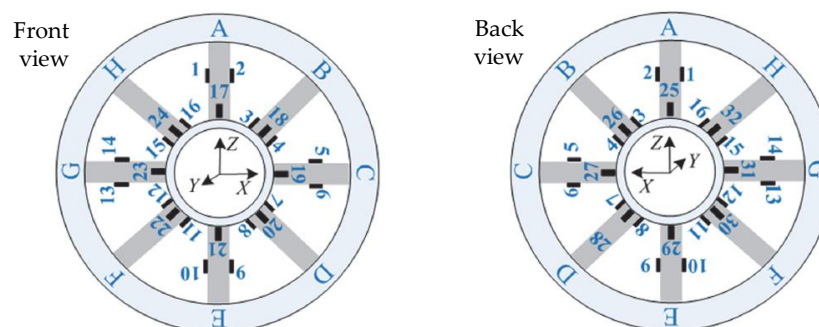
Figure 2-20: Strain gauge positions of a multi-component dynamometer to detect loads on a tire [52]

Piezoelectric Transducers are used by the company Kistler [53] in their measuring devices in order to determine spatial cutting forces and torques. The system is utilised to determine loads during chipping. Three crystal disc transducers are mounted under high preload to grant high accuracy. One of the discs is sensitive to pressure in one axis and the two others are sensitive to shear forces in the two other directions. Generally piezoelectric transducers are used to measure normal forces. However, with the suitable alignment of the crystals shear forces can be detected.

2.4 Data Acquisition Instruments

Professional data acquisition instruments were regarded. A high sampling frequency and a fine resolution enable the measurement of loads with high accuracy. Data acquisition instruments for measuring systems with strain gauges were regarded, as strain gauges were chosen for the implementation of the measuring system of this project.

The strain gauge supplier Hottinger Baldwin Messtechnik GmbH (HBM) provides a data acquisition system which consists of two instruments [54]. The strain gauges are connected to the first instrument depicted in Figure 2-21 a) which comprises the Wheatstone bridge circuitry, signal conditioners and an analogue to digital converter (A/D-converter). The QuantumX MX1615B [54] can be used for up to 16 strain gauges in quarter, half or full bridge configuration. The A/D-converter has 16 channels a resolution of 24 bit, a sampling frequency of 1 200 Hz and costs 7 000 € (65 000 NOK). The digital output of the QuantumX MX1615B is connected to the QuantumX CX22B-W [55] shown in Figure 2-21 b) which stores the data and is made for mobile application. The device for data acquisition costs 3 800 € (35 000 NOK).
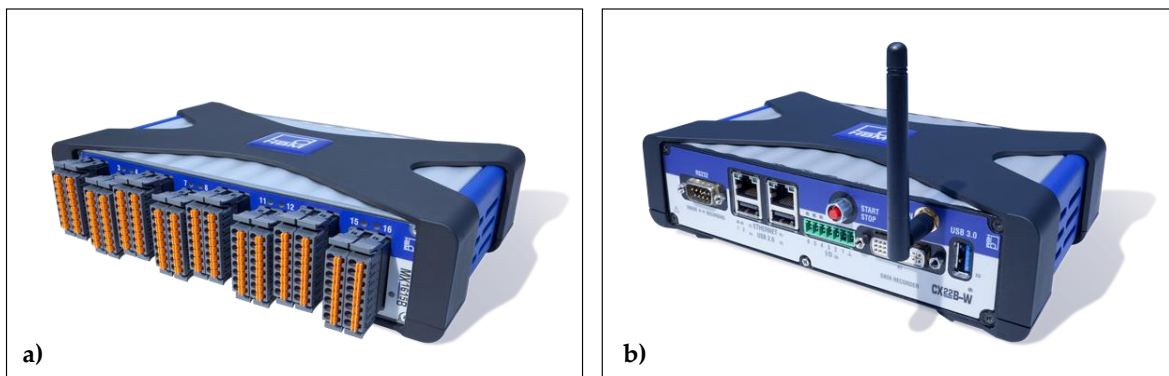
Figure 2-21: Data acquisition instruments from HBM: a) QuantumX MX1615B with bridge cirquitry, signal conditioners and A/D-converter; b) QuantumX CX22B-W data logger

National Instruments provides a similar system. The strain gauges are connected to the NI 9235 [56] with inbuilt Wheatstone bridges, signal conditioners and A/D-converters. The device has eight channels, 24-bit resolution, can sample at 10 000 Hz and costs 1 700 € (15 700 NOK). The measured data is stored with the cRIO-9024 [57] which costs 4 300€ (39 840 NOK). National Instruments provides a modular setup of their instruments. Up to four of the NI 9235 can be stored in a casing on which the cRio-9024 is mounted.

3 Motivation and Objectives

As described in chapter 2.2 no measuring system is available or described in the literature which matches the system required by RollerSafe and Rottefella. Therefore, a new measuring system for roller skis needed to be designed. More detailed information is given on the motivation and the objectives of the development of the required measuring system.

3.1 Motivation

Measuring systems used on skis and roller skis found in the literature are used to investigate the performance of different athletes and to improve the skiing technique. Different configurations to measure the loads acting on the roller ski were used. Similar to the system designed by the university of Jyväskylä [4] the more common measuring systems add sensors between the binding and the roller ski. This increases the distance between binding and ground which changes leverage and adds loads which commonly do not exist. These measuring systems are capable to measure one, two or three components of forces but not torques. A different design was invented by Bellizzi et al. [28] which measures two force components by determining the strain at brackets holding the wheel of the roller ski. Likewise, this system is not able to measure torques. Only for slalom skiing a measuring plate was developed by Friedrich and Berger [26] which is mounted under the binding and is capable to measure two torque components. In summary there is no measuring system which is capable of measuring spatial loads on skis or roller skis. Furthermore, most of the measuring systems change the roller ski – binding system and interfere with the common use of the roller ski. This might lead to results which do not match the common use.

The measurement of forces and torques will help to gain data for the optimisation of the skiing technique. Regarding the torques, which might be caused by unwanted instabilities of the athlete, a better understanding of efficiency in skiing will be achieved. Moreover, it will be possible for cross-country ski equipment suppliers to improve their design by increasing their knowledge on loads acting on their products. This will lead to better products, which enable a higher performance of the athlete and will lead to less incidents with malfunctioning equipment. Especially for the design of roller skis and roller ski bindings a safe dimensioning of the equipment is crucial as malfunctions commonly cause severe injuries.

The project partners RollerSafe and Rottefella will utilise the system to collect load data during roller skiing under regular conditions and peak load events. RollerSafe will use the load data for the design and dimensioning of a weight optimised roller ski made of carbon fibre. Rottefella needs the load data to develop future roller ski bindings. Moreover, they aim to establish more reliable laboratory tests for their bindings. Currently the tests are based on the standard ISO 9119:1990 [58], which defines test methods for bindings on cross-country skis as there is no standard available for the testing of roller ski bindings. The standard defines a binding to withstand a vertical pull-out force of 1600 N for adults and 1300 N for children [58]. Those values are insufficient for bindings on roller skis as break downs of the binding under peak load events occurred.

3.2   Objective

The main aim of this thesis was the development of a measuring system, which can detect both spatial forces and torques. As there is no such system described in the literature a suitable solution needed to be developed. Measuring systems from other fields were regarded to foster cross inventions in order to find an optimal solution.

The measuring system needs to be able to measure the forces and torques between the binding and the roller ski in all three directions. In order to measure the peak loads, it should sample at a frequency, which is sufficiently higher than the maximum frequency of the loads. In contrast to existing measuring systems the loads which are induced by external influences should be regarded in addition to the ones caused by the athlete. This makes a considerably higher sampling frequency necessary as the maximum frequency caused by a human is significantly lower than the one which is caused for example by skiing with high speed on an uneven road.

The measuring system is going to be used for in situ testing on the road. Therefore, a portable power supply is needed. Moreover, the measuring system needs to be water and dust resistant and needs to withstand the vibrations caused by the asphalt. Besides the tests on different underground like gravel roads and asphalt, the measuring system will be used to record data for different skiing styles and all situations which might occur during roller skiing.

For the realisation of the measuring system only a limited project budget was available. Hence, it was aimed to design a high quality solution with low cost components. Besides the financial restrictions the measuring system needed to be developed within the 20 weeks which are available for a master thesis at the NTNU.

The measuring system will be used by engineers from Rottefella and RollerSafe, athletes and academic staff of the NTNU. Not all of the users will be familiar with the design of the measuring system. Therefore, an intuitive design of the user interfaces and a high usability of the system is crucial.

4 Examination Method

In product development an optimal solution can be achieved if all requirements and constraints are considered. Therefore, it is essential to proceed methodologically and incrementally during the development of the product. Not the first solution which comes in to mind should be chosen as it might not be the best one. For this purpose, a methodology was used for the development of the measuring system.

The SPALTEN methodology introduced by Albers et al. [59] covers all the steps listed in the guideline VDI 2221 *Systematic approach to the development and design of technical systems and products* [60]. Therefore, the methodology is a suitable choice for the development of the measuring system. The systematic analysis of the initial situation, the structured search for solutions and the gradual implementation of the solution leads to a suitable result of the development project. In subsequent more information is given on the SPALTEN methodology itself and how it was implemented during this project.

4.1 Fundamentals of the SPALTEN Methodology

In 2005 Albers et al. [59] published a problem solving methodology for product development. If not mentioned otherwise this publication was used for this chapter. The SPALTEN methodology was developed based on research results in the field of problem solving and system engineering. The methodology considers the stages problem analysis, problem definition, system synthesis, system analysis, evaluation and decision of the guideline VDI 2221 *Systematic approach to the development and design of technical systems and products* [60]. SPALTEN consists of the seven stages which are listed in Figure 4-1. The stages are related to the topics of problem analysis, search for solutions and solution implementation and they can be worked through subsequently or dynamically. Depending on the project and the problem not all of the stages need necessarily be considered. At the beginning of each stage a problem solving team with appropriate abilities needs to be recruited. Before the start of a new stage an information check needs to be done in order to assure that the necessary information for the next stage is available.
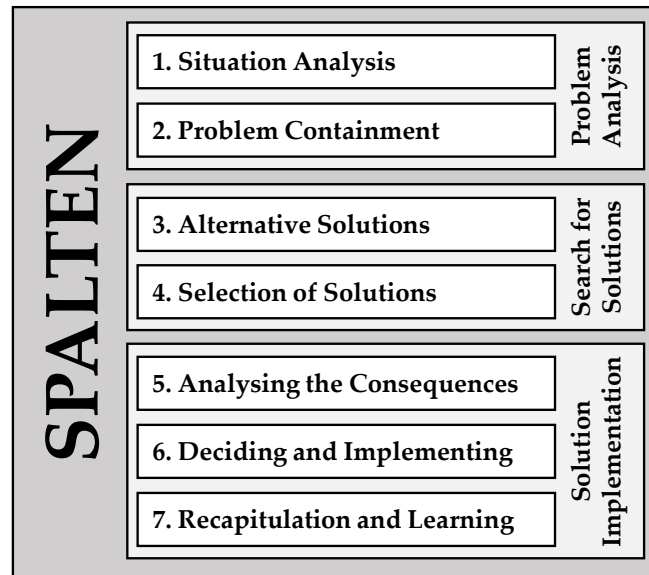
Figure 4-1: Stages of the SPALTEN methodology, adapted from [61]

Situation Analysis is the first step of SPALTEN. In order to understand the problem, it is important to assess the situation. This might be done by determining the actual state and the target state. Information about the problem needs to be collected, structured and documented. This is the basis for the subsequent steps of product development. Moreover, an approach to solve the problem needs to be chosen [62].

Problem Containment identifies the real problem. The information gathered in the situation analysis is used to determine the deviation between target state and actual state. The precise definition of the problem is the main outcome of the problem containment. A hypothesis of the reasons for the problem might be set up and proven. Furthermore, the goals of the problem solving process need to be determined.

Finding Alternative Solutions focuses on finding a high variety of solutions. Creativity techniques might foster the ingenuity which is needed for solution generation [61]. In order to avoid prejudiced solutions abstract wording of the solutions is important at that stage. Solutions should not be compared with each other in this stage. However, a feasibility check of the solutions is done on an individual basis [62].

Selection of Solutions is the juncture when the optimal solutions are selected considering technical and economic aspects [61]. The solutions generated during the previous stage are analysed regarding several eligibility criteria. Those criteria are set up and ranked following the requirements determined during the situation analysis. Using the eligibility criteria, the most promising solutions are chosen. This might be done by conducting a selection procedure such as a value benefit analysis in combination with a binary comparison. Solutions which are not selected are stored in a continuous idea storage [62].

Analysing the Consequences has the purpose to assess the chances and risks of the solutions chosen during the previous stage. In this context risk means influences which endanger the successful implementation of the chosen solution [61]. This intends to reveal critical aspects and to identify the causes for the risks. Schemes minimizing the risks are set up and will be considered during the implementation of the solution [62].

Deciding and Implementing is the realisation of the selected solutions considering the results of the stages selection of solutions and analysing the consequences. Actions which were determined to minimise the risks are implemented. Methods of project management are applied which consist of planning, conduction and control of the implementation process [61].

Recapitulation and Learning has the purpose of continuous improvement. The approach used for the development is optimised with use of the knowledge gained during the project and the improvements are documented. Results of the project are checked to be consistent with the target state and defects are eliminated [61].

4.2   SPALTEN Applied on this Project

For the development of the load measuring system the seven steps of the SPALTEN methodology were performed. The steps were adapted to the specific needs of the project and were conducted subsequently. A summary of all steps and related tasks is depicted in Figure 4-2

Situation Analysis was started with choosing the SPALTEN methodology for the development project. The sub tasks of the SPALTEN process were defined and a project plan was set up. In order to determine the target state there were meetings with the companies RollerSafe and Rottefella for which the system was designed. Detailed information on the measuring system was obtained using a questionnaire during the meetings. Furthermore, the situations the measuring system is used for were analysed in order to determine the necessary measuring range and the restraints of the surrounding. The situations during which the highest loads occur were assessed and the loads were ascertained by literature research or simplified calculations for those situations. Moreover, the needed sampling frequency of the measuring system was identified. The requirements were gathered in an initial requirement list which was continuously extended during the project. Classification of the requirements in *must have*, *should have* and *could have* was done and the requirements were priorized based on the available time and resources. In order to determine the actual state, existing solutions of measuring systems for skis and roller skis were researched.

Problem Containment is used to determine the deviation of the target state and the actual state. The demanded measuring system was compared with the existing solutions for measuring systems. Requirements which are not fulfilled by the existing measuring systems were listed and possible causes for the divergences were identified. The causes were investigated in order to find

out, whether the respective requirements are difficult or even impossible to fulfil. Furthermore, the goal of the development project was defined.

Alternative Solutions were generated for the main functions which are to measure forces and torques in all components. A systematic approach was used to generate a variety of convenient solutions to measure the loads and to log the measured data. Firstly, basic methods employed by the existing measuring systems were abstracted. Measuring systems for skis and roller skis were considered as well as systems from other fields. An analysis of measuring systems from other fields was done to foster cross inventions. Secondly, the number of sensors was reduced to the ones which could be used for the required measuring system. For the remaining sensors the previously extracted basic methods were adapted to the demanded measuring system in order to generate basic solutions. Solutions for the measuring of the loads and for the data acquisition were identified. A feasibility check was performed for all of the basic solutions.

Selection of Solutions dealt with the selection of the previously drafted solutions for the implementation. Selection criteria were defined and ranked based on the requirement list. The available time and resources were taken into account. Considering the selection criterions, a value benefit analysis was conducted and the best solution was found.

Analysing the Consequences focused on the prediction of chances and risks of the chosen solution. Critical aspects were revealed and causes for the risks were identified. Schemes how the risk could be minimised were set up. This was aimed to reduce errors in subsequent steps of the project.

Deciding and Implementing was done to develop and to build the final measuring system from the chosen basic solution. The schemes which were set up in the previous step to prevent the risks of the chosen solution were implemented. A set-based approach was used for the implementation of the solution. The measuring system was divided in sub-systems which were developed separately. For the sub-systems different solutions were engineered and tested with prototypes. The most capable solutions were connected to the final setup of the measuring system. Subsequently, the measuring system was calibrated.

Recapitulation and Learning was done to assess the success of the project and to learn for future projects. This was achieved by assessing how the measuring system matches the target state. The measuring system was validated and verified. Furthermore, the measuring accuracy was determined for the entire system. Moreover, the success of the applied methods to develop the measuring system was investigated.

SPALTEN				
1.	**Situation Analysis**	• The task was analysed and a project plan was set up • The requirements on the measuring system were analysed • An initial requirement list was set up • Existing measuring systems for skis and roller skis were researched	**Problem Analysis**
2.	**Problem Containment**	• The differences between the demanded and existing measuring systems were revealed • Causes for the differences were assessed • Goals for the intended measuring system were set up	
3.	**Alternative Solutions**	• Existing measuring systems were analysed to find basic methods to measure loads • The basic methods were adapted to the demanded system to find multiple solutions • A feasibility check of the basic solutions was conducted	**Search for Solutions**
4.	**Selection of Solutions**	• Suitable sensors were selected and ranked • Solutions for the measuring system were selected with a method which defines the technical value of the solutions • Two concepts were selected for further implementation	
5.	**Analysing the Consequences**	• Chances and risks of the chosen solution were assessed • Critical aspects were revealed and the causes for the risks were identified • Schemes to minimize the risks were set up	**Solution Implementation**
6.	**Deciding and Implementing**	• A set-based approach was used and different solutions for the sub-systems were developed in parallel • Prototypes for the solutions were built and tested • The best solutions for the sub-systems were connected • The measuring system was calibrated	
7.	**Recapitulation and Learning**	• Comparison of the resulting measuring system with the target state • Validation and verification • Learn about the measuring accuracy of the measuring system	

Figure 4-2: Stages of the development project and the related tasks

Fabian Tobias Mayer B.Sc.

5 Results

The result of this master thesis is the methodical development process of the measuring system which determines forces acting between the roller ski and the binding. For the development the seven stages of the SPALTEN methodology introduced by Albers et al. [59] were performed. Fundamentals of the SPALTEN methodology can be found in chapter 4.1. In the subsequent chapters, information is given how the measuring system was developed and what the resulting measuring system is capable of.

5.1 Situation Analysis

The objective of the situation analysis is to recognise and to understand the situation. Furthermore, a treatment of the situation has to be chosen. Analysing the given task, it turned out that SPALTEN is the methodology of choice to develop the measuring system.

After a thorough analysis of the development task given by RollerSafe and Rottefella a project plan was set up. The target state was evaluated by determining which kind of measuring system is required. Based on that knowledge a requirement list was set up. The actual state was assessed by investigating existing measuring systems which are able to detect loads during roller skiing and cross-country skiing.

5.1.1 Task Analysis and Project Plan

Meetings were arranged with the project partners RollerSafe and Rottefella in order to learn what is expected of the measuring system. The task was to develop a measuring system which is able to detect the loads acting between roller ski and binding during all situations which may occur during a common training.

A project plan was set up considering the stages of the SPALTEN methodology. The tasks which need to be fulfilled for each stage were listed and their duration was estimated. Including the settling-in period there were six months available to conduct the project.

5.1.2 Required Measuring System

It was investigated which kind of measuring system is needed in order to define the target state. Information was gathered from RollerSafe and Rottefella using a questionnaire during the meetings with them. The questionnaire was utilised to obtain detailed information on the measuring of the loads, the data output of the measuring system and the validation. Moreover, the equipment which should be used for the measurements, the restraints of the surrounding and the deadlines of the project were discussed based on the questionnaire.

The measuring system needs to be able to measure spatial forces and torques between binding and roller ski during classic and skate roller skiing. For Rottefella and RollerSafe it is most important to know the peak loads which they will use for the dimensioning of their systems and the development of laboratory test setups. Besides the absolute values of the peak loads the companies are interested during which events they occur. The system will be used with active and pro skiers and should be able to record data during two to three hours. The recorded data should be transferred to a computer. For the setup of the measuring system the roller skis from RollerSafe and the bindings from Rottefella have to be used. The setup of the roller ski – binding system should be changed as less as possible. In order to enable testing on the road the system needs to be water proof and dust resistant. Moreover, it needs to withstand vibrations and small drops. Most important is a safe design of the system in order not to endanger the athlete. The system should be finished and validated until the end of September.

Besides the information from RollerSafe and Rottefella further information was gathered. For the dimensioning of the measuring system the peak loads and the required sample rate were assessed. Together with more specific restraints of the surrounding this additional information was added to the target state and the requirement list.

Peak Loads during roller skiing were estimated for the dimensioning of the system as the two companies explicitly want to learn more about the maximum loads during roller skiing. There have been certain situations such as harsh braking or getting stuck on a curb stone with the roller ski during which the bond between the binding and roller ski failed. There are no situations known during which the binding failed due to minor forces which occur frequently such as vibrations caused by uneven roads. Therefore, it was agreed to focus on the measurement of maximum loads with high accuracy.

For the dimensioning of the measuring system the maximal loads were assessed. All situations during roller skiing were regarded. The different sub-techniques of skate and classic skiing were considered with respect to the push phase, glide phase and swing phase which occurs during all of this techniques. Besides common skiing other incidents like breaking, turning and jumping were taken into account.

The forces and torques which occur during these situations were ranked dependent on the expected loads and the situations with the highest ranking were determined. For those situations the loads were researched if load data was available in the literature. The remaining loads were assessed by simplified calculations. The entire procedure for the assessment of the maximal loads and the explanation of the different skiing techniques can be found in Appendix HAppendix I.

The highest force in roller ski direction was assessed to be $F_x = 562$ N caused by getting stuck on a curb stone with the roller ski. During breaking with the altering push brake the maxima of $F_y = 239$ N which is horizontal perpendicular to the skiing direction, $M_x = 13$ Nm around the beam of the roller ski and $M_z = 82$ Nm around the vertical axis occur. Diagonal stride was assessed to cause the maxima of $F_z = 1748$ N in the vertical direction and $M_y = 9$ Nm around the axis horizontal perpendicular to the skiing direction.

The Required Sampling Frequency was assessed using the Nyquist criterion which states that the sampling rate has to be two times higher than the frequency which needs to be measured [63]. However, for practical use a sampling frequency six to ten times higher than the maximum frequency is recommended. For the measurement system on the roller ski the maximum frequency caused by the athlete and by external sources was regarded. Mauritius [64] found out that most humans cannot move faster than 7 Hz which leads to a needed sampling frequency of at least 14 Hz according to Nyquist but better would be 42 to 70 Hz.

Considering the external load sources, the vibrations due to uneven asphalt cause the highest frequencies. Due to Rottefella the malfunction of their binding was caused by special incidents and not by vibrations. Therefore, the highest frequency which is caused by a single incident was regarded. Skiing downhill at $v = 40$ km/h and hitting a small stone with a classic roller ski wheel of the diameter $l = 60$ mm takes the time t.

$$t = \frac{l}{v} = \frac{1}{185} \text{ s} \tag{5-1}$$

In order to detect the frequency of 185 Hz which occurs the sampling frequency needs to be 370 Hz according to Nyquist but 1 110 Hz to 1 850 Hz would be better.

Regarding the Restraints of the Surrounding on the measuring system it needs to be recognised that roller skiing is very demanding for the equipment. Roller skis are used for training on roads and compressed gravel tracks which means the measuring system needs to be dust resistant and to withstand vibrations. Using the measuring system on wet roads or when it is raining water-resistance is needed. Enabling the collection of a lot of measurement data during numerous training sessions a sturdy and durable measuring system is needed.

For this purpose, all situations during roller skiing were analysed in order to estimate maximum loads which could act between binding and roller ski. Loads occurring during the different situ-

ations were rated and the maximum forces and torques in each direction were researched or estimated by doing simplified calculations.

5.1.3 Requirement List

The questionnaire which was worked through during the meeting with RollerSafe and Rottefella had the purpose to enable the project partners to express their demands on the measuring system. Based on the requests an initial requirement list was set up. The requests were classified into the following six topics. *Measurement* comprises information of the loads which are obliged to be detected under which conditions. *Data Output* describes how measured data needs to be provided. *Restraints of the Surrounding* entails information on the surrounding the measuring system needs to be designed for. *Test Equipment* explains which roller skis and bindings need to be used and how they might be modified. *Validation* defines the validation of the measuring system. *Deadlines* provides information on when the system needs to be finished. The initial requirement list was extended during the whole project and can be found in Appendix G.

The requirements on the measuring system were classified depending on their relevance like it is recommended in the standard VDI 2225 *Engineering design at optimum cost* [65]. A division in *must haves*, *should haves* and *could haves* was done. Requirements which were crucial in order to make the measuring system work like RollerSafe and Rottefella want it to were ranked with *must have*. *Should have* was used for requirements which enable a better fulfilment of the demanded properties of the measuring system. Requirements which are not necessarily needed are classified as *could have*. The result of the classification is found in the requirement list in Appendix G.

5.1.4 Existing Measuring Systems

Existing measuring system for skis and roller skis were investigated in order to determine the actual state. Several measuring systems were found in the literature. More detailed information on those systems in found chapter 2.2. Regarding Table 5-1 which is a summary of the existing measuring systems reveals that it is common to detect forces on the binding. Most of the systems are able to detect spatial forces. The system of the Neuromuscular Research Centre, University of Jyväskylä, Finland is used by the most research studies. Torques are rarely recorded. Respecting the detection of the applying torques there is the system of Friedrichs and Berger [26] only. Their System is able to detect M_x and M_y but there is no system which can detect M_z.

Furthermore, the systems were used to analyse the skiing technique and the physical performance of the athlete. This requires a significantly lower sampling frequency than the one which is needed to detect loads which are caused by external circumstances such as skiing over a curb or a stone on the road. Regarding the equipment which the found measuring systems utilised there was a budget which is considerably higher than the one which is available for this project.

Research Study	Used measuring setup	Used sensors	Detected forces / torques on the binding					
			F_x	F_y	F_z	M_x	M_y	M_z
Komi [14]	External force plates	Strain gauges	X		X			
Leppävuori et al. [17]		Strain gauges	X	X	X			
Vähäsöyprinki et al. [16]		Strain gauges	X		X			
Kehler et al. [15]		Strain gauges	X		X			
Pierce et al. [25]	Force sensors on the ski / roller ski	Strain gauges	X		X			
Street, Frederick [18]		Piezoelectric load cells		X	X			
Friedrichs, Berger [26]		Resistive force plate				X	X	
Bellizzi et al. [28]		Strain gauges		X	X			
Babiel [20]		Strain gauges	X	X	X			
Ohtonen [4]		Strain gauges	X	X	X			
Linnamo et al. [23]		Strain gauges	X	X	X			
Ohtonen et al. [21]		Strain gauges	X	X	X			
Ohtonen et al. [22]		Strain gauges	X	X	X			
Ainegren et al. [19]		Strain gauges	X	X	X			
Pohjola [24]		Strain gauges	X	X	X			
Stöggl et al. [31]		Strain gauges			X			
Lindinger et al. [29]	Pressure insoles				X			
Göpfert et al. [30]					X			

Table 5-1: Propperties of existing ski and roller ski measuring systems

5.2   Problem Containment

The intention of the problem isolation is to determine the divergence of the target state which is represented by the demanded measuring system and the actual state consisting of the existing measuring systems. Therefore, existing solutions for ski and roller ski specific measuring systems were compared with the measuring system demanded by RollerSafe and Rottefella. Furthermore, the possible causes for the revealed deviations were assessed. This is meant to identify possible complications to design the measuring system. Furthermore, the goals of the development project were defined.

5.2.1 Divergence of Required and Existing Measuring Systems

For the purpose of revealing the divergence between target state and actual state the requirement list in Appendix G was compared with the solutions of existing measuring systems described in chapter 2.2. The results were sorted in the categories measurement, validation, data output, test equipment and restraints of the surrounding.

Measurement considers the detection of spatial forces and torques. None of the existing roller ski or ski measuring systems is able to detect all forces and torques. It is common to detect spatial forces but torques have not been detected by a nordic system yet. Only the system of Friedrichs and Berger [26] made for alpine skiing is able to detect the torques M_x and M_y. M_z has not been determined yet. Moreover, the systems found in the literature were used to detect loads caused by the athlete. As the required measuring system has to detect loads which are acting at higher frequency an increased sampling frequency is needed.

The loads need to be determined between the binding and the roller ski. All systems using force plates between the binding and the roller ski fulfil this criterion. The criterion to analyse classic and skate skiing was accomplished by several existing systems as well.

Moreover, the measuring system needs to detect the loads during each situation which might occur during training. External force plates are not suitable to measure during a common training session because they are locally bound. It is not possible to integrate them in a common training session and to simulate all situations. The same applies for systems involving motion capturing.

Maximum forces need to be measured with high accuracy. For this purpose, most of the existing systems can be used. Evaluating the skiing technique and the energy output of the athlete absolute values are shown in most of the papers. Furthermore, the validation procedure is explained. When it comes to enable measuring over a long time for instance the system of Ohtonen et al. [21] was able to be used over several hours in cold conditions. As the tests were conducted with professional cross-country skiing athletes the measuring systems are assumed to withstand high forces.

Validation of the measuring system is necessary in order to generate reliable data which can be used for dimensioning. All of the existing measuring systems providing absolute values are expected to be validated. If absolute values are mentioned in the papers the validation procedure of the measuring system is documented as well.

Data output considers how measurement data should be transferred and evaluated. After the training the recorded data has to be transferred to a computer via USB port, SD card, Wi-Fi or Bluetooth. The software used for the evaluation needs to be available for RollerSafe and Rottefella. Both of the companies have access to Matlab.

Test equipment considers the equipment which needs to be used for the test and how it might be modified. It is required to use a roller ski model from RollerSafe. As there have not been tests

using Rollersafe roller skis the existing measuring systems need to be adapted. When it comes to the positioning and mounting of the measuring system the compressor unit and the pipes of the disc brake system need to be taken care of. Furthermore, Rottefella bindings have to be used for the tests. All existing measuring systems comprise Rottefella bindings or are at least able to be used with them. None the less, it has to be taken care that the distance between the interface of the binding has the same distance to the roller ski and the ground as before. The binding interface is the connection between boot and binding which constitutes the pin of the boot fastened by the binding. Existing measuring systems using force plates between roller ski and binding would need to be improved to fulfil this requirement. The weight of the roller ski and its centre of gravity should be changed as less as possible by mounting sensors and transducers. Ohtonen et al. [21] added 490 g to each ski by mounting their measuring system.

Restraints of the Surrounding need to be considered in order to enable the usage of the measuring system in the demanded surrounding. The system has to be water and dust resistant. Existing measuring systems used on snow fulfil this requirement. However, systems made to be used on treadmills are probably not made to withstand water and dust. None of the systems was used to detect loads during roller skiing on roads. Due to this reason, vibrations caused by uneven asphalt need to be taken care of if one of the existing measuring systems is used. Whether the existing measuring systems are able to withstand small drop tests is not mentioned. A sturdy and durable design of the existing systems is assumed as they have been used for research studies which required a lot of measuring sessions. Using the measuring systems on roller skis they are considered to be safe due to the reason that the athletes using the system have not been endangered.

The Budget of the measuring systems found in the ligature was large. This becomes clear regarding the components the systems are using. For this project there is a limited budget which is significantly lower. Therefore, a solution needs to be found which enables the design of a good measuring system with low cost components.

Summarizing the divergence of the target state and the actual state Figure 5-1 shows how existing measuring systems need to be improved and adapted in order to fulfil the demanded requirements. A solution has to been found to determine the torques M_x, M_y and M_z. Furthermore, it should be figured out how to sample at a higher frequency. The measuring system has to be mounted on a RollerSafe roller ski. Moreover, a measuring system which withstands vibrations and small drop tests is needed. Besides a solution is required for a low cost measuring system.
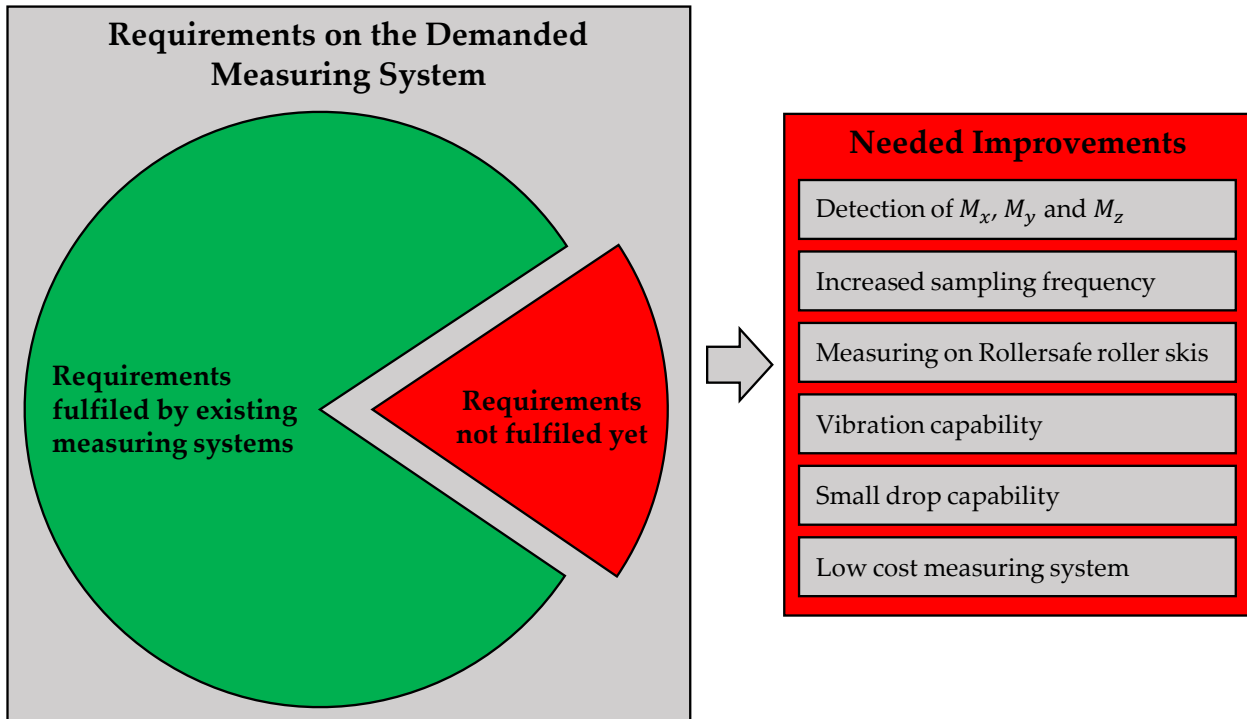
Figure 5-1: Requirements on the measuring system which have not been fulfilled yet

5.2.2 Reasons for Divergences

Divergences between solutions of existing measuring systems and the requirements on the demanded measuring system were revealed. In order to prevent complications caused by the additional requirements the causes for this divergences were assessed. It might be possible that some requirements have not been fulfilled yet because it turned out that they could hardly be fulfilled or that requirements interfere with each other.

During cross-country skiing the athlete applies forces on the ski in order to generate propulsion. Torques usually do not cause propulsion and most often they are related to instabilities or other unwanted events. The purpose of the research studies using measuring systems on roller skis is to analyse the technique and its efficiency. Therefore, forces and not torques are measured and it was sufficient to measure at a low sampling frequency in order to detect the loads caused by the athlete. Furthermore, measuring of too many variables at once causes interferences between the sensors. Ohtonen et al. [22] found out that separation of the measured variables on two skis is necessary for the purpose of a simple design of the measuring system and less crosstalk between the sensors.

Research studies including the measurement on roller skis were conducted on treadmills. There is no need for brakes on a treadmill. Furthermore, the brake system inside the roller ski makes it more difficult to mount a measuring system on the roller ski. This might be the reason why RollerSafe roller skis have not been used for tests yet. For this project it is essential to use their roller skis due to the reason that loads during braking with disc brakes need to be recorded.

The test procedures of the existing measuring systems were used for tests on treadmills or snow. A certain test course was chosen to conduct the tests on. Thereby reproducibility is granted and it is possible to compare the test runs. On the contrary the purpose of the demanded measuring system is to determine the overall maximum values of the forces. Therefore, tests will be conducted during common trainings on various kinds of asphalt and with athletes of different levels. The measuring system has to withstand vibrations caused by the road. Moreover, the measuring system needs to be durable. Small drop tests due to inadvertent handling by the athletes need to be withstood by the measuring system.

5.2.3 Goals of the Development Project

As a result of the development project the designed measuring system should match its target state. The measuring system was intended to detect spatial forces and torques. It was contemplated to be verified in the lab with tests which prove the accurate measurement of torques and forces. Furthermore, the system was intended to be validated by in-situ testing and comparison with measured data from research papers.

RollerSafe and Rottefella should be able to use the system in order to record data during common training with active skiers and pro skiers. The measured data should be supplied to a computer and has to be evaluated easily. RollerSafe will be able to use the recorded data in order to design a weight optimised roller ski out of carbon fibre. Rottefella will be enabled to optimise their roller ski binding and to establish more relevant laboratory test setups.

5.3 Search for Alternative Solutions

In this step of the project a high variety of solution principles to measure the loads between roller ski and binding needed to be found. The focus was on finding solutions for the main functions to measure forces and torques. A systematic approach was used to generate numerous apt solutions. The solution principles were not compared with each other at this stage. A feasibility check for each solution was performed individually.

In order to generate a high variety of suitable solutions the approach depicted in Figure 5-2 was used. Existing measuring systems for cross-country skiing, roller skiing and from other fields were considered. Especially systems from other fields have been taken into account for the purpose of making cross inventions possible. Most inventions are not completely new as they are solely solutions adapted from another field of application. The respective measuring systems are listed and explained in chapter 2. The function of the exiting measuring systems was abstracted and basic methods to measure loads were identified. The number of different types of sensors was reduced to the sensors which could be used. For the remaining sensors basic solutions were generated by adapting the previously found basic methods to the needed measuring system. Furthermore, possible solutions for the data acquisition were gathered. For all of the solutions a feasibility check was conducted and the weaknesses were revealed.
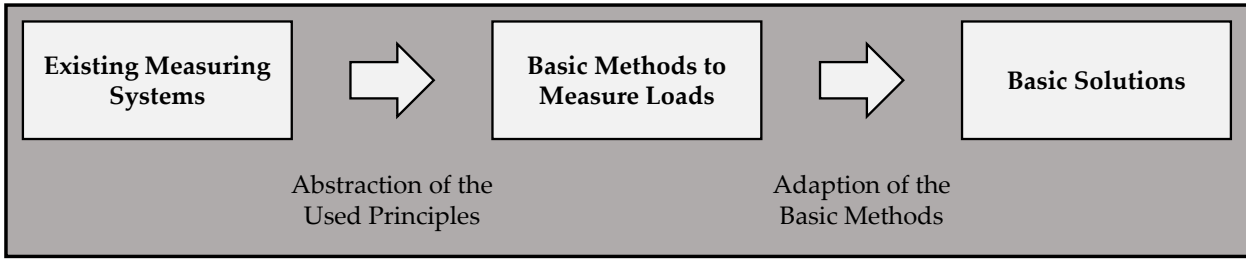
Figure 5-2: Process to find alternative solutions

5.3.1 Abstracted Methods to Measure Loads

An analysis of the measuring systems listed in chapter 2 revealed that spatial forces and torques can be measured by employing six force sensors. Three sensors are needed to measure spatial forces. However, six sensors are needed to detect spatial torques. For one torque two sensors are needed due to the reason that forces need to be measured at two points of the lever the torque is acting on. Nevertheless, only six sensors are needed to determine spatial torques and forces because sensors can be shared as it is depicted in Figure 5-3 a).

Sharing sensors for forces and torques requires a possibility to distinguish whether a force or torque is acting on the sensors. Figure 5-3 b) shows the effect of two forces and a torque acting on a lever equipped with two sensors measuring the reaction forces $F_{\text{sensor 1}}$ and $F_{\text{sensor 2}}$. The force F_b has the same effect on sensor one and two. However, the torque M causes a negative force on sensor one and a positive force on sensor two. Forces which are out of the centre of the lever like F_a have a combination of the effect explained before for force and torque. The sum of forces and torques acting on the centre of the lever can be determined by comparing the forces measured with sensor one and two. The average of the two sensors which is marked in green in Figure 5-3 b) is the sum of forces acting of the centre of the lever. The difference of the two sensors marked in red in Figure 5-3 b) is used to calculate the torque.
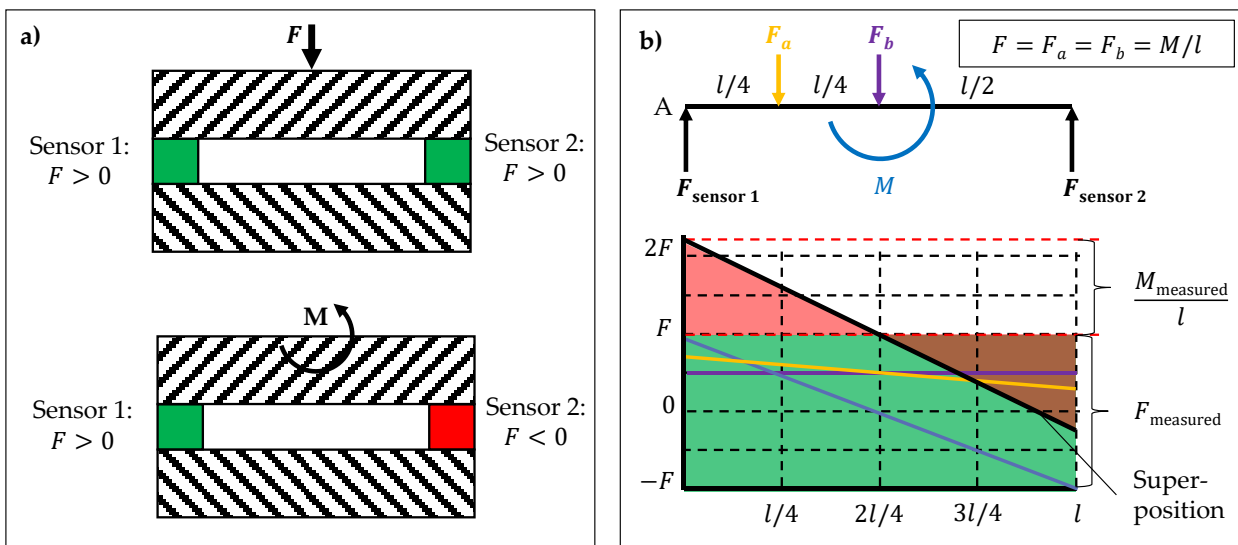
Figure 5-3: Separation of sensor signals caused by forces and torques: a) Setup with two sensors to measure force and torque, b) Illustration how forces and torques can be distinguished using two sensors

The determined torques and forces are referred to the centre of the lever which has the same distance to the sensors one and two. The resulting forces and torques can be transferred to any position by adding compensation torques which are required for the shifted forces.

One possibility to measure forces is to put a sensor into the flux of force. The sensor has to be aligned with the force. Another possibility is to measure the deformation of an element which already is in the flux of force. Torque is measured by determining the force at two points of a lever with a known length. In case there are no forces it would be possible to measure at one point of the lever only but then it is not possible to distinguish between forces and torques as explained before.

Analysing the different measuring systems listed in chapter 2 various sensors were found which are commonly used to measure loads. In Figure 5-4 transducers of force sensors, torque sensors and multi component dynamometers are listed. In the following the basic methods to measure the loads with the different sensors is explained. The methods are sorted by the sensor types which they utilise. At this point the focus is on how the transducers were deployed. Information on how they work can be found in chapter 2.1.2.
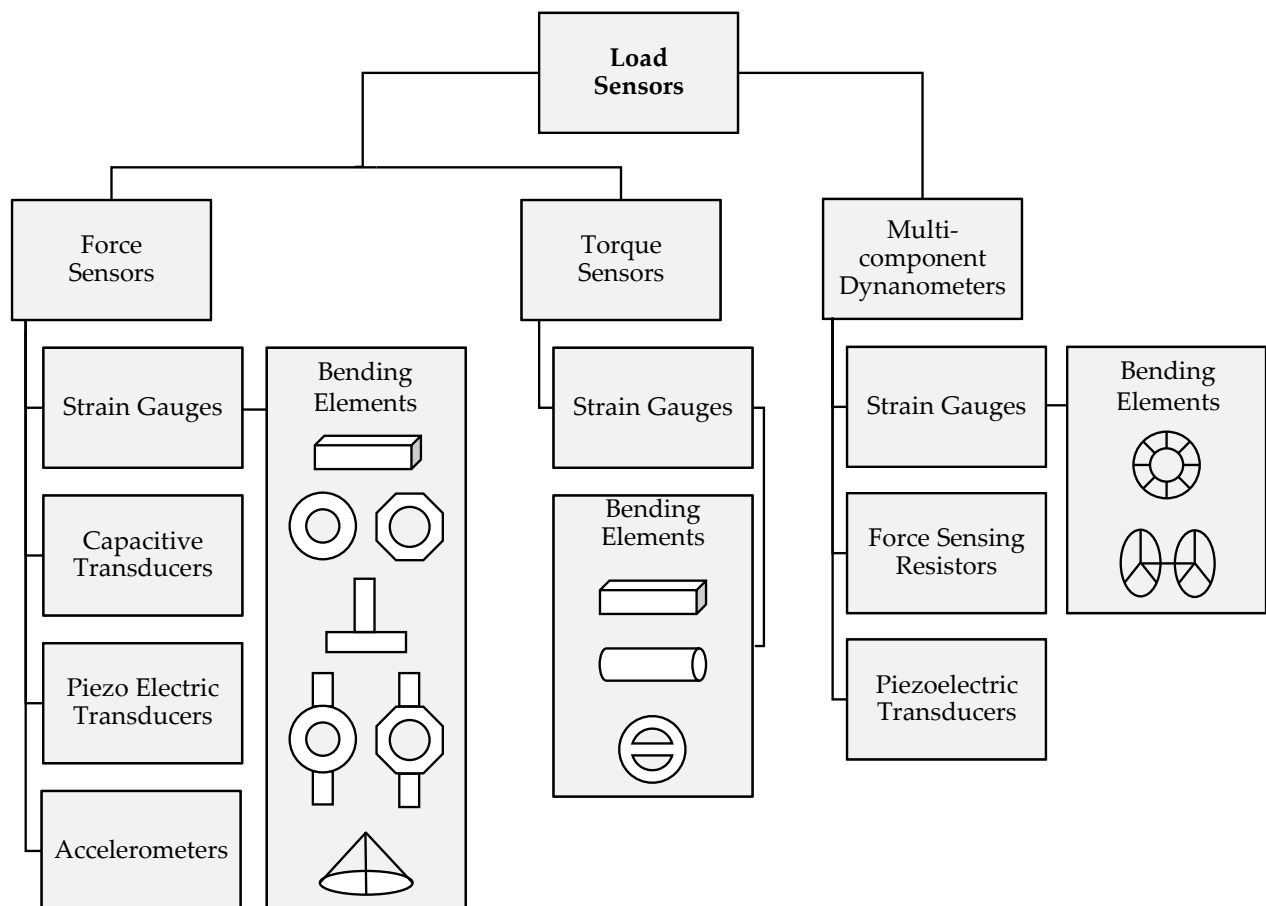
Figure 5-4: Load sensors utilised by the measuring systems found in the literature

Strain Gauges are used in combination with an elastic element to measure loads. The applied load causes a deflection of the elastic element which leads to a change in the resistance of the strain gauges placed on the elastic element. Due to previous calibration the according force value for a certain resistance change is known. Measuring setups can comprise different geometries as elastic elements like bending beams, tensile rods, torsion bars and combined elements. The following explanations of the principles are based of the related publications.

Bending beams are one possibility for an elastic element to measure forces with. Loading the beam with a force perpendicular to the longitudinal axis causes strain like it is depicted on the upper beam in Figure 5-5 a). The strain can be measured with strain gauges on the upper and lower side of the beam. Bending beams were used by Berli, Bönzli [33] and Caya et al. [34] in a scale and in a brake hood of a bike. Furthermore, bending beams were used in the beam load cell Pierce et al. [25] integrated in skis and in the force measuring binding the of the Neuromuscular Research Centre, University of Jyväskylä, Finland. Hoset et al. [27] used the beam of the roller ski as bending beam and Bellizzi et al. [28] did the same with the wheel holding brackets of the roller ski. In case forces which bend the beam in two directions additional strain gauges are needed at the front and back side of the beam. Multidimensional force components were determined utilizing bending beams with the measuring plates introduced by Komi [14], Vähäsöyprinki et al. [16] and Leppävuori et al. [17]. Their measuring plates comprised bending beams with strain gauges on different sides which determined the deflection of the beams in different direction caused by the forces applied by the athlete.

Bending beams can be used to measure torques as well. The lower beam in Figure 5-5 a) demonstrates how torques can be measured with one beam of known length. The resulting strain on the surface of the lever is measured with strain gauges to determine the torques. Huneycutt [46] measured the deflection on a single lever of a tech wrench. With multiple beams or multiple sensors on one beam, it is possible to distinguish between forces and torques. Figure 5-5 b) displays a multi lever setup which can be used when forces or torques apply at more than one point. The SRM power meter for bicycles measures the deflection of four levers [47]. Multidirectional torques might be measured utilizing bending beams. A two-dimensional lever is commonly used to determine spatial forces. A possible shape of the lever to measure spatial torques is the L-configuration shown in Figure 5-5 c). Which strain gauges are used to measure a specific torque direction is displayed with colours. The calculation of the spatial torques is simple due to the 90° orientation of the two parts of the lever.
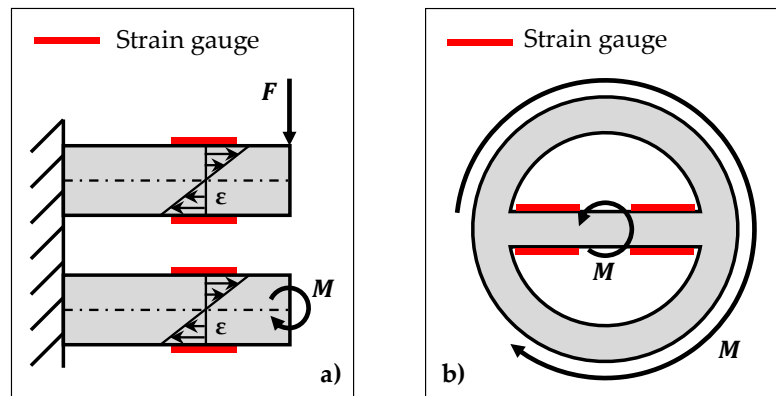
Figure 5-5: Bending beams as elastic elements with strain gauges: a) Bending beam with strain as a result of an applied force or torque, b) Setup with multiple bending beams

Tensile rods are used to measure forces which are parallel to the longitudinal axis of the rod. This causes strain like depicted on the lower beam in Figure 5-6 a). The strain is measured with strain gauges aligned with the longitudinal axis of the rod. Tensile rods can be used to measure multi-two force components in case the beams are in a special configuration as depicted in Figure 5-6 b). Spatial forces can be measured at the positions where the rods are connected. Entacher et al. [38] used bolts equipped with strain gauges to measure the forces action on the cutter of a tunnel boring machine. Strain gauge load cells were placed under the head of the bolts used to mount the cutter to the cutter saddle. Additionally, strain gauges were mounted inside the bolts.
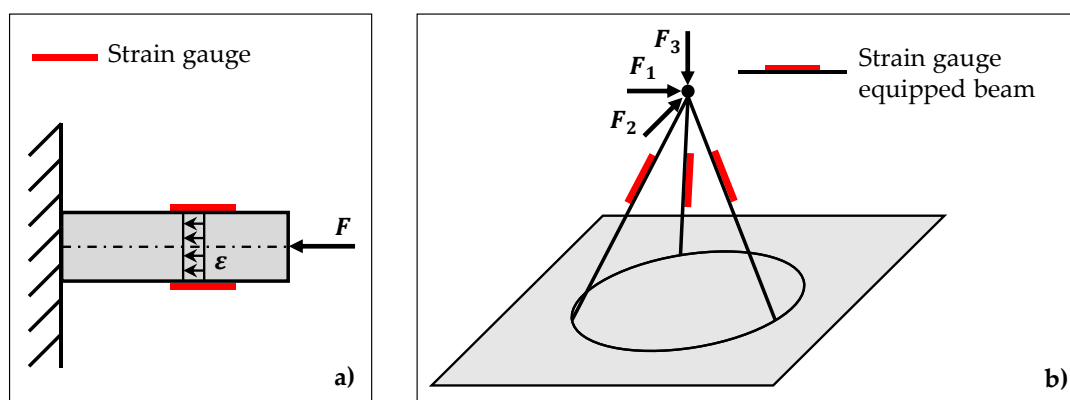
Figure 5-6: Multiple rod setup to measure spatial forces: a) Tensile rod with strain as a result of an applied force, b) Setup with three rods, adapted from [38]

Less strain occurs on the surface of a tensile rod than the on surface of a bending beam when the same force is applied. Therefore, it might be suitable to measure comparably small forces with a bending beam. However, one force component is necessarily aligned with a one-dimensional profile in case of spatial forces.

T-shaped profiles are a solution to measure spatial forces with bending beams. The profile is a combination a horizontal and a vertical bending beams. All of the three force components are registered by measuring the bending strain of the beam. Forces in the vertical direction are detected by measuring the bending strain of the horizontal beam of the T-shaped profile.

The two vertical force components are determined evaluating the bending strain of the vertical beam of the profile. The profile and the position of the sensors are depicted in Figure 5-7 a). Dai et al. [37] utilised T-shaped elastic elements to measure spatial gecko locomotion forces.

Octagonal rings are another suitable element to measure spatial forces. Each of the eight segments of the octagonal ring can be used as a sensor when it is equipped with strain gauges. At the section with the worst flexural rigidity the maximal strain occurs. Due to this reason the strain gauges are placed at these spots. In Figure 5-7 b) it is shown that octagonal rings have their maximum deformation for vertical forces at 90° and 270°. For horizontal forces the maximum is at 45° and 225°. If spatial forces occur at least two octagonal rings orientated perpendicularly to each other are needed. Octagonal rings were utilised by Parida et al. [35] for force detection during friction stir welding and lathing and Zhao et al. [36] to determine tool forces during turning.

It is possible to measure multidimensional forces with combined bending elements like depicted in Figure 5-7 c). Instead of the T-shaped bending element shown in Figure 5-7 a) a beam like in Figure 5-6 a) and a ring similar to the one in Figure 5-7 b) might be connected to measure spatial forces. The beam is used to measure bending forces and the ring to measure compression forces. Bourbonnais et al. [66] used such a combination of bending elements to measure forces which are applied by the hip of a patient.
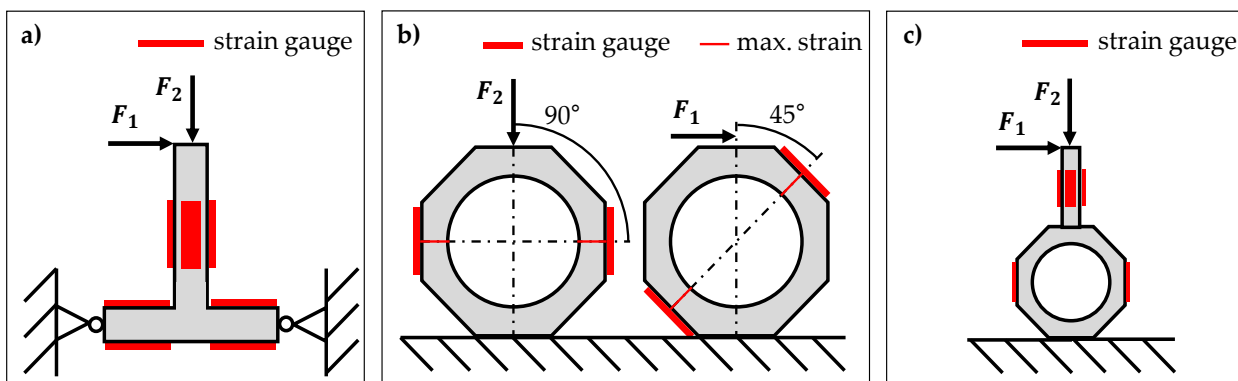
Figure 5-7: Possible bending elements and strain gauge locations: a) T-shaped profile, b) Octagonal ring, c) Combination of bending beam and octagonal ring

Torsion Rods can be used to determine one torque component aligned with the axis of the rod. The applied torque causes shear strain which can be measured with strain gauges on the surface of the rod. The strain gauges are levelled 45° to the axis of the cylinder like it is depicted in Figure 5-8. Yoxall, Rowson [48] measured the opening force subjects can apply on vacuum lug cans using this method. Zhu et al. [49] determined the start-stop torque of a valve by the same way.
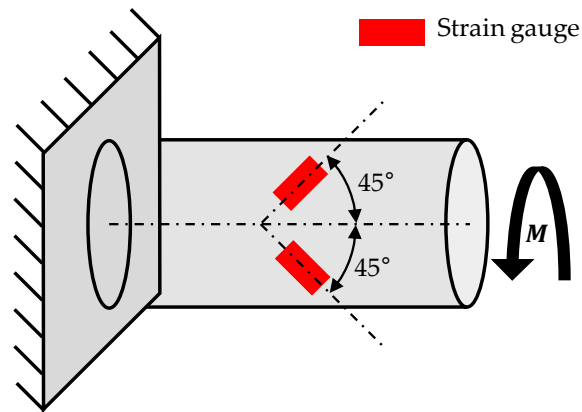
Figure 5-8: Setup to determine one torque component by measuring the 45° shear

Multi component dynamometers employ a combination of the previously explained elastic elements to measure torques and forces in different directions within one sensor. With a beam as elastic element it is possible to measure force components and torques which are perpendicular to the axis of the beam. As it is illustrated in Figure 5-2 b) sensing at two spots of a beam is necessary to enable division of the output signal into a force and a torque component. In order to measure the third force component, the beam needs to be regarded as tensile rod by measuring its elongation. The torque aligned with the axis of the beam can be measured with strain gauges which detect the shear strain of the beam. The setup of multi component dynamometers including the geometrical shape of the elastic elements and the position of the strain gauges is complex due to the variety of measured variables. The systems often are adapted for a specific measuring setup and usage in other fields is hardly possible. For a probing system of a coordinate measuring machine Liang et al. used two connected Y-type cross beams as elastic element. One of the Y-type cross beams was used to determine torque components and the other one to measure spatial forces [50]. Feng et al. connected two rings with eight beams. Measuring the deflection of the beams it was possible to determine spatial forces and torques [52].

Force Sensing Resistors are pressure sensitive transducers. Pressurising the transducer its resistance is decreasing. Similar to strain gauges the change in resistance can be used to determine the force acting on the sensor. Available sensors are not able to measure forces higher than 100 N accurately [13]. The transducers need to be set in the flux of force. It is possible determine one force component with a single sensor. That is what Hamid et al. [41] did integrating flexible force sensing resistors in the heel and thumb area of an ankle foot orthosis in order to control the movement of the orthosis. In Figure 5-9 it is depicted how to measure multidimensional torques and forces using several sensors. Comparing the output of sensor A and B with sensor C and D M_2 is determined. The output of Sensor A and D is compared with the output of sensor B and C to determine M_1. Foces are determined with the output signal of all four sensors. This set up was used by Friedrichs, Berger [26] to detect forces and torques between binding and ski during downhill skiing. They used customised force dependant resistors which are able to detect forces

higher than 100N. The methods to measure with force sensing resistors are based on the stated publications.
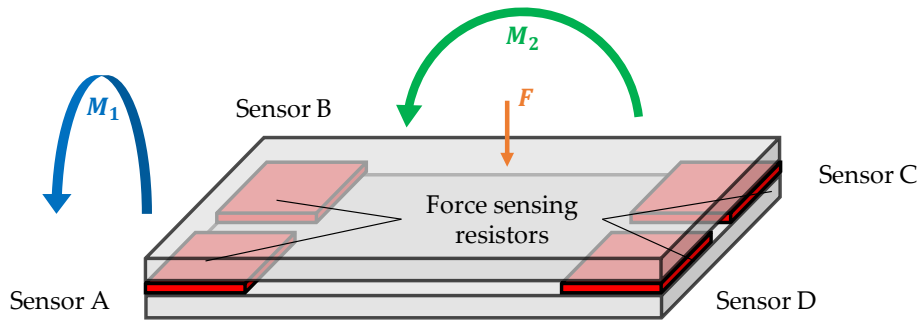
Figure 5-9: Measuring setup comprising force sensing resistors to measure two torque components and one force component

Capacitive Transducers change their capacitance when they are compressed by applying a load. In order to measure a force, the capacitor needs to be set into the flux of force. The pressure insoles used by Lindinger et al. [29], Göpfert et al. [30], Stöggl et al. [31], Stöggl et al. [32] to determine forces during skiing and roller skiing comprised numerous capacitive transducers. The methods to measure with capacitive transducers are based on the stated publications.

Piezo Electric Transducers generate charge proportional to the change of a force. The transducers are highly accurate for the measurement of dynamic loads. The transducers need to be set in the flux of force and need to be pre-stressed as depicted in Figure 5-10. A pre-stress plate is used to pretension the sensor which is needed for accurate measuring and to enable the measurement of negative forces. The pre-stress plate is pressed on the piezoelectric crystal with a pre-stress bolt. Due to the reason that the pre-stress plate and the piezo electric crystal are in series the same forces are acting on both of them. Degenstein, Winner [40] used piezoelectric transducers to detect forces during braking with a disk brake. The forces between friction element and the disk of a disk brake needed to be determined. The piezoelectric transducer was mounted on the backside of the friction material.

Multidimensional forces can be measured with piezoelectric transducers as well. For each force component one transducer needs to be set in the flux of force. Concerning the setup of multiple sensors, it needs to be take care that there is no cross talk between the single pre-stressed sensors. Street, Frederick [18] placed piezoelectric sensors between roller ski and binding to measure forces during roller skiing. They used two vertical transducers to measure vertical forces and two horizontal transducers to determine forces perpendicular to the skiing direction.

Piezoelectric transducers can be used for multi component dynanometer applications as well. The setup of the sensors might be similar to the one of force sensing resistors depicted in Figure 5-9. In order to enable the detection of spatial forces and torques additional transducers would be needed on the sides of the setup. Especially for the setup of multicomponent dynamometers it is

important to take care that there is no crosstalk between the sensors. The multi component dyna-mometer from Kistler [53] comprises multiple sensors in all three planes which enables the measurement of spatial tool forces and torques during chipping. The methods to measure with piezoelectric transducers is based on the stated publications if not marked differently.
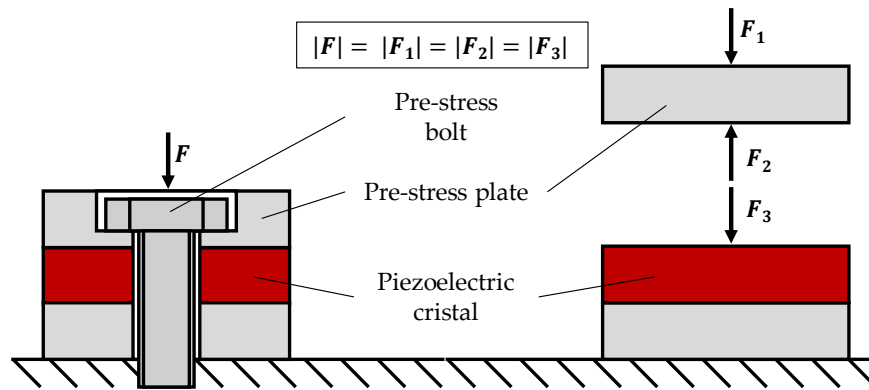
Figure 5-10: Set up to pre-stress piezo electric cristal transducers

Accelerometers are used to determine loads by measuring the acceleration the load causes on a body. As it is displayed in Figure 5-11 a stiff connection between the centre of gravity and the accelerometer is needed in order to measure the full amount of the load. If contact forces need to be measured the offset and the orientation of the contact point to the accelerometer needs to be known. Wei et al. [42] mounted accelerometers on a wheel set of a train to determine rail forces and Braghin et al. [43] used three-axial accelerometers in the wheel of a car to measure ground contact forces.
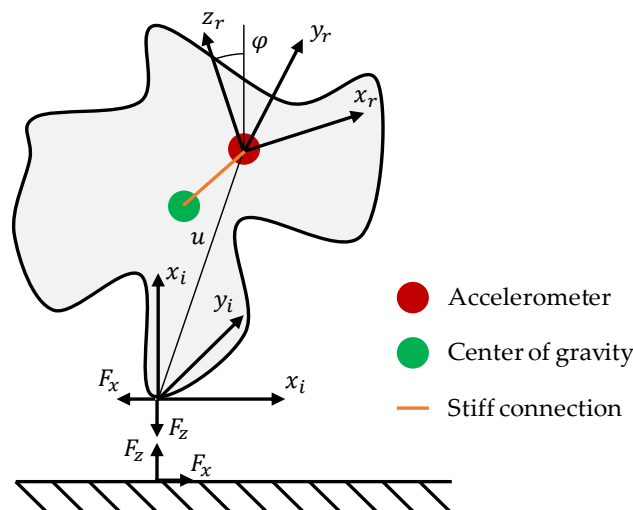
Figure 5-11: Setup to measure contact forces with an accelerometer

5.3.2 Basic Solutions to Measure Loads

The basic methods to measure loads which are listed in chapter 5.3.1 were adapted for the demanded measuring system in order to generate suitable solutions. Firstly, it was determined

which sensors generally could be used for the required measuring system. Subsequently, possible solutions were drafted for the remaining sensors and the feasibility of the solutions was checked.

The Sensors which were used for nordic measuring system and for measuring systems from other fields were reviewed whether they can be used for the demanded measuring system. Detailed information on the different sensor types is provided in chapter 2.1.2.

Force sensing resistors cannot be utilised as the maximum of their measuring range is 100 N [13]. There will be forces which are a lot higher. Andersson et al. [67] found out there are vertical forces up to $F_z = 1748N$ during diagonal stride in classic skiing.

Capacitive transducers are recommended not to be used for dirty conditions. Capacitive transducers are recommended to be used only in a clean surrounding due to their sensitivity to unwanted particles between the plates of the capacitor [12]. The measuring system should be used outside on dusty roads and gravel roads which disables the use of capacitive transducers. Furthermore, the elastic element between the plates might cause malleable properties setting the capacitor into the flux of force.

Piezoelectric transducers are suitable to measure dynamic loads with high accuracy. They cannot be used to measure absolute loads which have an unknown static load share. Charge leakage in the circuitry of the amplifier causes measuring errors for static forces [12]. A piezoelectric transducer generates about 10 pC/N [68] and the required charging amplifier has a charge leakage of about 0.05 pC/s [69]. Practically this would mean that measured weight of the athlete standing on the roller ski would decrease 1 N within 20 seconds. The drift of the static share of the load during a measuring session would disable the detection of the absolute peak loads even if the system is really accurate for the dynamic load share. In consultation with the company Kistler which is an expert for piezoelectric transducers it was advised better to use strain gauges for this measuring system. Consequently, the piezoelectric transducers are not a suitable choice for the desired measuring system.

Accelerometers could hardly be used for the measuring system. There are two possibilities where to put the sensors, on the roller skis or the athlete. There are situations during which loads are acting on the roller ski but there is no acceleration. For instance, during diagonal stride the ski at the pushing leg does not move but the propulsion is generated by pushing on this ski. Therefore, it is not possible to measure the loads with accelerometers on the roller ski. The sensors need to be placed on the body of the athlete as depicted in Figure 5-12. In order to enable the calculation of the forces acting between athlete and roller ski it is necessary to know the offset and orientation of the accelerometer to the roller ski. Furthermore, there needs to be a stiff connection between the centre of gravity of the athlete and the accelerometer or at least the offset and orientation needs to be known. As the athlete is moving the arms and legs continuously it is hardly possible to calculate the centre of gravity.
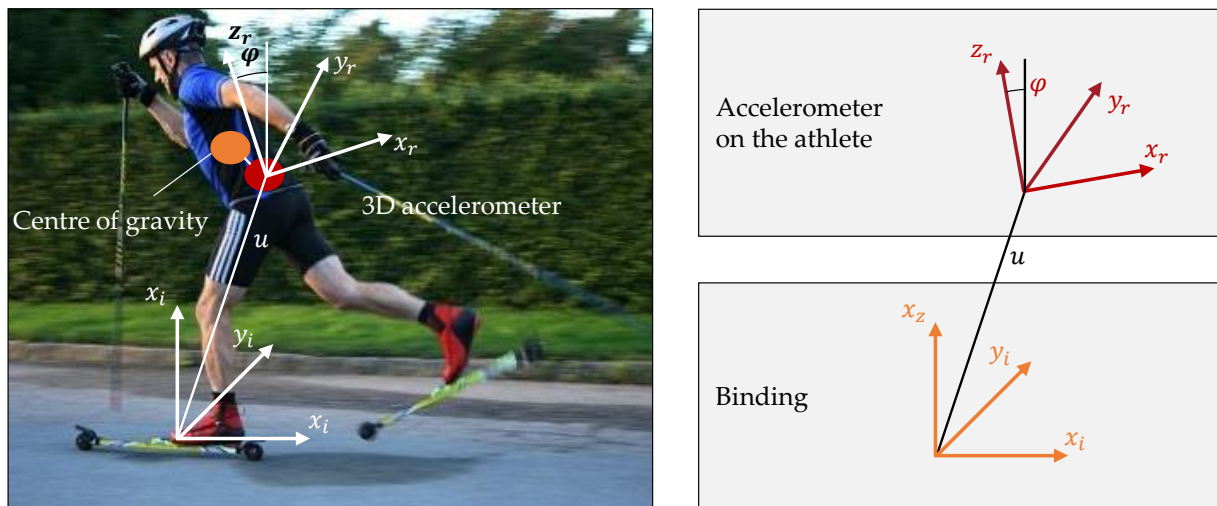
Figure 5-12: Basic solution comprising an accelerometer on the body of the athletes and offset and rotation of the accelerometer coordinate system to the one of the roller ski

The remaining sensors which can be used for the roller ski measuring system are strain gauges. They are the most commonly used sensors as they are available in a high variety and accessible. Depending on the elastic element which the load cell comprises there is a measuring range from 5 N up to 50 MN with a typical uncertainty from 0.02 % to 1 % [5]. Therefore, strain gauges are the sensors of choice for the measuring system. Four concepts comprising strain gauges were drafted and are explained hereinafter.

Screws With Strain Gauge Load Washers underneath were used by Entacher et al. [38] to measure spatial forces on a tunnel drilling machine. For the measuring system on the roller ski screws with load washers underneath could be used similarly. As depicted in Figure 5-13 the binding is mounted on a plate which is connected to the roller ski with seven screws equipped with strain gauge load washers. The positions of the equipped screws are marked with the numbers 1 to 7. Forces in x-direction are detected with the sensor at position 7 and forces in y-direction with the sensors at position 1 and 2. However, forces in z-direction are detected with the sensors on position 3, 4, 5 and 6. Torque in x-direction are determined comparing sensor 3 and 4 or sensor 5 and 6. For the detection of the torque in y-direction sensor 3 and 5 or sensor 4 and 6 are compared. Sensors 1 and 2 are compared to determine the torque in z-direction.
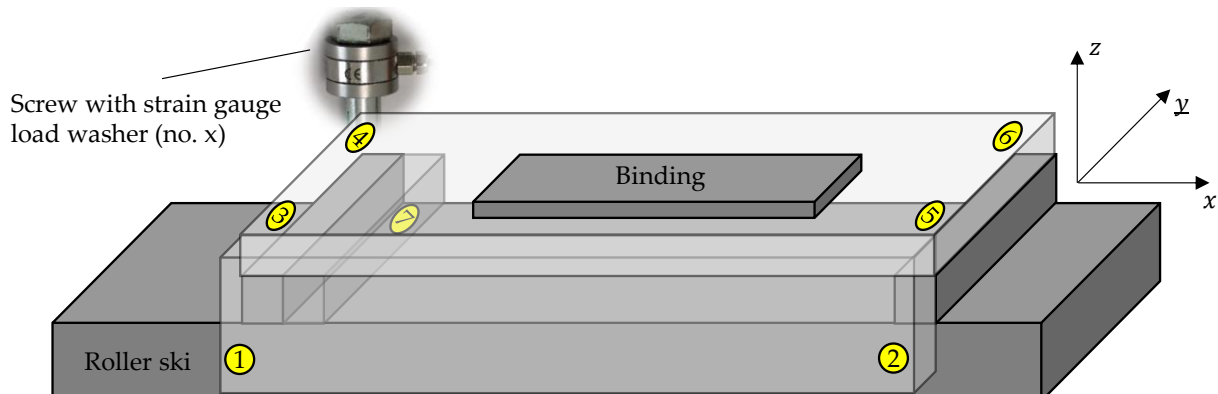
Figure 5-13: Basic solution with strain gauge load washers under pre-tensioned screws, with use of [38]

In order to enable the detection of forces and torques in both directions the screws need to be pre-stressed. Pre-stressing the sensors reduces the sensitivity of the other sensors. For instance, the force acting on the sensors 1 and 2 in y-direction is reduced because of the pre-stressing of sensor 3, 4, 5 and 6. Due to this reason this concept cannot be implemented.

T-Shaped Bending Elements on which the strain gauges are mounted were used by Dai et al. [37] to measure gecko locomotion forces. Connecting the binding and the roller ski with T-shaped bending elements as depicted in Figure 5-14 makes it possible to measure the required loads. The plate on which the binding is mounted is connected to the roller solely by the T-shaped elements. Forces in x-direction are measured with the strain gauge 4 which detects the bending of the vertical beam around the y-axis. The forces in y-direction are measured by the strain gauge 3 which determines the bending of the vertical beam around the x-axis. As a force causes higher strain at the surface of an element when bending it instead of stretching it the vertical forces in z-direction are measured at the horizontal beam with the strain gauges 1 and 2. In order to determine the torque in x-direction the strain gauges 1 and 2 are used as well. In contrast to the force in z-direction the torque in x-direction causes negative strain on the strain gauge 1 and positive strain on strain gauge 2. Those two loads can be distinguished by this. Torque in the y-direction is determined by comparing the forces in z-direction at the T-shaped elements A and B. The torque in z-direction determined comparing the forces in y-direction at the T-shaped elements A and B.

The force in y-direction and the torque in x-direction have the same effect on strain gauge 1 and 2. Therefore, it is not possible to use T-shaped bending elements to determine spatial forces and torques. This system can only be used if there either is a force in y-direction or a torque in x-direction.
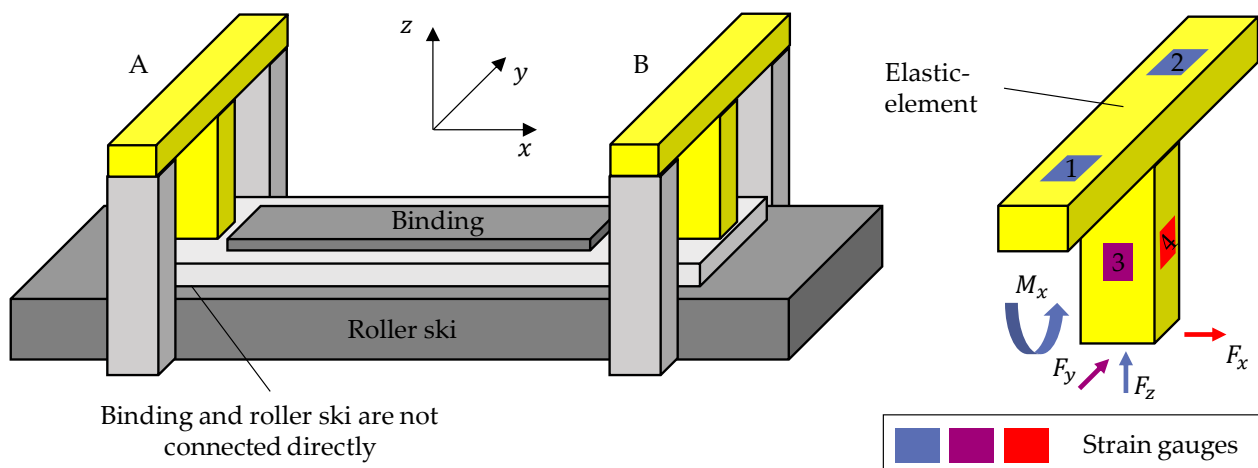
Figure 5-14: Basic solution with T-shaped bending elements and strain gauges connecting the roller ski and the binding

Octagonal Rings could be used as elastic elements on which the strain gauges are mounted like Parida et al. [35] did. The octagonal rings are placed between the beam of the roller ski and a plate on which the binding is mounted on. As depicted in Figure 5-15 there are two octagonal rings in

each corner perpendicular to each other. Having three corners equipped with sensors would be sufficient to determine spatial forces and torques but for the stability of the structure the fourth corner needs to be suspended as well. On each octagonal ring there is a pair of strain gauges in 45° orientation and another pair oriented 90° to the vertical axis. Horizontal forces in x-direction are measured by the 45° oriented strain gauges of octagonal rings 2, 3, 6 and 7. Whereas forces in y-direction are detected with the strain gauges in 45° orientation on position 1, 4, 5 and 8. Vertical forces in z-direction are detected by the strain gauges in 90° orientation on all octagonal rings. Torque in x-direction is determined comparing the vertical forces on the octagonal rings 1 and 8, 2 and 7, 3 and 6 or 4 and 5. In y-direction the torque is detected comparing the vertical forces measured on the positions 1 and 4, 2 and 3, 5 and 8 or 6 and 7. However, the torque in z-direction is determined by comparing the horizontal forces of the position 1 and 5, 2 and 6, 3 and 7 or 4 and 8. As there are several possibilities to determine the forces and torques from the strain gauges the number of strain gauges at the octagonal rings can be reduced for the implementation of the measuring system.

The strain gauges need to fit on the sides of the octagonal rings. Therefore, a minimum side length is required. Furthermore, an additional plate is needed between the octagonal rings and the binding. In order to grant the safety of the athlete it has to be taken care that the system is rigid enough. This leads to an offset between the binding and the beam of the roller ski which causes additional torque during skiing. Moreover, there might be interferences because the plate on which the binding is mounted and the beam of the roller ski are both bending. Differences in the bending behaviour of the beam and the binding could lead to tension in the octagonal rings which might be misinterpreted as force or torque during the measurement.
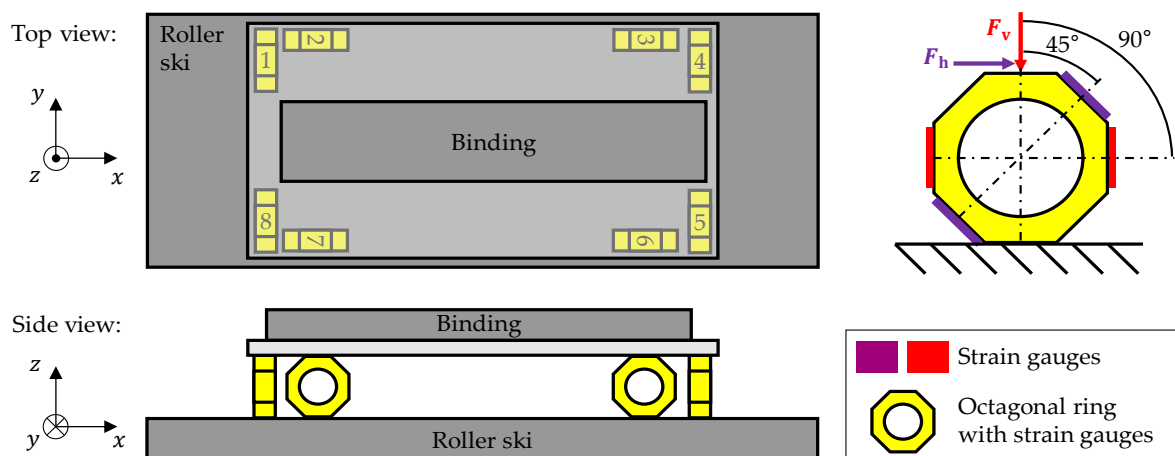
Figure 5-15: Basic solution with strain gauges on octagonal rings between the binding and the roller ski

The Beam of the Roller Ski can be used as the elastic element where the strain gauges are mounted on. Hoset et al. [27] were able to measure forces which are acting vertically on the roller ski with this setup. Nevertheless, Feng et al. [52] showed with their device to measure wheel forces of a car that is feasible to measure load in multiple directions by mounting several strain

gauges on the bending element. Furthermore, they showed that is possible to distinguish between the forces and torques which cause the bending of the elastic element. The principle of the device developed by Yoxall and Rowson [48] to measure the opening force of vacuum lug cans can be used for the determination of the torque which is twisting the beam of the roller ski.

In order to measure spatial forces and torques the strain needs to be measured at the eight positions which are marked in Figure 5-16. Due to the multiaxial stress state in the beam of the roller ski strain gauge rosettes need to be used to determine the strain at the different positions. The strain at the eight positions is compared in order to determine the proportion of the different forces and torques. Force in positive x-direction causes negative strain at positions 1, 2, 3 and 4 and negative strain at the positions 5, 6, 7 and 8. Torque in x-direction is determined by analysing the shear strain at the positions 2, 4, 6 and 8 measured by the rosettes. Forces in positive y-direction are measured by comparing the difference of the strain at the positions 2 and 4 with the difference at 2 and 4. As depicted in Figure 5-16 there is positive strain at position 4 and 8 and negative strain at position 2 and 6. The same is done for the force in z-direction by comparing the difference of position 1 and 3 with the difference at position 5 and 7. In contrast to the forces the torques in y- and z-direction cause different strain in front of the binding and behind it. As shown in Figure 5-16 for torque in positive y-direction there is negative strain at position 1, positive strain at position 3, positive strain at position 5 and negative strain at position 7. The torque in z-direction is determined by comparing the strain at position 2, 4, 6 and 8. The torques and forces which are measured are referred to the neutral layers of the elastic element and the middle between the sensors in the front of and behind the binding. Nevertheless, the determined loads can be transferred to any position by adding additional torques for forces which are relocated perpendicular to their acting direction.
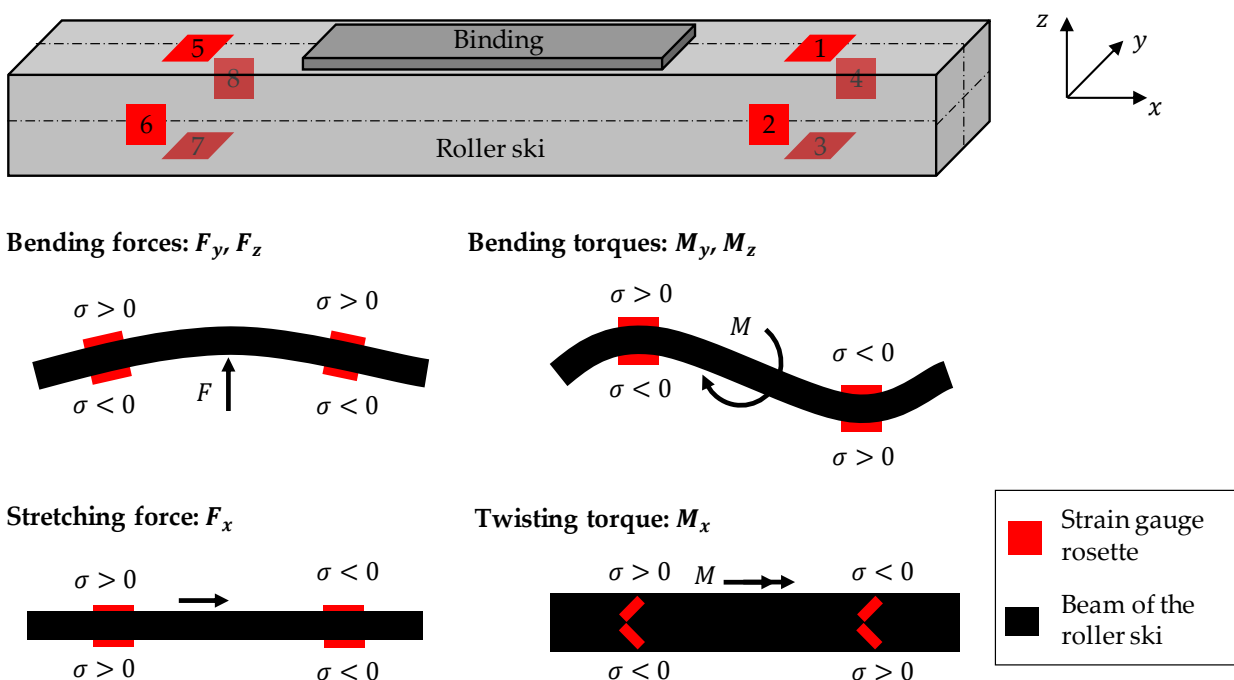
Figure 5-16: Strain gauge rosette positions and principles to detect the loads

Fabian Tobias Mayer B.Sc.

5.3.3 Basic Solutions for the Data Acquisition

The change of resistance of the strain gauges has to be determined and the values need to be stored until they can be processed by a computer in order to determine the loads. Suitable data acquisition instruments are needed for this purpose. The difference of the resistance of the strain gauges is determined with use of Wheatstone bridges. With signal conditioners the voltage output measured at the bridges is optimised for the subsequent analogue to digital conversion. The A/D-converter needs to have a sufficient resolution and a high sampling rate to measure the maximum loads. For the detection of the loads caused by the athlete a sampling frequency of 42 Hz to 70 Hz is required. However, for the detection loads caused by external circumstances like potholes a sampling frequency of 1 110 Hz to 1 850 Hz is needed. Furthermore, the data acquisition system needs to be portable in order to enable testing on the road.

The signal conditioning unit and the data acquisition module can be carried in a drinking belt or a rucksack. As the strain gauges are situated on the roller ski the measuring signal needs to be transferred through a connection cable as depicted in Figure 5-2.
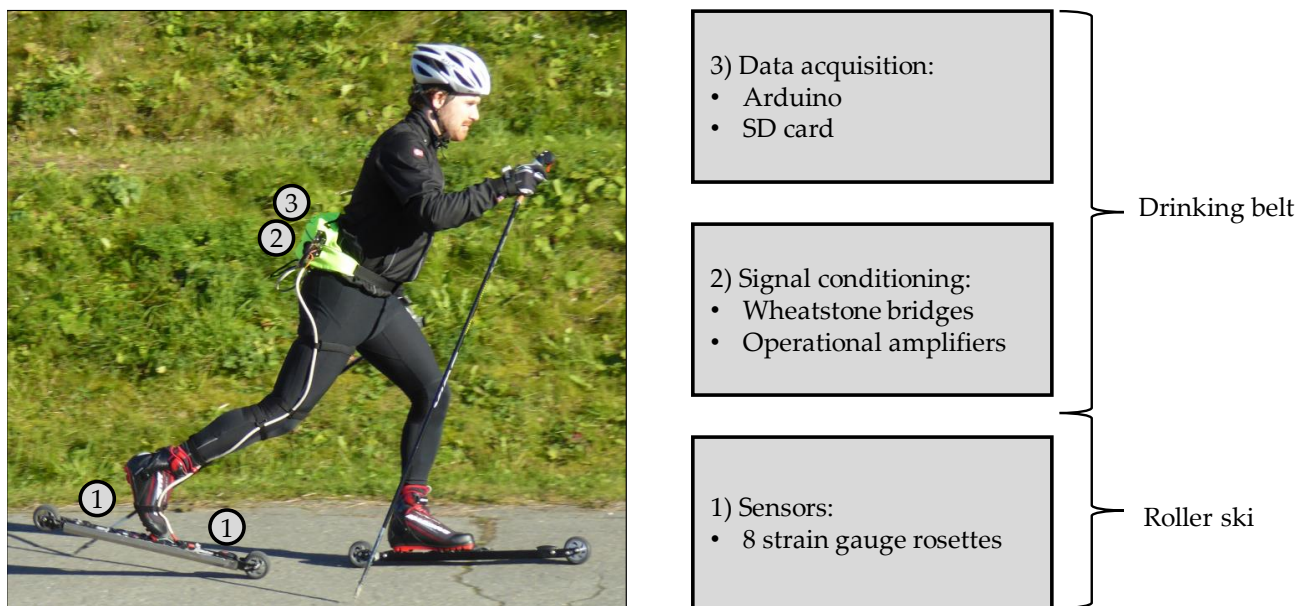
Figure 5-17: Position of the signal conditioning and data acquisition unit

The data acquisition systems from the HBM and National Instruments introduced in chapter 2.4 is capable of the mentioned requirements. Using the instruments from HBM the QuantumX CX22B-W would be needed. For the signal conditioning of 24 strain gauges two QuantumX MX1615B and are needed as well. Together the tools would cost 17 800 € (165 000 NOK) which exceeds the budget of this project by far [54][55]. Therefore, the solution from HBM could not be chosen.

For a solution with equipment from National Instruments a cRIO-9024 and three NI 9235 would be needed for 24 strain gauges. The required equipment from National Instruments would cost 9 400 € (87 420 NOK) [56] [57]. This is too expensive for this project as well.

Trying to keep the costs for the data acquisition as low as possible and having a suitable system on the same time a data acquisition system comprising an Arduino Zero and a self-manufactured circuitry was developed. The Wheatstone bridge circuits are used to determine the resistance of the strain gauges. Subsequently the output voltage of the Wheatstone bridges is amplified by instrumentation amplifier. An instrumentation amplifier comprises two operational amplifiers which rise the output signal of the two sides of the bridge [70]. A third operational amplifier is included which compares the output signal of the two other operational amplifiers. The output of the instrumentation amplifier is read by an analogue input pin of the Arduino Zero microcontroller. The microcontroller has six analogue inputs with a resolution of 12 bit. There is one A/D-converter with a sampling rate of 350 000 Hz which is used by all of the six input pins [71]. The measured voltage values are stored on a SD card. When the measurements are done the data is transferred to a computer. On the computer the data is processed using a Matlab script to determine the detected loads. One Arduino Zero only costs 43 € (400 NOK). Additionally, there are costs for the components which are needed for the amplification of the measuring signal but this should be in the range of the budget of the project.

5.4   Selection of Solutions

In the previous stage solutions for the setup of the sensors and for the data acquisition were determined. The three solutions for the data acquisition comprise either equipment from HBM or National Instruments or an Arduino Zero micro controller. As the costs for the solutions with the equipment from HBM or National Instruments exceed the budget of this project the solution of the self-built data acquisition with the Arduino Zero micro controller was chosen.

For the solution it was discerned that strain gauges are the right transducers for the needed measuring system. There were four basic solutions of which two can be implemented. One solution consists of octagonal rings equipped with strain gauges which are placed between the beam of the roller ski and a plate on which the binding is mounted on. The other solution employs the beam of the roller ski as elastic element on which the strain gauges are mounted. In order to select the best of those two solutions a systematic approach was chosen. Firstly, selection criteria were established and were weighted with a binary comparison. Secondly, the technically value of the two solutions was determined with use of the method introduced in the standard VDI 2225 *Engineering design at optimum cost* [65].

5.4.1   Selection Criteria for the Solutions

It has to be determined which are the crucial properties of the demanded measuring system in order to select the best solution. Those properties were used as selection criteria. Using the requirement list and considering the available time and resources the following selection criteria were chosen:

- Criterion 1:   The measuring system may not break and endanger the athlete
- Criterion 2:   The distance between the binding and the ground is not changed
- Criterion 3:   The weight of the roller ski is not increased
- Criterion 4:   The measuring system is easy to be built
- Criterion 5:   The loads can be derived easily from the measured values
- Criterion 6:   The measuring system is able to detect the loads accurately

As some of the properties are more important than others they need to be weighted. This was done with a binary comparison of the properties depicted in Table 5-2. For the binary comparison the properties are set in the first column and first row of a table. The property in a column is compared with the properties in the rows [61]. The cells are marked with a *1* if the property of the column is more important than the one of the row and cells are marked with a *0* if it is vice versa [61]. The sum of the values in column are the weight of the property in the column [61].

The result of the binary comparison in Table 5-2 is that *Criterion 1* is the most important and *Criterion 5* is of minor importance. This is reasonable as it is much more important to take care for the safety of the athlete than to simplify the calculations of the load.

Binary Comparison						
Colum criteria compared with row criteria	Criterion 1	Criterion 2	Criterion 3	Criterion 4	Criterion 5	Criterion 6
Criterion 1	-	0	0	0	0	0
Criterion 2	1	-	0	0	0	0
Criterion 3	1	1	-	0	0	1
Criterion 4	1	1	1	-	0	1
Criterion 5	1	1	1	1	-	1
Criterion 6	1	1	0	0	0	-
Weight of the criterion	**5**	**4**	**2**	**1**	**0**	**3**

Table 5-2: Binary comparison of the selection criteria

5.4.2   Technical Value of the Solutions

In order to select the best of the two solutions comprising octagonal rings and strain gauges on the beam of the roller ski their technical value was determined. The approach introduced in the standard VDI 2225 *Engineering design at optimum cost* [65] was used to determine the technical value of the solutions.

The solutions were ranked regarding the properties which were chosen in chapter 5.4.1. For each of the properties the solution was ranked compared with a fictional optimal solution. In case the solution fulfils a property very well and it is equal to the performance of a perfect solution the solution is ranked with *4*. If the solution fulfils a property well there is a *3*, for sufficient fulfilment there is a *2* and if the solution hardly fulfils a requirement there is a *1*. In case the solution performs unrewarding for a property there is a *0*. The technical value X of a solution is determined with equation (5-2). For the n-th selection criterion g_n is the weighting and P_n the performance of the solution. The best ranking which is possible for a solution for a selection criterion is $P_{max} = 5$.

$$X = \frac{g_1 P_1 + g_2 P_2 + \cdots + g_n P_n}{(g_1 + g_2 + \cdots + g_n) P_{max}} \tag{5-2}$$

The result of the technical value analysis of the two solutions is depicted in Table 5-3. The solution with the strain gauges directly on the roller ski has a technical value of 0.92 which is significantly higher than the technical value 0.38 of the solution comprising octagonal rings. Due to this reason the solution with strain gauges on the beam of the roller ski was chosen for the implementation of the measuring system. The chosen solution is only 8 % short of the perfect solution which is a really good result as the perfect solution does not exist.

Technical Value			
Selection criteria	Weight of the selection criteria g	Ranking of the solutions P	
		Octagonal Rings	Beam of the roller ski
The measuring system could not break and endanger the athlete	5	2	4
The distance between the binding and the ground is not changed	4	0	4
The weight of the roller ski is not increased	2	1	3
The measuring system is easy to be built	1	2	4
The loads can be derived easily from the measured values	0	3	2
The measuring system is able to detect the loads accurately	3	3	3
Technical value [-]		0.38	0.92

Table 5-3: Determination of the technical value of the solutions

5.5   Analyse the Consequences

The chances and risks of the chosen solution were analysed in order to be aware of them in the subsequent implementation of the measuring system. Critical aspects were revealed and schemes were set up to minimise the risks and to enable a successful implementation of the measuring system.

Mounting the strain gauges on the beam of the roller ski has the advantage that no elastic elements need to be added and it is a direct measurement on the real system. As the roller ski – binding system is not modified measuring under realistic conditions is possible. The distance between ground and the binding is not changed, consequently the leverage ratio is unchanged. But most important the athlete is not endangered as the structure of the roller ski is not changed. The influence of the added weight of the strain gauges is negligible compared to the weight of the roller ski. The strain gauge rosettes mounted underneath the roller ski could be damaged by hitting curb stones or bumpers. Therefore, those two strain gauge rosettes need to be protected with a cover. The protection of the strain gauges needs to be lightweight and should change the weight of the roller ski as little as possible. In order to record accurate measurement data using the strain gauges they need to be mounted correctly. The advised mounting procedures of the strain gauge suppliers need to be followed.

The signal conditioning unit with the Wheatstone bridges and the instrumentation amplifiers as well as the Arduino microprocessors for the data acquisition can be carried in a drinking belt or a rucksack. For this reason, they do not add any additional weight to the roller ski. It is no problem to connect the strain gauges via a connection cable of two meters. In case of constant temperature, the cable adds a constant resistance additionally to the resistance of the strain gauges. Therefore, the measured change in resistance of the strain gauges in the bridge configuration is still the same. Adding only the weight of the strain gauges and their protection to the roller ski makes sure that technique of the athlete is not influenced. Wearing a drinking belt or rucksack during roller skiing does not cause any problems as there are various cross-country skiing races like the Birkebeinerrennet during which the athletes need to carry rucksacks with up to 4 kg.

Building a data acquisition system instead of buying a commercially available one is cheaper but increases the risk of design and therefore measuring errors. The components of the data acquisition system and the whole system need to be properly tested for possible measuring errors. The advantage of the modular setup of the measuring system is that the components like the signal conditioners and the data acquisition can be exchanged easily in case a larger budget is available in later projects

The schemes which need to be taken into account during the implementation of the measuring system are:

- The rules of the supplier how to mount the strain gauges need to be followed.

- The strain gauges underneath the roller ski need to be protected with a cover.

- The cover should change the weight of the roller ski and its centre of gravity as less as possible

- The components of the data acquisition system and the whole system need to be properly tested for possible measuring errors

5.6 Deciding and Implementing

Deciding and Implementing means to develop and to build the final measuring system from the basic solution ideas. In the subsequent sections more detail is given how the solution for the measuring system was implemented Then the measuring chain of the system and the function of the subsystems is introduced. Finally, information on the calibration procedure is given.

The Implementation Strategy to realise the measuring system was a set-based approach. Therefore, the measuring system was divided in subsystems which were developed separately. Furthermore, the knowledge and the schemes to prevent failure from the *Analyse the Consequences* stage described in chapter 5.5 were used for the design. The components of the measuring system were properly tested in order to avoid measuring errors. Moreover, the rules of the strain gauge supplier HBM were followed to mount the strain gauges. Provisions were taken to protect the strain gauges at the roller ski from water and dust. Additionally, the strain gauges underneath the roller ski were protected with a cover to prevent abrasion. Moreover, it was taken care to add as less weight as possible to the roller ski and to change the centre of gravity of the roller ski as less as possible.

The purchase of the components needed was done early during the project to avoid delays. This was crucial as not all of the components needed were available in Norway causing to longer delivery times. Parcels from EU countries needed up to three weeks after ordering. The necessary components and their specifications were therefore investigated as early as possible in order to enable the early order strategy. This made it possible to avoid unoccupied time during the implementation of the solutions.

The production of the measuring system was time consuming. Besides the design of the units needed they had to be assembled manually. Mounting the strain gauges, their protection and the connection cables required a lot of time. Most time consuming was the assembly of the circuitries. Soldering and testing took several weeks.

The Overall Setup of the Measuring System consists of the *sensor* unit, the *signal conditioning* unit the *data acquisition* unit, the *power supply* and the *data processing* programme. The setup of the hardware is depicted in Figure 5-18. The signal from the strain gauges is transferred via a cable to the signal conditioning unit. There the change of resistance of the strain gauges is transduced

to a change of voltage using 24 Wheatstone bridges. The output of all 24 Wheatstone bridges is multiplexed to one set of instrumentation amplifiers. The voltage is raised to a level which the A/D-converter of the Arduino can handle. In order to use the full input voltage range of the Arduino the zero output of the instrumentation amplifier is adjusted to the middle of the measuring range by adding an offset voltage to the instrumentation amplifier with the Arduino. The measuring signal is digitalised by the Arduino and stored to the SD card. In addition to the measured data the amplification state of the instrumentation amplifier is stored on the SD card. The whole system is powered by a customised battery with a +6.4 V, 0 V and -6.4 V output and diodes. Schottky diodes are used to reduce the voltage to 3.3 V for the Wheatstone bridges and the Arduino. Similarly, the voltage is reduced to ±5 V for the multiplexers. The instrumentation amplifiers are directly run on the ±6.4 V.

The schematics of the electronic circuitry, the technical drawings of the housing of the measuring system and the Matlab- and Arduino-code can be found in the appendix.
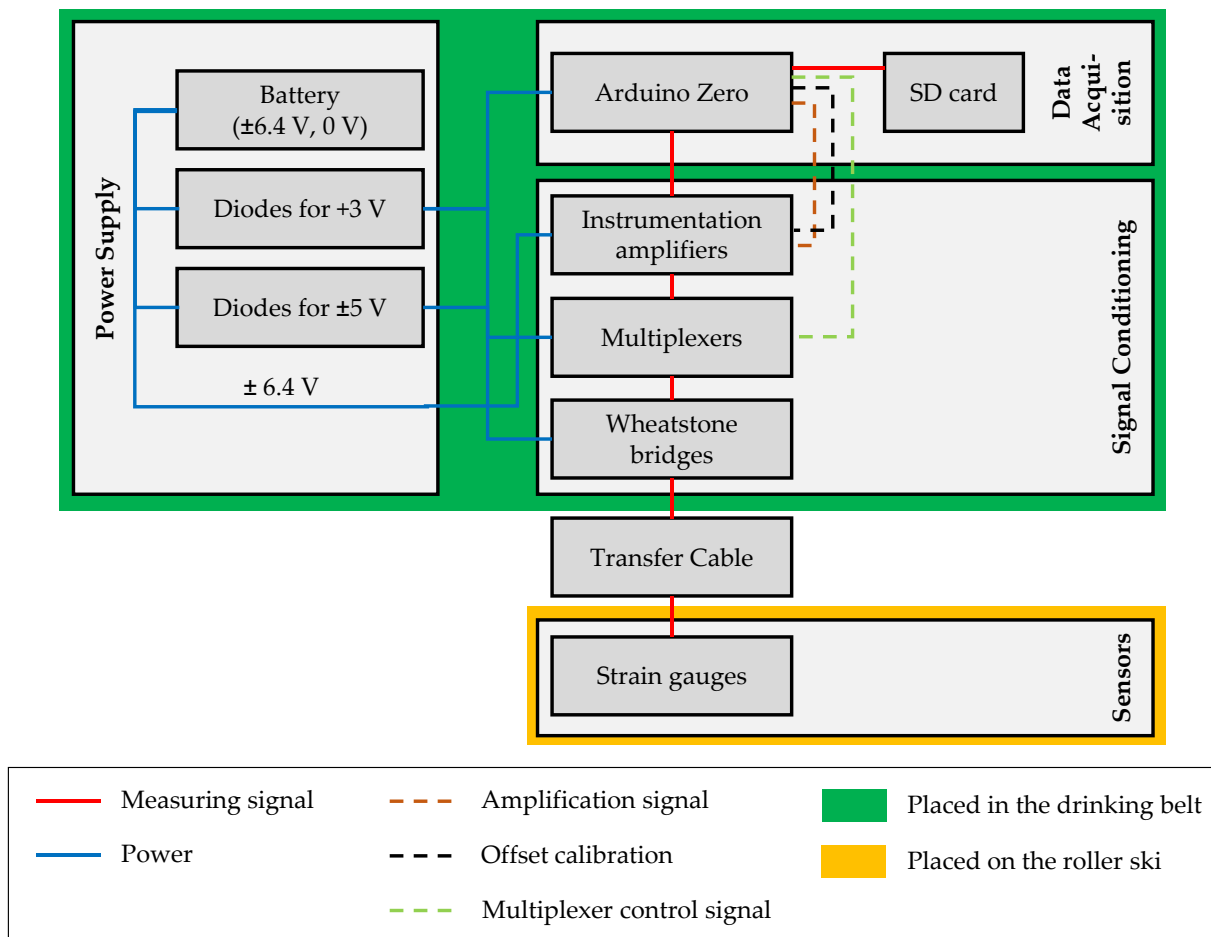
Figure 5-18: Comprehensive setup of the measuring system

5.6.1 Set-based Approach

For the implementation of the chosen principal solutions a set-based approach was used. This kind of development approach was already utilised by the Wright brothers to design the first airplane. The main purpose of the design strategy is to eliminate rework in later stages of the project. This is achieved by investigating possible solutions before deciding which one to use. Alternative ideas are investigated in parallel to span the full range of a design. Alternatives are tested and weak alternatives are sorted out. The strong solutions are used for the implementation of the solution. Information on the set-based approach is based on the publication of Kennedy et al. [72].

The application of the set-based approach for the implementation of the solution for the measuring system is depicted in Figure 5-19. First, the measuring system was split up in the subsystems *sensors*, *signal conditioning*, *data acquisition*, *power supply* and *data processing*. Then the interfaces between those subsystems were defined.

For each of the subsystems various solutions were developed in parallel. Testing several solutions for the subsystems made it possible to learn, how an optimal solution could be achieved and the critical aspects were revealed. In some cases, even further division of the subsystems was necessary in order to test critical functions separately. It was necessary to develop, test and optimise the subsystems separately as the entire system would have been far too complex to eliminate errors. Moreover, it was possible to determine the capability of the subsystems and to have a full understanding what happens within the system. The capability of the prototypes of the subsystems were tested with simulated interfaces. Knowing, which output a subsystem should show for a given input, it was possible to determine the performance of the subsystem.

For instances, the voltage of the measuring signal, which the data acquisition unit needs to read and store on the SD card, was simulated with potentiometers. For a known voltage input the data acquisition unit should write a certain value on the SD card. Comparing the deviation of the recorded value with the actual value it was possible to quantify how accurate the voltage is determined.

The solutions with the best performance for each subsystem were selected and connected to a comprehensive prototype of the measuring system. This was done in order to exclude errors, which are caused by interactions, which have not been regarded by the simulated interfaces. After the comprehensive prototype was approved to work like desired the final measuring system was built.
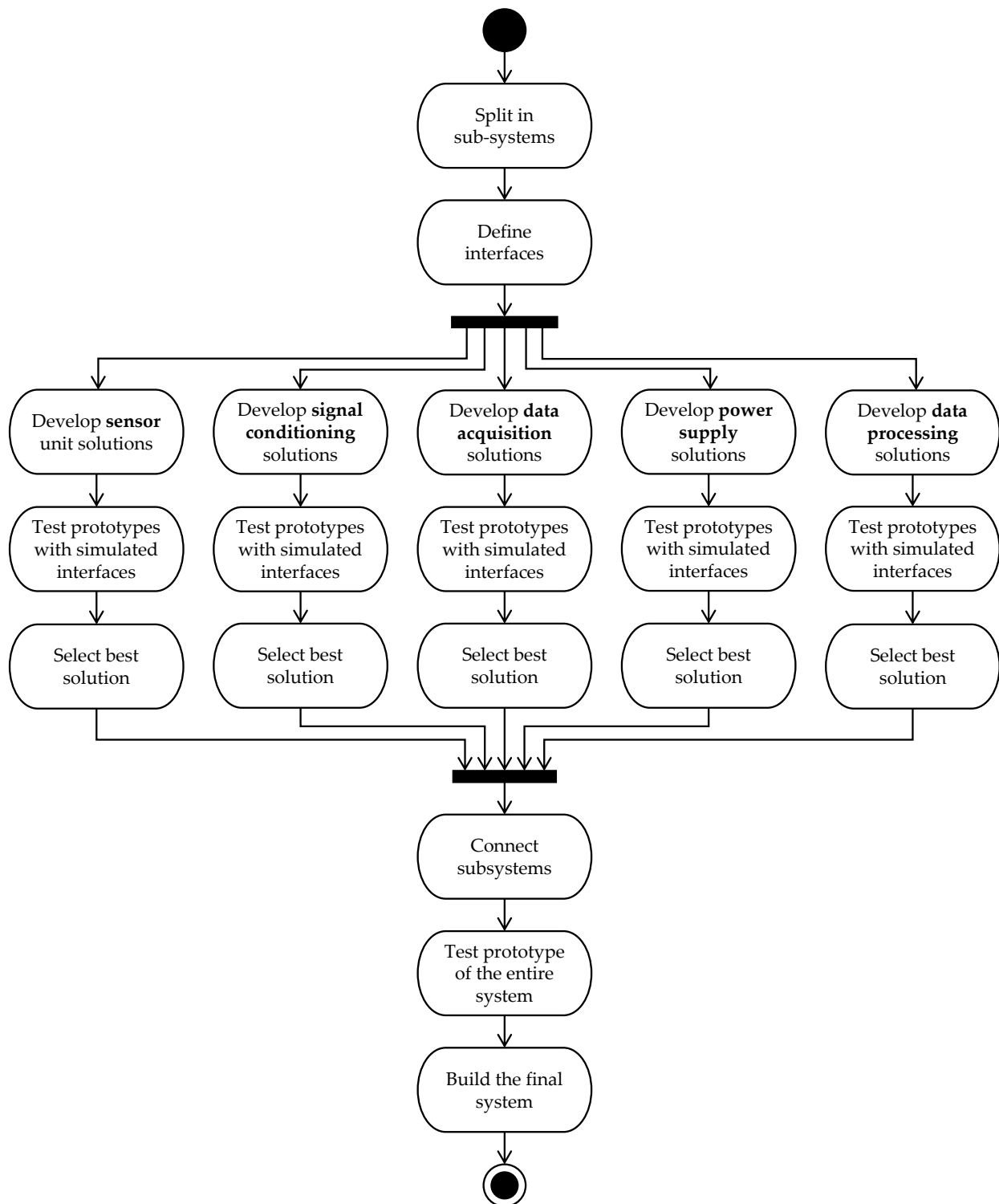
Figure 5-19: Activities of the set-based approach during the implementation of the measuring system

5.6.2 Optimisation of the Setup

With the set-based approach it was possible to optimise the entire setup of the measuring system. It was possible to reduce the number of needed Arduino Zeros from six boards to one board. Furthermore, the circuitry was reduced and the accuracy of the measuring system increased. In the following, the optimisation of the subsystems is explained. For the sensor unit comprising the

strain gauges on the roller ski the first prototype worked as desired. No other solutions were therefore developed.

The Signal Conditioning Unit was tested with different setups as depicted in Figure 5-20. First, there was a setup with 24 Wheatstone bridges, 24 amplifier modules and 24 A/D-converters. It was determined to be difficult to calibrate the 24 amplifier units to a similar gain and a similar offset. Furthermore, it was impossible to synchronise the sampling rate of the A/D-converters, which rendered the advantage to sample all 24 strain gauges at the same time void.

This lead to the setup which was finally used. The voltage output of the Wheatstone bridges is multiplexed to a single amplifier and the output is digitalised by a single A/D-converter. As the data acquisition unit controls the multiplexers it is possible to determine which measured voltage belongs to which Wheatstone bridge. This is a technique commonly used for data acquisition boards [73].
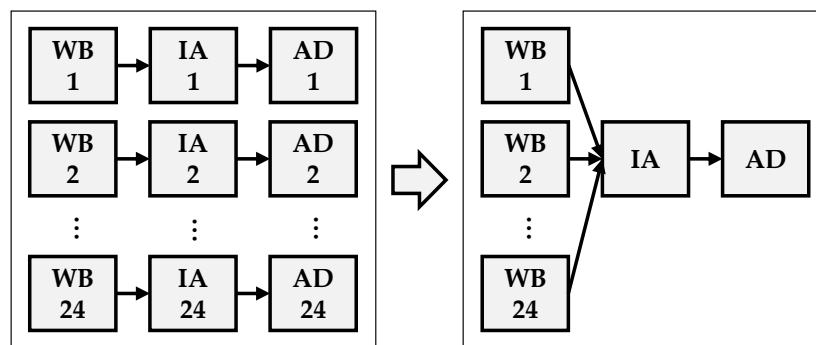
Figure 5-20: Improvement of the setup of the measuring system, with Wheatstone bridges (WB), instrumentation amplifiers (IA) and A/D-converter (AD)

The Data Acquisition Unit was optimised regarding accuracy and sampling frequency. Furthermore, it needed to be adapted to the changed setup of the signal conditioning unit. It was possible to reduce the number of required Arduino Zero boards to one and even the control of the multiplexers of the signal conditioning unit was integrated into this board.

For the initial setup 24 A/D-converters were needed. In order to read that number of analogue channels four Arduino Zero boards each comprising six analogue input pins were required. All of the boards had to be started and stopped by the user at the same time. Furthermore, they needed to be stopped when there is an error on one of the boards. As depicted in Figure 5-21 a setup with a master and slave boards was developed to enable the synchronisation of the measurements at the slave boards. The four slave Arduinos were controlled by one master Arduino. When the master got the signal from the user interface to measure, it triggered the slaves to start a measurement. In case one of the slaves was not able to sample, it sent an error to the master, which prompts all the slaves to stop the measurement and the user receives an error signal. When the error was corrected and the user reset the system by pushing the reset button the master and the slaves were reset.

Besides the high amount of hardware which is needed and the complex communication between the master and the slaves there was another significant disadvantage. The slaves were started and stopped by the master at the same time but in between they sampled at slightly different times. This was caused by the delay which irregularly occurs while writing to the SD card. The SPI bus communication to write on the SD cards enabled stable writing for most of the samples. However, there were disruptions after every 1000 samples which caused a delay in sampling between 80 ms and 100 ms. The sampling rate could have been decreased as low as the maximal delay in order to have synchronous sampling. This would lead to a sampling rate lower than 10 Hz.
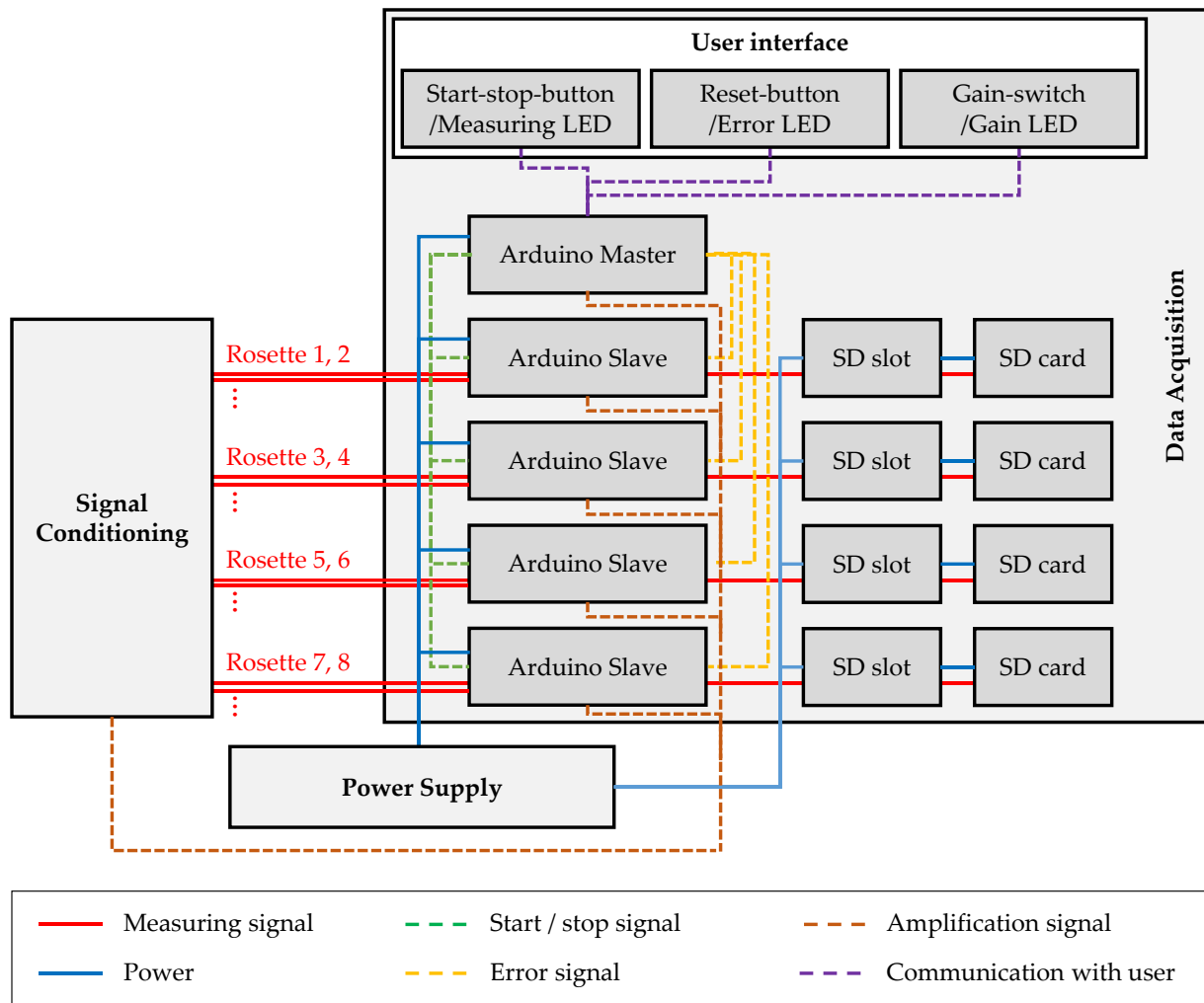
Figure 5-21: Data acquisition setup with 24 analogue inputs

For the final solution only one analogue input pin is required. Therefore, one Arduino Zero is sufficient. A detailed description of the setup is given in chapter 5.6.6. and the setup is depicted in Figure 5-31. Besides the reduction of the Arduino Zero boards of the data acquisition unit it was possible to integrate the control of the multiplexers of the signal conditioning unit to this board as well.

The Power Supply was optimised regarding the noise which it adds to the measuring system. Three different setups for the power supply were designed. First, there were DC/DC-converters

and adjustable voltage regulators to achieve the desired voltage output. Then linear voltage regulators were added in order to reduce the ripple on the output voltage. Finally, a customised battery in combination with diodes was used in order to reduce the noise drastically.

With the laboratory power supply unit TTi EL 155R and the oscilloscope Tektronix TDS 1002 the different output voltages were examined. The oscilloscope is capable to detect up to 60 MHz and has an accuracy of 2 mV.

First there was a setup with constant voltage regulators and DC/DC-converters in order to provide the voltage for the Wheatstone bridges, the Arduino board and the required symmetric power supply for the multiplexers and instrumentation amplifiers. The ripple on the output voltage of the constant voltage regulator LT1528CT from Linear Technology was measured to be 3.3 V peak to peak (pk-pk) at 10 kHz. However, it was possible to reduce the ripple to 7 mV pk-pk with a 470 µF bypass capacitor on the output. The direct current to direct current converter (DC/DC-converter) TMR 3-0521 used for the power supply of the multiplexers had a ripple of 710 mV pk-pk at 10 MHz. With 470 µF and 100 nF bypass capacitors between the output voltages and ground it was possible to reduce the ripple to 400 mV pk-pk. The TMR 0523 which was used for the voltage supply of the instrumentation amplifiers had a ripple of 320 mV pk-pk at 7 MHz. Using 470 µF and 100 nF bypass capacitors between the output voltages and ground the ripple was reduced to 250 mV pk-pk.

In summary the ripple of the setup with constant voltage regulators and DC/DC-converters could be reduced considerably by the use of bypass capacitors. However, the ripple of the DC/DC-converters is several times higher than the change in voltage which is caused by the strain gauges at the measuring terminals of the Wheatstone bridge. Due to this, a better setup for the power supply had to be found.

Linear voltage regulators are used to stabilise the voltage and to prevent ripple [74]. In order to provide stable voltages, the setup depicted in Figure 5-22 was designed. The voltage output of the power bank was regulated with the low drop voltage regulator LF33ABV to 3.3 V for the Wheatstone bridges and the Arduino. For the multiplexers and instrumentation amplifiers positive and negative voltages are needed as they need to be symmetrically powered. Therefore, the DC/DC-converters were still needed but the ripple was reduced with linear voltage regulators. For the multiplexers the ±12 V output of the TMR 6-0522 was smoothened with the linear voltage regulators LM7805 to +5 V and LM7905 to -5 V. The DC/DC-converter TMR 0523 with an output of ±15 V was utilised for the instrumentation amplifiers. For the smoothing the LM78L12ACZ with an output of +12 V and the LM79L12ACZ with -12 V were used. In order use the voltage regulators for the smoothing several bypass capacitors and protection diodes were needed. For the setup the application notes of the specific components were deployed. As a solution for a perfectly stable power supply was found this system was not tested anymore.
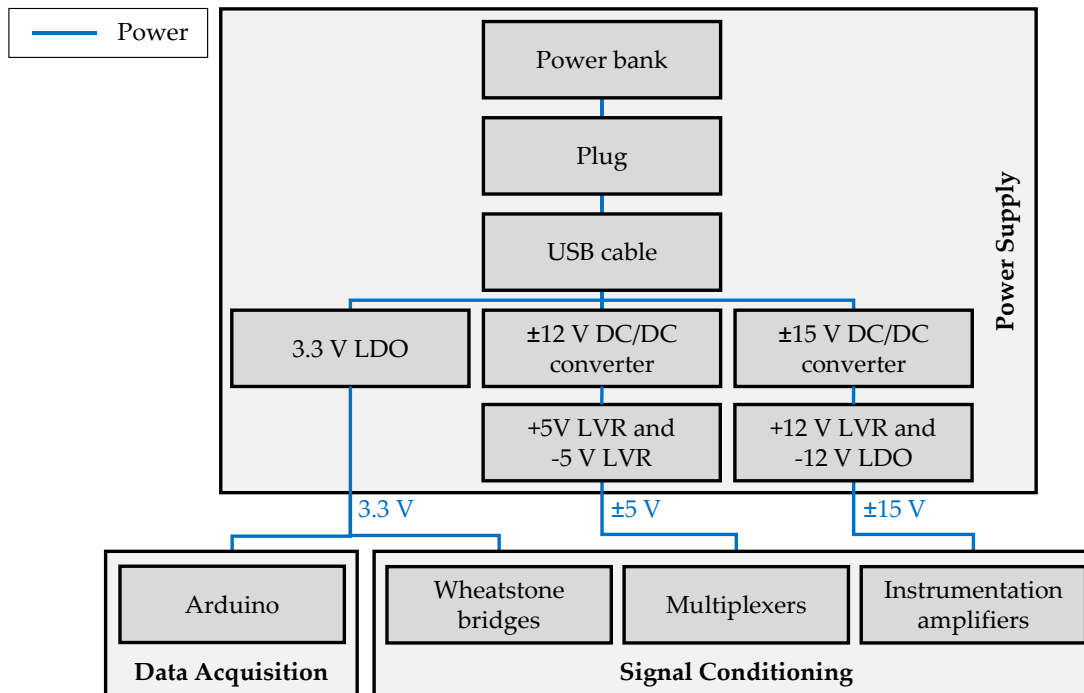
Figure 5-22: Setup of the power supply

The best solution for the power supply was a customised battery with a +6.4 V, 0 V and -6.4 V output. With Schottky diodes the output voltage of the battery was decreased to the levels needed. More detailed information on this setup is found in chapter 5.6.7. Measuring with the oscilloscope no ripple could detected. This is due to the fact that the battery and the diodes do not cause a ripple.

Data Processing was optimised regarding usability and computational cost. Furthermore, the programme needed to adapted to the changes of the data acquisition unit. First files were written on four SD cards which needed to be read. The speed to write the measured data on the SD card was not completely stable. As described in chapter 5.6.6 the SPI bus communication with the SD cards enables stable writing for most of the samples but there are periodic disruptions which cause a delay in sampling. Those disruptions caused that later samples on the different SD cards are at different times which makes an interpolation to an equidistant measuring time necessary. The measured data was linearly interpolated on an equidistant time increment. The increment on which the data was interpolated was automatically adapted by the code regarding the sampling frequency on the SD cards. In order to pass on the data as exact as possible the interpolation time increment was set equal with the fastest sampling time increment of the fastest SD card. The interpolation can cause slight unwanted smoothing of the measured values and maximal values might get lost. More accurate results could be achieved using a smaller time increment which requires increased computing capacity. Due to the vast amount of sampled data an approach needed to be used which enabled efficient interpolation of the data.

Furthermore, the time values from different SD cards needed to be shifted to start at 0 ms. This was necessary due to the different start up speed of the boards, which lead to different timing of

the internal clock of the Arduino boards. Moreover, the measuring duration needed to be adjusted. It happened that the measuring lasted one sampling longer on some of the slave Arduinos than on the others as they might have been in the sampling loop when the master Arduino triggered to stop the measurement. Therefore, the measurements which are later than the stop of the first slave Arduino were not taken into account.

For the final setup of the data processing programme no interpolation of the measured values on a common time step is needed as the data is logged by only one Arduino. Due to the same reason no matching of the first and last sampling is required. The system is designed to be easy to use that unexperienced users can easily utilise it. Furthermore, it was aimed to process the data as fast as possible and to include fail-safe solutions. More detailed information on the data processing programme can be found in chapter 5.6.8.

5.6.3 Measuring Chain

In order to explain, which steps need to be run through to determine the loads, the measuring chain is explained. The measuring chain is the process how the strain measured at the beam is translated to a force or a torque. Hardware modules like the sensors, the signal conditioning unit and the data acquisition as well as the software utilised for the calculation of the loads are included. The measuring chain is depicted in Figure 5-23.
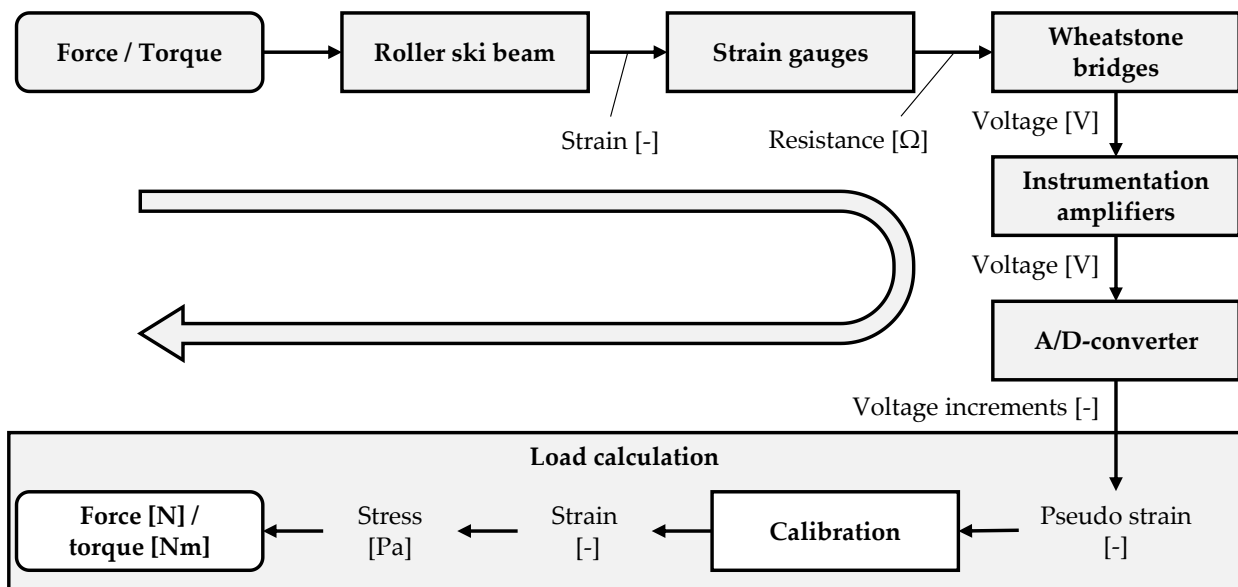
Figure 5-23: Measuring chain of the measuring system

The forces and torques acting on the beam of the roller ski cause strains which induces a change of resistance at the strain gauges. With the use of the Wheatstone bridges this change of resistance can be translated to voltage which is amplified by the instrumentation amplifiers. The amplified voltage is sensed by the A/D-converter and transformed to voltage increments of the measuring range.

Subsequently, the loads are reconstructed from the voltage increments. First the pseudo strain is calculated with the voltage increments. There is no actual strain as no calibration factors are considered until there. When the pseudo strain is multiplied with the determined calibration factors it is the actual strain. As the stress state is multiaxial the loads are not directly related to the strain. The principal stresses need to be calculated. With the principal stresses transferred to the roller ski coordinate system it is possible to calculate the forces and torques.

5.6.4 Sensors

The loads acting between the roller ski and the binding are determined by measuring the strain at different positions of the beam of the roller ski. Strain gauges are utilised to measure the strain at the beam. The strain gauges and their protection add 190 g to the roller ski which weighs 1500 g and the centre of gravity is shifted 4 mm back. The strain gauges are connected via a cable to the signal conditioning and data acquisition unit. The cable is mounted with hook and loop fasteners on the leg of the athlete. In Figure 5-24 the roller ski equipped with strain gauges and the connection cable is depicted.

The beams of the classic and skating roller ski from RollerSafe have the same cross section. It was sufficient to equip one beam with strain gauges as the wheel holding brackets and the wheels for skating and classic roller skiing can be mounted on the same beam. The beam of the classic ski was used as it is longer and there will be higher torques than on the skating beam as the leverage ratio is increased. Furthermore, it is hardly possible to mount strain gauges in front of the binding of the skating roller ski. There is not sufficient space as the charging box of the brake of the roller ski is placed really close to the binding.

For the development of the measuring system it was necessary to find out how to deal with the multiaxial stress state. Furthermore, the optimal position of the rosettes needed to be determined with the aid of a FEM model. A suitable way to connect the strain gauges to the signal conditioning and data acquisition unit was investigated and the accuracy of the setup was optimised.
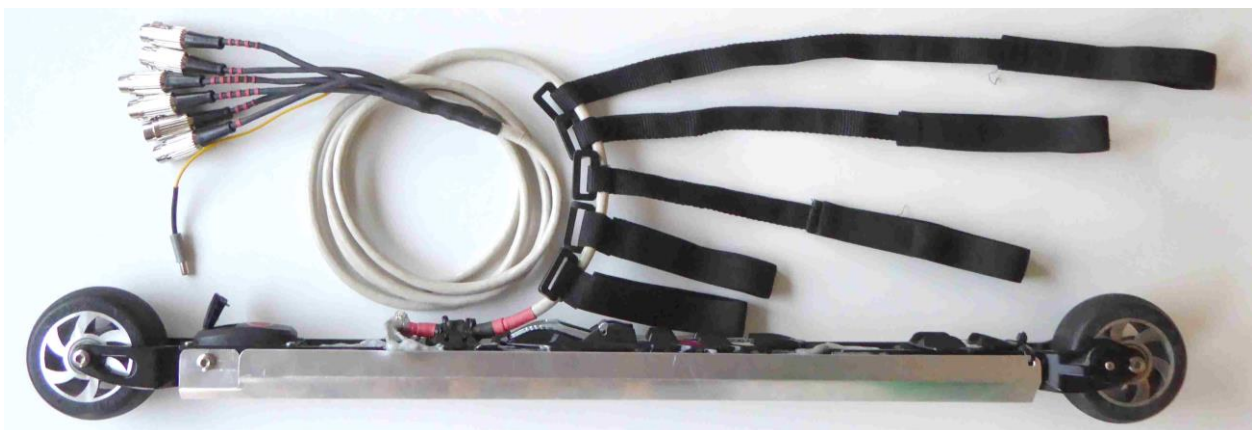
Figure 5-24: Equipped roller ski with strain gauges, cover plate and connection cable with hook and loop fasteners

The Multiaxial Stress State which acts at the beam of the roller ski makes it necessary to use strain gauge rosettes. If a force is acting on a beam in a known direction it is possible to measure with a single strain gauge which is aligned with the tension or compression caused by the force. The force can be determined with use of the measured strain and the one-dimensional Hook's law. If there is an additional force it is not possible any more to use only one strain gauge. The strain and the transverse deformation caused by the two forces are superimposed. Due to this, the one-dimensional Hook's law cannot be used. If the direction of the two forces is known the principal strain in the direction of the forces can be measured with two strain gauges and the principal stress is derived. However, if the direction of the forces is not known or if torques are superposed a strain gauge rosette comprising three strain gauges is needed. Knowing the strain in three directions it is possible to calculate the direction of the principal stresses [6]. More detailed information how the loads are derived from the measured strain is given in chapter 5.6.8.

As spatial forces and torques will be superposed for this measuring system strain gauge rosettes are needed. The rosettes HBM 1-RY93-3/350 with an alignment of the strain gauges a/b/c at 0°/45°/90° were chosen as it is easier to perform the transformation from the rosette based coordinate system to the roller ski coordinate system than for a 0°/60°/120° type. Furthermore, this rosette was chosen because it has a grid size which can withstand 3.3 V bridge excitation voltage and is small enough to be mounted at the desired position. A bridge excitation voltage of 3.3 V is necessary in order to grant high accuracy for the acquisition of the measured data. More detailed information why the voltage of the data acquisition and the Wheatstone bridges needs to be the same is given in chapter 5.6.7. The strain gauge rosette together with the solder terminal and the transfer cable is depicted in Figure 5-25.
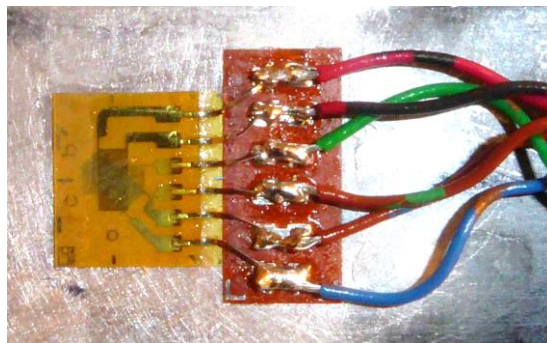
Figure 5-25: Strain gauge rosette HBM 1-RY93-3/350 at the beam of the roller ski with solder terminals and transfer cables

The Position of the Rosettes was determined with respect to an easy calculation of the loads with high accuracy. Regarding the principal setup for the measuring system in chapter 5.3.1 it turned out that six sensors are needed to measure spatial forces and torques. Mounting strain gauges at only three sides of the profile would have led to a more complex calculation of the loads than mounting them at four sides. With sensors on all four sides of the profile in front of the binding and on four sides behind the binding it is easy to calculate the loads. The rosettes on the left and

the right side are in the neutral layer of bending torques around the horizontal axis. Whereas, the rosettes at the bottom and the top side of the profile are in the neutral layer of bending torques around the vertical axes.

For bending forces and torques the neutral layers are in the centre of the intersectional area of the beam of the roller ski [75]. In Figure 5-26 the positions of the neutral layers are shown. The position of the vertical layer was easy to determine as the profile is symmetrical with respect to the z-axis. The symmetry axis is equal to the centroidal axis [76]. However, the position of the neutral layer in horizontal direction was more difficult to calculate as the profile is not symmetrical to the y-axis. The position of the neutral layer was determined to be $z_S = 14.8$ mm by calculating the centre of gravity for a compound of the geometric bodies the profile is composed of. For the calculations the computer algebra system Maple 18 was used. The detailed calculations can be found in Appendix I.
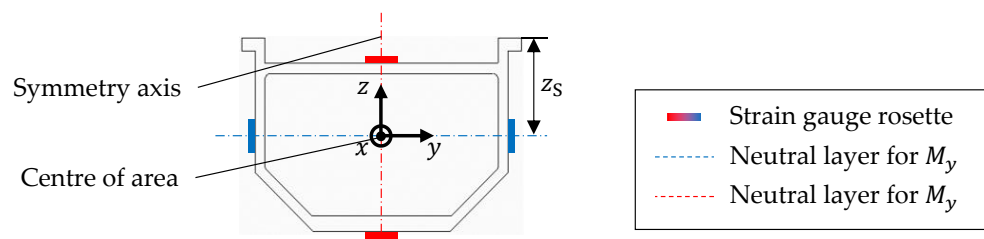
Figure 5-26: Cross section of the beam of the roller ski and its centre of area

The four rosettes at the front and the four at the back have the same distance to the binding. Furthermore, the strain gauges were mounted far enough from grooves and holes in order to obtain data which can be used for the accurate calculation of the loads. Information on how the optimal positions for the strain gauge rosettes were determined is given in the next paragraph.

Mounting rosettes underneath the beam of the roller ski requires a cover to protect the sensors from getting ripped off when accidentally getting stuck on bumpers or curb stones. A cover made of 0.8 mm thick aluminium sheet plate was bent. The cover is mounted with the screws of the wheel holding bracket at the front of the roller ski. At the back the cover was attached loosely with a tie wrap to the beam of the roller ski. This enabled to mount the cover to the roller ski without adding stiffness to the system which would interfere with the accuracy of the measurements. Furthermore, protection of the rosettes on all sides of the profile is needed to make them withstand dusty and wet conditions. The rosettes were covered with two component polyurethane adhesive Araldite 2018.

FEM Simulations of the strain distribution were done in order to exclude interference of the strain distribution with the accuracy of the measuring system. If grooves would induce excessive strain to the strain gauge for some of the load cases, there would be an error for the measurement. Therefore, it needed to be checked whether irregularities in the profile like groves and bores induce strain to the strain gauge positions. In order that the equations used for the load calculation

can be applied it is crucial that there is only elastic deformation at the position of the strain gauges. Therefore it was checked whether the stress does not exceed the tensile yield strength of 276 MPa of the aluminium 6061-T6 [77] which the beam of the roller ski consists of.

For the beam of the roller ski only the essential properties were modelled. The geometric body of the beam was generated with PTC Creo Parametrics 3.0. The original cross section of the profile was used, but only the notches and holes in the region of the strain gauges were modelled. Subsequently, a .STP-file was exported from Creo Parametrics and imported to Abaqus 6.14-1. The material parameters of the aluminium 6061-T6 of the beam were assigned to the profile. For the mesh the linear, tetrahedral, four node element C3D4 was used. The mesh was globally seeded with an approximate size of 1 mm. The loads were induced trough surface areas on the beam which correspond to the contact areas between binding and roller ski. The maximal expected loads described in chapter 5.1were applied.

In Figure 5-27 the results of the simulation of the E11 strain in the direction of the beam is depicted. For the displayed case the maximal expected loads were superposed. It can be seen that none of the strain gauge rosette positions is within the region of excessive strain. Furthermore, they are not placed in regions with a high strain gradient. The results of the FEM-simulation for positive and negative maximally expected loads can be found in Appendix L. Considering all load cases revealed that the optimal position of the strain gauges is 180 mm in front and behind the binding link. For none of the load cases the tensile yield strength was exceeded.
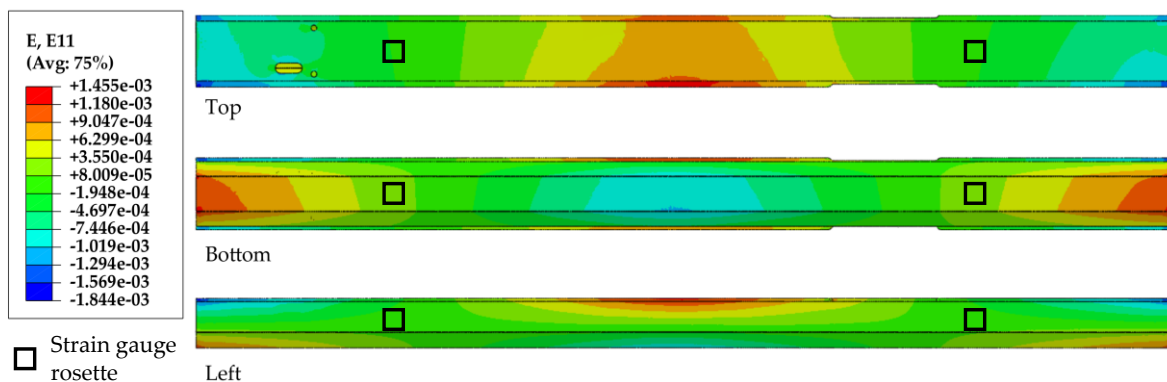
Figure 5-27: FEM simulation of the strain E11 in x-direction at the beam of the roller ski for the superposition of the maximal expected loads, with the positions of the strain gauge rosettes

Connections of the strain gauges to the data acquisition unit are necessary. There are 8 rosettes with 3 strain gauges and each strain gauge has two connection pins. In order to connect those 48 pins, the shielded cable 3600B-50 from 3M is used. Flexibility of the cable is granted with the stranded cores of the wire. The cable is mounted with elastic hook and loop fasteners to the leg of the athlete.

The cable was compared with one, which has solid cores, but the stranded wire is less sensitive to noise. The twisted pairs of the cable reduce the sensitivity to noise as well. On the roller ski,

the cable pairs need to be spread to the strain gauge rosettes. An attachable cable shield was used to protect the six wires which lead to each strain gauge. The same was done between the six plugs of the cable and the common shield. In order to activate the shielding function of the cable the shields were connected to ground where they are plugged to the signal conditioning and data acquisition unit.

Accuracy of the strain gauge sensors was taken into account by checking the strain distribution at the beam of the roller ski. The guide of the strain gauge supplier was used for the strain gauge application and influences caused by electromagnetic fields were eliminated.

The results of the strain modulation for the maximal load cases were used to check whether the strain gauges provide reliable output. As there was no plastic deformation at the beam of the roller ski a linear stress strain relation applies. Furthermore, no strain peaks were detected at the position of the strain gauges. Therefore, the strain gauges are placed at representative positions.

In order to detect the strain accurately the guide from HBM *Practical Hints for the Installation of Strain Gages* [78] was followed during the application of the strain gauges. The cleaning of the surface, the precise positioning methods and the use of the adhesive was done correctly. Furthermore, the strain gauges were tested as recommended. There were no short circuits between the strain gauge connections and the beam of the roller ski. All of the strain gauges were measured to have 350 Ω resistance. The deviation of the desired position of the rosettes was measured to be under 1 mm, consequently they are correctly aligned. In order to get accurate results for the loads, it is necessary that the four sensors at the front and the four at the back are within one layer.

The measuring system is protected from external influences on the accuracy of the measuring system caused by electro-magnetic fields induced by power lines. The cable to transfer the data from the strain gauges to the signal conditioning and data acquisition unit can be a flaw for the electro-magnetic influences. Therefore, shielded cable is used. In order to eliminate cross talk between the signals of the strain gauges a wire with twisted pairs is used. The resistance of the cable does not have any influence on the measuring accuracy as the resulting imbalance of the Wheatstone bridges is shifted to zero by the tare function of the data processing unit.

The Prototype of the sensor unit was used to conduct first tests on the behaviour of the strain gauge rosettes on the beam of the roller ski. The strain gauges of the rosettes were connected to a Wheatstone bridge on the bread board and the output of the bridge was measured with a multimeter. The system was loaded with the same weight for several times and the multimeter returned to the same voltage each time. The interface to the signal conditioning unit is between the connection wire of the strain gauges and the Wheatstone bridges. It was necessary to integrate the Wheatstone bridge to the prototype of the sensors as it was not possible to measure the change of the resistance of the strain gauges without the bridge circuitry and the multimeter.

With this prototype it was detected that the Wheatstone bridge is unbalanced even if there is no load and that the output of the bridge is in the range of 3 mV. Furthermore, it was used to get practice in mounting the strain gauges accurately.

5.6.5   Signal Conditioning

The signal conditioning unit is needed in order to transfer the changing resistance of the strain gauges to a voltage signal, which the Arduino Zero board can digitalise. The setup, the accuracy, the prototype and the production of the signal conditioning unit are described. The electronic schematics can be found in Appendix B.

The Setup of the of the signal conditioning unit is based on the common setup of data acquisition boards explained in *Measurement, Instrumentation and Sensors handbook* by Webster [73]. The implemented setup is visualised in Figure 5-28. The 24 Wheatstone bridges, which comprise the strain gauges, are connected to multiplexers. Three sets of two multiplexers with eight inputs each are used connect one Wheatstone bridge at the time is to the instrumentation amplifiers and the A/D-converter of the Arduino. This is done for all of the 24 bridges subsequently. As the multiplexers are steered by the Arduino which measures the output voltage of the signal conditioning unit, it is possible to refer the measured voltage to a certain bridge.

Connecting all strain gauges to only one Wheatstone bridge via multiplexers is not possible due to the reason that the on-resistance of the individual multiplexer channels can vary up to 6 Ω [79]. This variance in resistance is substantially higher than the one of the strain gauges. Basically only the change of the resistance of the multiplexers and not the strain at the strain gauges would be measured.
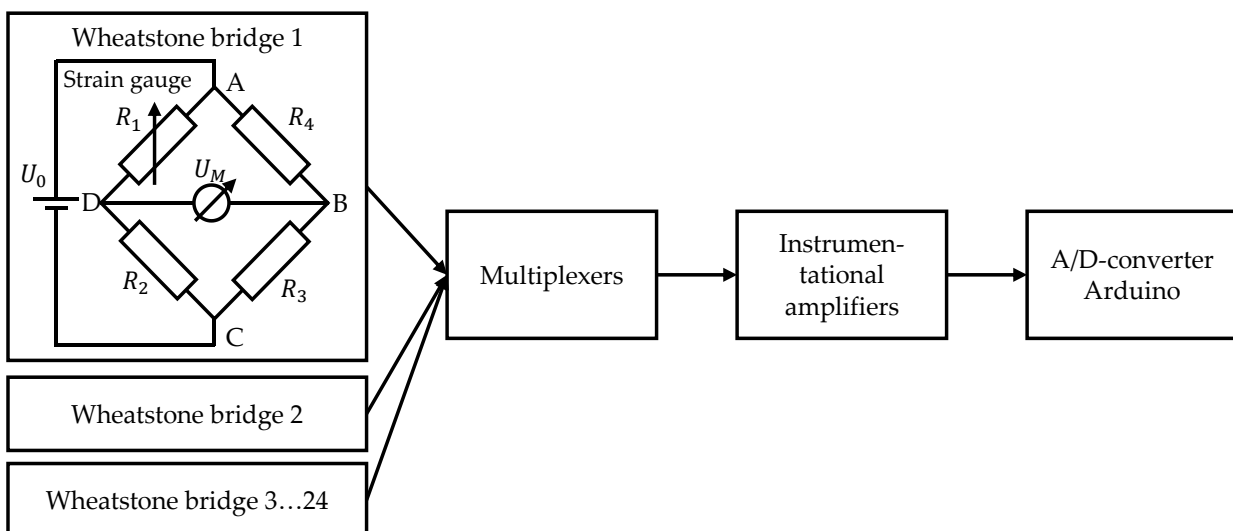
Figure 5-28: Setup of the signal conditioning unit

The strain gauges were connected to the position R_1 of the Wheatstone bridge in order to achieve a positive voltage output between D and B when there is an elongation of the strain gauge. On the remaining positions of the bridge resistors with 1 % resistance accuracy were placed. In order

to have equal bridges the resistors were measured and sorted by their resistance value before soldering them to their specific positions. The product of the resistors at the positions R_1 and R_2 and the product of the resistors at the positions R_3 and R_4 needs to be equal to fulfil the initial balance condition of the Wheatstone bridge [9]. In order to fulfil this condition, resistors with 350 Ω were placed on the position R_2 as the strain gauges at position R_1 were measured to have 350 Ω resistance as well. There were not enough 350 Ω resistors left for the positions R_3 and R_4 but there were enough 349 Ω resistors for both positions and consequently to fulfil the initial balance condition.

The measuring terminals at the positions B and D of the Wheatstone bridge were connected to two different multiplexers. This made it possible to connect both B and D to the first instrumentation amplifier at the same time. Six multiplexers 74HC 4051 from Texas Instruments are employed to connect the Wheatstone bridges to the instrumentation amplifier consecutively.

Bypass capacitors are needed for the supply voltage of the multiplexers. Otherwise the multiplexers would cause a ripple on the supply voltage due to the fast switching frequency between the channels. This would cause measuring errors as other components of the measuring system would be impeded by the ripple. Bypass capacitors with 100 nF from the positive and the negative supply voltage to the ground are used as well as a 47 μF capacitor from the positive to the negative supply voltage of the multiplexers.

The output signal of the Wheatstone bridges needs to be amplified in order to use as much of the measuring range of the A/D-converter of the Arduino as possible. The output voltage after the Wheatstone bridges is lower than 3 mV. Consequently, it needs to be raised to use the full range from 0 V to 3.3 V of the A/D-converter of the Arduino. The more of the measuring range is used the higher resolution is available for the data acquisition.

Therefore, the voltage is raised with two AD620 instrumentation amplifiers from Analog Devices. Amplification in two steps was necessary in order to not to exceed the bandwidth limit for the required output voltage and to reduce noise [70]. The higher gain was realised in the first amplification step in order to reduce the amplification of the noise caused by the instrumentation amplifiers. For the determination of the optimal gain the strain calculation for the strain gauge positions in Appendix J was used. This made it possible to assess the output voltage for the strain gauges at the different positions.

The gain of the instrumentation amplifiers is adjusted with resistors. For the first amplification step a fixed gain is used. However, the gain of the second step is adjusted by switching between two different resistors. The user can select between a gain setting for low loads and a setting for high loads. In vertical direction there are forces on the roller ski which are significantly higher than in the other directions as the weight of the athlete causes forces in this direction. With a gain adjustable for low loads the measuring accuracy of those loads is considerably increased.

For negative strain at the strain gauges there is a negative output voltage at the Wheatstone bridges. However, the A/D-converter of the Arduino can only read positive voltage values. For this reason, the reference voltage of the second instrumentation amplifier needs to be raised. At the reference terminal of the AD620 up to 2 V can be applied in order to define a new 0 V-reference [70]. This can be done with a static voltage or with an intelligent adjustment voltage like Moghimi [80] introduced. When the measuring system is powered or reset the Arduino adjusts the reference voltage of the second instrumentation amplifier. The amplified output of every channel is read and the reference voltage is increased until the output of all channels is between 1 V and 2 V. Owing to the adjustable reference voltage even more of the input range of the A/D-converter can be used as the system automatically adapts to imbalances of the Wheatstone bridges. Imbalances might occur for instance when the resistance of the connection cable increases due to higher external temperatures. In contrast to other Arduino boards which use pulse width modulation for the analogWrite-function the Arduino Zero has a digital to analogue converter with a steady output for pin A0. Nevertheless, a 100 nF bypass capacitor is used at the reference pin of the instrumentation amplifier in order to stabilise the reference voltage.

Similar to the multiplexers the voltage supply of the instrumentation amplifiers needed to be protected with bypass capacitors. For each of the instrumentation amplifiers 100 nF bypass capacitors are used from the positive and the negative supply voltage to the ground. Furthermore, a 47 μF capacitor between the positive and negative supply voltage of each instrumentation amplifier is used.

Next to the instrumentation amplifiers there is an over voltage protection in order to protect the analogue input pin of the Arduino board. Overvoltage occurs when high loads are applied when the gain of the signal conditioning unit is set for low loads. Schottky diodes BAT 43 were used for the realisation of the over voltage protection in combination with a 100 Ω resistor to prevent excessive current.

The Accuracy of the signal conditioning unit was tested by recording data when there was no load on the roller ski. There is a fluctuation of 50 N for forces and 1.3 Nm for torques of which 40 N and 1 Nm are caused by the A/D-converter of the data acquisition unit. Consequently, the signal conditioning unit induces a fluctuation of 10 N for forces and 0.3 Nm for torques.

An unexpected disbalance occurs at the Wheatstone bridges. For the 24 bridges there is an output voltage between 0.8 mV and 5.5 mV although the resistors were selected carefully by testing their resistance to fulfil the initial balance condition. The gain of the instrumentation amplifiers cannot be set as high as desired in order to have the output voltage of all bridges within the measuring range of the A/D-converter. The change of the output voltage is small compared to the disbalance of some bridges. For the maximal expected loads there is a change of 2.3 mV. Consequently, the change of the voltage is only within a small share of the measuring range of the A/D-converter which makes the accuracy of the A/D-converter more relevant.

The Prototype consists of several parts. First, the multiplexers and the instrumentation amplifiers were tested separately. The multiplexers were connected to a constant input voltage in order to determine whether they work in the desired way. With the constant voltage input the output voltage of the Wheatstone bridges was simulated. The instrumentation amplifiers were tested with a single Wheatstone bridge which comprised one strain gauge. This enabled to test whether the signal is amplified correctly. Furthermore, it was possible to determine whether appropriate gain was chosen. When the desired output was achieved the multiplexers and instrumentation amplifiers were connected.

In Figure 5-29 the prototype of the signal conditioning unit connected to the sensor unit and the data acquisition unit is shown. It was necessary to do comprehensive testing of the subsystems to grant functionality of the entire system before manufacturing it.
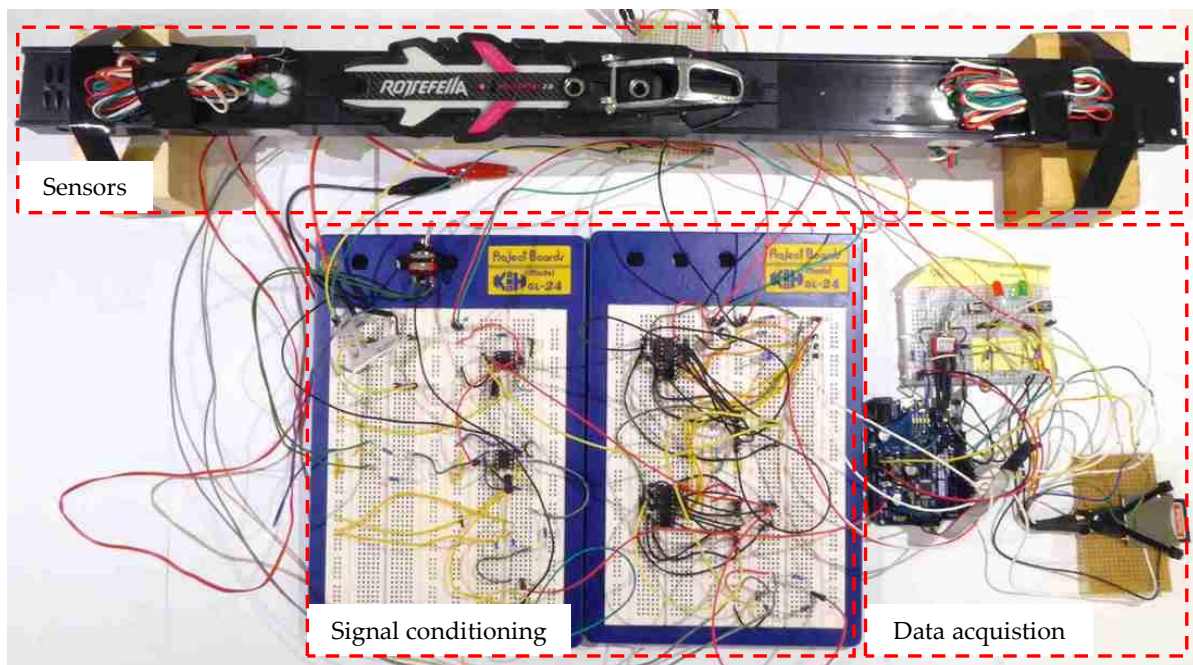
Figure 5-29: Prototype of the signal conditioning unit connected to the prototpyes of the sensor unit and the data acquisition unit

The Production of the board of the signal conditioning unit was done in-house. In order to enable the production of the complex circuitry the pencil-wiring technique was applied. Enamelled copper wire with a thin diameter is used to realise the needed connections. At the positions where the wire is soldered the enamel melts and the wire is not insulated at that spot any more. Thicker wire diameters are used for the power lines and thinner wires for the signal lines. Soldering of the enamelled copper wire is significantly more difficult than soldering common wires. It needs some time until the enamel of the wire melts but the electrical components which are connected should not be heated too much. Furthermore, it is difficult to handle and solder wires with a diameter that small. Testing the system regarding connections and short circuits during the production is crucial. The production of the board of the signal conditioning unit took several weeks.

Figure 5-30 a) shows the top side of the signal conditioning board and Figure 5-30 b) the bottom side with the cooper-coloured power lines and the red signal lines.

It is common practice to build prototype boards with the pencil-wiring technique. Once the circuitry is tested with the prototype board it is possible to layout a printed circuit board. Due to the high additional amount of time to layout the board and the delivery time only the pencil wired prototype is used.
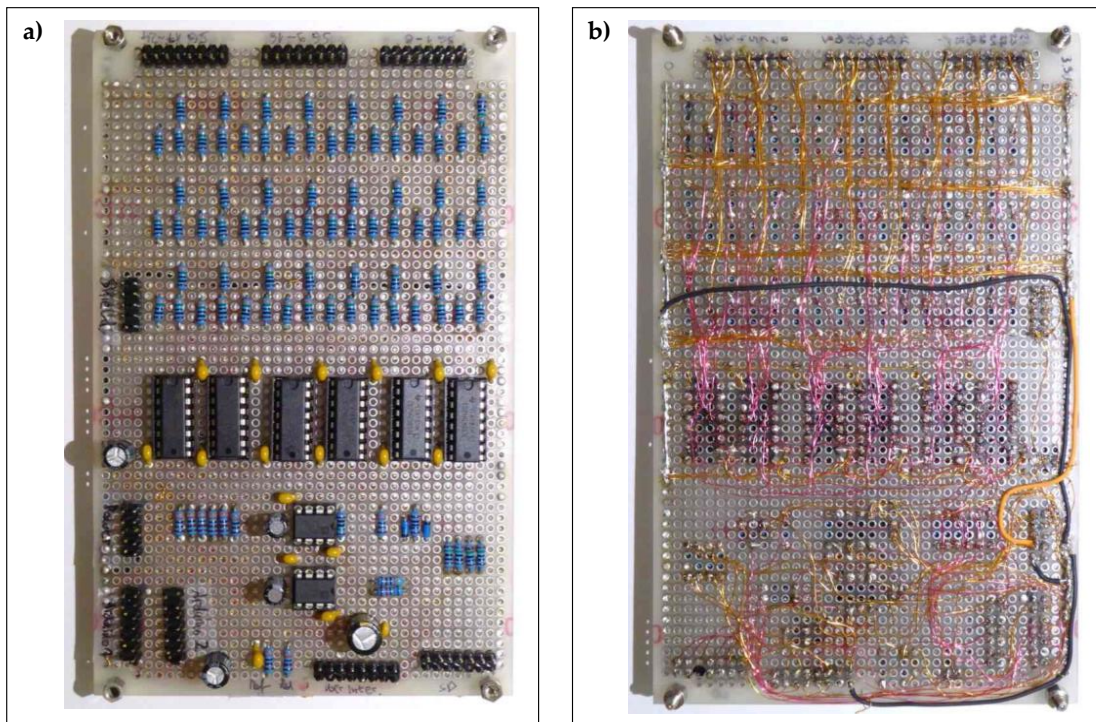
Figure 5-30: Board of the signal conditioning unit: a) Top side, b) Bottom side

5.6.6 Data Acquisition

The measuring system will be used for in situ testing on the road. Data needs to be stored to enable the calculation of the loads after measurement. The data acquisition is only used to store the data as processing of the data induces computational costs. The calculation of the actual loads is done on a computer after the measurement session. In order to enable storage of the measured analogue signal it needs to be converted to digital data. This is done by the A/D-converter of the Arduino Zero.

The final solution of the data acquisition unit is depicted in Figure 5-31. The electronic schematic and the programme code of the data acquisition can be found in Appendix B and Appendix E. One Arduino Zero board is utilised to communicate with the user through the user interface, to read the measuring signal and to store it on the SD card. This board also controls the multiplexers and calibrates the instrumentation amplifier of the signal conditioning unit. The system is able to sample at 33 Hz. Following, the function, the sampling frequency optimisation, the accuracy, the fail-safe design, the usability of the used data acquisition device and the prototype is explained.
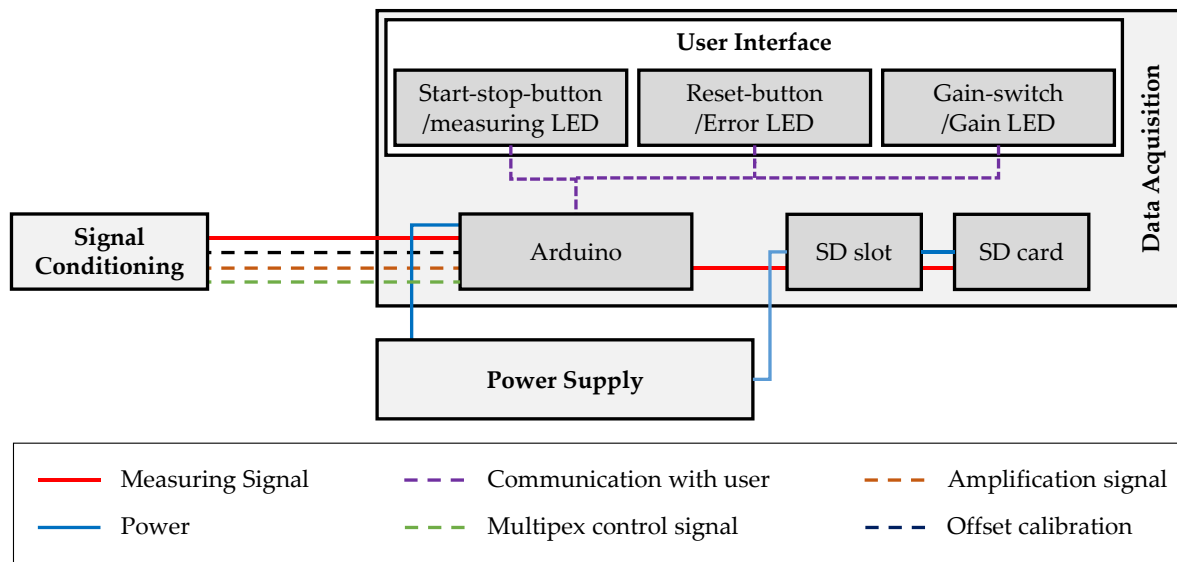
Figure 5-31: Final Setup of the data acquisition unit

The Functions of the data acquisition unit are separated into the setup, which is run when the system is powered or reset and the loop, which is run through continuously after the setup. The setup begins with determining the state of the gain state switch of the signal conditioning unit. This determines which amplification level applies to the measurement. Subsequently, the board warms up the multiplexers and instrumentation amplifiers of the signal conditioning unit by running through the switching states for several times until a stable output level is achieved.

Afterwards the board adjusts the output offset of the instrumentation amplifier of the signal conditioning unit by applying a voltage between 0 V and 2 V to the reference pin. The A/D-converter of the Arduino Zero is able to measure values between 0 V and 3.3 V. In order to enable the detection of negative strain at the strain gauges the 0 V-level is raised to the middle of the measuring range of the Arduino. If this is done by a fixed voltage a misbalance of the Wheatstone bridge due to temporal influences like the temperature cannot be adjusted. The zero-reference would not be in the middle of the measuring range of the Arduino any more. This is prevented by measuring the output of the instrumentation amplifier with the Arduino and increasing the voltage at the reference pin until the output is at the desired level. When the output of the instrumentation amplifier is adjusted a settling time is necessary during which the switch state of the multiplexers is continuously shifted. After three seconds the offset of the output voltage changes less than 4 µV and the setup is finished [70]. Now the user can start a measurement.

When the setup has finished the measuring loop is run continuously until the measuring system is reset or powered off. The user can start and stop data logging at any time. At the beginning of each loop it is checked, whether the gain state is still the same. If the gain state is changed an error is signalled to the user and the system needs to be reset. The reset is necessary in order to go through the calibration procedure of the setup again.

The 24 channels are connected to the analogue input pin subsequently by adjusting the multiplexers. When the multiplexers are set to a certain channel there is a settling time before the A/D-converter of the Arduino board takes a sample. The output rise and fall time of the multiplexers is only 1µs but the bandwidth limit of the instrumentation amplifier for gain 1000 is 10 kHz [79] [70]. Therefore, a settling time of 100 µs is required before a reliable sample can be taken.

When the values of all 24 channels are digitalised they are written to the SD card. Writing all of them together has the purpose that the file on the SD card only needs to be opened and closed once. The data is stored as comma separated values in .txt-files. In one row of the file the time of the sample is given, followed by the measured values for the 24 channels and at the last position there is the state of the gain switch.

When the number of samples within one file increases the writing time increases. Due to this, the data is written to a new file after 10000 samples. When the measurement is stopped by the user the signal of the 24 channels is still measured but the data are not written to the SD card. This has the purpose to keep the signal conditioning unit, comprising multiplexers and instrumentation amplifiers, at a constant temperature. Restart of a measurement is enabled at any time.

The Sampling Frequency Optimisation was done as the objective of the data acquisition device is to sample the measured data at the required sampling frequency. In chapter 5.1 the sampling frequency to determine loads caused by the athlete is determined to be at least 14 Hz but better 42 Hz to 70 Hz. For loads caused by external circumstances the sampling frequency is required to be at least 370 Hz but better 1110 Hz to 1850 Hz. The ATSAMD21G18 microcontroller of the Arduino Zero board comprises an A/D-converter which is capable to take 350 000 samples per second [71]. Unfortunately, this sampling frequency cannot completely be used for the measuring system. The frequency is reduced by the setting times needed for the signal conditioning unit. Furthermore, the 24 channels need to be switched trough and sampled. The most important reduction of the sampling frequency occurs because of the time needed to write the data on the SD card.

Due to the required high sampling rates a lot of effort was put into the development of a time efficient code for the Arduino. Especially the sampling loop was optimised regarding time efficiency. The biggest issue was the delay which occurs after a certain number of samples when writing on the SD card. In order to optimise the programme speed tests were conducted for the sections of the code. Different approaches were tested and the fastest one was used. For instance, it was tried whether a higher sampling rate can be achieved converting the measured values into a string before storing it on the SD card. It turned out that converting the data to a string before writing it to the SD card is 2 ms slower than writing the values separately on the SD card.

Furthermore, it was found out that the more samples are stored within one file at the SD card the longer it takes to write data in this file. The sampling time is increasing by 10 ms from sample one to sample 100 000. Due to this reason the programme does not put more than 10 000 samples

to one file which increases the sampling time only by 1 ms from the first to the last sample. In order to recognise, which files belong to a measurement session their naming is coded. The file name is xxxyyy.txt with xxx increasing from 001 to 999 when the user starts a new measurement and yyy increasing from 001 to 999 in case the data acquisition device starts a new file. For instance, the file 023014.txt belongs to the 23rd measurement on the SD card started by the user and this is the 14th automatically started sub file.

Besides the optimisation of how to sample and to write the data on the SD card it was investigated what kind of SD card and which formatting is most suitable. Tests with an 8 GB class 6 SDHC card from Addata and an 8 GB class 10 SDHC card from SanDisk were conducted. It was ascertained that it is 2 ms faster to sample on the class 10 card. Furthermore, it was tested whether writing on the SD card is faster when formatting it FAT 16 or FAT 32. With FAT 32 the sampling was 1 ms faster than with FAT 16. Unfortunately, the Arduino library which is used to write on the SD card only supports FAT 16 and FAT 32. Otherwise it might have been possible to achieve faster sampling rates with a FAT 64 formatted SD card.

Accuracy of the data acquisition unit was increased by methods to compensate errors by a supply voltage drop and steps to enable the acquisition of reliable data. Furthermore, errors caused by the data acquisition unit were revealed and their influence assessed.

Changes in the supply voltage of the Arduino cause a change of the reference voltage used for the A/D-converter. The 12-bit resolution is evenly distributed on the voltage range the Arduino is powered with. When there is a change of the supply voltage the increments will change which would lead to an error. This error was eliminated as the Wheatstone bridges are powered by the same voltage source. More detailed information how this error is eliminated can be found in chapter 5.6.7.

When the multiplexers are powered up, their resistance is changing, which would interfere with the accuracy of the measuring system. However, when they are warmed up, they have a stable resistance. Therefore, the data acquisition is enabled after the warm up time. Furthermore, those two minutes before a measurement is started are needed to get the voltage offset of instrumentation amplifiers to a stable level.

The A/D-converter of the ATSAMD21G18 microcontroller on the Arduino Zero board has a resolution of 12 bit [71]. With the measuring range between 0 V and 3.3 V [81] this results in an resolution of 0.8 mV. Tests with the A/D-converter have revealed that the readings fluctuate between 13 values of the 4096 increments. The accuracy is reduced by the fluctuation but there still is an accuracy of 10mV. It is not possible to transfer this uncertainty directly to a general uncertainty for the detected forces and torques. This is due to the ambiguity of the tangent used for the calculation of the principal stress. More information on how the loads are calculated is provided in chapter 5.6.8. It was possible to apply a static voltage to the analogue input pin and to process the data with the Matlab script which is used to calculate the forces und torques. With the gain

adapted for low loads there is a fluctuation of 40 N pk-pk for forces and 1 Nm pk-pk for torques. With the gain for high loads there is a fluctuation of 60 N pk-pk for forces and 1.5 Nm for torques.

The strain at all strain gauges needs to be measured within the smallest time difference possible. If the strain at one position is measured significantly later than at another position this would lead to inaccuracies when calculating the loads from those values. All strain gauges are measured within 12 ms which corresponds about 83 Hz.

Fail-safe System Design was aimed for the data acquisition device to prevent data loss and malfunction caused by the user. When powering up the system checks which file numbers already exist on the SD card, in order not to over write existing files. This would cause data, which cannot be processed with the Matlab code. Therefore, a number higher than the one of the existing files is chosen for the file, in which the new data are stored.

There are several errors which could occur if the data acquisition system is used incorrectly. When an error occurs the system gives feedback to the user by lighting a red LED on the reset button. Additionally, the measurement is stopped and it is not possible to start a new measurement until the error is corrected. The user has to check:

- Has the gain state not been changed while the system was powered on?
- Is the SD card in the slot?
- Is the SD card broken?
- Are not more than 999 measurements on the SD card?

When the error is corrected the user pushes the reset button. It is prevented that the user does sampling sessions without actually storing any measured data. Furthermore, there cannot be a failure in the measured data caused by the change of the gain state of the signal conditioning unit. After changing the gain state, a reset of the system is necessary because the adjustment procedure of the system needs to be run.

Usability was considered when designing the user interface of the data acquisition device depicted in Figure 5-32. During the setup and the adjustment of the measuring system both the measurement and error LED button are lit. When the system is ready to sample the lights are switched off.

The measurement is started by pushing the measurement button. If a measurement is running the measurement button is lit in green. To stop the measurement, the measurement button which is lit in green needs to be pushed again and the light switches off. If an error occurs the error button is lit in red and if a measurement was running the measurement LED is turned off. After going through the previously explained error check list, the user needs to push the lighted error led in order to restart the setup. Basically, the user only needs to push the button which is currently lit. The gain state is adjusted with the gain state switch to detect low loads or high loads.

Direct feedback which gain state is currently applied is given by the yellow LEDs besides the text *Low Forces and Torques* and *High Forces and Torques*. The LED besides the applied gain state is lit.

Figure 5-32: User interface of the data acquisition unit

Prototypes were used to test the data acquisition unit. Interfaces to the signal conditioning unit were simulated to test the functions of the data acquisition unit. It was possible to determine the performance of the data acquisition unit and to compare alternative solutions. For critical functions the data acquisition was divided in further subsystems for which prototypes were built and tested. The best solutions were used for the comprehensive prototype of the data acquisition unit, to which the subsystems were consecutively added. This approach enabled an effective trouble shouting and allowed to be aware of what the system is capable of.

Besides the main function of storing the data, the system needs to control the multiplexers and adjusts the instrumentation amplifier. In order to test the data acquisition system and its interaction with the other components of the measuring system the prototype depicted in Figure 5-33 was used.
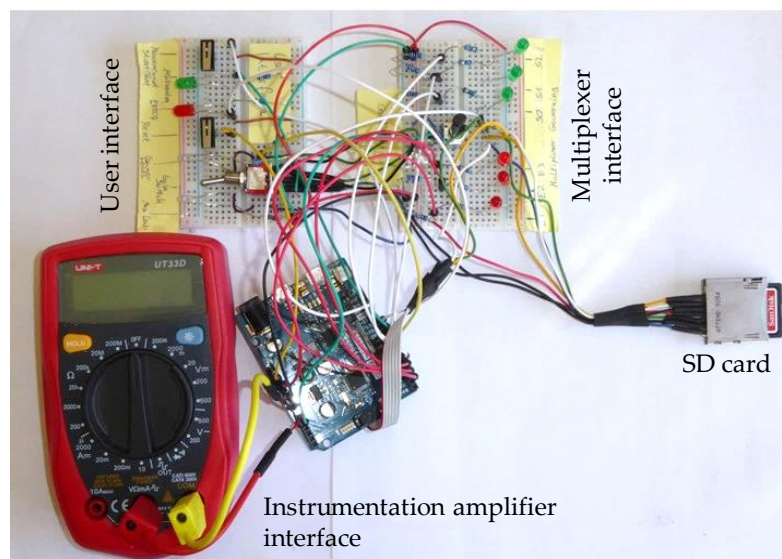
Figure 5-33: Prototype and simulated interfaces of the data acquisition unit

It was possible to simulate all functions of the user interface with start/stop-button, measuring-LED, reset-button, error-LED, amplification-switch and amplification-state-LEDs. For the interface with the multiplexers the adjustment signal for the multiplexers was visualised with green

and red LEDs. Furthermore, the interface with the instrumentation amplifier was set up with a potentiometer and a multimeter. The potentiometer was used to simulate the varying measuring signal which is sent from the instrumentation amplifier to the data acquisition unit. With the multimeter the voltage, which the data acquisition unit applies to the reference pin of the instrumentation amplifier, is visualised. The values logged by the data acquisition unit could be read from the SD card.

5.6.7 Power Supply

In order to power the measuring system a suitable power supply is needed. A mobile power supply is required as the in situ testing will take place on the road. Different voltages are needed for the modules of the measuring system. Following, information on the setup of the power supply is given. Furthermore, the influence of the power supply on the accuracy of the measuring system and the prototypes which was built is explained.

The Setup which was finally used for the measuring system comprises a customised battery produced by Altitec Service AS. The battery pack comprises two units which both provide 6.4 V. As they share the same ground a +6.4 V, a 0 V and a -6.4 V output is possible. For the setup the LiFePo4 battery 18650 is used. Two of the batteries are arranged in series. This leads to the 6.4 V output and enables a maximal current output of 4.5 A which is far above the required 300 mA. In total there is a capacity of 3 Ah which is sufficient for 10 hours of data logging. The two units of the battery pack need to be charged separately.

In order to provide the suitable voltage for the signal conditioning unit and data acquisition unit Schottky diodes are used. A combination of diodes in row with different output voltage drops leads to the required voltage drop. Schottky diodes are used as they have a more stable voltage drop than common diodes or Z-diodes have for changing temperatures. As depicted in Figure 5-34 the diodes were used for the voltage drop to 3.3 V needed for the Wheatstone bridges and the Arduino board and to ±5 V needed for the multiplexers. For the instrumentation amplifiers the ±6.4 V could be used without voltage reduction.

The Arduino Zero of the data acquisition module and the Wheatstone bridges of the signal conditioning unit are powered by the same voltage due to accuracy reasons. Using the same power supply for the excitation of the Wheatstone bridges and the Arduino has the purpose that an uncertain voltage drop of the battery would not lead to an error. When the excitation voltage U_0 of the Wheatstone bridge is changing the measured output voltage U_M of the bridge is changing as well. The input and the output voltage are linearly related to each other like shown in equation (5-3) [6]. The measured strain is ε and k is the bridge-factor of the strain gauge.

$$U_M = U_0 \, k \, \varepsilon \tag{5-3}$$

If the excitation voltage of the Wheatstone bridges drops the reference voltage of the Arduino drops as well which leads to a reduced measuring range of the A/D-converter. Within the reduced measuring range the reduced output voltage leads to a correct measurement.

A symmetric power supply of the multiplexers is needed as they only are able to transfer input voltages to their output which are within the supply range [79]. Both positive and negative strain needs to be measured which leads to a positive and negative output voltage of the Wheatstone bridge. Similar to the multiplexers a symmetric power supply is needed for the instrumentation amplifier to enable amplification of negative voltages [70].
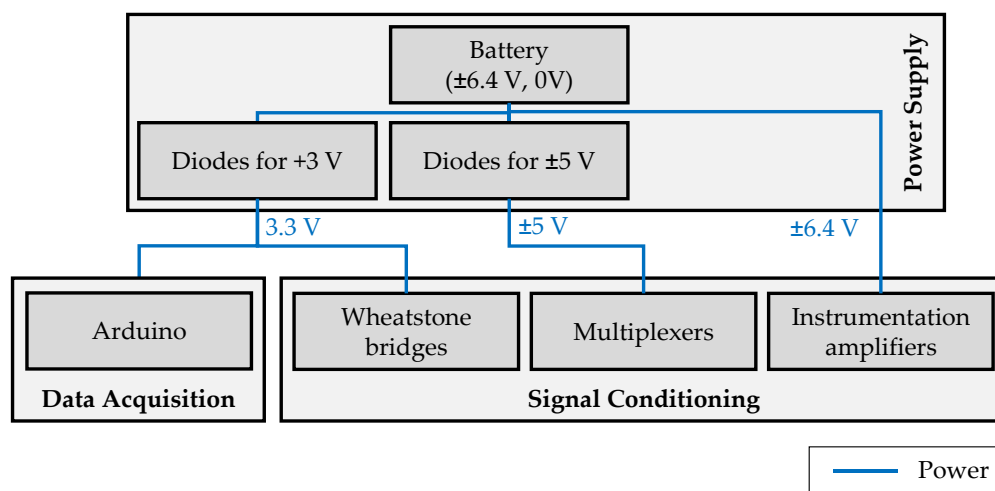
Figure 5-34: Setup of the power supply

Accuracy of the measuring system was taken care of by providing power with low noise. In order not to influence the signal which is passed through the multiplexers or amplified by the instrumentation amplifiers the voltage supply of those components may not induce any noise. Furthermore, the bridge excitation voltage and the voltage of the Arduino should not induce any noise. Therefore, the prototypes of the power supply were tested with an oscilloscope. The different subsystems of the power supply were tested separately and together, in order to find out which component the voltage ripple belongs to. Improving the solution for the power supply to a system which is solely based on batteries and diodes, there is now a power supply which only causes negligible noise.

Measuring errors due to a drop of the supply voltage were prevented by powering the Arduino board with the same voltage as the Wheatstone bridges. Furthermore, the multiplexers and the instrumentation amplifiers are powered with a voltage which is higher than required to lead the measuring signal trough and to amplify it.

The Prototypes of the power supply unit were tested with an oscilloscope. This was crucial in order to find out, how much noise is added to the measuring signal by the power supply. Furthermore, the output voltage was measured with multimeters at the interface of the power supply

to the rest of the measuring system. This was necessary in order not to destroy the measuring system due to overvoltage when connecting the power supply.

5.6.8 Data Processing

The data stored on the SD cards by the data acquisition device is transferred to the computer by the user. The files, which should be processed, are copied from the SD card to the folder *Test Data*. When the Matlab script is run, the data from this folder are processed and results are stored to the folder *Results*. Matlab generates a subfolder in the *Results* folder, which contains the processing date and time in its name. In this folder the measuring protocol and the figures of force and torque are stored. The automatically written protocol contains information on the sampling frequency of the measuring session, the gain the system was adjusted to, the maximal and minimal loads which occurred and when they occurred. The position for which the loads should be calculated can easily be adapted in the code. By default, it is set to the position which is at the intersection of the neutral layers of the beam and the binding link.

When the user starts the data processing are the loads are calculated automatically in four steps visualised in Figure 5-35. First, the data are imported from the .txt-file to Matlab. Then the strain of the different sensor positions is determined. As there is a multiaxial strain state the loads cannot be derived from the strain. Therefore, the stress at the positions of the strain gauge rosettes is determined and in the last step the loads are derived from the stress. The previously mentioned folders and the *Run* button in Matlab represent the user interface. The Matlab code can be found in Appendix F. Following, the steps of the data processing are explained.
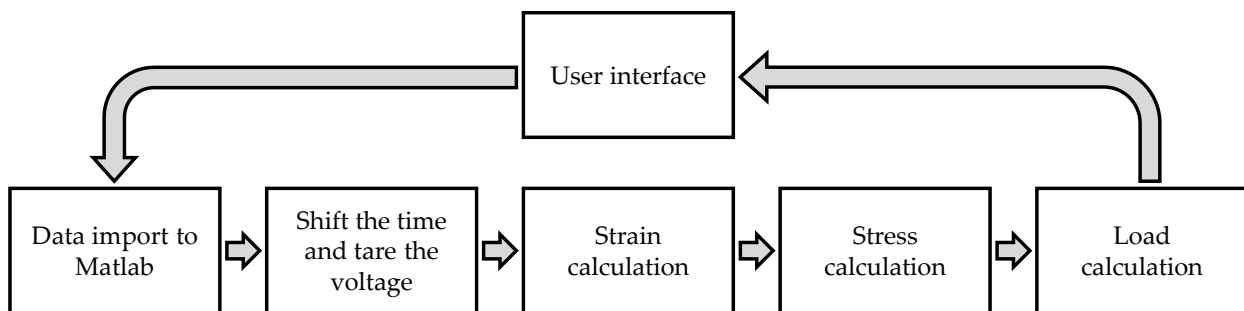
Figure 5-35: Processing of the measured data

Import of the data is done from the files, which are in the folder *Test Data*. If there are several sub files of measurements in the folder the data are automatically imported in chronological order.

The data from the SD card comprises a time vector in the first column, the measured voltages for the 24 strain gauges in column 2 to 25 and the gain state in column 26. The time vector shows the time determined by the millis-function of the Arduino. This function returns the time since the Arduino was booted. Therefore, the first measurement is not at 0 ms as the measurement is not directly started when the Arduino finished booting. The measured voltage is in the range between 0 V and 3.3 V and is given in values between 0 and 4095 as the microcontroller has a 12-bit

resolution. When the measuring system was set to a gain suitable to determine loads during common use, 1 is written in the last column. If the gain was set to enable acquisition of maximum loads, 2 is written in this column.

The time of the samples is shifted so that the first sample is at 0 ms. This enables to display the time in a comprehensive way. Furthermore, there is a tare function for the measured voltage in order to eliminate static influences on the accuracy of the measuring system. The mean value of the first 20 samples is subtracted from the measured voltage. This is done in order to compensate the imbalance of the Wheatstone bridges caused by temperature changes on the transfer cable and the resistance added by the multiplexers. Moreover, this sets the output of all strain gauges to the same level. The first 20 samples are averaged in order to compensate the fluctuation of the A/D-converter of the data acquisition unit. For the purpose of not to tare the system to a wrong level, the roller ski has to be unloaded for the first second when a measurement was started.

Strain Calculations are conducted with use of the imported data. As depicted in Figure 5-36 several steps are required to measure the actual strain at the strain gauges with the Arduino. The voltage U_M at the measuring points D and B of the Wheatstone bridge is amplified by the instrumentation amplifiers with the gain factor G to the voltage $U_{\overline{M}}$. For the calculation the offset added by the second instrumentation amplifier is not regarded because it is compensated by the previously explained tare function. The output of the instrumentation amplifiers is measured by the A/D-converter of the Arduino and written on the SD card in values N between 0 and 4095. The digitalisation is done with respect to the voltage increments U_{LSB} of the A/D-converter.
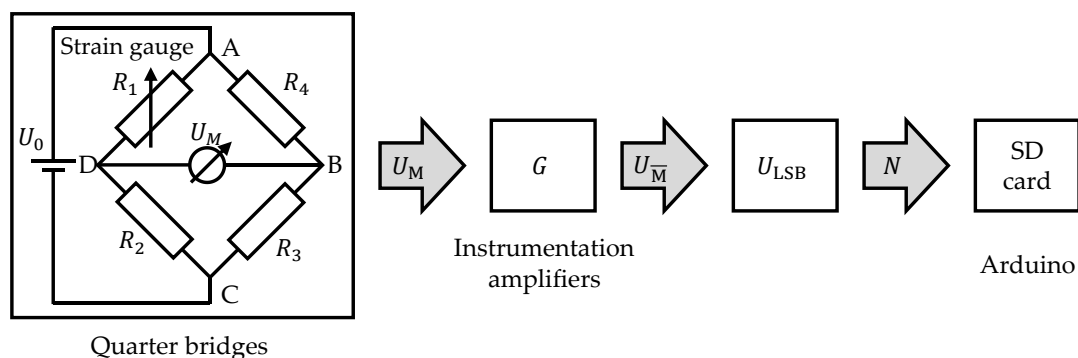
Figure 5-36: Processing of the recorded voltage and the strain at the strain gauges

The voltage U_M between the measuring points D and B of the Wheatstone bridge depicted in Figure 5-36 depends on the bridge excitation voltage U_0 and the resistance of the resistors R_1, R_2, R_3 and R_4 [6].

$$U_M = U_0 \left(\frac{R_1}{(R_1 + R_2)} - \frac{R_4}{(R_3 + R_4)} \right) \tag{5-4}$$

For the quarter bridge the resistor R_1 is a strain gauge and changes resistance by ΔR due to the applied strain. Equation (5-4) is rearranged to equation (5-5) with $R = R_2 = R_3 = R_4$ and $R_1 = R + \Delta R$ [6].

$$U_{\mathrm{M}} = U_0 \frac{\Delta R}{2\,(2\,R + \Delta R)} \tag{5-5}$$

Equation (5-5) can be simplified with $\Delta R \ll R$ to equation (5-6) as the change in resistance of the strain gauge is extremely small compared to its nominal resistance [6].

$$U_{\mathrm{M}} = U_0 \frac{\Delta R}{4\,R} \tag{5-6}$$

The dependency between the ratio $\Delta R/R$ and the strain ε is defined by equation (5-7) introducing the constant bridge factor k of the strain gauges [6].

$$\frac{\Delta R}{R} = k\,\varepsilon \tag{5-7}$$

With equation (5-6) and (5-7) the dependency between the voltage U_{M} and the strain ε results.

$$\varepsilon = \frac{4\,U_{\mathrm{M}}}{k\,U_0} \tag{5-8}$$

The instrumentation amplifiers scale the signal with the amplification factor G to the output signal $U_{\overline{\mathrm{M}}}$. The respective gain of the measurement is determined reading the gain state 1 for low loads or 2 for high loads from the last column of the data on the SD card. For the specific gain states, a gain factor G is set.

$$U_{\overline{\mathrm{M}}} = U_{\mathrm{M}}\,G \tag{5-9}$$

The voltage needs to be transferred to a real valued voltage as the Arduino stores the measured voltage in values N between 0 and 4095 of its 12-bit measuring range. Between two values N ther is the voltage increment U_{LSB} which is the relation between the measuring range of the A/D-converter and the 4096 possible output values.

$$N = \frac{U_{\overline{\mathrm{M}}}}{U_{\mathrm{LSB}}} \tag{5-10}$$

Equation (5-8), (5-9) and (5-10) result in equation (5-11) which is the dependence between the recorded values U_{Inc} on the SD cards and the strain ε at the strain gauges.

$$\varepsilon = \frac{4\,N\,U_{\mathrm{LSB}}}{k\,G\,U_0} \tag{5-11}$$

Stress Calculation is necessary as the loads cannot be derived directly from the strain due to the multiaxial strain state. More detailed information on the difficulty due to the multiaxial strain state is given in chapter 5.6.4. The strain needs to be transformed into normal and shear stress which are related to the loads. For the individual positions of the rosettes the stress is calculated

in three consecutive steps, illustrated in Figure 5-37. First, the principal stresses and their directions are derived from the strain measured at the individual strain gauges of the rosettes. Then the normal and shear stress in the a-c-coordinate system of the rosettes is calculated. Finally, the calculated normal and shear stress is transferred to the coordinate system of the roller ski. For the calculation of the stress the formulas of the book *Smart Materials* [6] of the strain gauge supplier HBM are used.
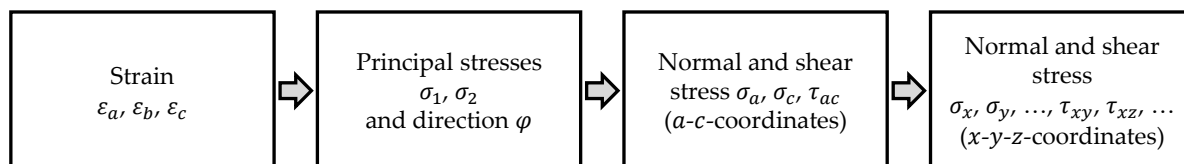
Figure 5-37: Calculation of normal and shear stresses from the strain at the strain gauges

The principal stresses are determined with equation (5-12). E is the Young's modulus and v the Poisson's ratio of aluminium 6061-T6, which the beam of the roller ski is made of. The strains ε_a, ε_b and ε_c are measured at the three strain gauges of the rosettes.

$$\sigma_{1,2} = \frac{E}{1-v} \frac{\varepsilon_a + \varepsilon_c}{2} \pm \frac{E}{\sqrt{2}(1+v)} \sqrt{(\varepsilon_a + \varepsilon_b)^2 + (\varepsilon_c + \varepsilon_b)^2} \qquad (5\text{-}12)$$

In Figure 5-38 the orientation of the three strain gauges is illustrated for the rosette type 1-RY93-3/350 which is used for the setup.
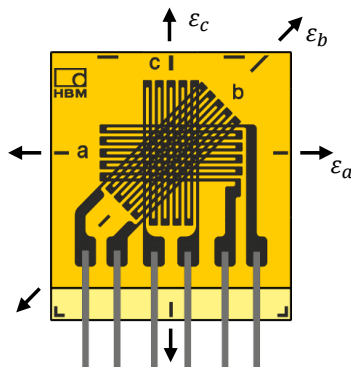
Figure 5-38: Orientation and alingnment of the strain gauges of the rosette 1-RY93-3/350, adapted from [6]

Due to the ambiguity of the tangent the direction φ of the first principal stress σ_1 has to be calculated in two steps. First, the smallest angle ψ between the a-axis of the rosettes and the σ_1-axis is calculated with equation (5-13), (5-14) and (5-15).

$$\psi = \arctan\left(\frac{N}{D}\right) \qquad (5\text{-}13)$$

$$N = 2\,\varepsilon_b - \varepsilon_a - \varepsilon_c \qquad (5\text{-}14)$$

$$D = \varepsilon_a - \varepsilon_c \qquad (5\text{-}15)$$

Secondly, cases have to be distinguished for positive and negative nominators (5-14) and denominators (5-15) of equation (5-13). As depicted in Figure 5-39 the angle φ between the direction of the first principal stress σ_1 and the a −axis is calculated with the formulae (5-16), (5-17), (5-18) or (5-19) depending on the algebraic sign of the nominator N and denominator D.

$$N \geq 0; D > 0: \qquad \varphi = \frac{1}{2}(0 + \psi) \tag{5-16}$$

$$N > 0; D \leq 0: \qquad \varphi = \frac{1}{2}(\pi - \psi) \tag{5-17}$$

$$N \leq 0; D < 0: \qquad \varphi = \frac{1}{2}(\pi + \psi) \tag{5-18}$$

$$N < 0; D \geq 0: \qquad \varphi = \frac{1}{2}(2\pi - \psi) \tag{5-19}$$
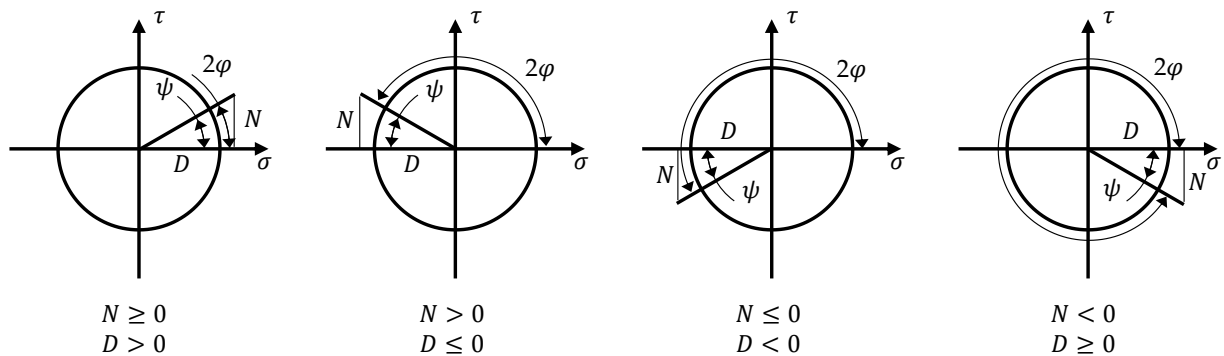
Figure 5-39: Ambiguity of the tangent: Relation between the algebraic sign of the nominator and denominator and the direction of the first principal stress σ_1, adapted from [6]

The normal stress in direction of the a-axis of the strain gauge rosette is calculated with equation (5-20) and the normal stress in direction of the c-axis with equation (5-21). For the shear stress τ_{ac} and τ_{ac} equation (5-22) is utilised.

$$\sigma_a = \frac{\sigma_1 + \sigma_2}{2} + \frac{\sigma_1 - \sigma_2}{2}\cos(2\varphi) \tag{5-20}$$

$$\sigma_c = \frac{\sigma_1 + \sigma_2}{2} - \frac{\sigma_1 - \sigma_2}{2}\cos(2\varphi) \tag{5-21}$$

$$\tau_{ac} = \tau_{ac} = \frac{\sigma_1 - \sigma_2}{2}\sin(2\varphi) \tag{5-22}$$

The transformation of the normal and shear stress from the a-c-coordinate system to the roller ski based coordinate system is done individually for each rosette depending on its orientation.

Load Calculation is conducted in the coordinate system which is situated in the centre of area of the intersectional area of the beam of the roller ski. The loads are determined by comparing the stress determined for the positions of the rosettes with respect to the geometric properties of the beam of the roller ski. The positions of the rosettes are depicted in Figure 5-40 a). The loads and

their directions at the rosette positions are shown in Figure 5-40 b). For the calculation of the loads a linear stress function over the height and the width is assumed. This assumption can be made as it is shown in chapter 5.6.4 that the sensors are placed at a sufficient distance from groves in the profile. Furthermore, the deformation was determined to be elastic with the FEM simulation introduced in chapter 5.6.4.
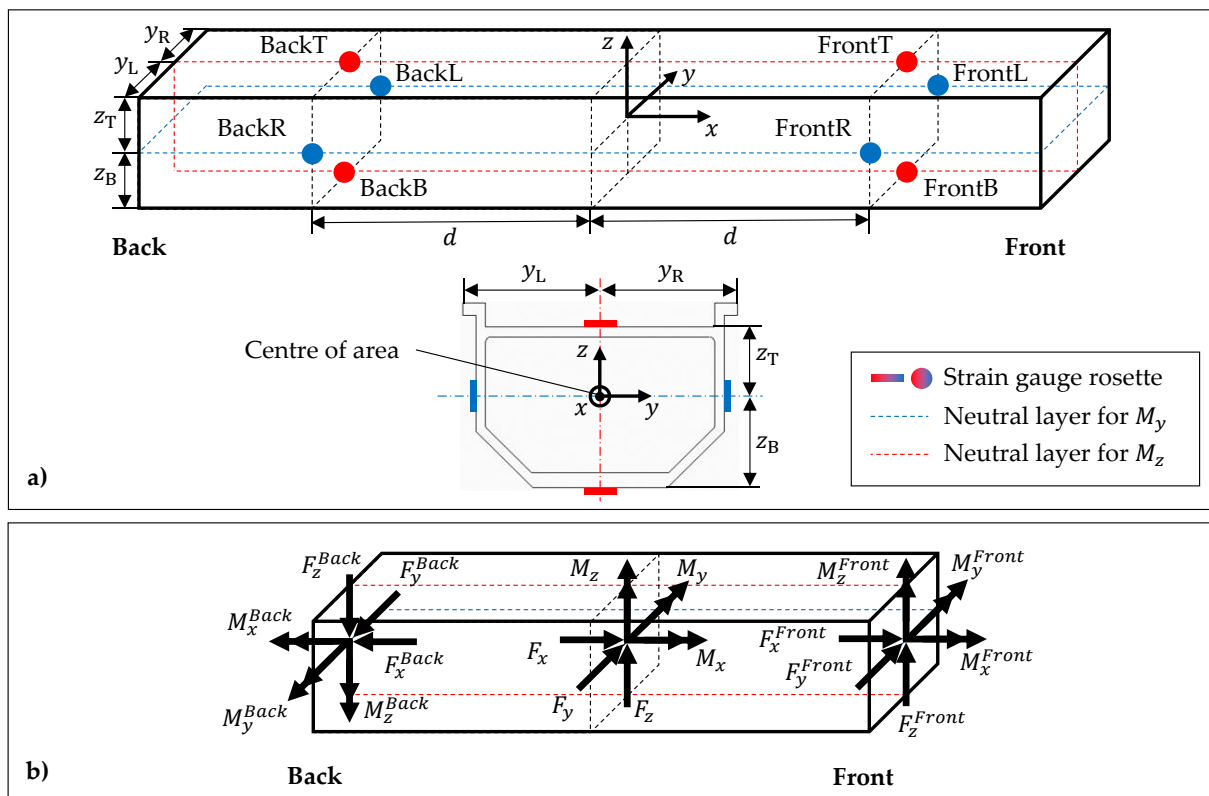
Figure 5-40: Measures and loads at the beam of the roller ski: a) Neutral layer for bending and the positions of the strain gauge rosettes, b) Direction of the forces and torques

The torque M_x is calculated by regarding the shear stress τ_{xz} at four positions. Equation (5-23) shows that for a torque M_T along the beam the maximal shear stress τ_{max} occurs at the position with the minimal thickness h_{min} of the profile.

$$\tau_{max} = \frac{M_T}{2\,A_m\,h_{min}} \tag{5-23}$$

A_m is the area which is surrounded by the middle line of the profile [75]. The minimal thickness is on the left-hand and right-hand side of the profile. Therefore, the four rosettes on the left-hand and right-hand sides of the profile were utilised for the calculation of M_x.

In addition to the shear caused by the twisting torque M_x the forces F_y and F_z perpendicular to the profile cause shear. However, the shear stress caused by a force has the same direction on the left-hand and the right-hand side of the profile as shown in Figure 5-41. Therefore, the influence of the shear forces can be eliminated by regarding the difference between the left-hand and right-hand side of the profile.

The difference of the shear stress τ_{xz}^{BackL} at the rear left-hand side and τ_{xz}^{BackR} at the rear right-hand side is used to determine the torque M_x^{Back} at the rear end. For the torque M_x^{Front} at the front end, the difference of the shear stress $\tau_{xz}^{\text{FrontL}}$ and $\tau_{xz}^{\text{FrontR}}$ on the left-hand and right-hand side is analysed.
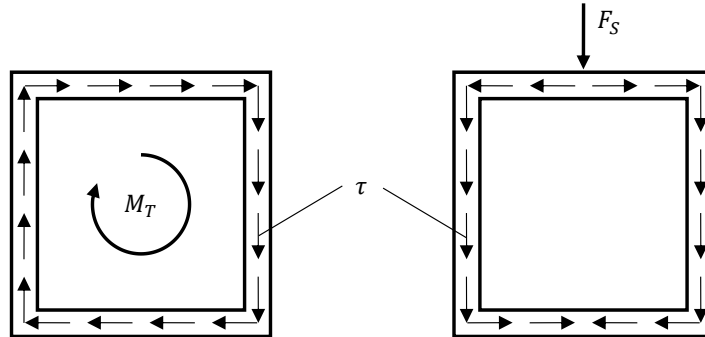
Figure 5-41: Shear stress caused by a torque and by a shear force, with [75]

The torque function along the beam has a step at the position of the binding where the athlete induces a torque. With Figure 5-40 b) the equation (5-24) for the torque M_x is determined. This leads to equation (5-25) with use of equations (5-23) for the coefficients.

$$M_x = M_x^{\text{Back}} - M_x^{\text{Front}} \tag{5-24}$$

$$M_x = \frac{A_{\text{m}}\, h_{\text{min}}}{4} \left[\left(\tau_{xz}^{\text{BackL}} - \tau_{xz}^{\text{BackR}} \right) - \left(\tau_{xz}^{\text{FrontL}} - \tau_{xz}^{\text{FrontR}} \right) \right] \tag{5-25}$$

The forces F_y and F_z and cause shear stress as depicted in Figure 5-41. It would be possible to use the shear function along the beam of the roller ski to calculate the forces F_y and F_z from the shear determined for the positions of the strain gauge rosettes. However, the shear stress caused by forces is relatively small compared to the shear stress caused by torque. It was found that the maximal expected load of $F_z = 1748$ N causes only $\tau_{xz} = 3656$ Pa which is extremely small compared to the $\tau_{xz} = 5.05$ MPa caused by the maximal expected torque $M_x = 13$ Nm. The calculations can be found in Appendix K. For small stress values the noise has a larger share than for high stress values as the noise is constant.

Due to this reason the forces F_y and F_z are determined considering the normal stress σ_x which they cause by bending the beam of the roller ski. For the maximal expected bending force $F_z = 1748$ N the normal stress on the lower side of the beam is $\sigma_x = 63$ MPa which is significantly higher than the resulting shear stress. Therefore the approach of Feng et al. [52] was used for the calculation of the remaining loads. They showed with their device to measure wheel forces of a car, how it is possible to determine loads in multiple directions mounting several strain gauges on the bending element.

The loads F_x, F_y, F_z, M_y and M_z cause normal stress σ_x by stretching or bending the beam of the roller ski. The measured normal stress σ_x at the different rosette positions is caused by superposition of the stress which is induced by the loads.

The force F_x is perpendicular to the cross section of the beam of the roller ski and is calculated with equation (5-26) considering the intersectional area A_S of the beam [75].

$$F_x = A_S \, \sigma_x \qquad (5\text{-}26)$$

Regarding the direction of the force F_x^{Back} in the rear and the force F_x^{Front} in the front in Figure 5-40 b) equation (5-27) was set up.

$$F_x = F_x^{\text{Back}} - F_x^{\text{Front}} \qquad (5\text{-}27)$$

As depicted in Figure 5-42 a) the force F_x causes the same stress σ_x at all four sides of the beam. With the mean value of the stress in x-direction at the front right-hand side σ_x^{FrontR} and the front left-hand side σ_x^{FrontL} it possible to calculate F_x^{Front}. Torques around the y-axis do not cause stress at the rosette positions at the right-hand and the left-hand side as they are in the neutral layer of M_y. The proportion of M_z of the stress is eliminated by utilizing the mean value of the stresses at the right-hand side and left-hand side.

For the calculation of F_x^{Back} the stress in x-direction at the rear right-hand side σ_x^{BackR} and rear left-hand side σ_x^{BackL} are utilised. With use of equation (5-26) the factors for F_x^{Front} and F_x^{Back} are determined and with equation (5-27) it is possible to set up equation (5-28) to determine F_x.

$$F_x = \frac{A_S}{2} \left[\left(\sigma_x^{\text{BackR}} + \sigma_x^{\text{BackL}} \right) - \left(\sigma_x^{\text{FrontR}} + \sigma_x^{\text{FrontL}} \right) \right] \qquad (5\text{-}28)$$

Figure 5-42 a) shows that the loads F_y, F_z, M_y and M_z bend the beam of the roller ski and can be determined by regarding the stress difference between the right-hand and the left-hand or the bottom and the top side. Regarding the difference of σ_x at the individual positions eliminates the influence of the force F_x. Furthermore, the calculated stress differences at the front side and the back side need to be compared in order to determine the proportion of the bending forces and the bending torques. As depicted in Figure 5-42 b) bending forces in the positive direction cause positive stress in the front and in the back at one side of the beam and negative stress on the other side. In contrast, positive bending torques cause positive stress on one side of the beam at the back and negative stress on the same side in the front. On the other side of the beam the algebraic sign of the stress is vice versa.
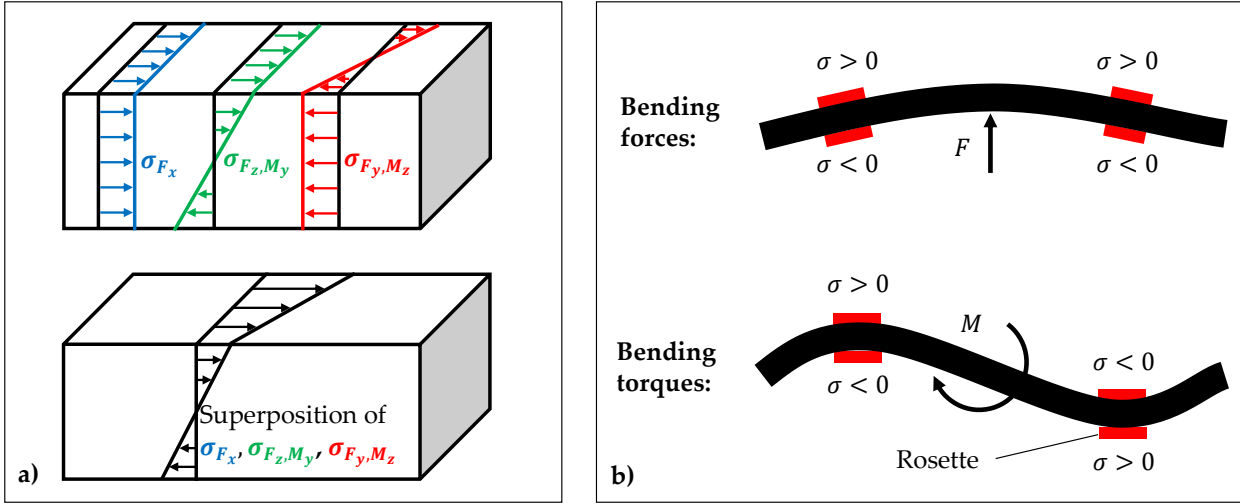
Figure 5-42: Different stress progression caused by the loads F_x, F_y, F_z, M_y and M_z: a) In the back or the front at beam of the roller ski, b) In the back and the front of the beam of the roller ski

The bending forces F_y or F_z are virtually shifted to the strain gauge positions and the couples M_z^{Back} and M_z^{Front} or M_y^{Back} and M_y^{Front} need to be added [76]. The couples are calculated with equation (5-29) and the lever d introduced in Figure 5-40 a) [76].

$$F = \frac{M}{d} \tag{5-29}$$

Equation (5-30) is utilised for the transfer from the torques to the normal stress σ_x [75].

$$\sigma_x = \frac{M_y}{I_y} \, z - \frac{M_z}{I_z} \, y \tag{5-30}$$

The second moments of inertia I_y and I_z were calculated for the profile with respect to the centre of area coordinate system. The calculations can be found in Appendix I. The forces F_y and F_z are calculated using the stress at the individual rosettes and the coordinates y and z. Equation (5-31) and (5-32) were used to calculate the forces.

$$F_y = \frac{I_z}{2\,d} \left[\left(\frac{\sigma_x^{\text{BackL}}}{y_{\text{L}}} - \frac{\sigma_x^{\text{BackR}}}{|y_{\text{R}}|} \right) + \left(\frac{\sigma_x^{\text{FrontL}}}{y_{\text{L}}} - \frac{\sigma_x^{\text{FrontR}}}{|y_{\text{R}}|} \right) \right] \tag{5-31}$$

$$F_z = \frac{I_y}{2\,d} \left[\left(\frac{\sigma_x^{\text{BackT}}}{z_{\text{T}}} - \frac{\sigma_x^{\text{BackB}}}{|z_{\text{B}}|} \right) + \left(\frac{\sigma_x^{\text{FrontT}}}{z_{\text{T}}} - \frac{\sigma_x^{\text{FrontB}}}{|z_{\text{B}}|} \right) \right] \tag{5-32}$$

Firstly, the difference of the stress caused by the bending on the left-hand and the right-hand side is regarded in order to eliminate the influence of the normal force F_x. Then the difference in the front and the back is used to eliminate the influence of the torques M_y and M_z. The coefficients are derived from equation (5-29) and (5-30). The position of the stress in relation to the intersection of the neutral layers for bending in y- and z-direction is given with y_{L} for the left-hand position, y_{R} for the right-hand position, z_{T} for the top position and z_{B} for the bottom position.

Torques can be virtually shifted without adding virtual forces or couples [76]. Similar to the calculation of the bending forces the influence of the normal force F_x is eliminated. Than the previously explained effect that the stress for torques is different in the front and the back is used. The effect of the bending forces is eliminated by analysing the difference of the strain in the front and in the back. This leads to equation (5-33) for M_y and equation (5-34) for M_z.

$$M_y = \frac{I_y}{2} \left[\left(\frac{\sigma_x^{BackT}}{z_T} - \frac{\sigma_x^{BackB}}{|z_B|} \right) - \left(\frac{\sigma_x^{FrontT}}{z_T} - \frac{\sigma_x^{FrontB}}{|z_B|} \right) \right] \tag{5-33}$$

$$M_z = -\frac{I_z}{2} \left[\left(\frac{\sigma_x^{BackL}}{y_L} - \frac{\sigma_x^{BackR}}{|y_R|} \right) - \left(\frac{\sigma_x^{FrontL}}{y_L} - \frac{\sigma_x^{FrontR}}{|y_R|} \right) \right] \tag{5-34}$$

The coefficients are derived from equation (5-30) which shows the relation of bending torque and normal stress.

The loads F_x, F_y, F_z, M_x, M_y and M_z are referred to the centre of area of the profile. However, they can be transferred to the position chosen by the user. The torques can just be shifted but for the shift of the forces a couple needs to be added [76]. For the chosen position the forces are given by the following equations.

$$F_{xS} = F_x \tag{5-35}$$

$$F_{yS} = F_y \tag{5-36}$$

$$F_{zS} = F_z \tag{5-37}$$

The torques depend on the position of the shifted system as the couples for the shift of the forces need to be added. With the shift by x_S, y_S and z_S depicted in Figure 5-43 the shifted torques result in the subsequent equations.

$$M_{xS} = M_x - F_y\, z_S + F_z\, y_S \tag{5-38}$$

$$M_{yS} = M_y + F_x\, z_S - F_z\, x_S \tag{5-39}$$

$$M_{zS} = M_z - F_x\, y_S + F_y\, x_S \tag{5-40}$$
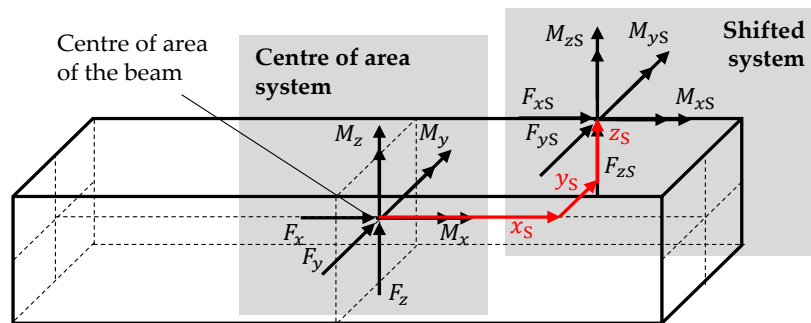
Figure 5-43: Loads in the centre of gravity and loads at a shifted coordinate system

5.6.9 Calibration

The guideline *Kalibierung von Dehnungsmessstreifen und DMS-basierten Sensoren* [82] published by the IMC Meßsysteme GmbH was followed for the calibration of the measuring system. The zero adjustment of the measuring system is done by the tare function included in the Matlab script for processing of the recorded sensor output. The initial sensor output at the beginning of a measurement is subtracted from the recorded output to shift the values to the right value in order to compensate disbalance of the Wheatstone bridges.

The amplification of the output signal of the strain gauges was calibrated by comparing the measured strain to the actual strain. With the setup depicted in Figure 5-44 a) it was possible to calibrate the strain gauges which are aligned with the beam of the roller ski. An increasing one-dimensional stress state aligned with the beam of the roller ski was applied adding weights to the weight container. For eight different loads the strain ε_R of the beam of the roller ski was calculated and compared to the measured strain ε_M of each strain gauge aligned with the longitudinal axis of the roller ski. The calibration factor k_C was added in order to equalise the measured and the real strain.

$$\varepsilon_R = k_C \, \varepsilon_M \tag{5-41}$$

The calibration factor k_C can be read from Figure 5-44 b) for the different strain gauges. It is the reciprocal of the line of best fit for the strain output of each strain gauge.
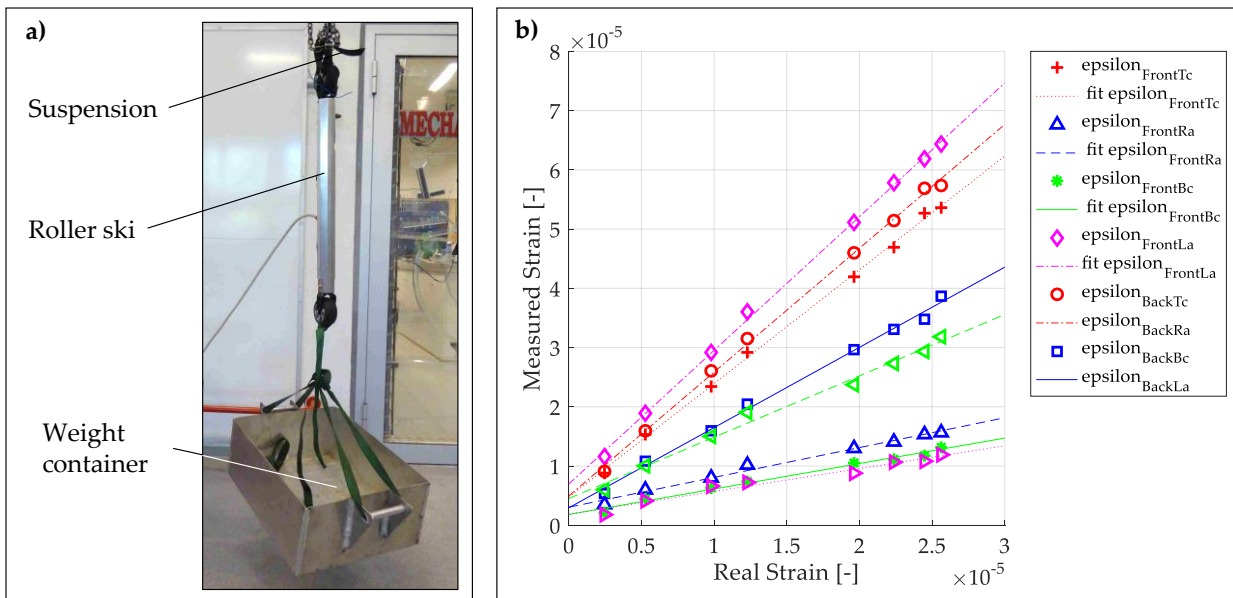
Figure 5-44: Calibration of the strain gauges alinged with the beam of the roller ski:
a) Calibration setup, b) Resulting strain output

For the strain gauges in 90° direction to the longitudinal axis of the roller ski no suitable calibration setup was available. However, it was possible to clamp the roller ski at the back wheel and to induce a torque around the longitudinal axis of the beam of the roller ski. For this load case the same shear strain should apply for all of the 90° strain gauges. The absolute value of the applied

torque was unknown but it was possible to equalise the measured strain of the 90° strain gauges to a mean output. The same was done for the strain gauges in 45° direction.

5.7 Recapitulation and Learning

For the purpose of continuous improvement, the development project and the resulting measuring system were scrutinised. In order to assess the success of the project the resulting measuring system was verified and validated. Verification was conducted by reviewing whether the measuring system meets the specifications of the requirement list. The system was ascertained to meet the target state. Validation was conducted in order to approve that the measuring system is applicable in the desired way and has the desired use. The success of the methodical approach for the development of the measuring system was analysed. A detailed discussion can be found in chapter 6.2.

5.7.1 Verification

The measuring system was approved to meet the desired target state in most of the specifications of the requirement list. It is possible to record spatial forces and torques during almost all situations which could occur during roller skiing. A more detailed discourse on the matching with the target state can be found in chapter 6.

The output of the measuring system was approved by applying static loads on the roller ski. Two athletes with different weight stood on the roller ski. The weight of the first athlete was determined to be 54.2 kg (532 N) with a common bathroom scale and the weight of the second athlete was 77.5 kg (760 N). In Figure 5-45 the output of the measuring system can be seen. Compared to the mean output of the measuring system there is a deviation of about 10 N only. Additionally, a fluctuation of about ±25 N occurs due to the noise added by the inaccuracy of the data logger.

Furthermore, it was tested whether the system is capable to detect rapidly changing loads caused by the athlete. The athletes bobbed up and down as fast as they could. In Figure 5-45 it can be seen, that the system was able to detect this as well. This proofs that 33 Hz are sufficient to detect loads caused by the athlete.
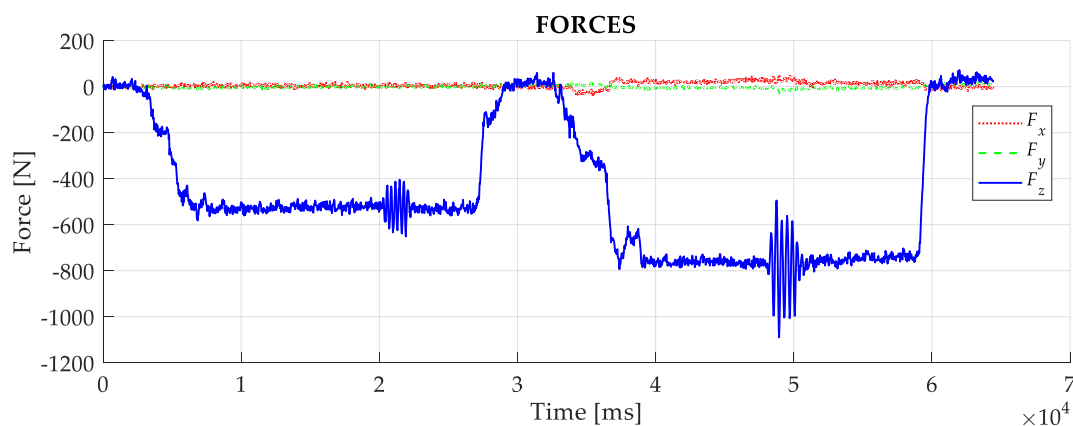
Figure 5-45: Static force applied in negative z-direction

5.7.2 Validation

The usability of the measuring system was investigated. It is easy to use the data acquisition box and the load data can be calculated easily with the Matlab script. During skiing there is no interference caused by the 190 g added to the weight of the roller ski. The transfer cable which is mounted on the leg of the athlete with hook and loop fasteners is not perceived at all. Furthermore, the drinking belt with the added 1600 g of the data acquisition box is experienced like a common drinking belt.

With the load data which can be recorded it will be possible to learn about the forces and torques caused by the athlete. This will enable the analysis and improvement of skiing technique. Comparing the recorded load functions with load data from the literature in Figure 5-46 it can be seen that the measuring system has a reliable output. Vertical forces on the roller ski during classic and skate skiing were compared with load data recorded by the most commonly used measuring system of the University of Jyväskylä in Finland.

In Figure 5-46 a) the forces are depicted which were detected during diagonal stride. The detected forces were compared with load data recorded by Ohtonen et al. [21]. When comparing the load force in vertical direction it needs to be known that positive forces of the developed measuring system are upwards in contrast to the measuring system of the University of Jyväskylä. It can be seen that the force progression is similar.
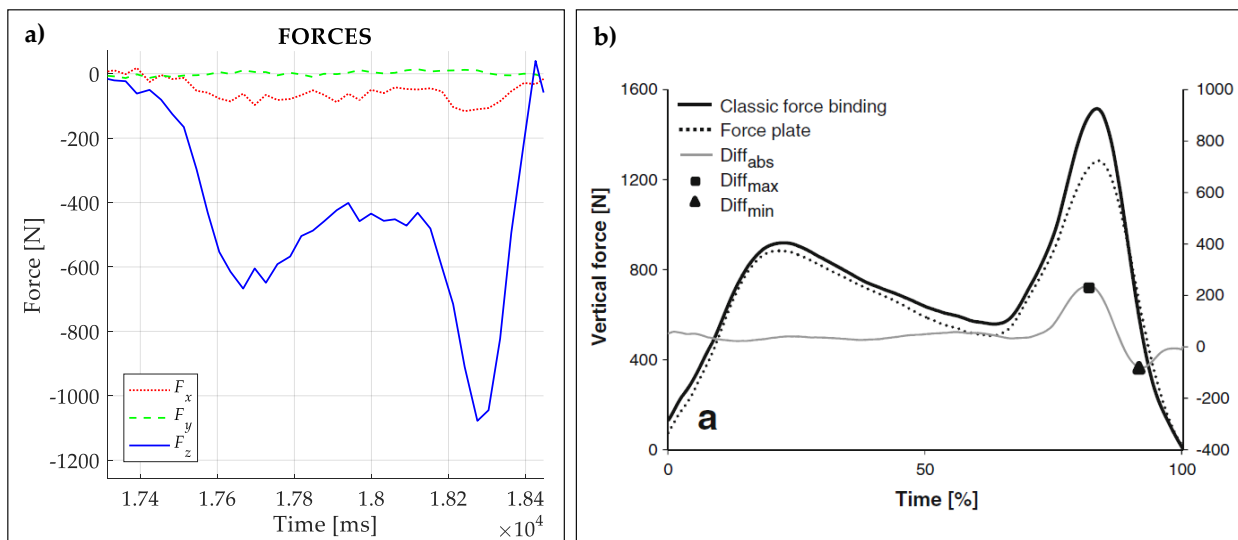
Figure 5-46: Validation of the recorded load data: a) Data with the developed measuring system recorded during classic skiing, b) Data recorded by the measuring system of the University of Jyväskylä in Finland during classic skiing [21]

It will not be possible to detect rapidly changing loads which occur for instance when skiing over a crack on the road at very high speed. However, it was possible to detect peak loads during jumping. This needs to be taken into account when using the load data for the dimensioning of roller skis or bindings.

6 Discussion

In this chapter the development process and the resulting measuring system are discussed. It is revealed how the measuring system matches the target state. Moreover, the reliability of the data which the measuring system records and the methodical approach which was used for the development is discussed in the following subchapters.

With the measuring system it is possible to record data during almost every situation which might occur during a roller ski training. Common loads as well as peak load events can be detected. The only situation which cannot be tested is getting stuck on a curb stone as there is the cover under the beam of the roller ski to protect the strain gauges.

The measuring system is able to measure spatial forces and torques without changing the roller ski-binding system. It was demonstrated that it is possible to measure spatial loads at the beam of the roller ski. The measuring systems detects reliable data as the leverage ratio is not changed and the weight of the roller ski was increased by only 190 g. The signal conditioning and data acquisition unit carried in a drinking belt weighs only 1600 g which is comparable to the weight of a drinking belt carried during a common training session.

The sampling frequency of the measuring system is 33 Hz which is sufficient to detect loads which are caused by the athlete. However, the measuring system is not capable to detect all of the loads which are caused by external circumstances for instance skiing over a crack. A sampling frequency higher than 1110 Hz would be needed to detect such events. The accuracy of the measuring system was determined to be 10 N for the mean value of vertical forces. For single force values there is an additional fluctuation of ±25 N. If a more potential measuring system should be achieved a higher budget and more time is needed.

The price of the electronical components for the final setup of the signal conditioning and data acquisition unit is about 500 € (4600 NOK). This is significantly lower than the price for commercially available solutions from HBM or National Instruments. The time needed for the development, testing and manufacturing of the system was substantial. The manufacturing of the measuring system excluding development and testing time took more than 250 hours. Though, it was demonstrated that it is possible to build a measuring system with low cost components.

As the entire measuring system is adapted to measure the loads acting between roller ski and binding it is easy to use. By pushing only one button on the data acquisition unit it is possible to record the data. Every athlete will be able to record data with this system. In order to evaluate the test data, it needs to be copied to a specific folder on the computer and the run-button in Matlab needs to be pushed.

6.1 Data Reliability

The accuracy of the measuring system was taken into account by several precautions to prevent errors in the sensor unit, the signal conditioning unit, the data acquisition unit and the power supply. In the following all of those precautions are summed up. More detailed information can be found in the respective subchapters of chapter 5.

The multiaxial stress state at the beam of the roller ski is taken into account by the use of the strain gauge rosettes. The rosettes enable the calculation of the principal stresses and their directions. With use of the principal stresses it is possible to calculate the loads correctly in contrast to calculating them from the strain directly.

FEM simulation of the strain distribution on the beam of the roller ski was done for the maximal expected loads in order to determine the optimal position of the strain gauges. It was ascertained that there is elastic strain only and that there is no excessive strain or a strain gradient at the positions of the rosettes caused by grooves or holes. Furthermore, the guidelines from the strain gauge supplier HBM were used to mount the strain gauges correctly. All of the strain gauges were mounted with a deviation less than 1 mm from their desired position and they are correctly aligned.

The connection between the strain gauges and the signal conditioning and data acquisition box is sensitive to noise caused by electromagnetic fields. Due to this reason cable shields are utilised to prevent influences from power lines and other sources of electromagnetic fields. In order to prevent cross talk between the output signal of the strain gauges a wire with twisted pairs is used.

The output signal of all 24 strain gauges is processed by the same instrumentation amplifiers and A/D-converter. Due to this reason the signal of all channels is amplified and digitalised equally. In order to achieve the same output voltage at all of the 24 Wheatstone bridges it was taken care to fulfil the initial balance condition by using suitable resistors. However, for the 24 bridges there is an unexpected disbalance between 0.8 mV and 5.5 mV. The linearity of the output signal is still granted but the amplification needed to be reduced to make sure that all of the channels are within the measuring range of the A/D-converter. The change of the output voltage caused by the strain gauges is small compared to the disbalance of some bridges. For the maximal expected loads there is a change of 2.3 mV only. Consequently, the change of the voltage uses only a small share of the measuring range of the A/D-converter which makes its accuracy more relevant. This

issue could be fixed by adding potentiometers in parallel with the strain gauges in order to regulate the output of the Wheatstone bridges to 0 V when there are no loads.

The stability of the measuring system is taken into account by a warm up time of 15 s for the entire system before sampling is enabled. Furthermore, the power supply of the multiplexers, instrumentation amplifiers, the SD card and the Arduino board is protected with bypass capacitors. Thus it is granted that the components do not induce a ripple on the power supply of the entire system which would cause a measuring error.

The measuring system is powered with batteries in order to not to add any noise to the system. For the A/D-converter at the Arduino board and for the Wheatstone bridges there is the same supply voltage. This prevents errors caused by a voltage drop at the batteries. Due to the linear correlation between the bridge excitation voltage and the output voltage of the bridges there is the same decrease at the reference voltage of the A/D-converter.

The multiplexers connect the 24 channels to the instrumentational amplifiers and the A/D-converter consecutively. When a channel is connected to the A/D-converter there is a setting time before sampling to enable the multiplexers and the instrumentation amplifier to rise the signal to the right level. As the channels are sampled consecutively there are 12 ms between the sample of the first and the last strain gauge. This might lead to an error of the load calculation in case of rapidly changing loads.

Between the channels there might be slight differences due to variances in the strain gauges, the connection cable and the Wheatstone bridges. Therefore, calibration of the measuring system is necessary. Loads were applied on the roller ski and the strain at the individual strain gauges was measured. With calibration factors the measured strain was adapted to the real strain which was calculated for the applied loads.

Data recorded with the measuring system was compared with available data from the literature and it was shown that the load functions fit very well. Furthermore, static tests for vertical forces were conducted. In order to assess the accuracy of all forces and torques a suitable test setup is needed.

6.2   Methodical Approach

The SPALTEN methodology introduced b Albers et al. [59] was used for the development process of the measuring system in order to achieve an optimal result. The stages *Situation Analysis* and *Problem Containment* allowed to learn what is really needed before starting to generate solutions and not to choose the first one which comes in mind. A precise definition of the target of the project helped especially in later stages to remain on the right track.

The methodical proceeding during *Search for Alternative Solutions* lead to the good solutions for the measuring system and even cross inventions were possible. Abstraction of the existing load

measuring systems made it possible to learn about their essential principles and enabled the combination of those principles. This enabled to find a solution for the measuring system which is capable to measure spatial forces and torques but does not change the roller ski-binding system and adds almost no weight to the roller ski.

The systematic selection of the solution during *Selection of Solutions* was important for later project stages. The best of the drafted solutions was selected. Moreover, the assurance was given that the effort is put into the right solution and not to switch to another one when difficulties occur.

The relevance of *Analysing the Consequences* might be underestimated. However, it is crucial to be aware what the risks of the selected solution are. Knowing the weaknesses of the selected concept it was possible to prevent errors during the implementation of the measuring system. Furthermore, it was possible to prevent malfunction of the system. The protective cover for the strain gauges and the testing of the circuitry was already determined to be important in this stage.

The set based approach described by Kennedy et al. [72] was used during the *Deciding and Implementing* stage of the SPALTEN process. The development of several solutions in parallel enabled to learn about the possibilities how the system can be implemented. With the separation in subsystems and the definition of interfaces it was possible to change the solutions of the subsystems without changing the entire system. This enabled to select the best solutions for each subsystem without having to rework the other subsystems due to the needed adaption. Therefore, it was possible to reduce the number of needed Arduino boards from six to one. Moreover, only one signal conditioning unit instead of 24 is needed for the 24 channels of the strain gauges.

Dividing the measuring system in subsystems made it possible to test the different solutions in order to select the best. Furthermore, trouble shooting was possible in the sub-systems. As it was possible to determine the capability of the sub-systems the capability of the entire system could be determined and there was full control on the entire system.

Evaluation and Learning helped to reflect the measuring system. Especially for RollerSafe and Rottefella it was important to evaluate what the accuracy of the measuring system is as they need to rely on the system when the use the recorded data for dimensioning of their products.

7 Conclusion and Prospective

The main outcome of this thesis and the next steps which might be done are elucidated in the following subchapters. The conclusion summarises the main results of the measuring system and its benefits. In the prospective there is information what the measuring will be used for and how it can be improved.

7.1 Conclusion

A measuring system was developed which is capable to detect spatial forces and torques between roller ski and binding. Common loads as well as maximum loads which occur during roller skiing on the road can be detected.

In the literature no measuring system which is able to detect spatial forces and torques is found. Due to this reason, a new setup needed to be developed. Moreover, a solution had to be found to achieve a sampling frequency higher than the one of the measuring systems for skiing and roller skiing found in the literature. This is due to the reason that this measuring system is intended to measure peak loads. Another target was to change the roller ski-binding system as less as possible and not to interfere with common skiing. None of the high end solutions from HBM and National Instruments could be used for the signal conditioning and the data acquisition as only a limited budget was available.

Strain gauge rosettes were mounted on the beam of the roller ski in order to determine the strain in three directions at eight positions of the beam. This enabled measuring without changing the roller ski-binding system. Mounting the measuring system on the roller ski the initial weight of the roller ski of 1500 g was increased by 190 g and the centre of gravity was shifted by 4 mm to the back of the roller ski. Amplification and acquisition of the sensor output signal is done with a circuitry especially designed for this project. Low cost components were used to build a system with a quality as high as possible. The low cost solution was payed with the time required for the development, testing and production of the system. With electrical components for about 500 € (4600 NOK) it was possible to build a signal conditioning and data acquisition unit with 33 Hz sampling frequency. The mean output of the measuring system has an accuracy of 10 N. Additionally, a fluctuation of about ±25 N occurs due to the noise added by the inaccuracy of the data

logger. Furthermore, the signal conditioning and data acquisition unit weighs only 1600 g and can be carried in a drinking belt or rucksack by the athlete as it has an autarkic power supply. The recorded data is transferred to a computer where it is processed by a Matlab script which derives the principal stresses and subsequently the loads from the measured strain. In Figure 7-1 the entire measuring system is depicted.
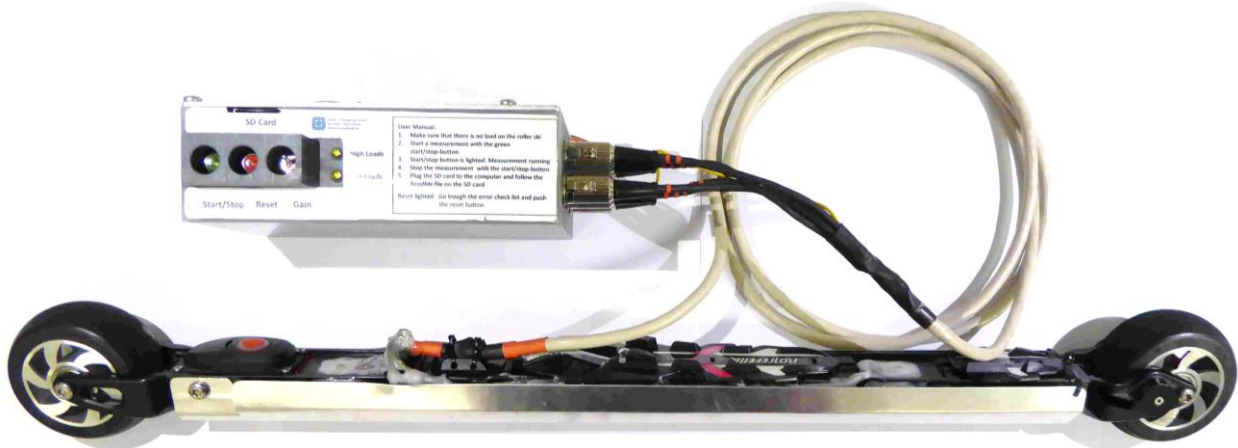
Figure 7-1: Final roller ski measuring system

The measuring system was developed with the SPALTEN methodology introduced by Albers et al. [59]. Measuring systems in the field of skiing and roller skiing as well as systems from other fields were considered in order to foster cross inventions. The solution for the measuring system was developed by combining the systems of Hoset et al. [27] who measured one force component on a roller ski, Feng et al. [52] who developed a device to measure wheel forces of a car and Yoxall and Rowson [48] who measured the opening force of vacuum lug cans. For the implementation of the solution a set-based approach introduced by Kennedy et al. [72] was used. Dividing the measuring system into sub-systems it was possible to develop solutions simultaneously, to test them independently and to use the best solutions of the sub-systems for the final setup. The measuring system was validated by applying static loads. Moreover, in situ test measuring was conducted to illustrate the capability of the measuring system. The recorded load data was approved to match the results of other roller ski measuring systems found in the literature.

The measuring systems will be used by the companies RollerSafe and Rottefella to improve their products and to develop more relevant laboratory test setups. Analysing the skiing technique with the measuring system knowledge might be achieved to improve the skiing technique as it was not possible to regard torques during skiing and roller skiing before. Besides the cross-country skiing specific use, the resulting measuring system shows that it is possible to determine spatial forces and torques at one elastic element with strain gauges. Furthermore, it was demonstrated how to build a measuring system with low cost components. The development process of the measuring system has shown that it is favourable to use the SPALTEN methodology in combination with the set-based approach to design and to built mechatronic systems.

The measuring system fulfils most of the requirements. It is possible to measure spatial loads. The roller ski-binding system is not modified and there is almost no weight added to the roller ski. Moreover, the system can be used to record loads during all situations which occur during roller skiing except getting stuck on a curb stone. A high accuracy of the measuring system was achieved with the low cost components for the signal conditioning unit and the data acquisition unit. However, with the limited project budget it was not possible to increase the sampling frequency in order to detect loads which are caused by external circumstances like skiing over a crack. Nevertheless, it is possible to detect the loads which are caused by the athlete.

7.2   Prospective

The project partners RollerSafe and Rottefella will use the measuring system to collect load data. Peak load events as well as common training will be recorded when the companies are testing all situations described in chapter 5.1. The comprehensive knowledge will help them to design better products. RollerSafe will use the load data for the dimensioning of their new roller ski made of carbon fibre. Rottefella will design new roller ski bindings with the earned knowledge and it is planned to develop more relevant laboratory test setups. Recording of load data with the measuring system during a common training is depicted in Figure 7-2.

Figure 7-2: Recording load data with the measuring system during common training

As there is no specific standard for the dimensioning and testing of roller ski bindings the standard ISO 9119:1990 [58] for skis is applied for roller skis as well. Based on the load data recorded with the new measuring system a more specific standard for roller skis and roller ski bindings might be issued.

Besides the commercial purposes, the measuring system can be used by research centres for cross-country skiing like Olympiatoppen. The skiing technique of elite skiers can be analysed in order to learn and improve the cross-country skiing technique. As there have not been measuring systems detecting torques during cross country skiing there will be new insights.

It is possible to rebuilt and to improve the measuring system as the electric schematics, technical drawings and the code of the measuring system is found in the appendix of the thesis. The modules *Sensors*, *Signal Conditioning* and *Data Acquisition* can be improved or exchanged separately.

The sensor unit might be improved by mounting the strain gauges on the inside of the beam of the roller ski. For this purpose, encapsulated strain gauges are needed which are equipped with connection cables as it is not possible to solder inside the beam or to attach a protective cover. Mounting the strain gauges inside the beam will make the external protection plate dispensable which will lead to an even lighter roller ski. Furthermore, the strain gauges are better protected and load data during getting stuck on a curb stone can be detected as well.

The signal conditioning unit might be improved by using potentiometers in parallel with the strain gauges in the Wheatstone bridges. It would be possible to adjust the bridge output voltage to 0 V when the strain gauges are unloaded. In case of a consistent output for the unloaded strain gauges it would be possible to use a higher amplification at the instrumentation amplifiers and the influence of the noise at the A/D-converter would be reduced. Besides the improvement of the in-house manufactured signal conditioning unit devices from the suppliers HBM and National Instruments could be used. Two of the Quantum X MX1615B from HBM or three of the NI 9235 from National Instruments would be needed for the 24 strain gauges.

The Arduino code of the data acquisition might be improved when there is more time and programming knowledge available. In several internet forums codes can be found how to sample with one analogue input at several thousand Hz on a SD card [83]. This exceeds the common Arduino programming. As the codes introduced in the forums are for the logging of one channel only it is not granted that they can be adapted for several channels which requires the steering of the multiplexers as well. Specific libraries and functions need to be designed in order to exclude the common safety settings of the predefined Arduino functions.

During the implementation of the measuring system a completely different solution was revealed for the signal conditioning and the data acquisition of the strain gauge output signal. The company Acam-Messelectronic GmbH [84] introduced a signal conditioning and data acquisition unit which is not based on the Wheatstone bridge as the common systems. A capacitor which was charged to a specific level is discharged through the strain gauge. The time until the voltage decreased to a certain level is measured with a time to digital converter. Dependent on the resistance of the strain gauge the period needed for the discharging varies. The PSØ9 has a 16-bit resolution and is able to sample with up to 10 kHz.

Independently from the devices which are used to record the sensor values the Matlab script developed for this master thesis can be used to derive the loads.

Further sensors than the strain gauges might be added to the measuring system in order to improve the linking between a certain incident and the measured loads. For instance, devices to determine the speed and the position could be used. Additionally, it is recommended to film the athlete during the measuring session in order to enable the linking between a specific event and the measured load when the data is evaluated.

Improvement of the calibration setup would increase the accuracy of the measuring system. A setup which enables the precise calibration of the strain gauges which are in 45° or 90° direction to the beam of the roller ski is needed additionally to the used setup.

An improved measuring system might be integrated into a commercially available roller ski. Competitive and pro skiers could use the system to analyse their skiing technique. Live feedback comparably to the WeMeMove [85] sports sensor for double pooling would be possible.

References

[1] F. Braghin *et al, The Engineering Approach to Winter Sports,* 1st ed. New York: Springer, 2016.

[2] Rollersafe AS, *Technology.* [Online] Available: http://www.rollersafe.no/all-about/technology/. Accessed on: Sep. 03 2016.

[3] Rottefella AS, *The Perfect Way to Maintain and Increas Your Skiing Performance.* [Online] Available: http://www.rottefella.com/product_categories/roller-ski/. Accessed on: Sep. 03 2016.

[4] O. Ohtonen, "The Effect of Ski Gliding Properties on the Force Production of V2-Technique," master thesis, Department of Biology; Department of Physical Activity, University of Jyväskylä, Jyväskylä, 2010.

[5] The Institute of Measurement and Control, *Guide to the measurement of force*. London: Wheight Measuring Panel, 1998.

[6] K. Hoffmann, *Smart Materials*. Berlin, Heidelberg: Springer Berlin Heidelberg, 2001.

[7] W. Bolton, *Engineering science,* 2nd ed. Oxford: Newnes, 1994.

[8] C. Bahra and J. Paros, *Instrumentation Reference Book,* 4th ed. Amsterdam: Elsevier, 2010.

[9] D. Ştefănescu, *Handbook of Force Transducers: Principles and components*. Berlin: Springer-Verlag, 2011.

[10] DEWESoft d.o.o, *Strain measurement.* [Online] Available: http://www.dewesoft.com/pro/course/strain-measurement-1. Accessed on: Oct. 06 2016.

[11] ME-Meßsysteme GmbH, *Einführung in die Dehnmessstreifen (DMS) Technik.* [Online] Available: http://www.me-systeme.de/de/basics/kb-straingage-1.pdf. Accessed on: May 11 2016.

[12] J. Wilson, *Sensor Technology Handbook*. Amsterdam: Elsevier, 2005.

[13] Interlink Electronics Inc, *FSR Force Sensing Resistor Integration Guide and Evaluation Parts Catalog: 400 Series Evaluation Parts With Suggested Electrical Interfaces.* [Online] Available:

References

https://www.sparkfun.com/datasheets/Sensors/Pressure/fsrguide.pdf. Accessed on: May 13 2016.

[14] P. Komi, "Force Measurements During Cross-Country Skiing," *Journal of the International Society of Biomechanics*, vol. 3, no. 4, pp. 370–381, 1987.

[15] A. Kehler, E. Hajkova, H. Holmberg, and R. Kram, "Forces and mechanical energy fluctuations during diagonal stride roller skiing running on wheels?," *Journal of Experimental Biology*, vol. 21, no. 217, pp. 3779–3785, 2014.

[16] P. Vähäsöyprinki *et al*, "Effect of Skiing Speed on Ski and Pole Forces in Cross-Country Skiing," *Medicine & Science in Sports & Exercise*, vol. 40, no. 6, pp. 1111–1116, 2008.

[17] A. Leppävuori, M. Karras, H. Rusko, and T. Viitasalo, "A New Method of Measuring 3-D Ground Reaction Forces Under the Ski During Skiing on Snow," *Journal of Applied Biomechanics*, no. 9, pp. 315–328, 1993.

[18] G. Street and E. Frederick, "Measurement of Skier-Generated Forces During Roller-Ski Skating," *Journal of Applied Biomechanics*, no. 11, pp. 245–256, 1995.

[19] M. Ainegren, P. Carlsson, M. Laaksonen, and M. Tinnsten, "The influence of grip on oxygen consumption and leg forces when using classical style roller skis," *Scand J Med Sci Sports*, vol. 24, no. 2, pp. 301–310, 2014.

[20] S. Babiel, "Studies on intra-individual variability of selected cross-country skiing techniques," *European Journal of Sport Science*, vol. 3, no. 3, pp. 1–10, 2003.

[21] O. Ohtonen, S. Lindinger, T. Lemmettylä, S. Seppälä, and V. Linnamo, "Validation of portable 2D force binding systems for cross-country skiing," *Sports Eng*, vol. 16, no. 4, pp. 281–296, 2013.

[22] O. Ohtonen, S. Lindinger, and V. Linnamo, "Effects of Gliding Properties of Cross-Country Skis on the Force Production During Skating Technique in Elite Cross-Country Skiers," *International Journal of Sports Science and Coaching*, vol. 8, no. 2, pp. 407–416, 2013.

[23] V. Linnamo *et al*, "Multi-dimensional force measurement binding used during skating in cross-country skiing," *Science and skiing*, no. 5, pp. 540–548, 2012.

[24] M. Pohjola, "Analysing Effectiveness of Force Application in Ski Skating Using Force and Motion Capture Data: A Model to Support Cross-Country Skiing Research and Coaching," master thesis, Department of Biology of Sport, University of Jyväskylä, Jyväskylä, 2014.

[25] J. Pierce *et al*, "Force Measurement in Cross-Country Skiing," *International Journal of Sport Biomechanics*, no. 3, pp. 382–391, 1987.

[26] E. Friedrichs and B. Berger, "Sensor Plates Designed for Measuring Forces Between Ski and Bidning - A Development Summary," *Science and skiing*, no. 1, 1997.

[27] M. Hoset, A. Rognstad, T. Rølvåg, G. Ettema, and Ø. Sandbakk, "Construction of an instrumented roller ski and validation of three-dimensional forces in the skating technique," *Sports Engineering*, vol. 17, no. 1, pp. 23–32, 2014.

[28] M. Bellizzi, K. King, S. Cushman, and P. Weyand, "Does the application of ground force set the energetic cost of cross-country skiing?," *Journal of Applied Physiology*, vol. 5, no. 85, pp. 1736–1743, 1998.

[29] S. Lindinger, C. Göpfert, T. Stöggl, E. Müller, and H. Holmberg, "Biomechanical pole and leg characteristics during uphill diagonal roller skiing," *Sports Biomechanics*, vol. 8, no. 4, pp. 318–333, 2009.

[30] C. Göpfert, H. Holmberg, T. Stöggl, E. Müller, and S. Lindinger, "Biomechanical characteristics and speed adaptation during kick double poling on roller skis in elite cross-country skiers," *Sports Biomechanics*, vol. 12, no. 2, pp. 154–174, 2013.

[31] T. Stöggl, W. Kampel, E. Müller, and S. Lindinger, "Double-Push Skating versus V2 and V1 Skating on Uphill Terrain in Cross-Country Skiing," *Medicine & Science in Sports & Exercise*, vol. 42, no. 1, pp. 187–196, 2010.

[32] T. Stöggl, E. Müller, and S. Lindinger, "Biomechanical comparison of the double-push technique and the conventional skate skiing technique in cross-country sprint skiing," *Journal of Sports Sciences*, vol. 26, no. 11, pp. 1225–1233, 2008.

[33] Mettler-Toledo International Inc, *Electronic Weighing Principles.* [Online] Available: https://www.mt.com/dam/mt_ext_files/Editorial/Generic/8/Weigh_Uncertain_Number4_0x0003d6750003db6700091749_files/elect_weigh_principles.pdf.

[34] A. Caya, Y. Champoux, and J. Drouet, Eds, *Dynamic behaviour and measurement accuracy of a bicycle brake hood force transducer*, 2012.

[35] B. Parida, S. Vishwakarma, and S. Pal, "Design and development of fixture and force measuring system for friction stir welding process using strain gauges," *Journal of Mechanical Science and Technology*, vol. 29, no. 2, pp. 739–749, 2015.

[36] Y. Zhao, S. Liang, and G. Zhou, "A high performance sensor for triaxial cutting force measurement in turning," *Sensors*, no. 15, pp. 7969–7984, 2015.

[37] Z. Dai, Z. Wang, and A. Ji, "Dynamics of gecko locomotion: a force-measuring array to measure 3D reaction forces," *The Journal of experimental biology*, vol. 214, no. Pt 5, pp. 703–708, 2011.

[38] M. Entacher *et al*, "Cutter force measurement on tunnel boring machines – System design," *Tunnelling and Underground Space Technology*, no. 31, pp. 97–106, 2012.

[39]   I. Kitayama, T. Kawauchi, R. Takahata, and N. Hirokawa, "Kinematic Analysis of Plastic Ankle-Foot Orthosis Using Force Sensors," *Journal of Sports Economics and Management*, no. 13, pp. 217–221, 2013.

[40]   T. Degenstein and H. Winner, *Dynamic Measurement of the Forces in the Friction Area of a Disc Brake During a Braking Process.* [Online] Available: http://www.fzd.tu-darm-stadt.de/media/fachgebiet_fzd/publikationen_3/2006/2006_degenstein_fisita.pdf. Accessed on: May 18 2016.

[41]   A. Hamid, M. Patar, and M. Ayub, Eds, *Force Sensor Detection and Performance Evaluation of New Active System Ankle Foot Orthosis*, 2012.

[42]   L. Wei, J. Zeng, P. Wu, and H. Gao, "Indirect method for wheel–rail force measurement and derailment evaluation," *Vehicle System Dynamics*, vol. 52, no. 12, pp. 1622–1641, 2014.

[43]   F. Braghin *et al*, "Measurement of contact forces and patch features by means of accelerometers fixed inside the tire to improve future car active control," *Vehicle System Dynamics*, vol. 44, no. sup1, pp. 3–13, 2006.

[44]   Honeywell International Incorporation, *Ways to Measure the Force Acting on a Rotating Shaft.* [Online] Available: https://measurementsensors.honeywell.com/techresources/appnotes/Pages/Ways_to_Measure_the_Force_Acting_on_a_Rotating_Shaft.aspx. Accessed on: May 18 2016.

[45]   Know Your Parts, *Electronic Power Steering.* [Online] Available: http://www.knowyourparts.com/technical-articles/electronic-power-steering/. Accessed on: May 20 2016.

[46]   Hot Rod Network, *Torque Wrench Myths - Matters of Precision.* [Online] Available: http://www.hotrod.com/how-to/additional-how-to/ctrp-1111-torque-wrench-myths/. Accessed on: May 19 2016.

[47]   SRM GmbH, *What is SRM?* [Online] Available: http://www.srm.de/srm-training-system/what-is-srm/. Accessed on: May 19 2016.

[48]   A. Yoxall and J. Rowson, "Talking about Torque: Measuring Pack Accessibility - a Review," *Packaging Technology and Science*, no. 28, pp. 1–14, 2015.

[49]   Q. Zhu *et al, Eds, Valve Torque Measuring Device Based on Strain Gauge*, 2010.

[50]   Q. Liang, D. Zhang, Y. Wang, and Y. Ge, "Development of a touch probe based on five-dimensional force/torque transducer for coordinate measuring machine (CMM)," *Robotics and Computer-Integrated Manufacturing*, vol. 28, no. 2, pp. 238–244, 2012.

[51]   ATI Industrial Automation Inc, *F/T Product Description and Features.* [Online] Available: http://www.ati-ia.com/products/ft/ft_productDesc.aspx. Accessed on: May 20 2016.

[52] L. Feng, G. Lin, W. Zhang, and D. Dai, "Inertia coupling analysis of a self-decoupled wheel force transducer under multi-axis acceleration fields," *PloS one*, vol. 10, no. 2, pp. e0118249, 2015.

[53] Kistler, *Reliable Measurement Results Thanks to High Reliable Measurement Results Thanks to HighNatural Frequencies: Cutting Force Measurement for Milling with Kistler.* [Online] Available: https://www.kistler.com/by/en/applications/sensor-technology/cutting-force-measurement/milling/products/#multi__component__dynamometer_up_to_60_k_n_9255_c. Accessed on: May 18 2016.

[54] Hottinger Baldwin Messtechnik GmbH, *All-rounder MX1615 from Quantum X series relies in reliable measurements.* [Online] Available: https://www.hbm.com/fileadmin/media-pool/hbmdoc/technical/s3571.pdf. Accessed on: Jul. 06 2016.

[55] Hottinger Baldwin Messtechnik GmbH, *QuantumX CX22B-W Autonomer Datenrekorder.* [Online] Available: https://www.hbm.com/de/2486/quantumx-cx22bw-datenrekorder-mit-wlan-funktionalitaet/. Accessed on: Jul. 06 2016.

[56] National Instruments Inc, *NI 9235, NI 9236.* [Online] Available: http://sine.ni.com/nips/cds/view/p/lang/en/nid/208790. Accessed on: Jul. 06 2016.

[57] National Instruments, *cRIO-9024.* [Online] Available: http://sine.ni.com/nips/cds/view/p/lang/en/nid/207371. Accessed on: Jul. 06 2016.

[58] *Cross-country skis -- Binding mounting area -- Requirements and test methods*, ISO 9119:1990, 1990.

[59] A. Albers, N. Burkardt, M. Meboldt, and M. Saak, Eds, *SPALTEN Problem Solving Methodology in the Product Development*, 2005.

[60] *Methodik zum Entwickeln und Konstruieren technischer Systeme und Produkte - Systematic approach to the development and design of technical systems and products*, VDI 2221, 1993.

[61] A. Albers and N. Burkardt, "Vorlesung Produktentstehung: Entwicklung,Werstoffkunde, Fertigung," lecture notes, IPEK - Institut für Produktentwicklung, Karlsruhe Institute of Technology, Karlsruhe, 2015.

[62] T. Deigendesch, "Kreativität in der Produktentwicklung und Muster als methodisches Hilfsmittel," research report, Karlsruhe Institute of Technology, Karlsruhe, 2009.

[63] M. Pelgrom, *Analog-to-digital conversion*, 2nd ed. New York: Springer, 2013.

[64] N. Maurits, *From Neurology to Methodology and Back: An Introduction to Clinical Neuroengineering*. New York: Springer, 2012.

[65] *Technisch-wirtschaftliches Konstruieren - Engineering design at optimum cost*, VDI 2225 - 3, 1998.

References

[66] D. Bourbonnais *et al*, "A Static Dynamometer Measuring Multidirectional Torques Exerted Simultaneously at the Hip and Knee," *Journal of Biomechanics*, vol. 26, no. 3, pp. 277–283, 1993.

[67] E. Andersson, B. Pellegrini, Ø. Sandbakk, T. Stüggl, and H. Holmberg, "The effects of skiing velocity on mechanical aspects of diagonal cross-country skiing," *Sports Biomechanics*, vol. 13, no. 3, pp. 267–284, 2014.

[68] Kistler Instrumente GmbH, *Press Force Sensor.* [Online] Available: https://www.kistler.com/?type=669&fid=55081&model=document&callee=frontend. Accessed on: Sep. 14 2016.

[69] Kistler Instrumente GmbH, *ICAM: Typ 5073A.* [Online] Available: https://www.kistler.com/?type=669&fid=54152&model=document. Accessed on: Sep. 14 2016.

[70] Analog Devices Inc, *AD620 Data Sheet.* [Online] Available: http://www.analog.com/media/en/technical-documentation/data-sheets/AD620.pdf. Accessed on: Aug. 18 2016.

[71] Atmel Inc, *SAM D21E / SAM D21G / SAM D21J Datasheet Complete: ATSAMD21G18, 32-Bit ARM Cortex M0+.* [Online] Available: http://www.atmel.com/Images/Atmel-42181-SAM-D21_Datasheet.pdf. Accessed on: Jul. 06 2016.

[72] B. Kennedy, D. Sobek, and M. Kennedy, "Reducing Rework by Applying Set-Based Practices Early in the Systems Engineering Process," *Systems Engineering*, vol. 17, no. 3, pp. 278–296, 2014.

[73] J. Webster and H. Eren, *Measurement Instrumentation and Sensors Handbook*. Boca Raton: CRC Press, 2014.

[74] Elektronik-Kompendium.de, *Integrierte Festspannungsregler (78xx/79xx).* [Online] Available: http://www.elektronik-kompendium.de/sites/bau/0204301.htm. Accessed on: Sep. 22 2016.

[75] D. Gross, W. Hauger, J. Schröder, and W. Wall, *Elastostatik,* 10th ed. Berlin Heidleberg: Springer, 2009.

[76] D. Gross, W. Hauger, J. Schröder, and W. Wall, *Statik,* 10th ed. Berlin Heidleberg: Springer, 2009.

[77] Aerospace Specification Metals Inc, *Aluminum 6061-T6; 6061-T651.* [Online] Available: http://asm.matweb.com/search/SpecificMaterial.asp?bassnum=MA6061t6. Accessed on: Aug. 27 2016.

[78] Hottinger Baldwin Messtechnik GmbH, *Practical Hints for the Installation of Strain Gages.* [Online] Available: https://www.hbm.com/fileadmin/mediapool/hbmdoc/technical/s1421.pdf. Accessed on: Aug. 28 2016.

[79] Texas Instruments Incorporation, *CDx4HC405x, CDx4HCT405x High-Speed CMOS Logic Analog Multiplexers and Demultiplexers.* [Online] Available: http://www.ti.com/lit/ds/symlink/cd74hc4052.pdf. Accessed on: Aug. 14 2016.

[80] Moghimi R, "Bridge-Type Sensor Measurements are Enhanced by Autozeroed Instrumentation Amplifiers with Digitally Programmable Gain and Output Offset," *Analog Dialogue*, vol. 5, no. 38, pp. 1–3, 2004.

[81] Arduino, *Arduino Zero & Genuino Zero.* [Online] Available: https://www.arduino.cc/en/Main/ArduinoBoardZero. Accessed on: Aug. 18 2016.

[82] IMC Meßsysteme GmbH, *Kalibierung von Dehnungsmessstreifen und DMS-basierten Sensoren.* [Online] Available: http://www.imc-berlin.de/fileadmin/Public/Downloads/Whitepapers/Kalibrierung-bei-Brueckenmessung-WhitePaper-20150128.pdf. Accessed on: Oct. 09 2016.

[83] Arduino, *Fastest Data Logging? With SD Card?* [Online] Available: http://forum.arduino.cc/index.php/topic,64813.0.html.

[84] acam-messelectronic GmbH, *Measurement Principles.* [Online] Available: http://www.acam.de/products/picostrain/measuring-method/. Accessed on: Sep. 19 2016.

[85] WeMeMove, *Din personliga realtidscoach.* [Online] Available: https://www.wememove.com/.

[86] Rottefella AS, *Xcelerator Roller Ski Skate.* [Online] Available: http://www.rottefella.com/product/xcelerator-2-0-roller-skate/. Accessed on: Oct. 04 2016.

[87] H. Rusko, G. Smith, O. Ronsen, and Y. Hanin, *Cross country skiing,* 1st ed. Oxford: Blackwell Science, 2003.

[88] B. Fasel, J. Favre, J. Chardonnens, G. Gremion, and K. Aminian, "An inertial sensor-based system for spatio-temporal analysis in classic cross-country skiing diagonal technique," *Journal of Biomechanics*, vol. 48, no. 12, pp. 3199–3205, 2015.

[89] Verdens Gang AS, *Slik blir du en stakemester.* [Online] Available: http://1.vgc.no/drpublish/images/article/2011/01/23/23209165/1/460x306/1628194.jpg. Accessed on: Apr. 29 2016.

[90] BASPO Bundesamt für Sport, *Skilanglauf-Technik.* [Online] Available: https://lh4.ggpht.com/aCcvpsulD-Zzujjrqhgbp3Qf6u0spjvYgNh0VjDDXHU5HdADK5IDPmBrmvJwHTLTJaY=h900. Accessed on: Apr. 29 2016.

[91] Faster Skier, *Johaug Tops Østberg to Win 2nd Tour de Ski; Diggins 10th; Stephen 3rd-Fastest to the Top.* [Online] Available: http://cdn.fasterskier.com/wp-content/blogs.dir/1/files/2016/01/Johaug02-700x526.jpg. Accessed on: Apr. 29 2016.

[92] Cross Country Ski Technique, *Effective Downhill Turns: What the Science Says - Cross Country Ski Technique.* [Online] Available: http://crosscountryskitechnique.com/effective-downhill-turns-what-the-science-says/. Accessed on: May 01 2016.

[93] R. Bryntesson, *Bryntes Bromstekniker.* [Online] Available: https://www.youtube.com/watch?v=MgfRAhkx75k. Accessed on: Apr. 30 2016.

[94] K. Ehrhardt, *SRB Benutzerhandbuch.* [Online] Available: http://www.ski-roller.de/media/Ski-Roller/pdf/Ski-Roller-Benutzerhandbuch.pdf. Accessed on: Apr. 30 2016.

[95] T. Böhlke, "Technische Mechanik 1 - Statik," lecture notes, Department for Technical Mechanics, Karlsruhe Institute of Technology, Karlsruhe, 2010.

Appendix

In the appendix there is information which has not been included to the main part of the master thesis for reasons of clarity and comprehensibility. Nevertheless, the following parts are outcomes of the thesis which lead to the final result. Furthermore, there is a user manual on how to use the measuring system in order to enable the usage of the measuring system for people who have not been involved in the development of the system.

Following the necessary information for the reproduction of the measuring system is given. Electronic schematics of the circuitry and a list of the required electronic components as well as the technical drawings of the housing are provided. Besides the information on the hardware the necessary software is given as well. The data logger code for the Arduino microcontroller and the Matlab code for the processing of the recorded data can be found.

Thereafter information and calculations are given which have not been included to the main part for clarity reasons. Firstly, the requirement list and the assessment of the expected loads on the measuring system are given. Thereafter, calculations and simulations can be found. The calculation of the second moment of inertia and the neutral layers of the beam of the roller ski is shown. Furthermore, the calculations of the force and momentum function at the beam of the roller ski for the expected maximal loads is given. Moreover, the results of the FEM simulation of the load cases on the beam of the roller ski are shown.

Appendix A: User Manual for the Measuring System

The measuring system is capable to detect loads during all situations except getting stuck on a curb stone. The strain gauges at the beam of the roller ski are protected by a cover. Nevertheless, it should be avoided to get stuck on bumpers or curb stones.

In order to enable to test classic or skate skiing the suitable wheel holding brackets and wheels need to be mounted on the beam of the roller ski. This is done by dismounting and mounting the four screws at the end of the beam. The cover plate of the strain gauges is fastened in the front with the two screws of the wheel holding bracket and in the back with a tie wrap. In the back the cover should not be mounted too tight as this would interfere with the measuring accuracy.

Hereinafter the user interface of the measuring system as well as the preparation procedure of the system for sampling is explained. Furthermore, there is information how to record strain data and how to process it to achieve the output of the forces and torques.

The user interface of the measuring system is depicted in Figure A 1. The gain for the data acquisition can be selected with the gain switch. The selected gain is displayed with the yellow LEDs besides the switch. If the range of the loads which should be detected is unknown the setting *High Loads* should be used first and can be adapted to low loads when it was ascertained that the measuring range is not exceeded. The setting *Low Loads* enables logging of low loads with high accuracy.

When the system is powered or the reset button has been pushed the setup is run through during which the system calibrates. The Start/Stop-button and the Reset-button are lighted at the same time in this case. During the setup it is crucial that there is no load on the roller ski because the system calibrates. This might be achieved by lifting the leg.

When the system is sampling the Start/Stop-button is lighted in green.

In case of an error the Reset-button is lighted in red and the error check list below needs to be gone through. This list can be found on the side of the measuring system as well.

- Has the gain state not been changed while the system was powered on?
- Is the SD card in the slot?
- Is the SD card broken?
- Are not more than 999 measurements on the SD card?
- Is the battery low?

When the error is corrected the measuring system needs to be reset. Make sure that there is no load on the roller ski during the setup which is signalised by the lit Start/Stop-button and Reset-button.

Figure A 1: User interface of the measuring system

Preparation for sampling:

1. Make sure that there is an SD card in the slot. Only use high quality class 10 SD cards. SD cards of low quality will reduce the sampling rate.

2. Place the data acquisition box in the drinking belt.

3. Plug in the connection cable to the data acquisition box. Use the coding on the wires to plug them in on the right position. Do not forget to plug the yellow shield cable in.

4. Connect the battery pack to the measuring system. Use the coding on the wire to plug it correctly. Connecting the battery wrong will destroy the measuring system.

5. Use the hook and loop fasteners to attach the transfer cable on the leg of the athlete.

Do not place a mobile phone in the drinking belt. It will interfere with the accuracy of the measuring system. If it is desired to use the phone for GPS tracking, set it to the flight mode.

Sampling:

1. Select the suitable gain.

2. Reset the system by pushing the Reset-button. Make sure that there is no load on the roller ski when the system is reset and the setup is running.

3. When the setup is done both the light of the Start/Stop-button and of the Reset-button are switched of and the system is ready to sample.

4. Sampling can be started now by pushing the Start/Stop-button. Make sure that the roller ski is unloaded when starting a measurement. Otherwise there will be an error as the tare function will shift the loads to a wrong level.

5. When a measurement is running the Start/Stop-button is lit in green.

6. Sampling is stopped by pushing the Start/Stop-button. The green light at the Start/Stop-button switches off.

7. Sampling can be restarted by pushing the Start/Stop-button

Processing of the sampled data:

1. Plug the SD card into the computer

2. Select the measurement which you want to process and copy it to the folder *Test Data*. Put only the files of the one measurement desired to be processed in this folder. The file names are encoded. A file name is xxxyyy.txt with xxx increasing from 001 to 999 when the user starts a new measurement and yyy increasing from 001 to 999 in case the data acquisition automatically starts a new file in order not to exceed a certain file size. All of the sub files of one measurement need to be copied into the folder *Test Data*.

3. Start the Matlab script *Data Processing* and press the run button.

4. The results are automatically stored in a subfolder of the folder *Results*. The subfolders are named depending on the time of the processing of the data. The naming is year_month_day_hour_minute_second. In this folder a summary of the results is given as well as the plot of the force and torque functions. Furthermore, a excel output file of the calculate loads can be found in this folder.

In the default setting the loads are calculated for the coordinate system which is under the middle of the binding pin where the roller ski and the binding are attached to each other. An offset of the coordinate system for which the loads should be calculated can be added in the Matlab script. The direction of the loads can be seen in Figure A 2.
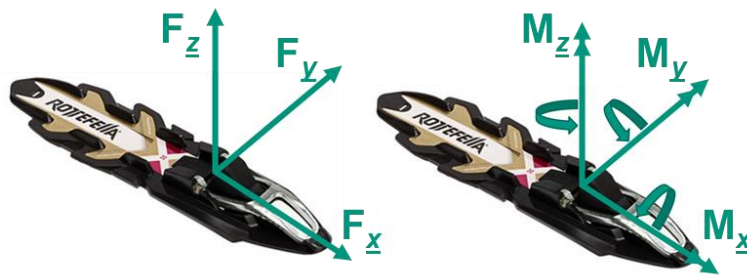
Figure A 2: Direction of forces and torques, adapted from [86]

Appendix B: Electronic Schematics

The electronic schematics of the signal conditioning unit and the data acquisition unit as well as the power supply are shown hereinafter. With use of the signal conditioning unit it is possible to rise the output signal of the strain gauges to a level which the Arduino microcontroller can read. The resulting output is logged by the data acquisition unit. Both units were powered by the displayed power supply.
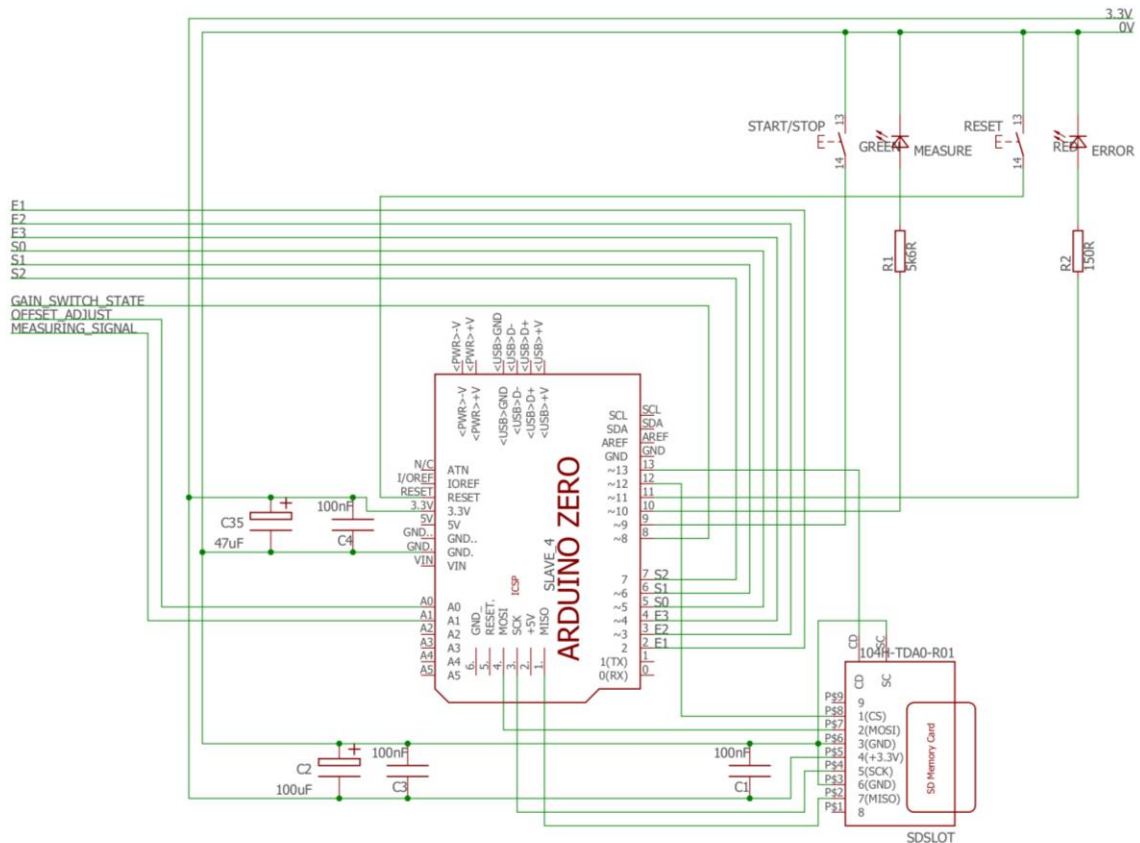
Figure A 3: Electronic schematics of the data acquisition unit
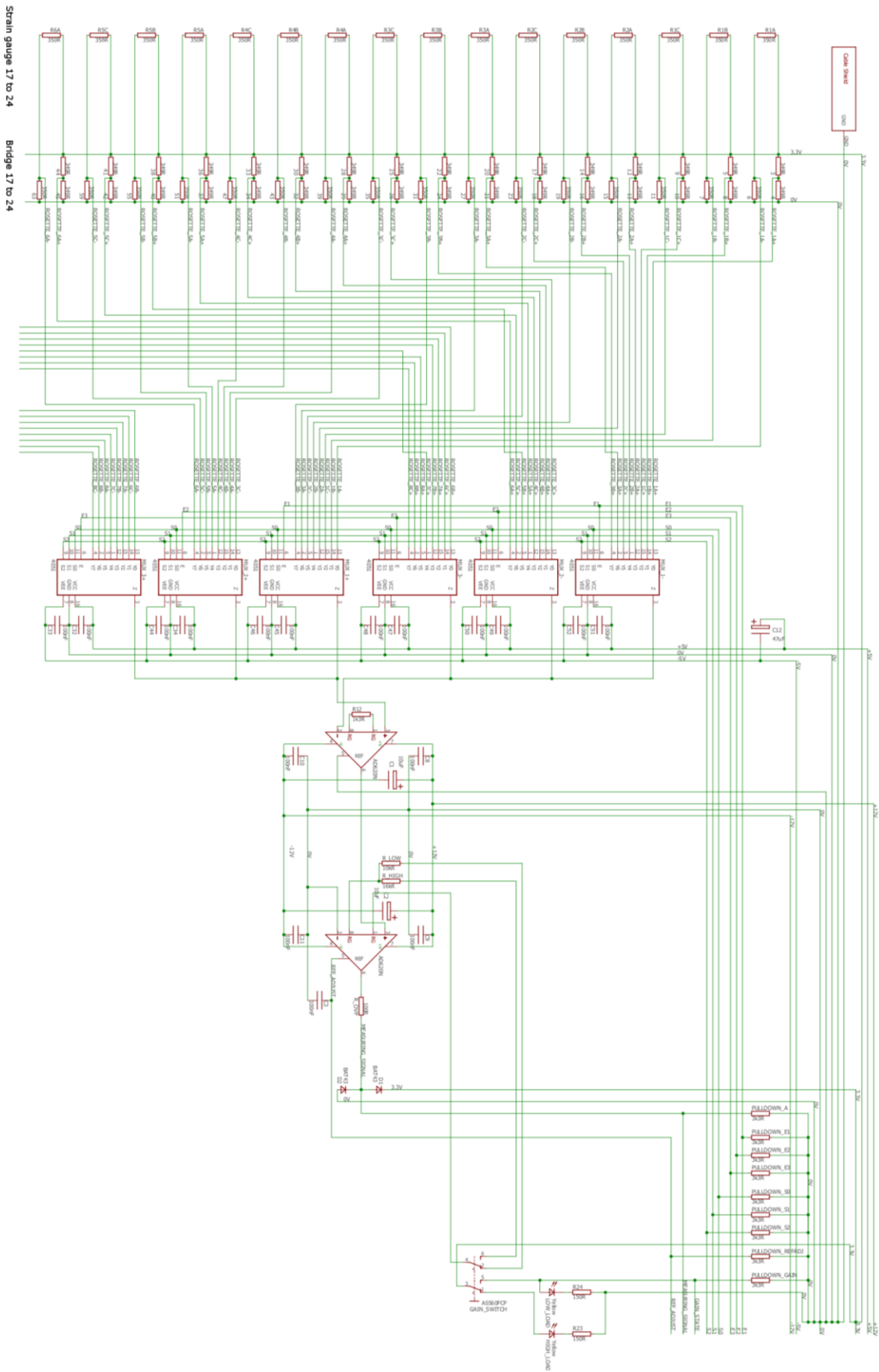
Figure A 4: Electronic schematics of the signal conditioning unit
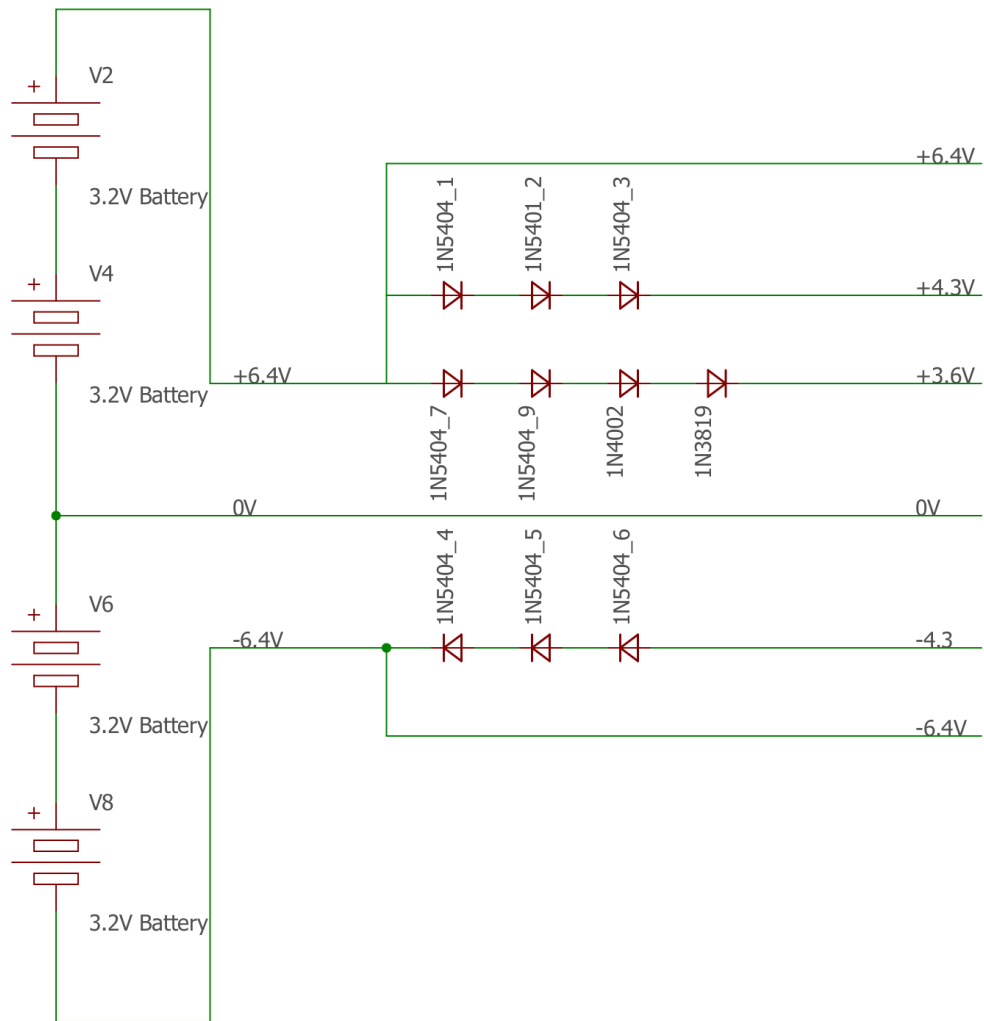
Figure A 5: Electronic schematics of the power supply

Appendix C: Electronic Components

In the following a list of the required electronic components can be found which are used for the entire setup of the measuring system.

Description		Type No.	Quantity
Resistors	150 Ohm	MRA0207 150R B 15PPM TA	1
	300 Ohm	MF55SSF/MF0204	1
	350 Ohm	MF0W4FF3500KIT	72
	1 kOhm	RC55Y-1K0BI	1
	3.3 kOhm	RC55Y-3K3BI	9
	5.6 kOhm	RC55Y-5K6BI	1
	10 kOhm	RC55Y-10KBI	1
	16 kOhm	MF55SSF/MF0204	1
Capacitors	Ceramic, 100 nF, 35 V	Z5U-5 100N	20
	Aluminium electrolytic, 10 µF, 35 V	ESMG101ELL100MF11D	2
	Aluminium electrolytic, 47 µF, 35 V	KR470M1HE11VU	2
	Aluminium electrolytic, 100 µF, 35 V	EEUFM1H101	1
Other electronic components	Prototype obard	H25PR200	2
	Multiplexer	74HC 4051	6
	Instrumentation amplifier	AD620	2
	Arduino Zero board	Genuino Zero	1
	SD card	SDSDUN-008G-G46	1
	SD card slot	Attend 104H-TDA0-R01	1
	Diode	SKA1/17	11
	Battery, +6.4 V / 0 V / -6.4 V	customised	1
Sensors	Strain gauge rosette	1-RY93-3/350	10
	Solder terminals	LS7	10
	Strain gauge glue	1-Z70	1
Buttons and lamps	Push-button with green LED	1.15.106.502/1500	1
	Push-button with red LED	1.15.106.501/1300	1
	Yellow LED	352-509-04	2
Cables and connections	Shielded 48 core cable	3600B-50	3 m
	Attachable shield 3 mm diameter	RAY90-3.0	2 m
	Attachable shield 4 mm diameter	RAY90-4.0	1 m
	DIN Plug with 8 connectors, female	650-0800	6
	DIN Plug with 8 connectors, male	590-0800	6
	Hook and loop fasteners	DRFUNDA	5
	Gain Switch	AS 500FPC	1

Table A 1: Electronic components of the measuring system

Appendix D: Technical Drawings

The technical drawings of the housing of the signal conditioning and data acquisition unit are displayed in the following.
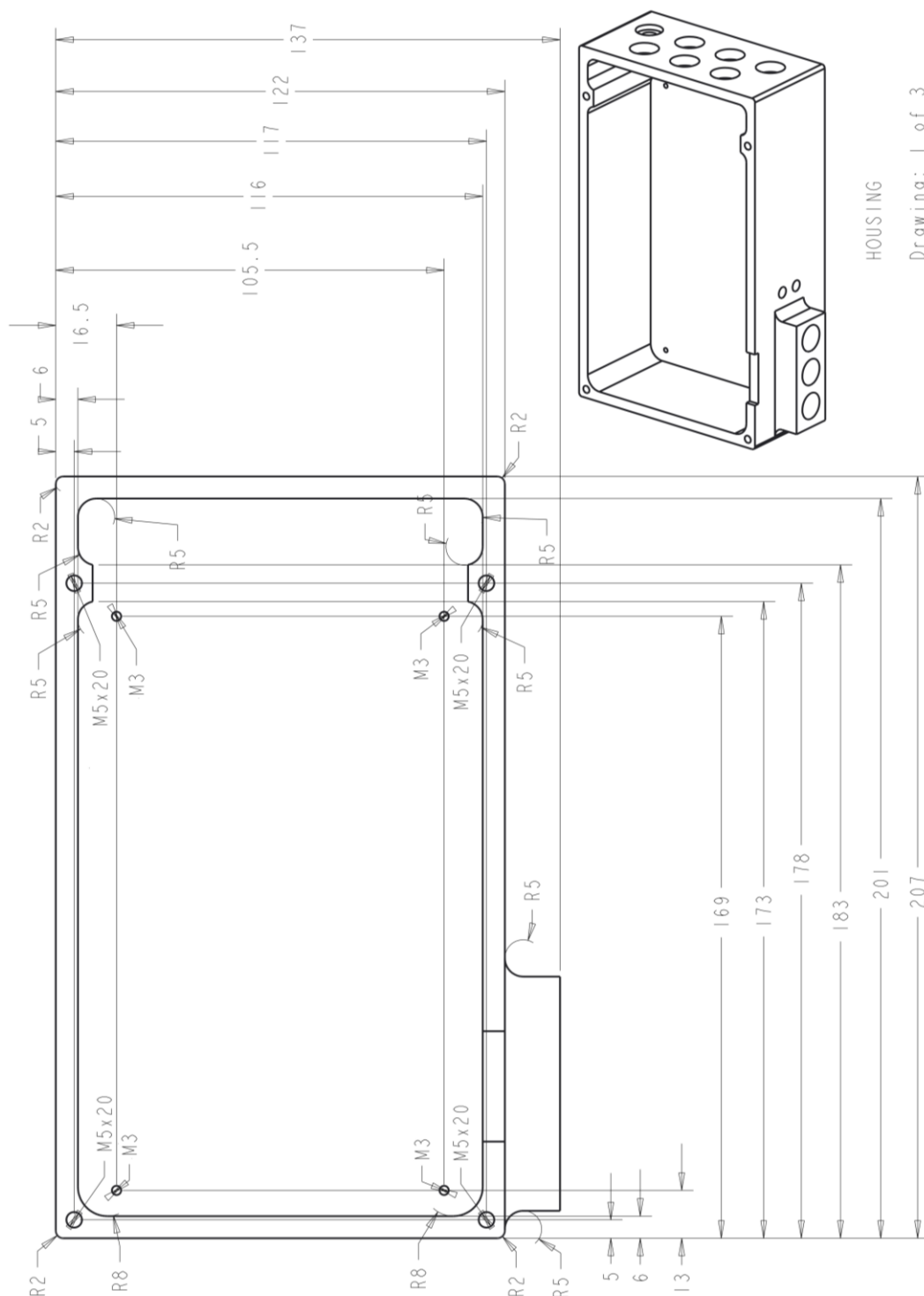
Figure A 6: Technical drawing one of the housing
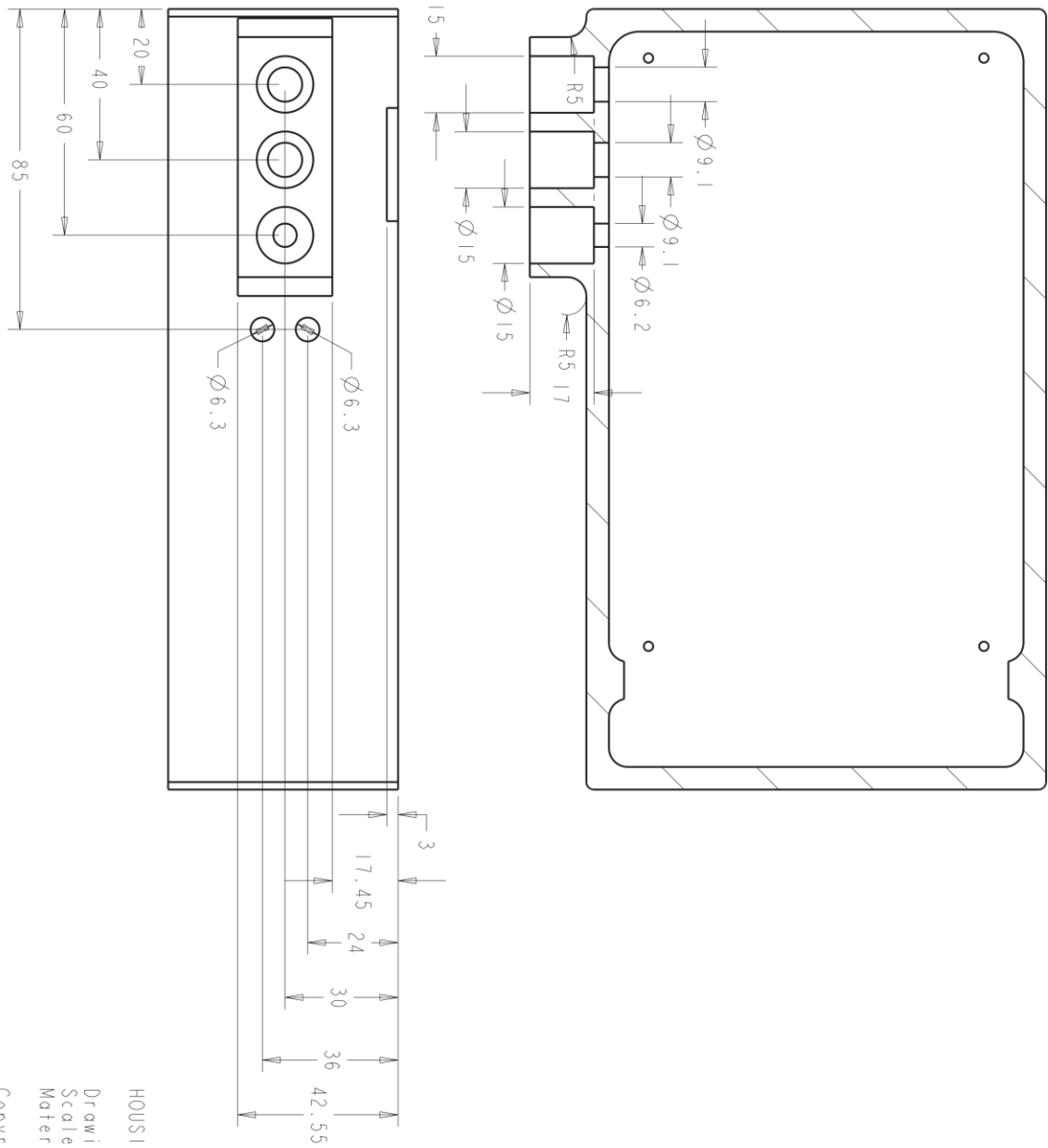
Figure A 7: Technical drawing two of the housing
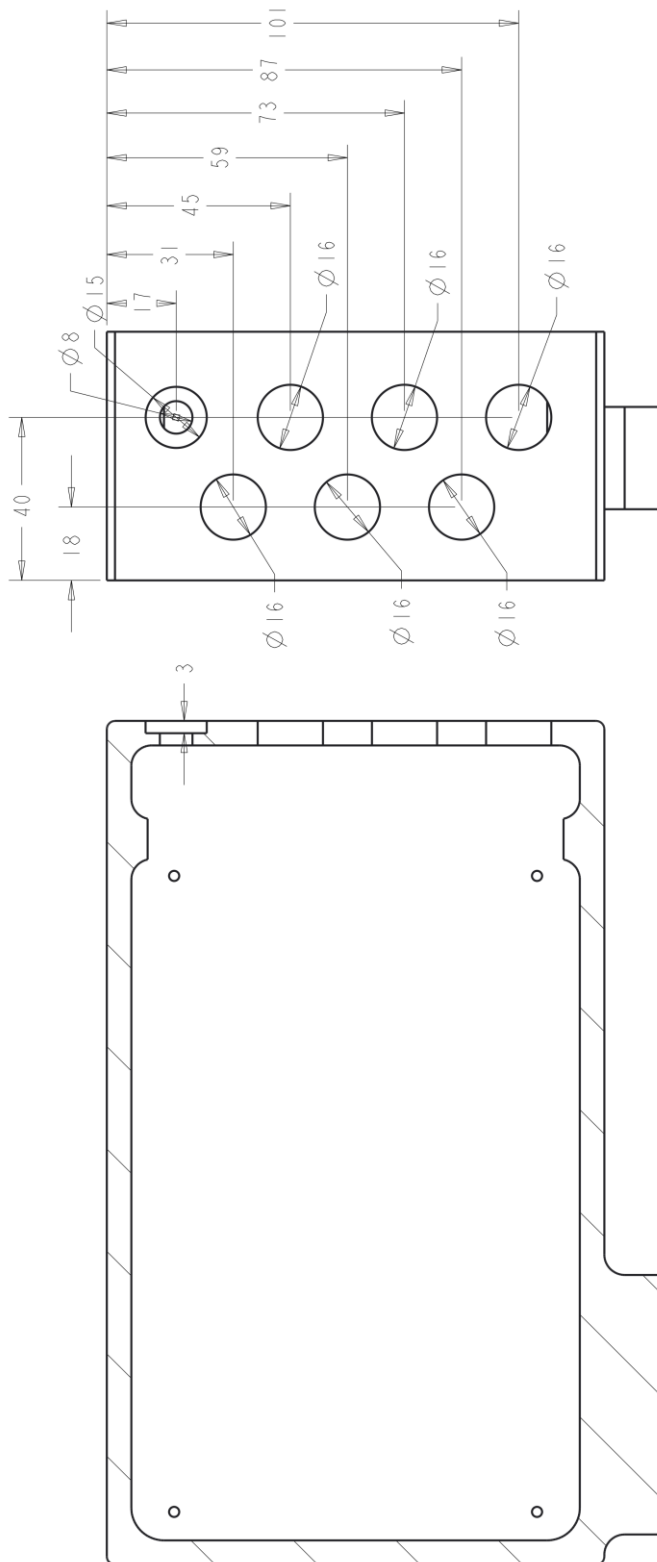
Fabian Tobias Mayer B.Sc.

Figure A 8: Technical drawing three of the housing
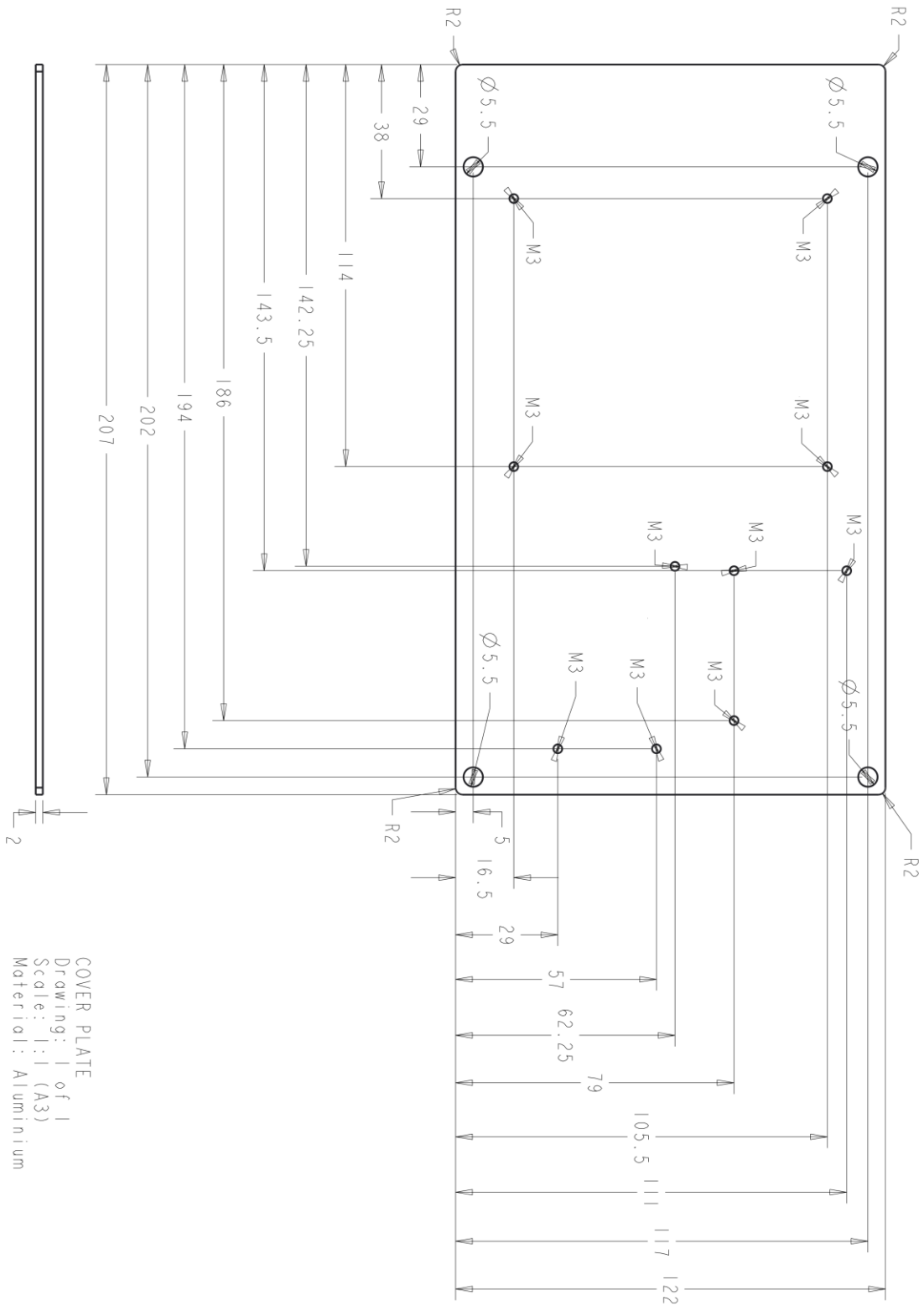
Figure A 9: Technical drawing of the cover plate

Appendix E: Arduino Code Data Logger

In the following the code which was used to log the measuring signal with use of the Arduino
Zero board is displayed. Detailed information on the data acquisition unit of the measuring unit
can be found in chapter 5.6.6.

```
/* **************************************************************************
   ARDUINO DATA LOGGER CODE

   Version: Z11_Optimised (final)
   Date: 29.09.2016

   Copyright 2016 by Fabian Tobias Mayer (fabianmayer@web.de)
   This code may not be used for purposes which are not related to
   the master thesis of Fabian Tobias Mayer without his prior
   written consent.
   **************************************************************************

   Function Summary:
   - Warm up for the multiplexers
   - Adjustment of the reference pin of the instrumentational amplifiers
   - Setting time for the instrumentational amplifiers (still multiplexing)
   - Set the E and S0…S2 pins HIGH and LOW to govern the multiplexers
   - Read the measurement value for the specific multiplexer settings
   - Store the values on the SD card (return error when it is not possible to
     initialise or write on the SD card)
   - Determine the gain state (return error when gain state is changed)
   - Start and stop the logging on the SD card when the start and stop button
     is pushed (light the green LED when measuring)
   - Automatically start a new file when there are more than 10 000 samples
     in the file (to keep the opening and closing time low
   - Differently increasing file names when restarting manually or
     automatically new files
   - Stop the Measurement when there is an error and light the red error LED

   Function *Setup*:
   - Set error and measurement LED high to show that the setup is running
   - Return an error when the SD card is missing and switch the green LED off
   - Deactivate all Multiplexers by setting the E pins HIGH
   - Determine the initial gain state
   - Set error and measurement LED low to show that the setup is done and the
     system is ready to log
   - Determine the highest file name on the SD card not to overwrite existing
     files
   - Make the multiplexers to warm up
   - Determine the maximum voltage of the channels and adjust it to 1.9 V
     (the reference voltage of the instrumentation amplifier is not raised
     higher than 1.9 V; the adjustment is only done during an allowed
     adjustment time)
   - There is a setting time for the instrumentational amplifier before the
     logging is enabled which is signalised by switching off the error and
     measurement LED

   Function *Loop*:
   - Determine the current gain state and set errorState true when it changed
   - Actions which should be taken if the errorState is true: Light the
     errorLed, set measuring state false
   - Determine the start stop button state and de-bounce it with 30ms
   - Set the MSState false or true dependant whether a measurement is running
   - When the MSState was set true the fileNo (first three numbers of the
     File name) is increased to write to a new file when the next measurement
```

is started
- The sample counter is reset when sampling on a new file is started
  manually
- When the maximum number of samples per file is reached a new file is
  Started (The last three digits of the file name are increased)
- The file sample counter is reset when a new measurement file is
  started automatically
- Set the E pins that the first multiplexer set is enabled and the other
  two disabled
- Go through the S pin HIGH/LOW combinations to connect the channels to
  the output after each other (there is a delay between the channels in
  order to grant stability of the signal before reading it)
- Adapt and read all inputs of the first multiplexer set
- Disable the first multiplexer set and do the same procedure for the
  second and third multiplexer set
- Write the measured data of all channels on the SD card when MSstate true
- The data is logged and sampling counter increases as long as the file
  name is the same

Connections:
- Pin 2 (OUTPUT) connected to the inhibit Pin E of multiplexer 1+ and 1-
  !!!Requires external pull down resistors!!!
- Pin 3 (OUTPUT) connected to the inhibit Pin E of multiplexer 2+ and 2-
  !!!Requires external pull down resistors!!!
- Pin 4 (OUTPUT) connected to the inhibit Pin E of multiplexer 3+ and 3-
  !!!Requires external pull down resistors!!!
- Pin 5 (OUTPUT) connected to the S0 Pin of all multiplexes
  !!!Requires external pull down resistors!!!
- Pin 6 (OUTPUT) connected to the S1 Pin of all multiplexes
  !!!Requires external pull down resistors!!!
- Pin 7 (OUTPUT) connected to the S2 Pin of all multiplexes
  !!!Requires external pull down resistors!!!
- Pin 8 (INPUT) connected to the gain low side of the gain state switch
  !!!Requires external pull down resistor!!!
  (INPUT_PULLUP cannot be used as this pin is never connected to ground)
- Pin 9 (INPUT_PULLUP) connected to the button to start and stop the
  measurement (connected to ground when button pushed)
- Pin 10 (OUTPUT) connected to the green LED which is lighted, when data
  is logged
- Pin 11 (OUTPUT) connected to the red error LED which is lighted when
  there is an error
- Pin 12 (-) used for the chip select (CS) of the SPI communication with
  the SD card
- Pin 13 (INPUT_PULLUP) connected to the detection switch of the SD card,
  (connected to ground, when the SD card is present)
- Pin A0 (OUTPUT) connected to the reference terminal of the
  instrumentational amplifier
- Pin A1 (INPUT) connected to the output of the second instrumentation
  Amplifier (more accurate with external pull down than with internal pull
  up resistor) !!!Requires external pull down resistor!!!
- SPI (-) connector connected to the SD card
- Reset Pin (-) connected to a button which connects to ground when pushed

User Interface:
- Both LEDs are lighted during the setup. When both LEDs are of the setup
  and calibration is done and data can be logged
- Start/stop button: Start and stop the data logging on the SD card
- Green measurement LED: If the green LED is lighted data is logged
- Red error LED: If the red LED is lighted the user needs to go through
  the error check list
- Reset button: To be pressed to restart the system after an error was
  corrected

```
    - Name of the file the data is logged on is aaabbb.txt
      (aaa is increasing from 001 to 999 when the user starts and stops a
      measurement; bbb is increasing from 001 to 999 when a new file is
      started after 10 000 samples)

    Error State: (Reset needed to get out of the error state)
    --> Measurement is stopped
    --> Green measurement LED is switched off
    --> Red errorLED is lighted
    - Error when the SD card is missing when the measuring system is powered
    - Error when gain state is changed after the Arduino is started up
    - Error when the SD card cannot be initialised (no SD card available / SD
      card broken
    - Error when it cannot be written on the SD card any more (full/ removed/
      broken)
    - Error when the fileNo (more than 999 measurements started by the user)
      or measNo (more than 999 sub files started by the Arduino)


**************************************************************************
*/


//_____Libraries_____
#include <SPI.h>
#include <SD.h>


//_____Definitions_____

//-----Define Pins-----
//Multiplexer Governing:
#define E1Pin 2             //Select the output pin to enable mux 1+ and 1-
#define E2Pin 3             //Select the output pin to enable mux 2+ and 2-
#define E3Pin 4             //Select the output pin to enable mux 3+ and 3-
#define S0Pin 5             //Select the output pin for steering the mux
                            //output S0
#define S1Pin 6             //Select the output pin for steering the mux
                            //output S1
#define S2Pin 7             //Select the output pin for steering the mux
                            //output S2

//Reference adjustment:
#define refAdjPin A0        //Select the output to adjust the
                            //instrumentational amplifier with at the
                            //reference terminal

//Determine gain state:
#define GSPin 8             //Select the input pin to determine the gain
                            //state (connected to +3.3V when common forces)

//Start/stop logging on the SD card:
#define measSSPin 9          //Select the input pin to start and stop the
                             //measurement (connected to 0V when pushed)
#define ledMSPin 10          //Select the output pin for the LED which shows
                             //whether data is logged

//Error:
#define errorLedPin 11      //Select the output pin for the errorLED

//Write to SD card:
const int chipSelect = 12;
```

```
//Check presence of SD card:
#define sdDetectPin 13      //Select the input pin to determine whether the
                            //SD card is present
                            //(connected to 0V when present)

//Determine Measrued Values:
#define MSPin A1            //Select the input pin for the measurement signal


//-----Define Variables-----
//Warm up and reference adjustment:
unsigned long startWU = 0;  //Variable to store the time [ms] when the
                            //warm up begins
int WUTime = 2000;          //Time [ms] to warm up before starting with the
                            //adjustment of the instrumentational amplifier
int adjTime = 10000;        //Time [ms] how long adjustment should be done
int chMax = 0;              //Variable to store the maximal voltage
                            //[0...4095] output of the channels 1 to 24
int vSenseMax = 2482;       //Voltage 2V [0...4095] the highest output
                            //channel of the instrumentational amplifier
                            //should not be adjusted over (vAdj/3.3*4096)
int vAdjInc = 2;            //Voltage increment [0...1023] with which the
                            //voltage is increased for the adjustment
int vAdjMax = 590;          //Voltage which is maximal apply on the
                            //reference pin 1.9V (not more than 2V allowed
                            //by the supplier)
int vAdj = 0;               //Variable to store the voltage [0...1023]
                            //applied to the reference pin of the
                            //instrumentation amplifier
int settingTime = 3000;     //Time [ms] required until the output voltage
                            //is stable (changes less than 3 uV)

//Naming of the data files:
String fileName = "";       //Variable to store the file number
int fileNo = 1;             //Variable for the file name for a new
                            //measurement started by the user
int measNo = 1;             //Variable for the file name for a new
                            //measurement started by the programme

//Automatic new sub file:
int sampleNo = 0;           //Variable to count the samples in one file
int sampleNoMax = 10000;    //Variable how many samples should be written
                            //to one file

//Error:
boolean errorState = false; //Variable to store whether there is an error

//Start and stop logging on the SD card:
boolean buttonState = false; //Variable to store the button state
boolean msState = false;    //Variable to store whether logging to the SD
                            //card should be done

//Multiplexer steering:
int tSet = 100;             //Setting time in microseconds (10^-6) after
                            //switching before the measurement is done
                            //Setting time multiplexers: 400-1000ns
                            //Setting time instrumentation amplifiers:15us
                            //Output voltage drop when higher than 10kHz
                            //--> 100 micro seconds
```

```
//Determine Measured Values:
int ch01 = 0;               //Variable to store the measured data of channel 1
int ch02 = 0;               //Variable to store the measured data of channel 2
int ch03 = 0;               //Variable to store the measured data of channel 3
int ch04 = 0;               //Variable to store the measured data of channel 4
int ch05 = 0;               //Variable to store the measured data of channel 5
int ch06 = 0;               //Variable to store the measured data of channel 6
int ch07 = 0;               //Variable to store the measured data of channel 7
int ch08 = 0;               //Variable to store the measured data of channel 8
int ch09 = 0;               //Variable to store the measured data of channel 9
int ch10 = 0;               //Variable to store the measured data of channel 10
int ch11 = 0;               //Variable to store the measured data of channel 11
int ch12 = 0;               //Variable to store the measured data of channel 12
int ch13 = 0;               //Variable to store the measured data of channel 13
int ch14 = 0;               //Variable to store the measured data of channel 14
int ch15 = 0;               //Variable to store the measured data of channel 15
int ch16 = 0;               //Variable to store the measured data of channel 16
int ch17 = 0;               //Variable to store the measured data of channel 17
int ch18 = 0;               //Variable to store the measured data of channel 18
int ch19 = 0;               //Variable to store the measured data of channel 19
int ch20 = 0;               //Variable to store the measured data of channel 20
int ch21 = 0;               //Variable to store the measured data of channel 21
int ch22 = 0;               //Variable to store the measured data of channel 22
int ch23 = 0;               //Variable to store the measured data of channel 23
int ch24 = 0;               //Variable to store the measured data of channel 24

//Determine gain state:
int startGS = 0;            //Variable of the gain state when stating the
                            //system (1 for low loads; 2 for high loads)
int nowGS = 0;              //Variable of the current gain state
                            //(1 for common forces; 2 for maximum forces)


//****************************** SETUP **********************************


void setup() {

  //-----Serial Interface-----

  Serial.begin(115200);


  //-----Pins Settings-----

  //Multiplexer steering:
  pinMode(E1Pin, OUTPUT);       //Define the pin 2 as OUTPUT
  pinMode(E2Pin, OUTPUT);       //Define the pin 3 as OUTPUT
  pinMode(E3Pin, OUTPUT);       //Define the pin 4 as OUTPUT
  pinMode(S0Pin, OUTPUT);       //Define the pin 5 as OUTPUT
  pinMode(S1Pin, OUTPUT);       //Define the pin 6 as OUTPUT
  pinMode(S2Pin, OUTPUT);       //Define the pin 7 as OUTPUT

  //Adjustment of the reference terminal:
  pinMode(refAdjPin, OUTPUT);   //Define pin A0 as output
  analogWriteResolution(10);    //Set the analogWrite resolution to its
                                //maximum at 10-bit

  //Gain State:
  pinMode(GSPin, INPUT);        //Define the pin 8 as INPUT
                                //(INPUT_PULLUP here not possible as this pin
                                //is never connected to ground)
```

```
//Start and stop logging on the SD card:
pinMode(measSSPin, INPUT_PULLUP);    //Define pin 9 as INPUT_PULLUP
pinMode(ledMSPin, OUTPUT);           //Define pin 10 as OUTPUT

//Error:
pinMode(errorLedPin, OUTPUT);        //Define the pin 11 as OUTPUT

//SD Card detection:
pinMode(sdDetectPin, INPUT_PULLUP);  //Define pin 11 as INPUT_PULLUP

//Measure:
pinMode(MSPin, INPUT);               //Define the pin A1 as INPUT
analogReadResolution(12);            //Set the analogue read resolution of
                                     //the Arduino Zero to the max at 12-bit


//-----Disable Multiplexers-----

digitalWrite(E1Pin, HIGH);
digitalWrite(E2Pin, HIGH);
digitalWrite(E3Pin, HIGH);


//-----Signalise Setup Is Running-----

digitalWrite(ledMSPin, HIGH);
digitalWrite(errorLedPin, HIGH);


//-----Error Mode When SD Card Missing-----

if (digitalRead(sdDetectPin) == HIGH) {
  errorState = true;
  digitalWrite(ledMSPin, LOW);
  Serial.println("SD card missing in Setup");
}


//-----Determine the Gain State-----

//Low loads:
if (digitalRead(GSPin) == HIGH) {
  startGS = 1;
}
//High loads:
else if (digitalRead(GSPin) == LOW) {
  startGS = 2;
}


//-----Initialise SD Card-----

Serial.print("Initializing SD card...");

//Check if the card is present and can be initialised:
if (!SD.begin(chipSelect)) {
  errorState = true;
  Serial.println("Card failed, or not present");
}
Serial.println("card initialised.");
```

```
//-----Prevent File Overwriting-----

//Generate the lowest file name possible:
fileName = "00" + String(fileNo) + "00" + String(measNo) + ".txt";

//Increase file number until a file name is generated which does not exist:
//(This number is kept than to sample on)
while (SD.exists(fileName)) {
  fileNo = fileNo + 1;

  //Generate the file name:
  if (fileNo < 10) {                          //fileNo [0,9]
    fileName = "00" + String(fileNo) + "00" + String(measNo) + ".txt";
  }
  else if (fileNo < 100 && fileNo >= 10) {          //fileNo [10,99]
    fileName = "0" + String(fileNo) + "00" + String(measNo) + ".txt";
  }
  else if (fileNo < 1000 && fileNo >= 100) {        //fileNo [100,999]
    fileName = String(fileNo) + "00" + String(measNo) + ".txt";
  }

  //Send an error if there are already more than 999 manually started
  //measurements on the SD card
  else {                                      //fileNo >999
    Serial.println("More than 999 files on the card");
    errorState = true;
  }
}


//_____Multiplexer Warm Up and Reference Adjustment_____

//Store the time when the warm up is started:
startWU = millis();

//Conduct the warm up of the multiplexers, adjust the instrumentation
//amplifier and let the system a set after the adjustment:
while (millis() < (startWU + WUTime + adjTime + settingTime)) {

  //-----Multiplexing-----
  Serial.println("Mux warm up and Ref adjust");

  //-----Multiplexer Set 1-----
  //Enable Multiplexer Set 1:
  digitalWrite(E1Pin, LOW);

  //A0 Mux 1 connected:
  digitalWrite(S0Pin, LOW);
  digitalWrite(S1Pin, LOW);
  digitalWrite(S2Pin, LOW);
  delayMicroseconds(tSet);
  ch01 = analogRead(MSPin);

  //A1 Mux 1 connected:
  digitalWrite(S0Pin, HIGH);
  digitalWrite(S1Pin, LOW);
  digitalWrite(S2Pin, LOW);
  delayMicroseconds(tSet);
  ch02 = analogRead(MSPin);

  //A2 Mux 1 connected:
  digitalWrite(S0Pin, LOW);
  digitalWrite(S1Pin, HIGH);
```

```
digitalWrite(S2Pin, LOW);
delayMicroseconds(tSet);
ch03 = analogRead(MSPin);

//A3 Mux 1 connected:
digitalWrite(S0Pin, HIGH);
digitalWrite(S1Pin, HIGH);
digitalWrite(S2Pin, LOW);
delayMicroseconds(tSet);
ch04 = analogRead(MSPin);

//A4 Mux 1 connected:
digitalWrite(S0Pin, LOW);
digitalWrite(S1Pin, LOW);
digitalWrite(S2Pin, HIGH);
delayMicroseconds(tSet);
ch05 = analogRead(MSPin);

//A5 Mux 1 connected:
digitalWrite(S0Pin, HIGH);
digitalWrite(S1Pin, LOW);
digitalWrite(S2Pin, HIGH);
delayMicroseconds(tSet);
ch06 = analogRead(MSPin);

//A6 Mux 1 connected:
digitalWrite(S0Pin, LOW);
digitalWrite(S1Pin, HIGH);
digitalWrite(S2Pin, HIGH);
delayMicroseconds(tSet);
ch07 = analogRead(MSPin);

//A7 Mux 1 connected:
digitalWrite(S0Pin, HIGH);
digitalWrite(S1Pin, HIGH);
digitalWrite(S2Pin, HIGH);
delayMicroseconds(tSet);
ch08 = analogRead(MSPin);

//Disable Multiplexer 1
digitalWrite(E1Pin, HIGH);

//-----Multiplexer Set 2-----
//Enable Multiplexer Set 2:
digitalWrite(E2Pin, LOW);

//A0 Mux 1 connected:
digitalWrite(S0Pin, LOW);
digitalWrite(S1Pin, LOW);
digitalWrite(S2Pin, LOW);
delayMicroseconds(tSet);
ch09 = analogRead(MSPin);

//A1 Mux 1 connected:
digitalWrite(S0Pin, HIGH);
digitalWrite(S1Pin, LOW);
digitalWrite(S2Pin, LOW);
delayMicroseconds(tSet);
ch10 = analogRead(MSPin);

//A2 Mux 1 connected:
digitalWrite(S0Pin, LOW);
```

Fabian Tobias Mayer B.Sc.

```
digitalWrite(S1Pin, HIGH);
digitalWrite(S2Pin, LOW);
delayMicroseconds(tSet);
ch11 = analogRead(MSPin);

//A3 Mux 1 connected:
digitalWrite(S0Pin, HIGH);
digitalWrite(S1Pin, HIGH);
digitalWrite(S2Pin, LOW);
delayMicroseconds(tSet);
ch12 = analogRead(MSPin);

//A4 Mux 1 connected:
digitalWrite(S0Pin, LOW);
digitalWrite(S1Pin, LOW);
digitalWrite(S2Pin, HIGH);
delayMicroseconds(tSet);
ch13 = analogRead(MSPin);

//A5 Mux 1 connected:
digitalWrite(S0Pin, HIGH);
digitalWrite(S1Pin, LOW);
digitalWrite(S2Pin, HIGH);
delayMicroseconds(tSet);
ch14 = analogRead(MSPin);

//A6 Mux 1 connected:
digitalWrite(S0Pin, LOW);
digitalWrite(S1Pin, HIGH);
digitalWrite(S2Pin, HIGH);
delayMicroseconds(tSet);
ch15 = analogRead(MSPin);

//A7 Mux 1 connected:
digitalWrite(S0Pin, HIGH);
digitalWrite(S1Pin, HIGH);
digitalWrite(S2Pin, HIGH);
delayMicroseconds(tSet);
ch16 = analogRead(MSPin);

//Disable Multiplexer 1
digitalWrite(E2Pin, HIGH);

//-----Multiplexer Set 3-----
//Enable Multiplexer Set 3:
digitalWrite(E3Pin, LOW);

//A0 Mux 1 connected:
digitalWrite(S0Pin, LOW);
digitalWrite(S1Pin, LOW);
digitalWrite(S2Pin, LOW);
delayMicroseconds(tSet);
ch17 = analogRead(MSPin);

//A1 Mux 1 connected:
digitalWrite(S0Pin, HIGH);
digitalWrite(S1Pin, LOW);
digitalWrite(S2Pin, LOW);
delayMicroseconds(tSet);
ch18 = analogRead(MSPin);

//A2 Mux 1 connected:
```

```
    digitalWrite(S0Pin, LOW);
    digitalWrite(S1Pin, HIGH);
    digitalWrite(S2Pin, LOW);
    delayMicroseconds(tSet);
    ch19 = analogRead(MSPin);

    //A3 Mux 1 connected:
    digitalWrite(S0Pin, HIGH);
    digitalWrite(S1Pin, HIGH);
    digitalWrite(S2Pin, LOW);
    delayMicroseconds(tSet);
    ch20 = analogRead(MSPin);

    //A4 Mux 1 connected:
    digitalWrite(S0Pin, LOW);
    digitalWrite(S1Pin, LOW);
    digitalWrite(S2Pin, HIGH);
    delayMicroseconds(tSet);
    ch21 = analogRead(MSPin);

    //A5 Mux 1 connected:
    digitalWrite(S0Pin, HIGH);
    digitalWrite(S1Pin, LOW);
    digitalWrite(S2Pin, HIGH);
    delayMicroseconds(tSet);
    ch22 = analogRead(MSPin);

    //A6 Mux 1 connected:
    digitalWrite(S0Pin, LOW);
    digitalWrite(S1Pin, HIGH);
    digitalWrite(S2Pin, HIGH);
    delayMicroseconds(tSet);
    ch23 = analogRead(MSPin);

    //A7 Mux 1 connected:
    digitalWrite(S0Pin, HIGH);
    digitalWrite(S1Pin, HIGH);
    digitalWrite(S2Pin, HIGH);
    delayMicroseconds(tSet);
    ch24 = analogRead(MSPin);

    //Disable Multiplexer 1
    digitalWrite(E3Pin, HIGH);

    //-----Adapt the Reference Pin-----
    //Calculate the current maximum output of the channels 1 to 24 [0...4096]:
    chMax = 0;          //Set chMax to 0 that it can be increased again for the
                        //following loop
    if (chMax < ch01) {
      chMax = ch01;
    }
    if (chMax < ch02) {
      chMax = ch02;
    }
    if (chMax < ch03) {
      chMax = ch03;
    }
    if (chMax < ch04) {
      chMax = ch04;
    }
    if (chMax < ch05) {
      chMax = ch05;
    }
```

Fabian Tobias Mayer B.Sc.

```
    if (chMax < ch06) {
      chMax = ch06;
    }
    if (chMax < ch07) {
      chMax = ch07;
    }
    if (chMax < ch08) {
      chMax = ch08;
    }
    if (chMax < ch09) {
      chMax = ch09;
    }
    if (chMax < ch10) {
      chMax = ch10;
    }
    if (chMax < ch11) {
      chMax = ch11;
    }
    if (chMax < ch12) {
      chMax = ch12;
    }
    if (chMax < ch13) {
      chMax = ch13;
    }
    if (chMax < ch14) {
      chMax = ch14;
    }
    if (chMax < ch15) {
      chMax = ch15;
    }
    if (chMax < ch16) {
      chMax = ch16;
    }
    if (chMax < ch17) {
      chMax = ch17;
    }
    if (chMax < ch18) {
      chMax = ch18;
    }
    if (chMax < ch19) {
      chMax = ch19;
    }
    if (chMax < ch20) {
      chMax = ch20;
    }
    if (chMax < ch21) {
      chMax = ch21;
    }
    if (chMax < ch22) {
      chMax = ch22;
    }
    if (chMax < ch23) {
      chMax = ch23;
    }
    if (chMax < ch24) {
      chMax = ch24;
    }

    //Increase the voltage:
    //- if the warm up time is over
    //- if the maximal adjustment time is not over
    //- if the voltage on the output is not higher than vSenseMax
```

```
    //- if the maximum on the reference pin is lower than the allowed vAdjMax
    if (millis() > (startWU + WUTime) && millis() < (startWU + WUTime +
        adjTime) && vAdj < (vAdjMax + vAdjInc) && chMax < vSenseMax) {
      vAdj = vAdj + vAdjInc;
      analogWrite(refAdjPin, vAdj);
      Serial.println("IncreasingVoltage:");
      Serial.print("vAdj= ");
      Serial.println(vAdj * 3.3 / 1024);
    }
  }


  //_____Setup Done_____
  digitalWrite(ledMSPin, LOW);
  digitalWrite(errorLedPin, LOW);
}


//***************************** LOOP *****************************


void loop() {

  //_____Error State_____

  //-----Error State for Changed Gain-----
  //Find out the current gain state:
  if (digitalRead(GSPin) == HIGH) {
    nowGS = 1;
  }
  else if (digitalRead(GSPin) == LOW) {
    nowGS = 2;
  }

  //Find out whether the gain state is still the same:
  if (nowGS != startGS) {
    errorState = true;
  }

  //-----Error State for Removed SD-----
  if (digitalRead(sdDetectPin) == HIGH) {
    errorState = true;
    Serial.println("SD removed in loop");
  }

  //-----Output for Error State-----
  if (errorState == true) {
    msState = false;
    digitalWrite(errorLedPin, HIGH);
    digitalWrite(ledMSPin, LOW);
    Serial.println("ERROR");
  }


  //_____Start and Stop Logging_____

  //-----Start/Stop Button Is Pressed-----
  //Set buttonState true if the button is pressed and button state is false:
  if (digitalRead(measSSPin) == LOW && buttonState == false) {
    delay(30);                              //Wait to de-bounce the switch
```

```
// Check whether the button is still pressed:
    if (digitalRead(measSSPin) == LOW) {
      buttonState = true;

      //-----Start Measurement-----
      //Set the msState high if no measurement is running and there is no
      //error:
      if (msState == false && errorState == false) {
        msState = true;                              //Enable measuring
        digitalWrite(ledMSPin, HIGH);          //Light measurement LED
      }

      //-----Stop Measurement-----
      //Set the msState low if a measurement is running and there is no error
      else if (msState == true && errorState == false) {
        msState = false;                            //Disable measuring
        digitalWrite(ledMSPin, LOW);           //Switch measurement LED off

        //-----Increase File Name for Next Measurement-----
        //Increase fileNo by one that data is written in one file higher than
        //the last measurement:
        fileNo = fileNo + 1;
        //Set the measNo back to 1:
        sampleNo = 0;      //Reset sample counter as new file will be used
        measNo = 1;        //That new sub files start from 001

        //Generate the file name:
        if (fileNo < 10) {                               //fileNo [0,9]
          fileName = "00" + String(fileNo) + "00" + String(measNo) + ".txt";
        }
        else if (fileNo < 100 && fileNo >= 10) {         //fileNo [10,99]
          fileName = "0" + String(fileNo) + "00" + String(measNo) + ".txt";
        }
        else if (fileNo < 1000 && fileNo >= 100) {       //fileNo [100,998]
          fileName = String(fileNo) + "00" + String(measNo) + ".txt";
        }

        //Send an error if more than 999 manually started measurements are on
        //the SD card:
        else {                                            //fileNo >999
          Serial.println("More than 999 files on the card");
          errorState = true;
        }
      }
    }
  }

  //-----Start/Stop Button Was Released-----
  //Set buttonState false if the button is not pressed and buttonState true:
  else if (digitalRead(measSSPin) == HIGH && buttonState == true) {
    delay(30);                                   //Wait to debounce the switch

    // Check whether the button is still pressed:
    if (digitalRead(measSSPin) == HIGH) {
      buttonState = false;
    }
  }
```

```
//_____Automatic New File Name_____

if (sampleNo > sampleNoMax - 1) {     //-1 because the counter is increased
                                      //after writing

  //Increase the measNo by one that the data is stored on a file named
  //higher than the last measurement:
  measNo = measNo + 1;
  sampleNo = 0;          //Reset sample counter because the file will be used

  //Generate the new file name:
  //fileNo [1,9], measNo [1,9]
  if (fileNo < 10 && measNo < 10) {
    fileName = "00" + String(fileNo) + "00" + String(measNo) + ".txt";
  }
  //fileNo [1,9], measNo [10,99]
  else if (fileNo < 10 && measNo >= 10 && measNo < 100) {
    fileName = "00" + String(fileNo) + "0" + String(measNo) + ".txt";
  }
  //fileNo [1,9], measNo [100,999]
  else if (fileNo < 10 && measNo >= 100 && measNo < 1000) {
    fileName = "00" + String(fileNo) + String(measNo) + ".txt";
  }
  //fileNo [10,99], measNo [1,9]
  else if (fileNo >= 10 && fileNo < 100 && measNo < 10) {
    fileName = "0" + String(fileNo) + "00" + String(measNo) + ".txt";
  }
  //fileNo [10,99], measNo [10,99]
  else if (fileNo >= 10 && fileNo < 100 && measNo >= 10 && measNo < 100) {
    fileName = "0" + String(fileNo) + "0" + String(measNo) + ".txt";
  }
  //fileNo [10,99], measNo [100,999]
  else if (fileNo >= 10 && fileNo < 100 && measNo >= 100 && measNo < 1000){
    fileName = "0" + String(fileNo) + String(measNo) + ".txt";
  }
  //fileNo [100,999], measNo [1,9]
  else if (fileNo >= 100 && fileNo < 1000 && measNo < 10) {
    fileName = String(fileNo) + "00" + String(measNo) + ".txt";
  }
  //fileNo [100,999], measNo [10,99]
  else if (fileNo >= 100 && fileNo < 1000 && measNo >= 10 && measNo < 100){
    fileName = String(fileNo) + "0" + String(measNo) + ".txt";
  }
  //fileNo [100,999], measNo [100,999]
  else if (fileNo >= 100 && fileNo < 1000 && measNo >= 100 && measNo <
          1000) {
    fileName = String(fileNo) + String(measNo) + ".txt";
  }

  //Send an error if there are already more than 999 automatically started
  //sub measurements on the SD card:
  else {                             //Error when fileNo > 999 or measNo > 999
    errorState = true;
    Serial.println("Too long measurement (too many sub files)");
  }
}


//_____Multiplex and Analog Read_____

//-----Multiplexer Set 1-----
//Enable Multiplexer Set 1:
```

```
digitalWrite(E1Pin, LOW);

//A0 Mux 1 connected:
digitalWrite(S0Pin, LOW);
digitalWrite(S1Pin, LOW);
digitalWrite(S2Pin, LOW);
delayMicroseconds(tSet);
ch01 = analogRead(MSPin);

//A1 Mux 1 connected:
digitalWrite(S0Pin, HIGH);
digitalWrite(S1Pin, LOW);
digitalWrite(S2Pin, LOW);
delayMicroseconds(tSet);
ch02 = analogRead(MSPin);

//A2 Mux 1 connected:
digitalWrite(S0Pin, LOW);
digitalWrite(S1Pin, HIGH);
digitalWrite(S2Pin, LOW);
delayMicroseconds(tSet);
ch03 = analogRead(MSPin);

//A3 Mux 1 connected:
digitalWrite(S0Pin, HIGH);
digitalWrite(S1Pin, HIGH);
digitalWrite(S2Pin, LOW);
delayMicroseconds(tSet);
ch04 = analogRead(MSPin);

//A4 Mux 1 connected:
digitalWrite(S0Pin, LOW);
digitalWrite(S1Pin, LOW);
digitalWrite(S2Pin, HIGH);
delayMicroseconds(tSet);
ch05 = analogRead(MSPin);

//A5 Mux 1 connected:
digitalWrite(S0Pin, HIGH);
digitalWrite(S1Pin, LOW);
digitalWrite(S2Pin, HIGH);
delayMicroseconds(tSet);
ch06 = analogRead(MSPin);

//A6 Mux 1 connected:
digitalWrite(S0Pin, LOW);
digitalWrite(S1Pin, HIGH);
digitalWrite(S2Pin, HIGH);
delayMicroseconds(tSet);
ch07 = analogRead(MSPin);

//A7 Mux 1 connected:
digitalWrite(S0Pin, HIGH);
digitalWrite(S1Pin, HIGH);
digitalWrite(S2Pin, HIGH);
delayMicroseconds(tSet);
ch08 = analogRead(MSPin);

//Disable Multiplexer 1
digitalWrite(E1Pin, HIGH);
```

```
//-----Multiplexer Set 2-----
//Enable Multiplexer Set 2:
digitalWrite(E2Pin, LOW);

//A0 Mux 1 connected:
digitalWrite(S0Pin, LOW);
digitalWrite(S1Pin, LOW);
digitalWrite(S2Pin, LOW);
delayMicroseconds(tSet);
ch09 = analogRead(MSPin);

//A1 Mux 1 connected:
digitalWrite(S0Pin, HIGH);
digitalWrite(S1Pin, LOW);
digitalWrite(S2Pin, LOW);
delayMicroseconds(tSet);
ch10 = analogRead(MSPin);

//A2 Mux 1 connected:
digitalWrite(S0Pin, LOW);
digitalWrite(S1Pin, HIGH);
digitalWrite(S2Pin, LOW);
delayMicroseconds(tSet);
ch11 = analogRead(MSPin);

//A3 Mux 1 connected:
digitalWrite(S0Pin, HIGH);
digitalWrite(S1Pin, HIGH);
digitalWrite(S2Pin, LOW);
delayMicroseconds(tSet);
ch12 = analogRead(MSPin);

//A4 Mux 1 connected:
digitalWrite(S0Pin, LOW);
digitalWrite(S1Pin, LOW);
digitalWrite(S2Pin, HIGH);
delayMicroseconds(tSet);
ch13 = analogRead(MSPin);

//A5 Mux 1 connected:
digitalWrite(S0Pin, HIGH);
digitalWrite(S1Pin, LOW);
digitalWrite(S2Pin, HIGH);
delayMicroseconds(tSet);
ch14 = analogRead(MSPin);

//A6 Mux 1 connected:
digitalWrite(S0Pin, LOW);
digitalWrite(S1Pin, HIGH);
digitalWrite(S2Pin, HIGH);
delayMicroseconds(tSet);
ch15 = analogRead(MSPin);

//A7 Mux 1 connected:
digitalWrite(S0Pin, HIGH);
digitalWrite(S1Pin, HIGH);
digitalWrite(S2Pin, HIGH);
delayMicroseconds(tSet);
ch16 = analogRead(MSPin);

//Disable Multiplexer 1
digitalWrite(E2Pin, HIGH);
```

```
//-----Multiplexer Set 3-----
//Enable Multiplexer 3 Set:
digitalWrite(E3Pin, LOW);

//A0 Mux 1 connected:
digitalWrite(S0Pin, LOW);
digitalWrite(S1Pin, LOW);
digitalWrite(S2Pin, LOW);
delayMicroseconds(tSet);
ch17 = analogRead(MSPin);

//A1 Mux 1 connected:
digitalWrite(S0Pin, HIGH);
digitalWrite(S1Pin, LOW);
digitalWrite(S2Pin, LOW);
delayMicroseconds(tSet);
ch18 = analogRead(MSPin);

//A2 Mux 1 connected:
digitalWrite(S0Pin, LOW);
digitalWrite(S1Pin, HIGH);
digitalWrite(S2Pin, LOW);
delayMicroseconds(tSet);
ch19 = analogRead(MSPin);

//A3 Mux 1 connected:
digitalWrite(S0Pin, HIGH);
digitalWrite(S1Pin, HIGH);
digitalWrite(S2Pin, LOW);
delayMicroseconds(tSet);
ch20 = analogRead(MSPin);

//A4 Mux 1 connected:
digitalWrite(S0Pin, LOW);
digitalWrite(S1Pin, LOW);
digitalWrite(S2Pin, HIGH);
delayMicroseconds(tSet);
ch21 = analogRead(MSPin);

//A5 Mux 1 connected:
digitalWrite(S0Pin, HIGH);
digitalWrite(S1Pin, LOW);
digitalWrite(S2Pin, HIGH);
delayMicroseconds(tSet);
ch22 = analogRead(MSPin);

//A6 Mux 1 connected:
digitalWrite(S0Pin, LOW);
digitalWrite(S1Pin, HIGH);
digitalWrite(S2Pin, HIGH);
delayMicroseconds(tSet);
ch23 = analogRead(MSPin);

//A7 Mux 1 connected:
digitalWrite(S0Pin, HIGH);
digitalWrite(S1Pin, HIGH);
digitalWrite(S2Pin, HIGH);
delayMicroseconds(tSet);
ch24 = analogRead(MSPin);

//Disable Multiplexer 1
digitalWrite(E3Pin, HIGH);
```

```
//_____Write Measured Values on the SD Card_____

//Write on the SD card if a measurement is Running:
if (msState == true) {

  //------Determine the Numbers of Samples on Current File----------
  //Is reset in the block where and when the file number changes
  sampleNo = sampleNo + 1;

  //Open File on the SD card:
  File dataFile = SD.open(fileName, FILE_WRITE);

  //-----Write the Measured Values on the SD Card-----
  //If the file is available, write to it:
  if (dataFile) {
    //Save values on the SD card:
    dataFile.print(millis());
    dataFile.print(",");
    dataFile.print(ch01);
    dataFile.print(",");
    dataFile.print(ch02);
    dataFile.print(",");
    dataFile.print(ch03);
    dataFile.print(",");
    dataFile.print(ch04);
    dataFile.print(",");
    dataFile.print(ch05);
    dataFile.print(",");
    dataFile.print(ch06);
    dataFile.print(",");
    dataFile.print(ch07);
    dataFile.print(",");
    dataFile.print(ch08);
    dataFile.print(",");
    dataFile.print(ch09);
    dataFile.print(",");
    dataFile.print(ch10);
    dataFile.print(",");
    dataFile.print(ch11);
    dataFile.print(",");
    dataFile.print(ch12);
    dataFile.print(",");
    dataFile.print(ch13);
    dataFile.print(",");
    dataFile.print(ch14);
    dataFile.print(",");
    dataFile.print(ch15);
    dataFile.print(",");
    dataFile.print(ch16);
    dataFile.print(",");
    dataFile.print(ch17);
    dataFile.print(",");
    dataFile.print(ch18);
    dataFile.print(",");
    dataFile.print(ch19);
    dataFile.print(",");
    dataFile.print(ch20);
    dataFile.print(",");
    dataFile.print(ch21);
    dataFile.print(",");
    dataFile.print(ch22);
    dataFile.print(",");
```

```
      dataFile.print(ch23);
      dataFile.print(",");
      dataFile.print(ch24);
      dataFile.print(",");
      dataFile.println(startGS);

      //Close the SD card:
      dataFile.close();
    }

    //If the file cannot be opened, return an error:
    else {
      errorState = true;
      Serial.println("Error opening file!");
    }
  }
}
```

Appendix F: Matlab Code Data Processing

The Matlab code which was used to process the recorded measuring signal in order to calculate the loads acting on the roller ski can be found hereinafter. Detailed information on the calculation can be found in chapter 5.6.8.

```matlab
%*************************************************************************
%  MATLAB DATA PROCESSING CODE
%
%  Version: DataProcessingFinal
%  Date: 09.10.2016
%
%  Copyright 2016 by Fabian Tobias Mayer (fabianmayer@web.de)
%  This code may not be used for purposes which are not related to
%  the master thesis of Fabian Tobias Mayer without his prior
%  written consent.
%*************************************************************************


%-------------------------------------------------------------------------
clear;          % Remove variables from the work space
close all;      % Close all plots
clc;            % Clear the command window


%-------------------------------------------------------------------------
%% User Interface

%!!!!!!!!!!!!!!!!!!!!!!!!!!!!!!!!!!!!!!!!!!!!!!!!!!!!!!!!!!!!!!!!!!!!!!!!!
% Data acquisition:
% - Roller ski needs to be unloaded for the first second when the system
%   is started
%   (otherwise the tare function will lead to an error)
% - Data needs to be copied into the folder TestData
%   (all sub files of the measurement need to be copied,
%    only one measurement can be processed at a time)
%!!!!!!!!!!!!!!!!!!!!!!!!!!!!!!!!!!!!!!!!!!!!!!!!!!!!!!!!!!!!!!!!!!!!!!!!!

% Direction of the coordinate axes:
% x-axis: Aligned with the beam of the roller ski
% y-axis: Horizontal, perpendicular to the beam of the roller ski
% z-axis: Vertical, perpendicular to the beam of the roller ski

% -----Position for which the loads should be calculated--------
% (offset to the neutral layers and the binding pin)

% Position of the neutral layer:
% - in x direction: The plane which intersects with the binding pin
% - in y direction: The plane in the geometric middle of the beam
% - in z direction: The plane which is 14.78 mm offset in negative
%                   z direction under the top of the beam of the roller
%                   ski where the binding and the roller ski are

xS=0;              % Position in x direction [m]
yS=0;              % Position in y direction [m]
zS=0.01478;        % Position in z direction [m]

% !!!!!!!!!!!!!!!!!!!!!!!!!!!!!!!!!!!!!!!!!!!!!!!!!!!!!!!!!!!!!!!!!!!!!!!!
%                   !!! NO CHANGES UNDERNEATH !!!
% !!!!!!!!!!!!!!!!!!!!!!!!!!!!!!!!!!!!!!!!!!!!!!!!!!!!!!!!!!!!!!!!!!!!!!!!
```

```
%%----------------------------Data Processing----------------------------

% Function:
% 0) Parameters
%    0.1) Data Acquisition Parameters
%    0.2) Material Parameters
%    0.3) Geometric Parameters
%    0.4) Calibration Parameters
% 1) Import Data from SD Card
%    1.1) Import Data
%    1.2) Shift the date to start at 0ms and tare the measured values
% 2) Determine the Strain at the Strain Gauges
% 3) Calibration of the calculated strain output
% 4) Determine the Stress at the Rosette Positions with the
%    SkiPositionStress function
% 5) Calculation of the loads
%    5.1) Calculate them for the neutral layers
%    5.2) Calculate them for the selected position
% 6) Results
%    6.1) Sampling frequency
%    6.2) Gain state
%    6.3) Selected position
%    6.4) Max and min loads
% 7) Plots
%    7.1) Results
%    7.2) Plots
% 8) Write Results and Plots to Results
%    8.1) Generate new sub folder
%    8.2) Write the results as .xls-file
%    8.3) Safe the plots
%    8.4) Write command window output to .txt-file
%
% User interface:
% - Roller ski needs to be unloaded for the first second when the system
%   is started
%   (otherwise the tare function will lead to an error)
% - Data needs to be copied into the folder TestData
%   (all sub files of the measurement need to be copied, only one
%   measurement can be processed at a time)


%%---------------------------0) Parameters----------------------------

% 0.1) Data Acquisition Parameters:

k=2.05;               % k-factor of the strain gauges
GL=333.33;            % Gain for low load setting
GH=223.08;            % Gain for high load setting
U0=3.3;               % Bridge excitation voltage
URange=3.3;           % Measuring range of the Arduino analogue input
res=4096;             % Possible values of the 12 bit resulution of the
                      % analogue input pin of the arduino

% 0.2) Material Parameters:

E=68.9e9;             % Young's modulus [Pa]
nu=0.33;              % Poisson's ratio [-]

% 0.3) Geometric Parameters:

A_S=0.00020521;       % Intersectional area of the profile [m^2]
h_min=1.5/1000;       % Minimal thickness of the profile (at the position
```

```
                              % of the left and right strain gauges) [m]
I_y=2.139939429e-8;           % I_y second moment of inertia for the torque
% in y direction [m^4]
I_z=3.703968513e-8;           % I_z second moment of inertia for the torque
                              % in z direction [m^4]
d=180/1000;                   % Horizontal distance from the strain gauges to the
                              % coordinate system [m]
z_T=(14.77979714-3.5)/1000;    % Distance of the top strain gauges to the
                              % coordinate system
% (in the centre of area of the profile) [m]
y_R=38/(2*1000);                 % Distance of the right strain gauges to the
                              % coordinate system
                              % (in the centre of area of the profile) [m]
z_B=(28.5-14.77979714)/1000;   % Distance of the bottom strain gauges to the
                              % coordinate system
                              % (in the centre of area of the profile) [m]
y_L=38/(2*1000);                 % Distance of the left strain gauges to the
                              % coordinate system
                              % (in the centre of area of the profile) [m]


% 0.4) Calibration Parameters:

%Strain Calibration:
cFrontTa=-1;
cFrontTb=-1;
cFrontTc=-1;

cFrontRa=-1;
cFrontRb=-1;
cFrontRc=-1;

cFrontBa=-1;
cFrontBb=-1;
cFrontBc=-0.9;

cFrontLa=-1;
cFrontLb=-1;
cFrontLc=-1;

cBackTa=-1;
cBackTb=-1;
cBackTc=-0.8;

cBackRa=-1;
cBackRb=-1;
cBackRc=-1;

cBackBa=2;
cBackBb=-1;
cBackBc=4.5;

cBackLa=-1;
cBackLb=-1;
cBackLc=-1;

% Load Calibration:
c_Fx=-1;
c_Fy=1;
c_Fz=1.87;
```

```matlab
c_Mx=1;
c_My=1;
c_Mz=1;

%%---------------------------1) Import---------------------------------

% 1.1) Import Data:

% Store the names of the files
list=dir('TestData/*.txt');      % Determine the .txt-files in the folder
                                 % and store them in the list


noOfFiles=length(list);          % Determine the number of sub files


measData=[];                     % Initialise matrix for the measured Data

% Write the measured data of the sub files under each other with increasing
% sub measuring no.
for i=1:noOfFiles
    %  fileName=list(i).name;                  % Get the filenames
    fileName=['TestData/',list(i).name];        % Define the filenames with
                                                % search path
    measData=[measData;dlmread(fileName)];      % Read the data from the file
                                                % and store it under the last
                                                % measurement
end


% 1.2) Shift Time and Tare:

% Time Shift:
% Shift the data that the first sample is at 0 ms
lengthData=size(measData,1);
measData(1:lengthData,1)=measData(1:lengthData,1)-measData(1,1);

% Tare:
% Tare system with the mean value of the first 20 samples
% (system needs to be unloaded)
for i=2:25
    if lengthData>=20
        meanTare=mean(measData(1:20,i));
        measData(1:lengthData,i)=measData(1:lengthData,i)-meanTare;
    else
        measData(1:lengthData,i)=measData(1:lengthData,i)-measData(1,i);
    end
end

%%------------------------2) Strain Calculation-------------------------

% Define the matrix in which time and strain is stored
strainData=zeros(lengthData,25);

% Write the time in the first column
strainData(1:lengthData,1)=measData(1:lengthData,1);

% Determine which gain was set:
if measData(1,26)==1          % Low loads
    G=GL;
elseif measData(1,26)==2      % High loads
    G=GH;
end
```

```
% Calculate the strain and write it to the columns
for i=2:25

strainData(1:lengthData,i)=4*URange/(k*U0*G*res)*measData(1:lengthData,i);
end

%%--------------------------3) Strain Calibration--------------------------

strainData(:,2)=cFrontTa*strainData(:,2);
strainData(:,3)=cFrontTb*strainData(:,3);
strainData(:,4)=cFrontTc*strainData(:,4);
strainData(:,5)=cFrontRa*strainData(:,5);
strainData(:,6)=cFrontRb*strainData(:,6);
strainData(:,7)=cFrontRc*strainData(:,7);
strainData(:,8)=cFrontBa*strainData(:,8);
strainData(:,9)=cFrontBb*strainData(:,9);
strainData(:,10)=cFrontBc*strainData(:,10);
strainData(:,11)=cFrontLa*strainData(:,11);
strainData(:,12)=cFrontLb*strainData(:,12);
strainData(:,13)=cFrontLc*strainData(:,13);

strainData(:,14)=cBackTa*strainData(:,14);
strainData(:,15)=cBackTb*strainData(:,15);
strainData(:,16)=cBackTc*strainData(:,16);
strainData(:,17)=cBackRa*strainData(:,17);
strainData(:,18)=cBackRb*strainData(:,18);
strainData(:,19)=cBackRc*strainData(:,19);
strainData(:,20)=cBackBa*strainData(:,20);
strainData(:,21)=cBackBb*strainData(:,21);
strainData(:,22)=cBackBc*strainData(:,22);
strainData(:,23)=cBackLa*strainData(:,23);
strainData(:,24)=cBackLb*strainData(:,24);
strainData(:,25)=cBackLc*strainData(:,25);

%%--------------------------4) Stress calculation--------------------------

% Extrackt the stress of the rosettes
strainRosetteFrontT=strainData(1:lengthData,2:4);
strainRosetteFrontR=strainData(1:lengthData,5:7);
strainRosetteFrontB=strainData(1:lengthData,8:10);
strainRosetteFrontL=strainData(1:lengthData,11:13);
strainRosetteBackT=strainData(1:lengthData,14:16);
strainRosetteBackR=strainData(1:lengthData,17:19);
strainRosetteBackB=strainData(1:lengthData,20:22);
strainRosetteBackL=strainData(1:lengthData,23:25);

% Use the SkiPositionStress function to determine the stresses at the
% positions of the rosettes:

% Orientation of the strain gauge rosettes:
%     1: Top, pins in positive x-direction
%     2: Top, pins in negative x-direction
%     3: Right, pins in positive z-direction
%     4: Bottom, pins in positive x-direction
%     5: Bottom, pins in negative x-direction
%     6: Left, pins in positive z-direction

%Rosette1 Front Top:
[sigma_x_FrontT,sigma_y_FrontT,sigma_z_FrontT,tau_xy_FrontT,tau_xz_FrontT]=Sk
iPositionStress(2,strainRosetteFrontT,E,nu);
```

```
%Rosette2 Front Right:
[sigma_x_FrontR,sigma_y_FrontR,sigma_z_FrontR,tau_xy_FrontR,tau_xz_FrontR]=Sk
iPositionStress(3,strainRosetteFrontR,E,nu);
%Rosette3 Front Bottom:
[sigma_x_FrontB,sigma_y_FrontB,sigma_z_FrontB,tau_xy_FrontB,tau_xz_FrontB]=Sk
iPositionStress(5,strainRosetteFrontB,E,nu);
%Rosette4 Front Left:
[sigma_x_FrontL,sigma_y_FrontL,sigma_z_FrontL,tau_xy_FrontL,tau_xz_FrontL]=Sk
iPositionStress(6,strainRosetteFrontL,E,nu);

%Rosette5 Back Top:
[sigma_x_BackT,sigma_y_BackT,sigma_z_BackT,tau_xy_BackT,tau_xz_BackT]=SkiPo
sitionStress(1,strainRosetteBackT,E,nu);
%Rosette6 Back Right:
[sigma_x_BackR,sigma_y_BackR,sigma_z_BackR,tau_xy_BackR,tau_xz_BackR]=SkiPo
sitionStress(3,strainRosetteBackR,E,nu);
%Rosette7 Back Bottom:
[sigma_x_BackB,sigma_y_BackB,sigma_z_BackB,tau_xy_BackB,tau_xz_BackB]=SkiPo
sitionStress(4,strainRosetteBackB,E,nu);
%Rosette8 Back Left:
[sigma_x_BackL,sigma_y_BackL,sigma_z_BackL,tau_xy_BackL,tau_xz_BackL]=SkiPo
sitionStress(6,strainRosetteBackL,E,nu);

%%--------------------------5) Load Calculation--------------------------

% 5.1) Calculate the loads from the measured strain:

%       - The forces and torques are calculated for the position at the
%         centre of area in the middle between the front and back sensors
%         (is in the middle of the beam under the binding link)

% F_x=-F_xFront+F_xBack:
F_x=c_Fx*A_S*((sigma_x_BackR+sigma_x_BackL)/2-
(sigma_x_FrontR+sigma_x_FrontL)/2);

% F_y (compare bottom and top to eliminate normal forces
% and add front and back because forces have the same effect in the front
% and in the back):
F_y=c_Fy*I_z/(2*d)*((sigma_x_BackL/y_L-
sigma_x_BackR/y_R)+(sigma_x_FrontL/y_L-sigma_x_FrontR/y_R));

% F_z (same proceeding like for F_y):
F_z=c_Fz*I_y/(2*d)*((sigma_x_FrontT/z_T-
sigma_x_FrontB/z_B)+(sigma_x_BackT/z_T-sigma_x_BackB/z_B));

% M_x=-M_xFront+M_xBack:
M_x=c_Mx*A_S*h_min/2*((tau_xz_BackL-tau_xz_BackR)-(tau_xz_FrontL-
tau_xz_FrontR));

% M_y (compare bottom and top to eliminate normal forces and subtract front
% and back because torques have different effects in the front
% and in the back):
M_y=c_My*I_y/2*((sigma_x_BackT/z_T-sigma_x_BackB/z_B)-(sigma_x_FrontT/z_T-
sigma_x_FrontB/z_B));

% M_z (same proceeding like for M_y):
M_z=-c_Mz*I_z/2*((sigma_x_BackL/y_L-sigma_x_BackR/y_R)-(sigma_x_FrontL/y_L-
sigma_x_FrontR/y_R));
```

```matlab
% 5.2) Calculate the loads for the selected position

F_xS=F_x;
F_yS=F_y;
F_zS=F_z;
M_xS=M_x-F_y*zS+F_z*yS;
M_yS=M_y+F_x*zS-F_z*xS;
M_zS=M_z-F_x*yS+F_y*xS;

%%-----------------------------6) Results-----------------------------

% 8.1) Generate a new sub folder in the results folder

formatOut = 'yyyy/mm/dd/HH/MM/SS';
timeNow=datestr(now,formatOut);
timeNowNew=strrep(timeNow,'/','_');
folderDirect=['Results\',timeNowNew];
mkdir(folderDirect);

% 8.4) Write Command Window output to a .txt-file

folderDirectResultsTXT=[folderDirect,'\1_Results.txt'];
diary (folderDirectResultsTXT);

disp('----------------------------------------------------------------');
disp('------------------------RESULTS---------------------------------');
disp('----------------------------------------------------------------');

% Extract the time vector for further calculations and the plots
time=strainData(1:lengthData,1);

% 6.1) Sampling frequency:

disp('SAMPLING FREQUENCY');
% Calculate the time increment between two measures
timeInc=zeros(lengthData,1);    % Define the vector to store the time inc.
timeInc(1,1)=0;                 % First increment is zero

for i=1:lengthData-1           % Calculate the other increments
    timeInc(i,1)=time(i+1,1)-time(i,1);
end

fMax=1000/min(timeInc);         % Maximal sampling frequency [Hz]
fMean=1000/mean(timeInc);       % Mean sampling frequency [Hz]
fMin=1000/max(timeInc);         % Minimal sampling frequency [Hz]

% Return the frequencies on the command window:
disp(['Mean sampling frequency [Hz]: ',num2str(fMean)]);
disp(['Lowest sampling frequency [Hz]: ',num2str(fMin)]);

disp('---------------------------------------------------------------');

% 6.2) Show whether the gain was adapted for high or low forces

disp('AMPLIFICATION');
if measData(1,26)==1
    disp('Gain was adapted set for: LOW LOADS (limited measuring range)');
elseif measData(1,26)==2
    disp('Gain was adapted set for: HIGH LOADS (lower accuracy');
end
```

Fabian Tobias Mayer B.Sc.

```matlab
disp('-----------------------------------------------------------------');

% 6.3) Position for which the loads were calculated

disp('POSITION');
disp(['Position for which the loads are calculated (x,y,z) [m]:
',num2str(xS),' , ',num2str(yS),' , ',num2str(zS)]);


disp('-----------------------------------------------------------------');

% 6.4) Maximum loads

% Determine the maximum and minimum values of the forces and torques and
% when they happened
[F_xSMin,F_xSMinI]=min(F_xS);
[F_ySMin,F_ySMinI]=min(F_yS);
[F_zSMin,F_zSMinI]=min(F_zS);
[M_xSMin,M_xSMinI]=min(M_xS);
[M_ySMin,M_ySMinI]=min(M_yS);
[M_zSMin,M_zSMinI]=min(M_zS);


[F_xSMax,F_xSMaxI]=max(F_xS);
[F_ySMax,F_ySMaxI]=max(F_yS);
[F_zSMax,F_zSMaxI]=max(F_zS);
[M_xSMax,M_xSMaxI]=max(M_xS);
[M_ySMax,M_ySMaxI]=max(M_yS);
[M_zSMax,M_zSMaxI]=max(M_zS);


% Output them on the display
disp('LOADS');
disp(['F_x: minimum ',num2str(F_xSMin),' (at
',num2str(time(F_xSMinI,1)/1000),' sec) | maximum ',num2str(F_xSMax),' (at
',num2str(time(F_xSMaxI,1)/1000),' sec)']);
disp(['F_y: minimum ',num2str(F_ySMin),' (at ',num2str(time(F_yS-
MinI,1)/1000),' sec) | maximum ',num2str(F_ySMax),' (at ',num2str(time(F_yS-
MaxI,1)/1000),' sec)']);
disp(['F_z: minimum ',num2str(F_zSMin),' (at
',num2str(time(F_zSMinI,1)/1000),' sec) | maximum ',num2str(F_zSMax),' (at
',num2str(time(F_zSMaxI,1)/1000),' sec)']);
disp(['M_x: minimum ',num2str(M_xSMin),' (at
',num2str(time(M_xSMinI,1)/1000),' sec) | maximum ',num2str(M_xSMax),' (at
',num2str(time(M_xSMaxI,1)/1000),' sec)']);
disp(['M_y: minimum ',num2str(M_ySMin),' (at ',num2str(time(M_yS-
MinI,1)/1000),' sec) | maximum ',num2str(M_ySMax),' (at ',num2str(time(M_yS-
MaxI,1)/1000),' sec)']);
disp(['M_z: minimum ',num2str(M_zSMin),' (at
',num2str(time(M_zSMinI,1)/1000),' sec) | maximum ',num2str(M_zSMax),' (at
',num2str(time(M_zSMaxI,1)/1000),' sec)']);


disp('-----------------------------------------------------------------');


diary off;


%%----------------------------7) Plots--------------------------------

% Plot of the loads F_xS, F_yS, F_zS for the selected position
figure;
hold on
plot(time,F_xS,'r:','Linewidth',1);
plot(time,F_yS,'g--','Linewidth',1);
```

```matlab
plot(time,F_zS,'b-','Linewidth',1);
grid on;
set(gca,'FontWeight','normal','FontSize',12,'FontName','Palatino Linotype');
xlabel('Time [ms]')
ylabel('Force [N]')
legend('{\itF_x}','{\itF_y}','{\itF_z}');
title('FORCES')

% Plot of the loads M_xS, M_yS, M_zS for the selected position
figure;
hold on
plot(time,M_xS,'r:','Linewidth',1);
plot(time,M_yS,'g--','Linewidth',1);
plot(time,M_zS,'b-','Linewidth',1);
grid on;
set(gca,'FontWeight','normal','FontSize',12,'FontName','Palatino Linotype');
xlabel('Time [ms]')
ylabel('Torque [Nm]')
legend('{\itM_x}','{\itM_y}','{\itM_z}');
title('TORQUES')

%%-----------------------8) Safe the Results and Plots-------------------

% 8.2) Write measured data to an excel-file:

folderDirectXls=[folderDirect,'\2_Load Logfile'];
outputmatrix=[time,F_x,F_y,F_z,M_x,M_y,M_z];
header = {'Time [ms]' 'F_x [N]' 'F_y [N]' 'F_z [N]' 'M_x [Nm]' 'M_y [Nm]'
'M_z [Nm]'};
xlswrite(folderDirectXls, header, 'sheetname'); % by defualt starts from A1
xlswrite(folderDirectXls, outputmatrix , 'sheetname','A2'); % array under the
header.

% 8.3) Safe the figures to the folder:

folderDirectForcesXls=[folderDirect,'\3_Forces.fig'];
folderDirectTorqueXls=[folderDirect,'\4_Torques.fig'];
saveas(figure (1),folderDirectForcesXls);
saveas(figure (2),folderDirectTorqueXls);
```

```
%****************************************************************************
%  MATLAB DATA STRESS CALCULATION CODE
%
%  Version: skiPositionStress
%  Date: 09.10.2016
%
%  Copyright 2016 by Fabian Tobias Mayer (fabianmayer@web.de)
%  This code may not be used for purposes which are not related to
%  the master thesis of Fabian Tobias Mayer without his prior
%  written consent.
%****************************************************************************

function [ sigma_x,sigma_y,sigma_z,tau_xy,tau_xz ] = SkiPositionStress( posi-
tion,strainRosette,E,nu )
% Summary:
% Calculation of the normal and shear stress in the roller ski based
% coordinate system from the strains in in the rosette systems
%
% Function:
% 1) Calculation of principal stress at the rosette positions with the
%    measured strain
% 2) Calculation of the direction of the principal stress:
%    - Calculation of a smallest angle to the a-axis (necessary because of
%      ambiguity of the tangent)
%    - Calculation of the angle between the positive a-axis and the
%      direction of the 1st principal stress (counter clockwise, [rad])
% 3) Calculation of Normal and Shear Stress in the Rosette coordinate system
% 4) Transformation Normal and Shear Stress in Roller Ski coordinate system
%
% Input Variables:
% - position: orientation of the rosette
%     1: Top, pins in positive x-direction
%     2: Top, pins in negative x-direction
%     3: Right, pins in positive z-direction
%     4: Bottom, pins in positive x-direction
%     5: Bottom, pins in negative x-direction
%     6: Left, pins in positive z-direction
%     Else: "Non-existent rosette position": If position for the rosette
%            was not chosen / does not exist
% - epsilo_a, epsilon_b, epsilon_c: strain in the rosettes strain gauges
% - E: Young's modulus in the beam of the roller ski
% - nu: Poisson ratio
%
% Output Variables:
% - sigma_x: Normal stress in positive x direction (skiing direction)
% - sigma_y: Normal stress in positive y direction (horizontal,
%            perpendicular, left in skiing direction
% - sigma_z: Normal stress in positive z direction (vertical, upwards)
% - tau_xy: Shear stress in plane perpendicular to x in positive y
%            direction
% - tau_xz: Shear stress in plane perpendicular to x in positive z
%            direction


%% Separate strain vectors for the rosette matrix:
epsilon_a=strainRosette(:,1);
epsilon_b=strainRosette(:,2);
epsilon_c=strainRosette(:,3);


%%-----------------------Principal Stresses-----------------------------

% Number of Measurements (to initialise vector in order to save comp. costs)
n=size(strainRosette,1);
```

```matlab
% Initialize vectors for principal stresses:
sigma_1=zeros(n,1);
sigma_2=zeros(n,1);

% Calculation of principal stresses [Pa]:
for i=1:n
    sigma_1(i)=E/(2*(1-nu))*(epsilon_a(i)+epsi-
lon_c(i))+E/(sqrt(2)*(1+nu))*sqrt((epsilon_a(i)-epsilon_b(i))^2+(epsi-
lon_c(i)-epsilon_b(i))^2);
    sigma_2(i)=E/(2*(1-nu))*(epsilon_a(i)+epsilon_c(i))-
E/(sqrt(2)*(1+nu))*sqrt((epsilon_a(i)-epsilon_b(i))^2+(epsilon_c(i)-epsi-
lon_b(i))^2);
end

%%---------------------Direction of Principal Stresses--------------------

% Calculation of a smallest angle to the a-axis (necessary because of
% ambiguity of the tangent):

numerator=2*epsilon_b-epsilon_a-epsilon_c;
denominator=epsilon_a-epsilon_c;
fraction=numerator./denominator;

psi=atan(fraction); % Smallest angle to the a-axis [rad]

% Calculation of the angle between the positive a-axis and the
% direction of the 1st principal stress (counter clockwise, [rad]):

rho=zeros(n,1); %initialize vector of the angle

for i=1:n
    if numerator(i)>=0 && denominator(i)>0
        rho(i)=psi(i)/2;
    elseif numerator(i)>0 && denominator(i)<=0
        rho(i)=(pi-psi(i))/2;
    elseif numerator(i)<=0 && denominator(i)<0
        rho(i)=(pi+psi(i))/2;
    elseif numerator(i)<0 && denominator(i)>=0
        rho(i)=(2*pi-psi(i))/2;
    else
        disp(['Numerator and Denominator Zero (no loads check
Setup)',num2str(i)]);
        rho(i)=0;
    end
end

%%--Calculation of Normal and Shear Stress in the Rosette Coordinate System--

% Notation from Gross et al. 2009 (Not from HBM!)

% Normal stress in rosette a-axis [pseudo Pa]:
sigma_a=((sigma_1+sigma_2)+(sigma_1-sigma_2).*cos(2*rho))/2;
% Normal stress in rosette c-axis [pseudo Pa]:
sigma_c=((sigma_1+sigma_2)-(sigma_1-sigma_2).*cos(2*rho))/2;
% Shear stress in rosette ac-direction [pseudo Pa]:
tau_ac=-(sigma_1-sigma_2).*sin(2*rho)/2;
```

```matlab
%%---Transformation Normal and Shear Stress in Roller Ski Coordinate System--

% Directions:
%     1: Top, pins in positive x-direction
%     2: Top, pins in negative x-direction
%     3: Right, pins in positive z-direction
%     4: Bottom, pins in positive x-direction
%     5: Bottom, pins in negative x-direction
%     6: Left, pins in positive z-direction

% Cases for the possible positions of the rosettes
switch position
    case 1 % Top, pins in positive x-direction
        sigma_x=sigma_c;
        sigma_y=sigma_a;
        sigma_z=zeros(n,1);
        tau_xy=-tau_ac;
        tau_xz=zeros(n,1);
    case 2 % Top, pins in negative x-direction
        sigma_x=sigma_c;
        sigma_y=-sigma_a;
        sigma_z=zeros(n,1);
        tau_xy=-tau_ac;
        tau_xz=zeros(n,1);
    case 3 % Right, pins in positive z-direction
        sigma_x=-sigma_a;
        sigma_y=zeros(n,1);
        sigma_z=-sigma_c;
        tau_xy=zeros(n,1);
        tau_xz=-tau_ac;
    case 4 % Bottom, pins in positive x-direction
        sigma_x=sigma_c;
        sigma_y=-sigma_a;
        sigma_z=zeros(n,1);
        tau_xy=-tau_ac;
        tau_xz=zeros(n,1);
    case 5 % Bottom, pins in negative x-direction
        sigma_x=sigma_c;
        sigma_y=sigma_a;
        sigma_z=zeros(n,1);
        tau_xy=tau_ac;
        tau_xz=zeros(n,1);
    case 6 % Left, pins in positive z-direction
        sigma_x=sigma_a;
        sigma_y=zeros(n,1);
        sigma_z=-sigma_c;
        tau_xy=zeros(n,1);
        tau_xz=-tau_ac;

    otherwise % If position for the rosette was not chosen / does not exist
        disp('Non-existent rosette position')
        sigma_x=NaN;
        sigma_y=NaN;
        sigma_z=NaN;
        tau_xy=NaN;
        tau_xz=NaN;
end

end
```

Appendix G: Initial Requirement List

Requirements List					
Topic	No.	Requirement Description	Requirement Source	Date	Requirement type
Measurement	1	3D forces and torques need to be measured	Rottefella and Rollersafe	20./21.4.	must have
	2	The forces and torques need to be determined between binding and roller ski	Rottefella and Rollersafe	20./21.4.	must have
	3	Classic and skate skiing needs to be evaluated	Rottefella and Rollersafe	20./21.4.	must have
	4	Other situations which occur during roller skiing need to be evaluated	Rottefella and Rollersafe	20./21.4.	must have
	5	Expected maximum loads need to be recorded: F_x=562N; F_y=239N; F_z=1748N; M_x=13Nm; M_y=9Nm; M_z=82Nm	Assessed	10.5.	must have
	6	Required Sampling Frequency for loads caused by the athlete: min. 14 Hz better 42-70 Hz (athlete: 7 Hz)	Assessed	10.05.	must have
	7	Required Sampling Frequency caused by external circumstances: min. 370 Hz better 1110-1850 Hz (external: 185 Hz)	Assessed	10.05.	must have
	8	The system needs to be accurate for high forces	Rottefella and Rollersafe	20./21.4.	must have
	9	Recording of lower loads than the peak loads	Rottefella and Rollersafe	20./21.4.	could haves
	10	Smaller forces do not need to be recorded as accurate as the high forces	Rottefella and Rollersafe	20./21.4.	could have
	11	Maximum forces are most important	Rottefella and Rollersafe	20./21.4.	must have
	12	The time the forces and torques occur needs to be determined	Rottefella and Rollersafe	20./21.4.	should have
	13	Measurement over a long time has to be possible	Rottefella and Rollersafe	20./21.4.	must have
	14	Large data storage capacity is needed	Rottefella and Rollersafe	20./21.4.	must have
	15	The measuring system needs to be able to detect forces and torques in each situation during roller skiing	Rottefella and Rollersafe	20./21.4.	must have
	16	The measuring system needs to withstand tests with pro skier	Rottefella and Rollersafe	20./21.4.	must have
Validation	17	The measuring system needs to be completely validated (3D forces and torques)	Rottefella and Rollersafe	20./21.4.	must have
Data Output	18	The recorded data should be transferred to a computer after the training by USB-cable/SD card/Wi-Fi/Bluetooth	Rottefella and Rollersafe	20./21.4.	must have
Test Equipment	19	The measuring system needs to be placed on a Rollersafe roller ski (brake system might be removed)	Rottefella and Rollersafe	20./21.4.	must have
	20	The Rottefella binding may be adapted but the distance between binding pin and roller ski needs to	Rottefella and Rollersafe	20./21.4.	should have
	21	The Distance between binding and ground should not be changed	Rottefella and Rollersafe	20./21.4.	should have
	22	The weight of the measuring system should be as less as possible	Rottefella and Rollersafe	20./21.4.	should have
Restrains of the Surrounding	23	Water resistant measuring system	Rottefella and Rollersafe	20./21.4.	should have
	24	Dust resistant measuring system	Rottefella and Rollersafe	20./21.4.	should have
	25	Withstand small drop tests	Rottefella and Rollersafe	20./21.4.	could have
	26	Withstand vibrations	Rottefella and Rollersafe	20./21.4.	must have
	27	Sturdy and durable measuring system	Rottefella and Rollersafe	20./21.4.	should have
	28	Safe construction (not to hurt the athlete while usage)	Rottefella and Rollersafe	20./21.4.	must have
Deadlines	29	End of September the measuring system needs to be finished	Rottefella and Rollersafe	20./21.4.	should have

Table A 2: Initial requirement list

Appendix H: Peak Load Assessment

The loads which are expected to act between roller ski and binding were assessed in order to determine the requirements of the measuring system and for dimensioning calculations. All situations which occur during roller skiing were analysed in order to estimate the maximal loads which could act between binding and roller ski. Loads occurring during the different situations were rated and the maximum forces and torques in each direction were researched or estimated by doing simplified calculations.

Analysing the different situations during roller skiing there are the different skiing styles, break techniques and other events. Regarding the different skiing styles there are the two main techniques classic and skate skiing. Both of them comprise several sub techniques which are listed in in Figure A 10 for classic skiing and in Figure A 11 for skate skiing [87]. The sub techniques might be segmented into three phases. Fasel et al. introduced a trust phase and a glide phase to analyse classic skiing [88]. For the purpose of analysing the loads a further subdivision was done in push phase, glide phase and swing phase. Firstly, there is the push phase during which the athlete generates propulsion by applying forces to the roller ski and the poles. Subsequently the glide phase takes place. Finally, there is the swing phase in order to get back to the starting position. The loads acting on the equipment during the different skiing techniques depend on the skills of the athlete. While pro skiers generate high forces in propulsion direction beginners apply high torques to the equipment caused by instabilities during the glide phase.
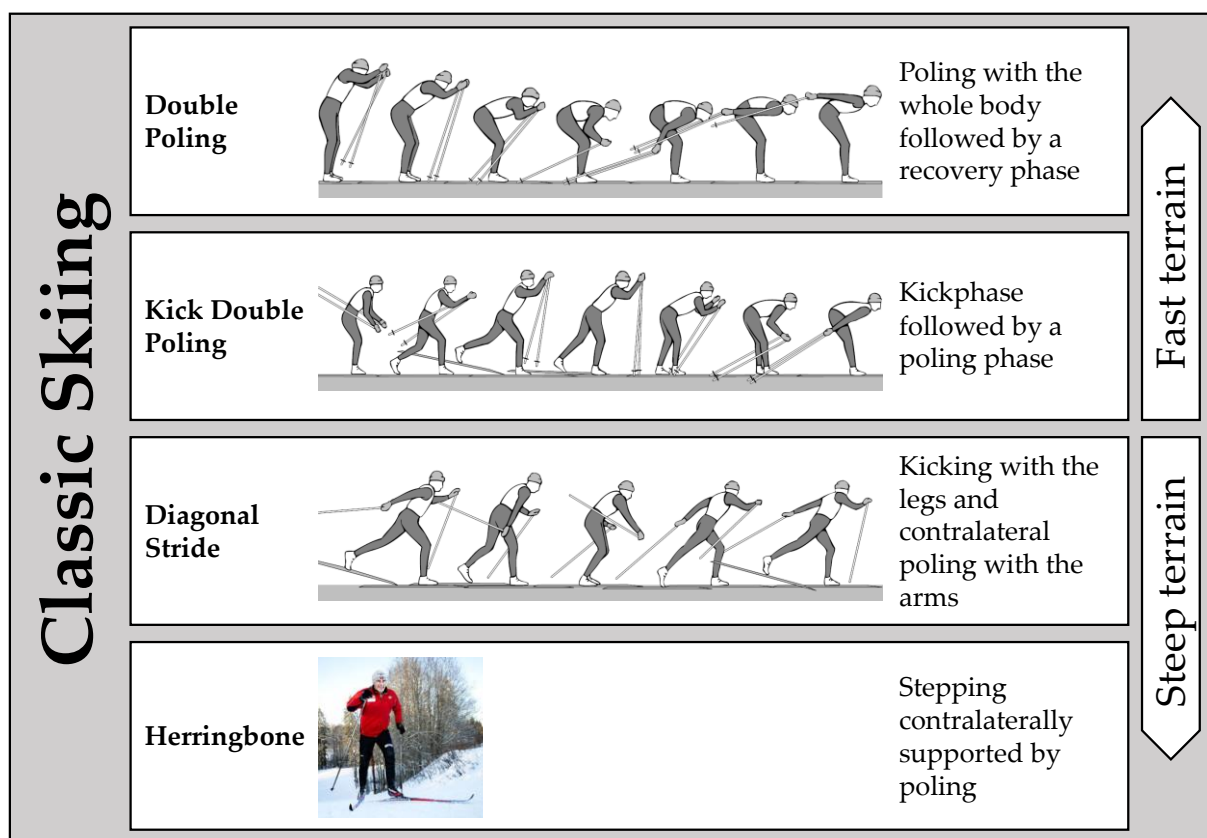
Figure A 10: Classic skiing techniques, with[87], [89]

Free Skating		Skating stroke using the pendulum movement of the arms
Open Field Skating		Double poling movement with every second skating stroke
V2 Skating		Double poling movement with each skating stroke
V1 Skating		Offset double poling movement with every second skating stroke
Flying Herringbone		Stepping contralaterally supported by poling, including a glide phase

Figure A 11: Skate skiing techniques, with [87], [90], [91]

Braking is probably the most difficult technique during roller skiing. Certain brake techniques are applied by the athletes on downhill tracks to reduce their speed or to brake when obstacles appear. Depending on the skills of the athlete the efficiency of the techniques varies. Loads on the equipment vary dependant on the performance of the athlete as well. All brake techniques are explained in Figure A 12.

Other events might be turning, fast downhill sections, jumping, or accidental incidents. Dependent on level of the athlete the curves are skied with different techniques. Curves can be skied without stepping by moving the centre of gravity. During step turning the athlete might stay at the same speed. Accelerating during step turning is possible by applying strong skate pushes with the outer leg while pushing the inside leg in skiing direction [92]. Jumping is important when unexpected obstacles like small gaps or potholes appear. For descending from a curb stone at high speed jumping is used as well. Besides planed actions on roller skis there might be unplanned situations. One of the most common incidents is to get stuck with the roller ski on a curb

stone at low speed. Furthermore, winter road sand can be problematic when it gets stuck between wheel holding bracket and wheel which leads to blocking of the wheel.

Brake Techniques			
	Air brake		Creating as much wind resistance as possible
	T brake		One roller ski pressed down perpendicular to the direction of movement
	V brake and Pole brake		Simmilar to snowplow on snow, pole tips can be used to increase braking
	Alterning push brake		Alternating snowplow for each roller ski, increased by the pole tips
	Serpentine technique		Stepping turning to reduce the speed by driving serpentines
	One ski off-road technique		Skiing with one roller ski in the slower gravel or lawn besids the road
	Emergency brake		Skiing on the lawn with performing a telemark step
	Breaking with Rollersafe		Using the disc brakes of the roller ski to brake

Better speed reduction

Figure A 12: Brake techniques, with [93], [94]

For the assessment only the absolute loads were regarded. F_x is the force in positive skiing direction, F_y is the force horizontal-perpendicular to the skiing direction and F_z is the force vertical-perpendicular to the skiing direction. The torques M_x, M_y, and M_z are rotating around the respective axes of previously explained forces.

The loads were ranked using the values zero to three. Zero means negligible forces and loads. Forces similar to the force Fz caused by the athlete's bodyweight were ranked with value two. Higher forces were ranked with value three and lower forces with value one. Torques were ranked with value one if they are similar to the torque My which occurs turning the boot to compress the rubber block of the binding. Torques were ranked as value two if they are similar to the torque Mx caused by instabilities during the glide phase. Toques which were expected to be higher were ranked with value three. The events during which the highest loads occur are highlighted in Table A 4 and Table A 3. If there have been several events with the highest value, the toughest situation was marked.

Event		Expected loads (right binding, athletes point of view)					
		$\vert F_x \vert$	$\vert F_y \vert$	$\vert F_z \vert$	$\vert M_x \vert$	$\vert M_y \vert$	$\vert M_z \vert$
Poole brake	Poole brake	1	0	2	1	0	0
T brake	Left rollerski lateral	1	0	2	1	0	1
	Right rollerski lateral	1	2	2	2	0	2
V brake		1	2	2	3	2	2
Altering	Pressure on the left rollerski	1	1	1	2	0	2
push brake	**Pressure on the right rollerski**	1	**2**	2	**3**	1	**3**
Serpentine	left-hand bend	1	2	3	3	1	2
technique	right-hand bend	1	1	2	3	1	2
One ski off-	Left rollerski off-road	1	0	2	2	1	1
road	Right rollerski off-road	3	0	2	2	0	2
Emergency	Emergency brake	3	0	1	2	1	0
Rollersafe	Left rollerski in the ahead	2	0	2	1	0	1
breaking	Right rollerski in the ahead	3	0	3	1	0	1
Accelerating	left-hand bend	1	1	3	2	1	2
turning	right-hand bend	1	1	2	2	1	1
Stepping	left-hand bend	1	1	2	2	1	2
turning	right-hand bend	1	1	2	2	1	2
Non-	left-hand bend	1	0	2	2	0	1
stepping	right-hand bend	1	0	2	2	0	1
Downhill	Downhill	1	0	2	1	0	0
Jumping	Jumping	1	0	3	3	1	1
Skiing on compact gravel roads		2	0	2	0	0	0
Hitting the wheel screws on each other		3	0	2	0	0	0
Slipping during classic skiing and pushing		3	0	2	0	0	0
Get stuck	left rollerski caught	1	0	2	2	0	2
on a curb	**right rollerski caught**	**3**	0	2	2	1	2
stone	both rollerskis caught	3	0	2	1	1	1

Table A 3: Ranking of other situations which might occur during roller skiing

 Fabian Tobias Mayer B.Sc.

Event			$\mathbf{|F_x|}$	$\mathbf{|F_y|}$	$\mathbf{|F_z|}$	$\mathbf{|M_x|}$	$\mathbf{|M_y|}$	$\mathbf{|M_z|}$
			Expected loads (right binding, athletes point of view)					
Skate skiing	Free skating	Push phase	1	1	3	2	1	2
		Glide phase	1	0	2	2	0	1
		Swing phase	0	0	0	0	1	1
	Open field skating (pole plant: left)	Push phase	1	1	3	2	1	2
		Glide phase	1	0	0	2	0	1
		Swing phase	0	0	0	0	1	1
	Open field skating (pole plant: right)	Push phase	1	1	3	2	1	2
		Glide phase	1	0	0	2	0	1
		Swing phase	0	0	0	0	1	1
	V2 skating	Push phase	1	1	3	2	1	2
		Glide phase	1	0	2	2	0	1
		Swing phase	0	0	0	0	1	1
	V1 skating (leading arm: left)	Push phase	1	1	3	2	1	2
		Glide phase	1	0	2	2	0	1
		Swing phase	0	0	0	0	1	1
	V1 skating (leading arm: right)	Push phase	1	1	3	2	1	2
		Glide phase	1	0	2	2	0	1
		Swing phase	0	0	0	0	1	1
	Flying herringbone	Push phase	1	2	3	2	1	2
		Glide phase	1	0	2	2	0	1
		Swing phase	0	0	0	0	1	1
Classic Skiing	Double poling	Push phase	1	0	1	1	1	0
		Glide phase	1	0	2	1	0	0
		Swing phase	1	0	3	1	1	0
	Kick double poling (left leg pushing)	Push phase	1	0	2	2	0	0
		Glide phase	1	0	2	1	0	0
		Swing phase	1	0	2	2	0	0
	Kick double poling (right leg pushing)	Push phase	2	0	3	2	1	0
		Glide phase	1	0	2	1	0	0
		Swing phase	1	0	1	2	1	0
	Diagonal stride	**Push phase**	2	0	**3**	2	**1**	0
		Glide phase	1	0	2	2	0	0
		Swing phase	1	0	1	2	1	0
	Herringbone	Push phase	1	2	3	3	1	1
		Glide phase	0	0	0	0	0	0
		Swing phase	0	0	0	0	1	0

Table A 4: Ranking of the different situations during common skiing

For F_x the highest load occurs during catching a curb stone. The maximum of F_y, M_x and M_z occurs during breaking with the altering push brake. The maximum of F_z and M_y occurs during the diagonal stride.

In order to find out which maximal forces and torques the measuring system needs to detect and to withstand the loads were calculated for the previously determined load events. For the calculation of the forces the tilting criteria based was used. A body depicted in Figure A 13 has a centre of gravity marked in red. Knowing the distance from the centre of gravity CG to the tilting point A in horizontal direction w and vertical direction h it is possible to calculate the tilting force F. The torque equilibrium around the tilting point A was set up [95].

$$0 = Fh - F_G w \tag{7-1}$$

The gravitational force F_G depends on the mass m and gravitational constant g as followed

$$F_G = mg \tag{7-2}$$

The tilting force F results as:

$$F = mg\frac{w}{h} \tag{7-3}$$
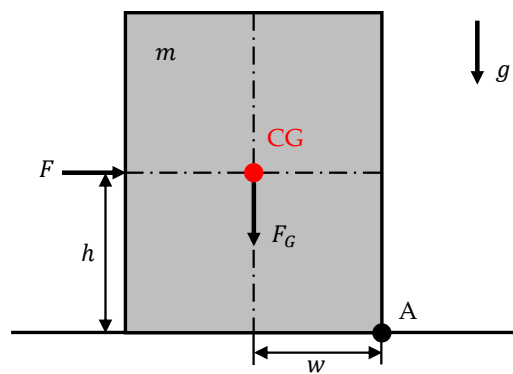
Figure A 13: Tilting body

The maximum value for $F_{\underline{x}}$ is determined analysing the situation catching on a curb stone. Skiing up or down a curb stone the athlete might get stuck with the beam of the roller ski which results in a high force in the skiing direction. Similar forces apply when the athlete gets stuck on the surface peaks of uneven roads. Sizable forces occur if the skier expects getting stuck and he performs a telemark movement as depicted in Figure A 14 a). The maximum forces occur when the athlete tilts over the roller ski in the front. An angle of $\alpha_c = 34°$ is reasonable like it is depicted in Figure A 14 a). The length l is between the tilting point at the binding link and the centre of gravity which is assumed to be at the hip of the athlete. With use of the relation

$$\frac{w}{h} = \frac{\sin(\alpha_c)\, l}{\cos(\alpha_c)\, l} = \tan(\alpha_c) \tag{7-4}$$

Equation (7-3 can be written as followed.

$$F_{\underline{x}} = m_A g\tan(\alpha_c) \tag{7-5}$$

Fabian Tobias Mayer B.Sc.

For the force $F_{\underline{y}}$ a similar tilting calculation is performed. The maximum forces in this direction occur during altering push braking. An angle up to $\alpha_b = 16°$ might occur between the vertical axis and the leg of the athlete like displayed in Figure A 14 b). This enables the calculation of $F_{\underline{y}}$ utilizing the following equation.

$$F_{\underline{y}} = m_A g \tan(\alpha_b) \qquad (7\text{-}6)$$

The torque $M_{\underline{x}}$ during altering push braking is calculated with use of the force $F_{\underline{y}}$ and the distance $l_{bg} = 0.055\text{m}$ between the ground and the upper side of the skating roller ski's beam shown in Figure A 14 d). The beam of the skating roller ski is higher than the one of the classic roller ski due to the bigger skating wheels.

$$M_{\underline{x}} = F_{\underline{y}} l_{bg} \qquad (7\text{-}7)$$

During altering push braking the front or back wheel touches the ground prior to the other one which leads to the torque $M_{\underline{z}}$. In order to evaluate the maximum torque, the lever $l_{wb} = 0.342\text{m}$ shown in Figure A 14 c) is used in combination with $F_{\underline{y}}$ to calculate the torque $M_{\underline{z}}$. For l_{wb} is the length of the classic roller ski is used which is longer than the one of the skating roller ski.

$$M_{\underline{z}} = F_{\underline{y}} l_{wb} \qquad (7\text{-}8)$$

The maximum forces $F_{\underline{z}}$ which are expected to occur during the push phase of diagonal stride were measured by Andersson et al. [67]. They analysed diagonal stride and measured maximum values of $F_{\underline{z}} = 1748\text{N}$ for the demanded force. The torque $M_{\underline{y}}$ during the push phase is caused by the compression of the rubber block of the binding. $M_{\underline{y}}$ was measured by determining the force $F_{\underline{b}} = 34.3 \text{ N}$ at the end of the boot with a luggage scale. $F_{\underline{b}}$ was measured for the compression of a new classic rube block with the hardest stiffness. The boot was bent until there was an angle $\alpha_{bb} = 45°$ between the boot and the binding. The setup is shown Figure A 14 e). The measured force $F_{\underline{b}}$ was multiplied with the lever $l_{bb} = 0.251\text{m}$ which is measured between the end of the boot to the binding link.

$$M_{\underline{y}} = F_{\underline{b}} l_{bb} \qquad (7\text{-}9)$$

Figure A 14: Peak load events: a) Catching a curbe stone performing a telemark movement, b) altering push braking, c) side few during alterning push braking, d) side view of the skating roller ski, e) measurement of the binding rubber compression torque

The values $m_A = 85\text{kg}$ for the weight of the athlete and $g = 9.81\ \frac{\text{m}}{\text{s}}$ for the gravitational constant were used for the calculations. With these values the forces and torques listed in Table A 5 were determined. These are the maximum loads which the measuring system needs to be able to withstand and to detect.

Event	Calculated and researched loads [N, Nm]					
	$\lvert F_x \rvert$	$\lvert F_y \rvert$	$\lvert F_z \rvert$	$\lvert M_x \rvert$	$\lvert M_y \rvert$	$\lvert M_z \rvert$
Catching a curb stone (right roller ski caught)	562	-	-	-	-	-
Altering push brake (pressure on right ski)	-	239	-	13	-	82
Classic skiing: Diagonal stride (push phase)	-	-	1748	-	9	-
Maximal loads	562	239	1748	13	9	82

Table A 5: Calculated and researched maximal loads between the roller ski and the binding

Appendix I: Second Moment of Inertia and Neutral Layers
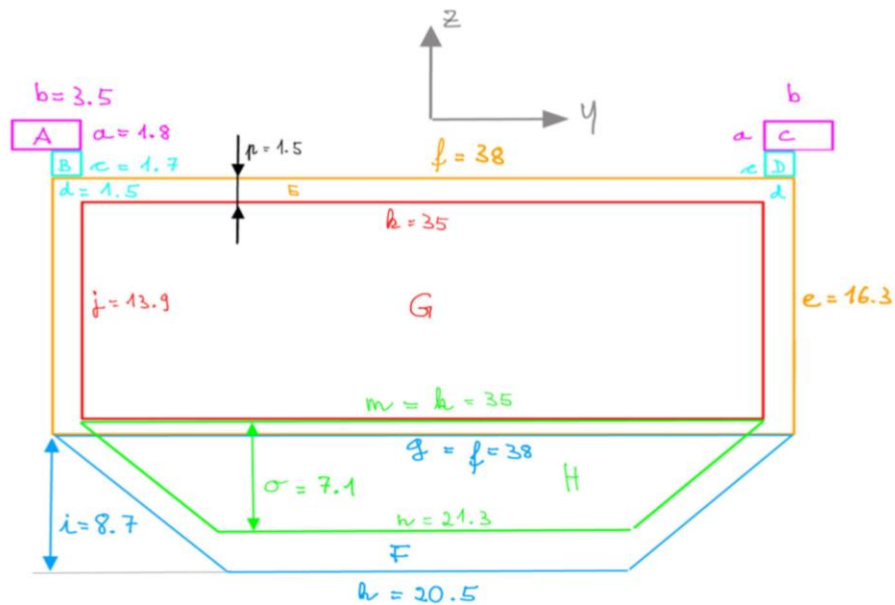
⎡Intersectional area of the profile:
⎣**>** $A\_S := A\_A + A\_B + A\_C + A\_D + A\_E + A\_F - A\_G - A\_H:$
⎡Center of area in z direction (roller ski system, on the top rail):
⎢**>** $z\_S := (A\_A * z\_AS + A\_B * z\_BS + A\_C * z\_CS + A\_D * z\_DS + A\_E * z\_ES + A\_F * z\_FS$
⎣ $- A\_G * z\_GS - A\_H * z\_HS) / A\_S:$
⎡Second moment of inertia of the whole profile (roller ski systte, on the top rail):
⎢**>** $Iy\_Stotal := Iy\_AS + Iy\_BS + Iy\_CS + Iy\_DS + Iy\_ES + Iy\_FS - Iy\_GS - Iy\_HS:$
⎢ $Iz\_Stotal := Iz\_AS + Iz\_BS + Iz\_CS + Iz\_DS + Iz\_ES + Iz\_FS - Iz\_GS - Iz\_HS:$

⎡**Second moment of inertia of the whole profile (center of area system):**
⎣(Could be shifted with Steiner but was not done to keep the Steiner Shifting as a control)
⎢**>** $Iy\_Ctotal := Iy\_AC + Iy\_BC + Iy\_CC + Iy\_DC + Iy\_EC + Iy\_FC - Iy\_GC - Iy\_HC:$
⎣ $Iz\_Ctotal := Iz\_AC + Iz\_BC + Iz\_CC + Iz\_DC + Iz\_EC + Iz\_FC - Iz\_GC - Iz\_HC:$
⎡**Area A:**
⎢area [mm^2],

offset in y and z directio of the center of area of the individual area to the coordinate system on top of the roller ski [mm],
offset in y and z directio of the center of area of the individual area to the coordinate system in the center of area of the whole profile [mm],
second moment of inertia in y and z direction [mm^4],
second moment of inertia shifted to the coordinate system on top of the roller ski [mm^4],
second moment of inertia shifted to the center of area of the whole crossectional area[mm^4]

> $A\_A := a * b :$
$y\_AS := -(f/2 - d + b/2) :$
$z\_AS := -a/2 :$
$y\_AC := -\left(\dfrac{f}{2} - d + \dfrac{b}{2}\right) :$
$z\_AC := -(z\_S - z\_AS) :$
$Iy\_A := b * a^3/12 :$
$Iz\_A := a * b^3/12 :$
$Iy\_AS := Iy\_A + z\_AS^2 * A\_A :$
$Iz\_AS := Iz\_A + y\_AS^2 * A\_A :$
$Iy\_AC := Iy\_A + z\_AC^2 * A\_A :$
$Iz\_AC := Iz\_A + y\_AC^2 * A\_A :$

Area B:
area [mm^2],
offset in y and z directio of the center of area of the individual area to the coordinate system on top of the roller ski [mm],
offset in y and z directio of the center of area of the individual area to the coordinate system in the center of area of the whole profile [mm],
second moment of inertia in y and z direction [mm^4],
second moment of inertia shifted to the coordinate system on top of the roller ski [mm^4],
second moment of inertia shifted to the center of area of the whole crossectional area[mm^4]

> $A\_B := c * d :$
$y\_BS := -(f/2 - d/2) :$
$z\_BS := -(a + c/2) :$
$y\_BC := -\left(\dfrac{f}{2} - \dfrac{d}{2}\right) :$
$z\_BC := -(z\_S - z\_BS) :$
$Iy\_B := d * c^3/12 :$
$Iz\_B := c * d^3/12 :$
$Iy\_BS := Iy\_B + z\_BS^2 * A\_B :$
$Iz\_BS := Iz\_B + y\_BS^2 * A\_B :$
$Iy\_BC := Iy\_B + z\_BC^2 * A\_B :$
$Iz\_BC := Iz\_B + y\_BC^2 * A\_B :$

Area C:
area [mm^2],
offset in y and z directio of the center of area of the individual area to the coordinate system on top of the roller ski [mm],
offset in y and z directio of the center of area of the individual area to the coordinate system in the center of area of the whole profile [mm],
second moment of inertia in y and z direction [mm^4],
second moment of inertia shifted to the coordinate system on top of the roller ski [mm^4],
second moment of inertia shifted to the center of area of the whole crossectional area[mm^4]

> $A\_C := a * b :$
$y\_CS := f/2 - d + b/2 :$
$z\_CS := -a/2 :$
$y\_CC := \dfrac{f}{2} - d + \dfrac{b}{2} :$
$z\_CC := -(z\_S - z\_CS) :$
$Iy\_C := b * a\text{^}3 / 12 :$
$Iz\_C := a * b\text{^}3 / 12 :$
$Iy\_CS := Iy\_C + z\_CS\text{^}2 * A\_C :$
$Iz\_CS := Iz\_C + y\_CS\text{^}2 * A\_C :$
$Iy\_CC := Iy\_C + z\_CC\text{^}2 * A\_C :$
$Iz\_CC := Iz\_C + y\_CC\text{^}2 * A\_C :$

Area D:
area [mm^2],
offset in y and z directio of the center of area of the individual area to the coordinate system on top of the roller ski [mm],
offset in y and z directio of the center of area of the individual area to the coordinate system in the center of area of the whole profile [mm],
second moment of inertia in y and z direction [mm^4],
second moment of inertia shifted to the coordinate system on top of the roller ski [mm^4],
second moment of inertia shifted to the center of area of the whole crossectional area[mm^4]

> $A\_D := c * d :$
$y\_DS := f/2 - d/2 :$
$z\_DS := -(a + c/2) :$
$y\_DC := \dfrac{f}{2} - \dfrac{d}{2} :$
$z\_DC := -(z\_S - z\_DS) :$
$Iy\_D := d * c\text{^}3 / 12 :$
$Iz\_D := c * d\text{^}3 / 12 :$
$Iy\_DS := Iy\_D + z\_DS\text{^}2 * A\_D :$
$Iz\_DS := Iz\_D + y\_DS\text{^}2 * A\_D :$
$Iy\_DC := Iy\_D + z\_DC\text{^}2 * A\_D :$
$Iz\_DC := Iz\_D + y\_DC\text{^}2 * A\_D :$

Area E:
area [mm^2],
offset in y and z directio of the center of area of the individual area to the coordinate system on top of the roller ski [mm],
offset in y and z directio of the center of area of the individual area to the coordinate system in the center of area of the whole profile [mm],
second moment of inertia in y and z direction [mm^4],
second moment of inertia shifted to the coordinate system on top of the roller ski [mm^4],
second moment of inertia shifted to the center of area of the whole crossectional area[mm^4]

> $A\_E := e * f :$
$z\_ES := -(a + c + e/2) :$
$z\_EC := -(z\_S - z\_ES) :$
$Iy\_E := f * e\text{^}3 / 12 :$
$Iz\_E := e * f\text{^}3 / 12 :$

$Iy\_ES := Iy\_E + z\_ES^\wedge2 * A\_E:$
$Iz\_ES := Iz\_E:$
$Iy\_EC := Iy\_E + z\_EC^\wedge2 * A\_E:$
$Iz\_EC := Iz\_E:$

Area F:

area [mm^2],
offset in y and z directio of the center of area of the individual area to the coordinate system on top of the roller ski [mm],
offset in y and z directio of the center of area of the individual area to the coordinate system in the center of area of the whole profile [mm],
second moment of inertia in y and z direction [mm^4],
second moment of inertia shifted to the coordinate system on top of the roller ski [mm^4],
second moment of inertia shifted to the center of area of the whole crosssectional area[mm^4]

> $A\_F := (g + h) / 2 * i:$
$S\_F := i/3 * (g + 2 * h) / (g + h):$
$z\_FS := -(a + c + e + S\_F):$
$z\_FC := -(z\_S - z\_FS):$
$Iy\_F := i^\wedge3/36 * (h^\wedge2 + 4 * h * g + g^\wedge2) / (h + g):$
$Iz\_F := i/48 * (h^\wedge4 - g^\wedge4) / (h - g):$
$Iy\_FS := Iy\_F + z\_FS^\wedge2 * A\_F:$
$Iz\_FS := Iz\_F:$
$Iy\_FC := Iy\_F + z\_FC^\wedge2 * A\_F:$
$Iz\_FC := Iz\_F:$

Area G:

area [mm^2],
offset in y and z directio of the center of area of the individual area to the coordinate system on top of the roller ski [mm],
offset in y and z directio of the center of area of the individual area to the coordinate system in the center of area of the whole profile [mm],
second moment of inertia in y and z direction [mm^4],
second moment of inertia shifted to the coordinate system on top of the roller ski [mm^4],
second moment of inertia shifted to the center of area of the whole crosssectional area[mm^4]

> $A\_G := k * j:$
$z\_GS := -(a + c + p + j/2):$
$z\_GC := -(z\_S - z\_GS):$
$Iy\_G := k * j^\wedge3 / 12:$
$Iz\_G := j * k^\wedge3 / 12:$
$Iy\_GS := Iy\_G + z\_GS^\wedge2 * A\_G:$
$Iz\_GS := Iz\_G:$
$Iy\_GC := Iy\_G + z\_GC^\wedge2 * A\_G:$
$Iz\_GC := Iz\_G:$

Area H:

area [mm^2],
offset in y and z directio of the center of area of the individual area to the coordinate system on top of the roller ski [mm],

offset in y and z directio of the center of area of the individual area to the coordinate system in the center of area of the whole profile [mm],
second moment of inertia in y and z direction [mm^4],
second moment of inertia shifted to the coordinate system on top of the roller ski [mm^4],
second moment of inertia shifted to the center of area of the whole crossectional area[mm^4]

> $A\_H := (m+n)/2*o$:
$S\_H := o/3*(m+2*n)/(m+n)$:
$z\_HS := -(a+c+p+j+S\_H)$:
$z\_HC := -(z\_S - z\_HS)$:
$Iy\_H := o\char94 3/36*(n\char94 2 + 4*n*m + m\char94 2)/(n+m)$:
$Iz\_H := o/48*(n\char94 4 - m\char94 4)/(n-m)$:
$Iy\_HS := Iy\_H + z\_HS\char94 2*A\_H$:
$Iz\_HS := Iz\_H$:
$Iy\_HC := Iy\_H + z\_HC\char94 2*A\_H$:
$Iz\_HC := Iz\_H$:

Parameters

Measures from the technical drawing :

> $a := 1.8$:
$b := 3.5$:
$c := 3.5 - 1.8$:
$d := 3.5 - 2$:
$e := 18 - c$:
$f := 38$:
$g := f$:
$h := 20.5$:
$i := 28.5 - a - c - e$:
$j := 13.9$:
$k := 35$:
$m := 35$:
$n := 21.3$:
$o := 21 - j$:
$p := 1.5$:

Results

Offset of the center of area in z direction in the roller ski system (from top of the roller ski) [mm] :
> z_S;
$$-14.77979714 \tag{3.1}$$

Distance of the center of area to the outer 45° edge [mm]:
> $28.5 - i + z\_S$;
$$5.02020286 \tag{3.2}$$

Intersectional area of the profile [m^2]:
> $A\_S/1000\char94 2$;
$$0.0002052100000 \tag{3.3}$$

Second Moment of Inertia, Iy and Iz [m^4] (in roller ski system, on the top in the middle of the ski):

> $\dfrac{Iy\_Stotal}{1000^4}$;

$$6.622595981 \ 10^{-8} \tag{3.4}$$

> $\dfrac{Iz\_Stotal}{1000^4}$;

$$3.703968513 \ 10^{-8} \tag{3.5}$$

Second moment of inertia, Iy and Iz [m^4] (in the system of the center of area of the whole intersection):

> $\dfrac{Iy\_Ctotal}{1000^4}$;

$$2.139939429 \ 10^{-8} \tag{3.6}$$

> $\dfrac{Iz\_Ctotal}{1000^4}$;

$$3.703968513 \ 10^{-8} \tag{3.7}$$

Test (shift Iy from the center of area to the roller ski system with Steiner. Needs to be simmilar so Iy_Stotal) [m^4]:

> $\dfrac{\left(Iy\_Ctotal + z\_S^2 \cdot A\_S\right)}{1000^4}$;

$$6.622595991 \ 10^{-8} \tag{3.8}$$

Fabian Tobias Mayer B.Sc.

Appendix J: Shear and Momentum Function at the Roller Ski

Forces and torques acting on the Beam of the Roller Ski

The loads were calculated as followed:
1) Making assumptions
2) Calculating the bearing reactions
3) Deviding the profice in three sections
4) Calculation of the loads at the intersections of the sections

1) Assumptions:

The Torques around the y-axis in A and B are zero as the wheels can rotate freely around the wheel axis.

The Torques around the z-axis in A and B are zero as the wheel can rotate around the contact point on the ground.

The Force F_Bx in B is zero as the rachette is in A

The Torques M_Ax and M_Bx are equal as it is assumed that there is the same friction force at the ground contact point of both wheels

Forces in y-direction are assumed not to have a z-lever. As a consequences they do not cause torques in the x-direction.

Forces in the z-direction are assumed not to have an y-lever so that they do not cause torques torques in the x-direction.

Forces in the x-direction are assumed to have neither a z-lever nor an y-lever. Therefore they do not cause torques in the y- and z-direction.

These assumptions are made because levers in the y- and z-direction are much smaller than levers in the x direction. This is due to the diemnsions of the roller ski and due to the fact that forces applied by the athlete act on top of the roller ski.

2) The bearing reactions were calculated by hand and directly added to the intersectional loads

3) Deviding the profile in three sections
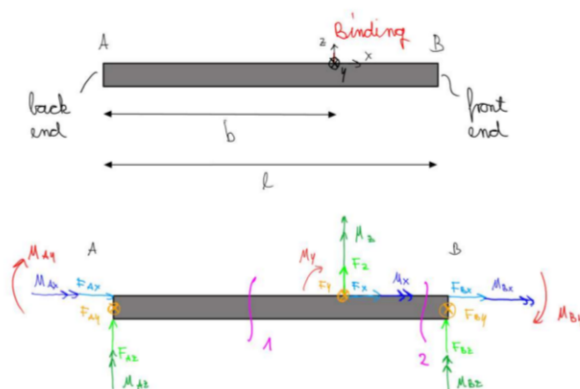
The beam is connected to the wheels in A and B
The back wheel with the rachette is in A.
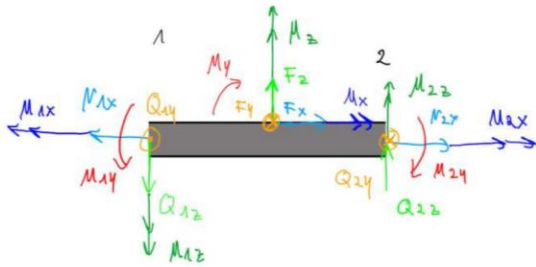
Strain gauges are placed in front of and behind the binding. The forces and torques in the positions of the strain gauges can be calculated as the loads which are obtained at the cuts 1 and 2.
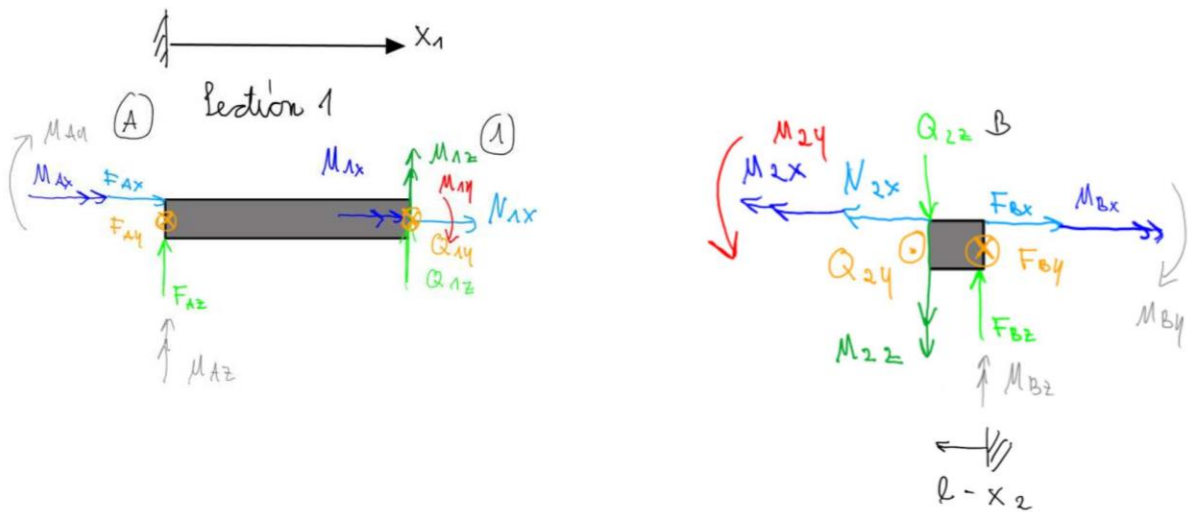
4) Calculation of the loads in the intersections
(the bearing reactions are already added and the formula were simplified by hand)

The forces and torques at the rear cut (behind the binding) can be calculated as follows :
(With length of the roller ski L, distance of the binding from the back end of the Skiroller b and distance of the left cut from the back of the roller ski x_1)

Force in the x-direction acting on the rear cut:
> $N\_1x := F\_x :$
Force in the y-direction acting on the rear cut:

> $Q\_1y := \left(1 - \dfrac{b}{L}\right) \cdot F\_y - \dfrac{1}{L} \cdot M\_z :$

Force in the z-direction acting on the rear cut:

> $Q\_1z := \left(1 - \dfrac{b}{L}\right) \cdot F\_z + \dfrac{1}{L} \cdot M\_y :$

Torque in the x-direction acting on the rear cut:

> $M\_1x := \dfrac{M\_x}{2} :$

Torque in the y-direction acting on the rear cut:

> $M\_1y := x\_1 \cdot \left(1 - \dfrac{b}{L}\right) \cdot F\_z + \dfrac{x\_1}{L} \cdot M\_y :$

Torque in the z-direction acting on the rear cut:

> $M\_1z := x\_1 \cdot \left(\dfrac{b}{L} - 1\right) \cdot F\_y + \dfrac{x\_1}{L} \cdot M\_z :$

The forces at the front cut (in front of the binding) can be calculated as follows:
(With length of the roller ski L, distance of the binding from the back end of the Skiroller b and distance of the right cut from the front end of the roller ski x_2)

Force in the x-direction acting on the front cut
(is zero as it is assumed that the force on the front end of the roller ski is zero, because the rachette is at the back end)

> $N\_2x := 0 :$

Force in the y- direction acting on the front cut

> $Q\_2y := -\dfrac{b}{L} \cdot F\_y - \dfrac{1}{L} \cdot M\_z :$

Force in the z-direction acting on the front cut

> $Q\_2z := -\dfrac{b}{L} \cdot F\_z + \dfrac{1}{L} \cdot M\_y ;$

$$Q\_2z := -\dfrac{b\,F\_z}{L} + \dfrac{M\_y}{L} \qquad\qquad (1.1)$$

Torque in the x-direction acting on the front cut

> $M\_2x := -\dfrac{M\_x}{2} :$

Torque in the y-direction acting on the front cut

> $M\_2y := \dfrac{(x\_2 - L)}{x\_2} \cdot (M\_y - F\_z \cdot b) :$

Torque in the z-direction acting on the front cut

> $M\_2z := \dfrac{(x\_2 - L)}{L} \cdot (M\_z + F\_y \cdot b) :$

Parameters, Moments of Inertia

Geometry of the roller ski
L = length [m]
b = position of the binding: distance from the back end [m]

> $L := 0.58 :$
> $b := 0.302 :$

Distance of the Strain gauge layers to the binding [m]

> $a\_SgB := 0.18$:

Position of the strain gauges [m]
(distance from the front and from the back end)

> $x\_1 := b - a\_SgB;$
> $x\_2 := b + a\_SgB;$

$$x\_1 := 0.122$$
$$x\_2 := 0.482 \tag{2.1}$$

E=Young's Modulus [Pa]

> $E := 68.9 \cdot 10^9;$

$$E := 6.890000000 \ 10^{10} \tag{2.2}$$

Intersectional Loads for applied Maximal Loads

Maximal Forces and Torques acting on the binding [N or Nm]

> $F\_x\_max := 0$: *#562:*
> $F\_y\_max := 0$: *#239:*
> $F\_z\_max := 1748$:
> $M\_x\_max := 0$:*#13:*
> $M\_y\_max := 0$:*#9:*
> $M\_z\_max := 0$:*#82:*

Forces and torques acting on the left rear gauge position (= left cut / behind the binding) [N or Nm]

> $N\_1x\_max := eval(N\_1x, F\_x = F\_x\_max);$
> $Q\_1y\_max := eval(Q\_1y, [F\_y = F\_y\_max, M\_z = M\_z\_max]);$
> $Q\_1z\_max := eval(Q\_1z, [F\_z = F\_z\_max, M\_y = M\_y\_max]);$
> $M\_1x\_max := eval(M\_1x, M\_x = M\_x\_max);$
> $M\_1y\_max := eval(M\_1y, [F\_z = F\_z\_max, M\_y = M\_y\_max]);$
> $M\_1z\_max := eval(M\_1z, [F\_y = F\_y\_max, M\_z = M\_z\_max]);$

$$N\_1x\_max := 0$$
$$Q\_1y\_max := 0.$$
$$Q\_1z\_max := 837.8344827$$
$$M\_1x\_max := 0$$
$$M\_1y\_max := 102.2158069$$
$$M\_1z\_max := 0. \tag{3.1}$$

Forces and torques acting on the front strain gauge position (= right cut / in front of the binding) [N or Nm]

> $N\_2x\_max := eval(N\_2x, F\_x = F\_x\_max);$
> $Q\_2y\_max := eval(Q\_2y, [F\_y = F\_y\_max, M\_z = M\_z\_max]);$
> $Q\_2z\_max := eval(Q\_2z, [F\_z = F\_z\_max, M\_y = M\_y\_max]);$
> $M\_2x\_max := eval(M\_2x, M\_x = M\_x\_max);$
> $M\_2y\_max := eval(M\_2y, [F\_z = F\_z\_max, M\_y = M\_y\_max]);$
> $M\_2z\_max := eval(M\_2z, [F\_y = F\_y\_max, M\_z = M\_z\_max]);$

$$N\_2x\_max := 0$$
$$Q\_2y\_max := -0.$$
$$Q\_2z\_max := -910.1655173$$
$$M\_2x\_max := 0$$

$$M\_2y\_max := 107.3315519$$
$$M\_2z\_max := -0. \tag{3.2}$$

Stress and Strain Caused for the applied Loads

Moments of Inertia in the center of area system [m^4] (calculated in "Newtral Layer for Torques and 2nd mom of inert")

> $I\_y := 2.139939429 \; 10^{-8}$:
  $I\_z := 3.703968513 \; 10^{-8}$:

Cross-sectional area of the profile [m^2] (calculated in "Neutral Layer for Torques and 2nd mom of inert")

> $A := 0.00020521$:

▼ Stress

(*coordinate system* in *the center of area of the intersection*)
Rear strain gauge positions (behind the binding)
Stress caused by the maximum torques and forces [Pa]

> $sigma\_tension\_x1 := \dfrac{N\_1x\_max}{A}$;

$$sigma\_tension\_x1 := 0. \tag{4.1.1}$$

> $sigma\_bending\_My1 := \dfrac{M\_1y\_max}{I\_y} \cdot z$;

$$sigma\_bending\_My1 := 4.776574772 \; 10^9 \, z \tag{4.1.2}$$

> $sigma\_bending\_Mz1 := -\dfrac{M\_1z\_max}{I\_z} \cdot y$;

$$sigma\_bending\_Mz1 := -0. \tag{4.1.3}$$

Sum of the bending and normal stress:

> $sigma\_ges1 := unapply(sigma\_tension\_x1 + sigma\_bending\_My1$
  $+ \; sigma\_bending\_Mz1, y, z)$

$$sigma\_ges1 := (y, z) \rightarrow 4.776574772 \; 10^9 \, z \tag{4.1.4}$$

Front strain gauge positions (in front of the binding)
Stress caused by the maximum torques and forces [Pa]

> $sigma\_tension\_x2 := \dfrac{N\_2x\_max}{A}$;

$$sigma\_tension\_x2 := 0. \tag{4.1.5}$$

> $sigma\_bending\_My2 := \dfrac{M\_2y\_max}{I\_y} \cdot z$;

$$sigma\_bending\_My2 := 5.015635043 \; 10^9 \, z \tag{4.1.6}$$

> $sigma\_bending\_Mz2 := -\dfrac{M\_2z\_max}{I\_z} \cdot y$;

$$sigma\_bending\_Mz2 := 0. \tag{4.1.7}$$

Sum of the bending and normal stress:

> $sigma\_ges2 := unapply(sigma\_tension\_x2 + sigma\_bending\_My2$
> $+ sigma\_bending\_Mz2, y, z);$
$$sigma\_ges2 := (y, z) \rightarrow 5.015635043 \; 10^9 \, z \qquad \textbf{(4.1.8)}$$

▼ Strain

sigma = E*epsilon [-]

> $epsilon\_ges1 := unapply\left(\dfrac{sigma\_ges1(y, z)}{E}, y, z \right);$
$$epsilon\_ges1 := (y, z) \rightarrow 0.06932619408 \, z \qquad \textbf{(4.2.1)}$$

> $epsilon\_ges2 := unapply\left(\dfrac{sigma\_ges2(y, z)}{E}, y, z \right);$
$$epsilon\_ges2 := (y, z) \rightarrow 0.07279586419 \, z \qquad \textbf{(4.2.2)}$$

>

▼ Results at the Strain Gauge Positions

Position of the strain gauges [m] :

> $y\_left := -\dfrac{38}{2 \cdot 1000}$:

> $y\_right := \dfrac{38}{2 \cdot 1000}$:

> $z\_top := \dfrac{(14.77979714 - 1.8 - 1.7)}{1000}$:

> $z\_bottom := -\dfrac{(28.5 - 14.77979714)}{1000}$:

Strain on the different strain gauges [-] :

> $epsilon\_front\_top := epsilon\_ges2(0, z\_top);$
$$epsilon\_front\_top := 0.0008211225807 \qquad \textbf{(4.3.1)}$$

> $epsilon\_front\_right := epsilon\_ges2(y\_right, 0);$
$$epsilon\_front\_right := 0. \qquad \textbf{(4.3.2)}$$

> $epsilon\_front\_bottom := epsilon\_ges2(0, z\_bottom);$
$$epsilon\_front\_bottom := -0.0009987740241 \qquad \textbf{(4.3.3)}$$

> $epsilon\_front\_left := epsilon\_ges2(y\_left, 0);$
$$epsilon\_front\_left := 0. \qquad \textbf{(4.3.4)}$$

> $epsilon\_back\_top := epsilon\_ges1(0, z\_top);$
$$epsilon\_back\_top := 0.0007819854057 \qquad \textbf{(4.3.5)}$$

> $epsilon\_back\_right := epsilon\_ges1(y\_right, 0);$
$$epsilon\_back\_right := 0. \qquad \textbf{(4.3.6)}$$

> $epsilon\_back\_bottom := epsilon\_ges1(0, z\_bottom);$
$$epsilon\_back\_bottom := -0.0009511694463 \qquad \textbf{(4.3.7)}$$

> $esilom\_back\_left := epsilon\_ges1(y\_left, 0);$
$$esilom\_back\_left := 0. \qquad \textbf{(4.3.8)}$$

Appendix K: Shear Stress by Forces and Torques

Geometry

For the calculations a simplified profile was used as only the relation of the shear strain caused by different loads was of interest.
The width of the simplified profile of the roller ski is 38 mm, its height 25 mm, the wall thickness is 1.5 mm

Calculation of shear stress caused by shear forces

Shear force

$$> F\_QZ := \left(1 - \frac{b}{l}\right) \cdot F\_z + \frac{1}{l} \cdot M\_y :$$

Maximum shear stress caused by shear forces for a thin-walled profile

$$> tau\_shear\_max := unapply\left(\frac{F\_QZ}{I\_y} \cdot S\_ymax, F\_z, M\_y\right) :$$

Second moment of area

$$> I\_y := \frac{(2 \cdot B + delta) \cdot (2 \cdot H + delta)^3}{12} + \frac{(2 \cdot B - delta) \cdot (2 \cdot H - delta)^3}{12} :$$

first moment of area

$$> S\_ymax := delta \cdot B \cdot H + \frac{delta \cdot H^2}{12} :$$

Calculation of shear stress caused by torque

shear stress caused by torque for a thin-walled profile

$$> tau\_torque := \frac{M\_x}{2 \cdot A\_M \cdot h} :$$

The stress is maximal where the thickness of the wall is minimal as the thickness is constant h = h_min = delta

$$> tau\_torque\_max := \frac{M\_xmax}{2 \cdot A\_M \cdot delta} :$$

A_M is the area circumscribed by the midline of the profile

$$> A\_M := 2 \cdot B \cdot 2 \cdot H :$$

Parameters

The width of the roller ski is 38 mm, its height 25 mm, the wall thickness is 1.5 mm --> values will be used in m

$$> delta := 1.5e{-}3 :$$
$$H := \frac{(25e{-}3 - 1.5e{-}3)}{2} :$$
$$B := \frac{(38e{-}3 - 1.5e{-}3)}{2} :$$

The sectional torque [Nm]

$$> M\_xmax := 13 :$$

l = length of the beam of the roller ski

b = position of the binding relatively to the back wheel
F_zmax = maximal expected force the athlete applies in tz z-direction
M_y = maximal expected torque the athlete applies around the y-axis

> $b := 0.342$:
  $l := 0.68$:
  $F\_zmax := 1748$:
  $M\_ymax := 9$:

Maximal expected shear for the force F_zmax [Pa]
Maximal expected shear for force and torque F_zmax and M_ymax [Pa]
Maximal expected shear **for** the torque M_xmax [Pa]

> $tau\_shear\_max(F\_zmax, 0)$;
  $tau\_shear\_max(F\_zmax, M\_ymax)$;
  tau_torque_max;

$$3656.365887$$
$$3712.063170$$
$$5.051977075 \ 10^6 \tag{4.1}$$

Proportion caused by the shear of force/ force and bending torque compared with the one caused by twisting torque

> $\dfrac{tau\_torque\_max}{tau\_shear\_max(F\_zmax, 0)}$;
  $\dfrac{tau\_torque\_max}{tau\_shear\_max(F\_zmax, M\_ymax)}$;

$$1381.693526$$
$$1360.962043 \tag{4.2}$$

Appendix L: FEM Simulation of the Beam of the Roller Ski

FEM simulation of the different maximum load cases was done in order to evaluate the positions of the strain gauges. It was necessary to regard all load cases to make sure that none of the loads cause excessive stress at the positions of the strain gauges and that there is a low stress gradient over the strain gauge. The positions of the strain gauges are shown in chapter 5.6.4.
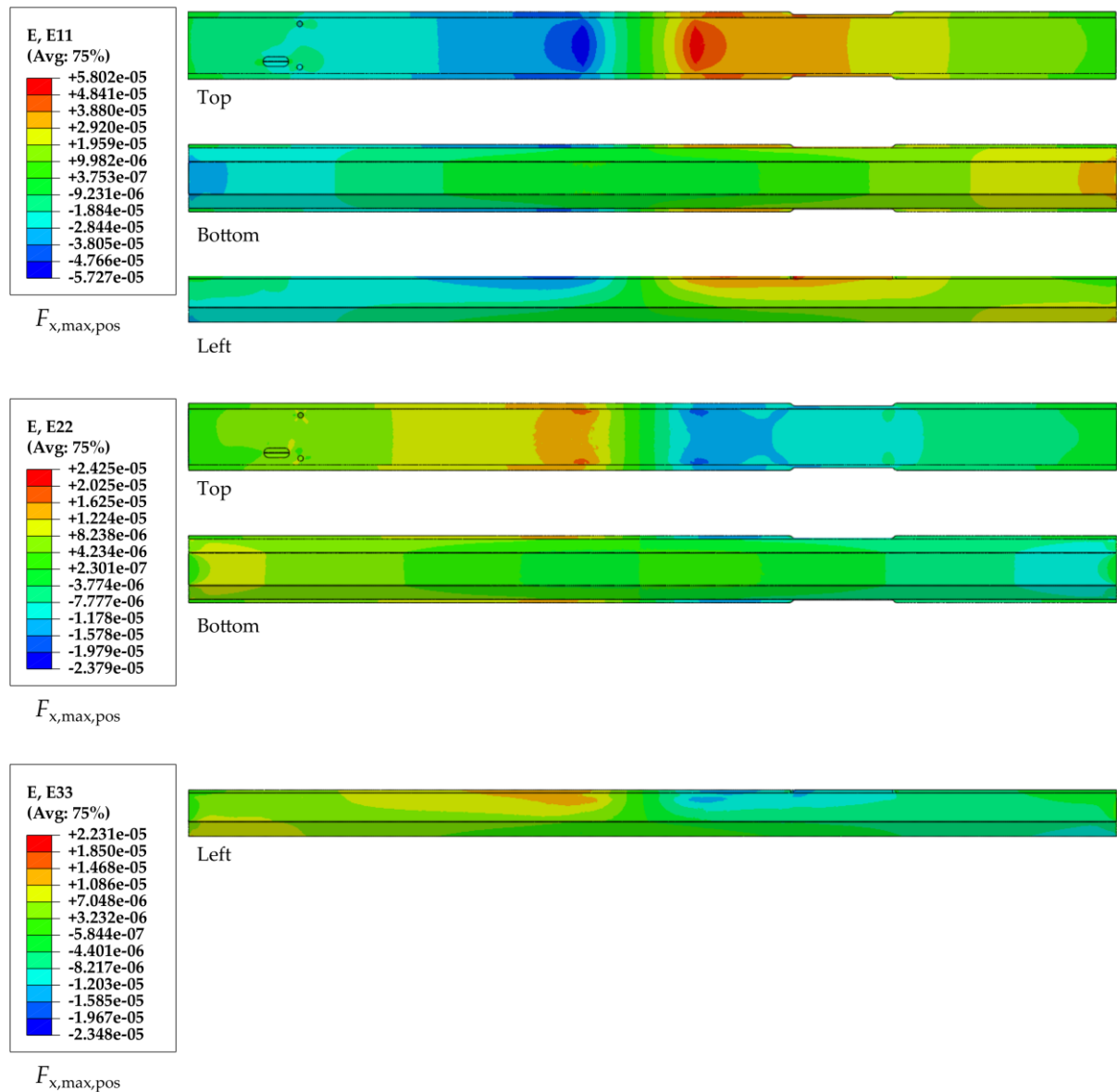
Figure A 15: FEM simulation of the strain for the maximal expected positive force F_x
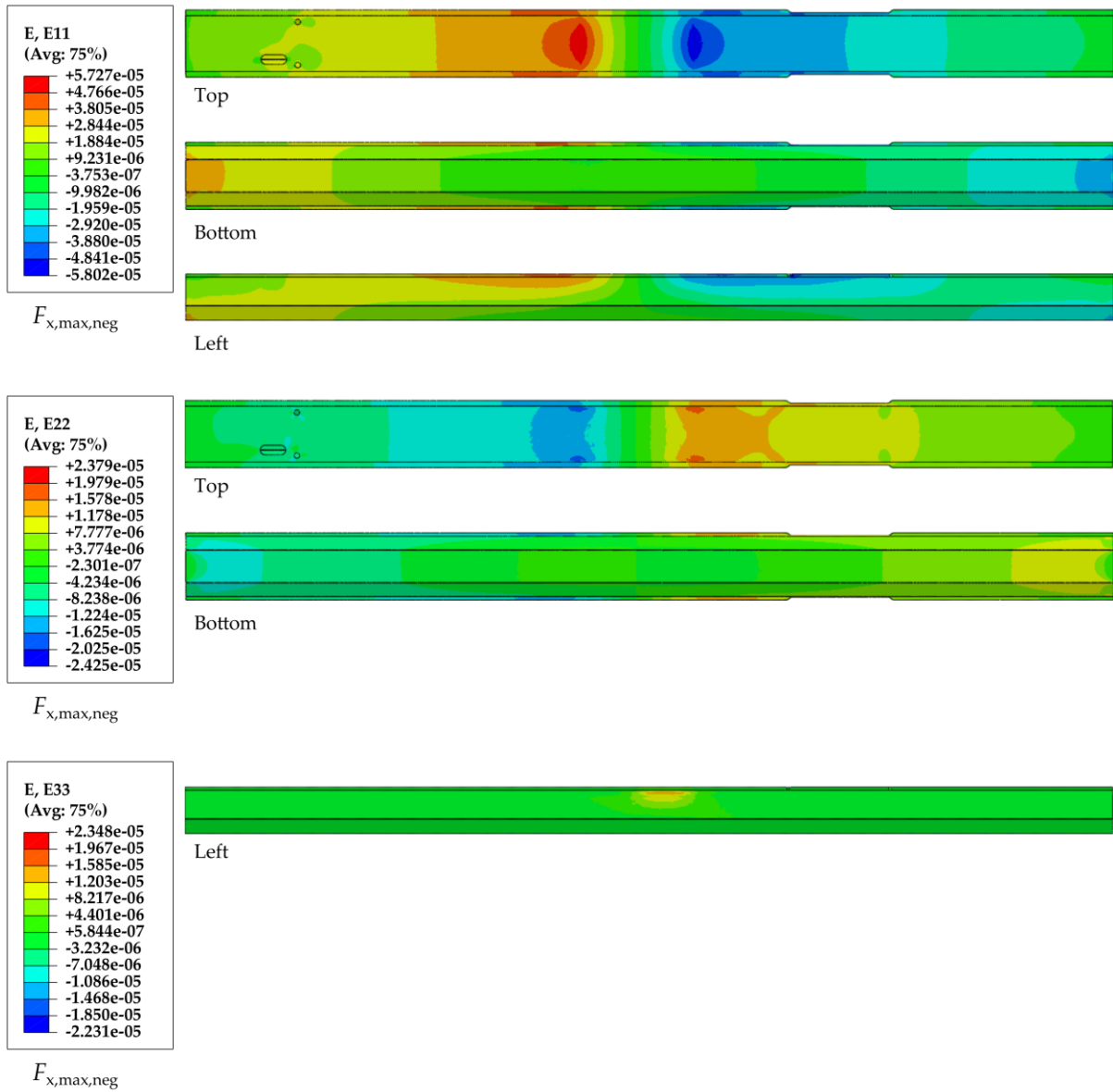
Figure A 16: FEM simulation of the strain for the maximal expected negative force F_x
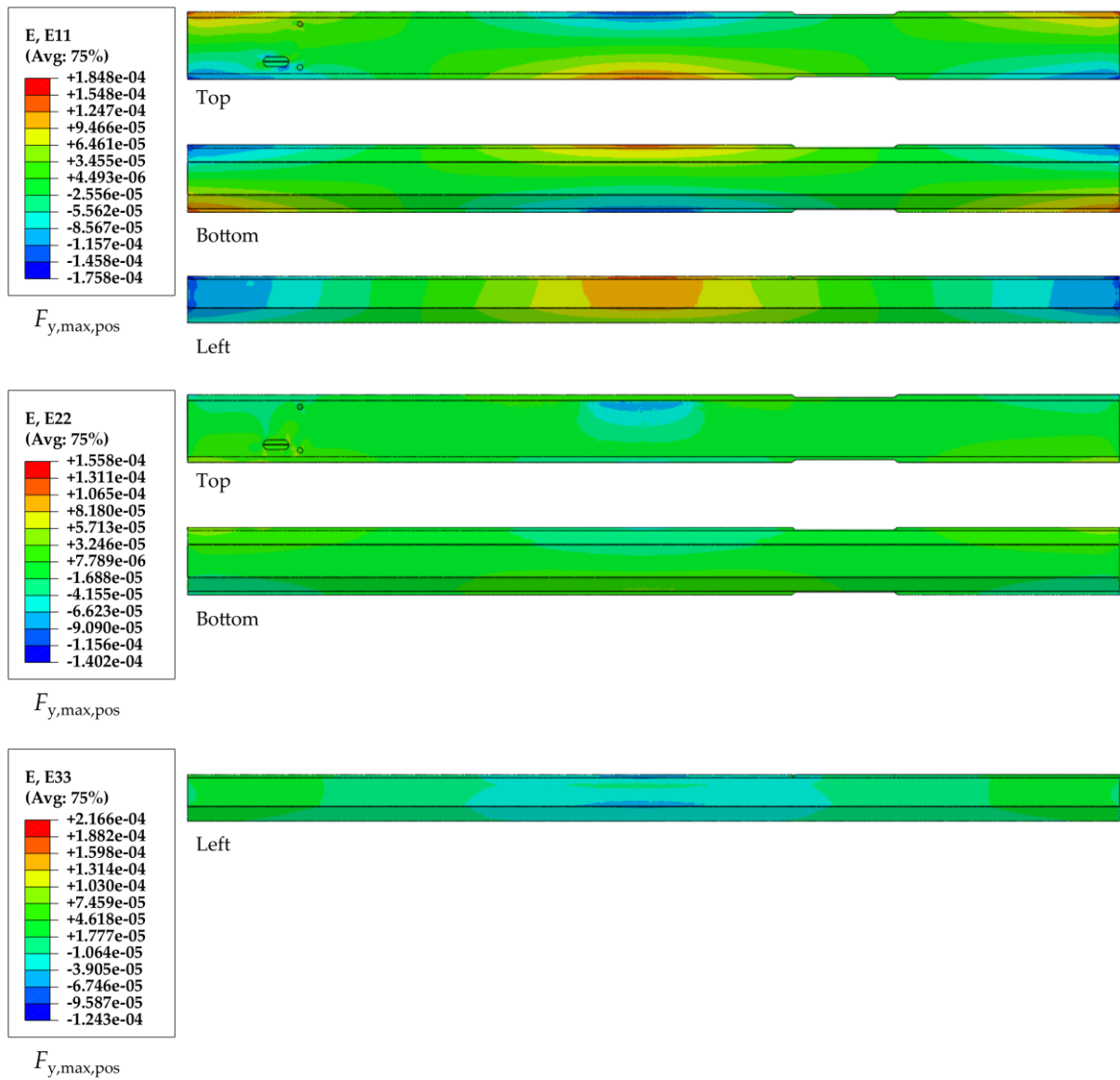
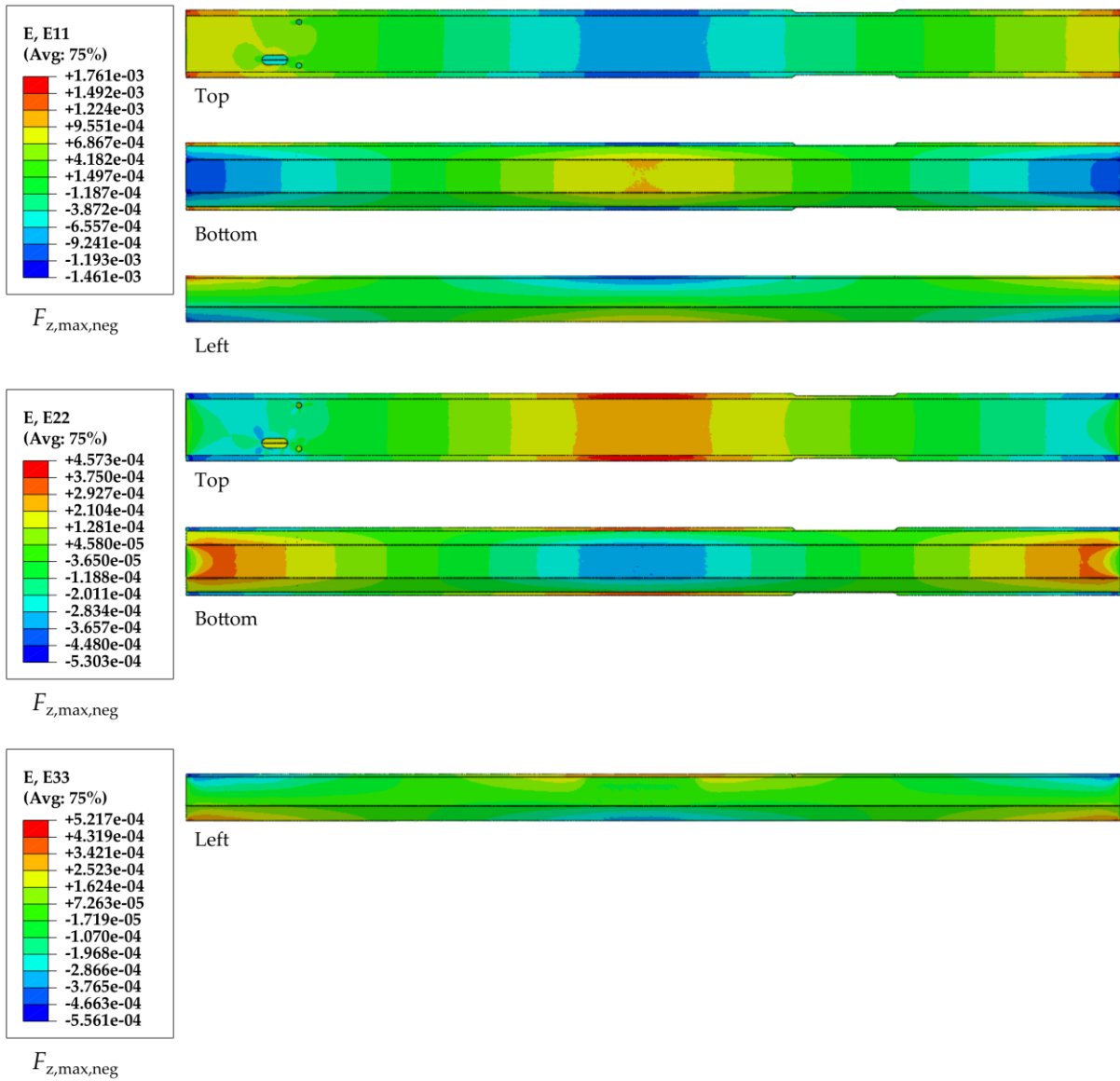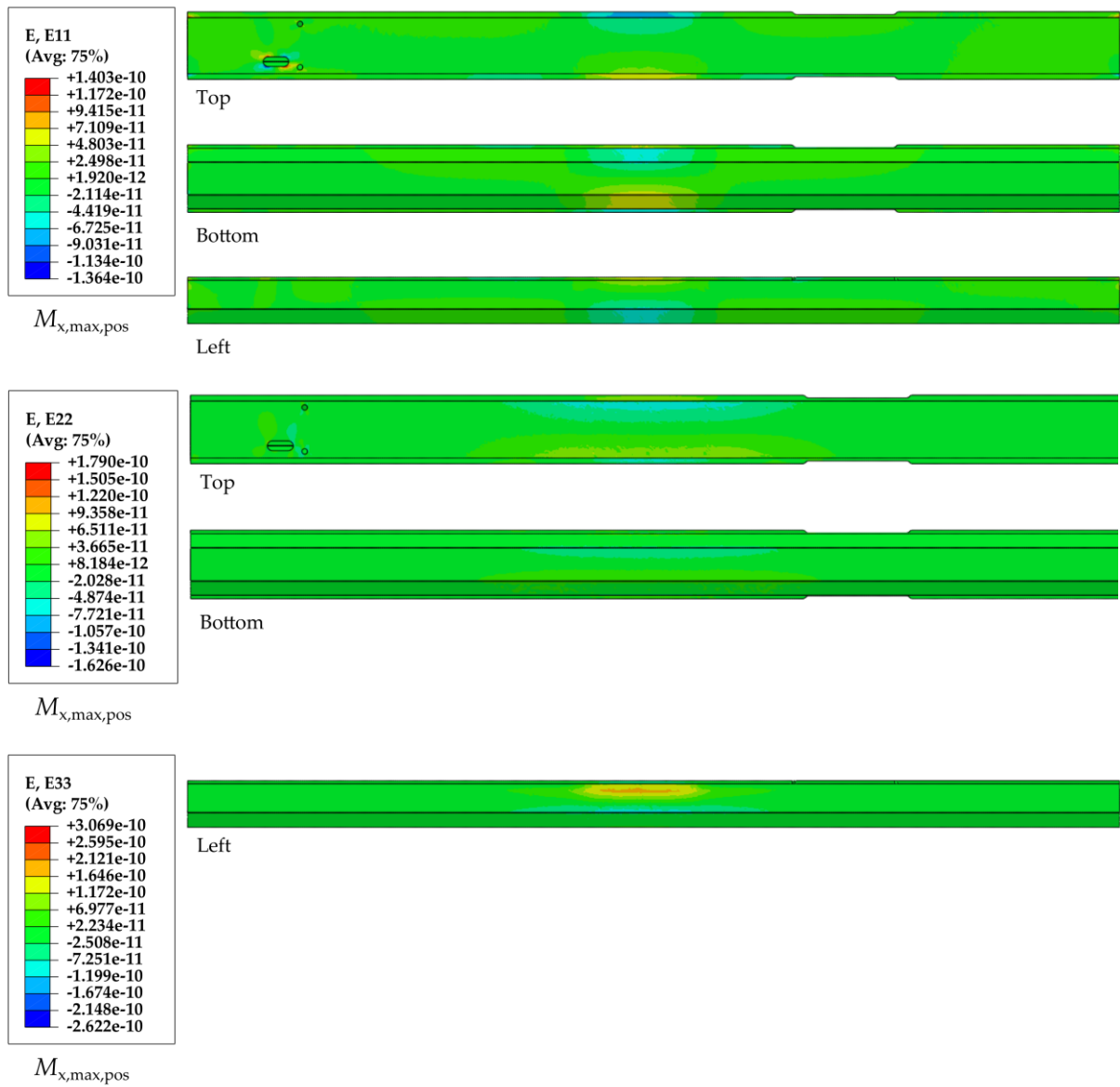Figure A 17: FEM simulation of the strain for the maximal expected positive force F_y
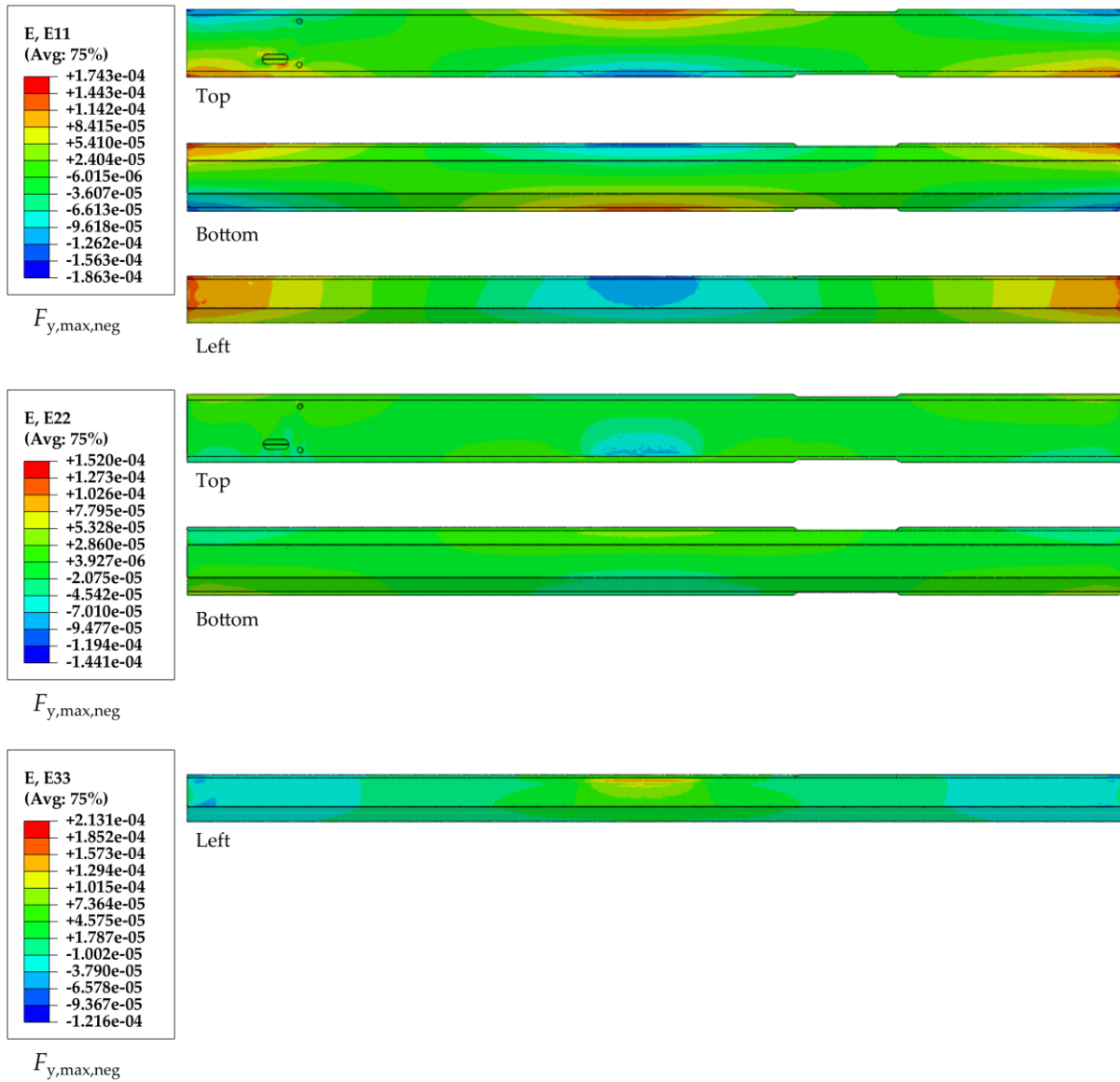
Figure A 18: FEM simulation of the strain for the maximal expected negative force F_y

Fabian Tobias Mayer B.Sc.
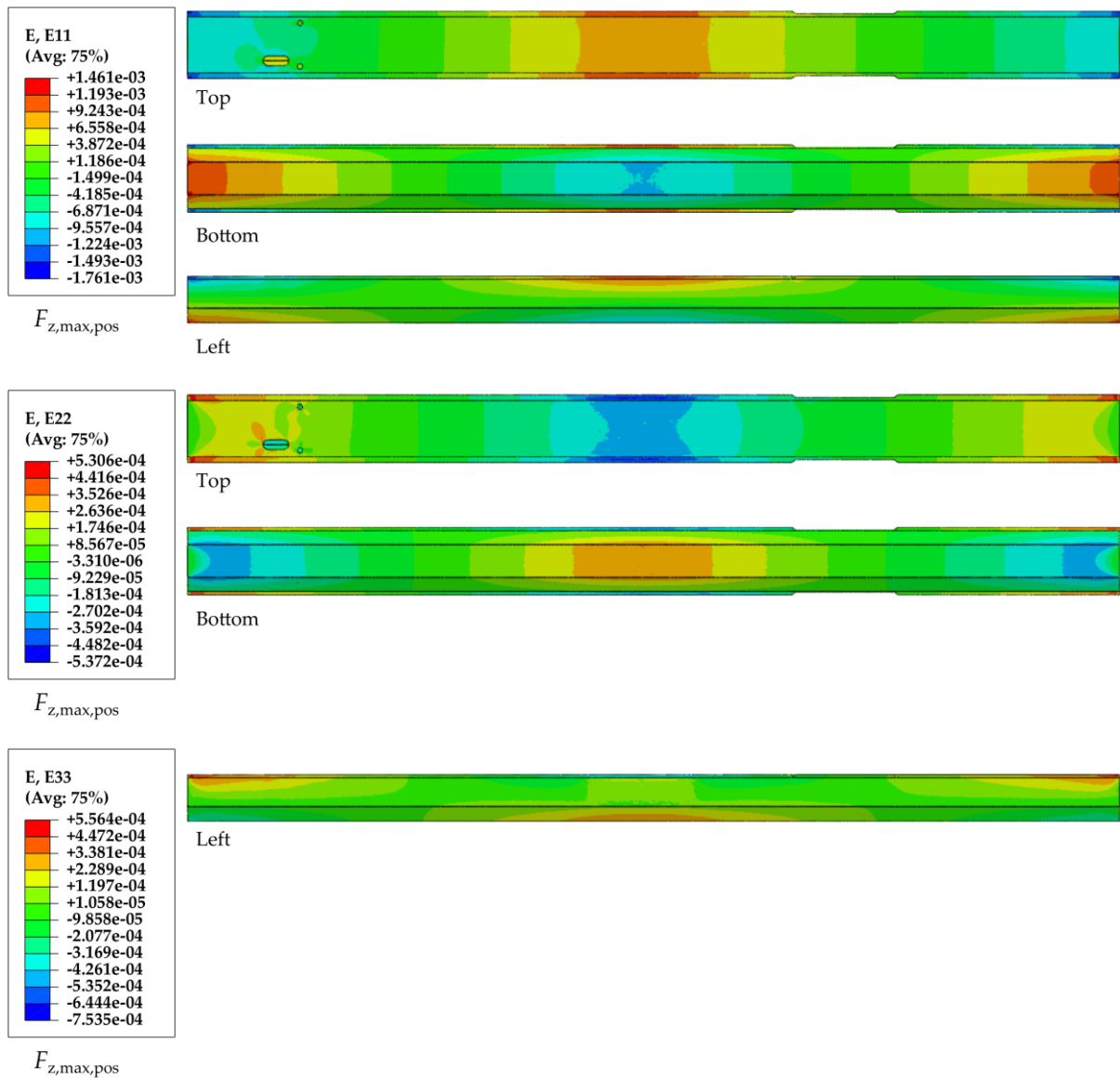
Figure A 19: FEM simulation of the strain for the maximal expected positive force F_z

Figure A 20: FEM simulation of the strain for the maximal expected negative force F_z

Figure A 21: FEM simulation of the strain for the maximal expected positive torque M_x
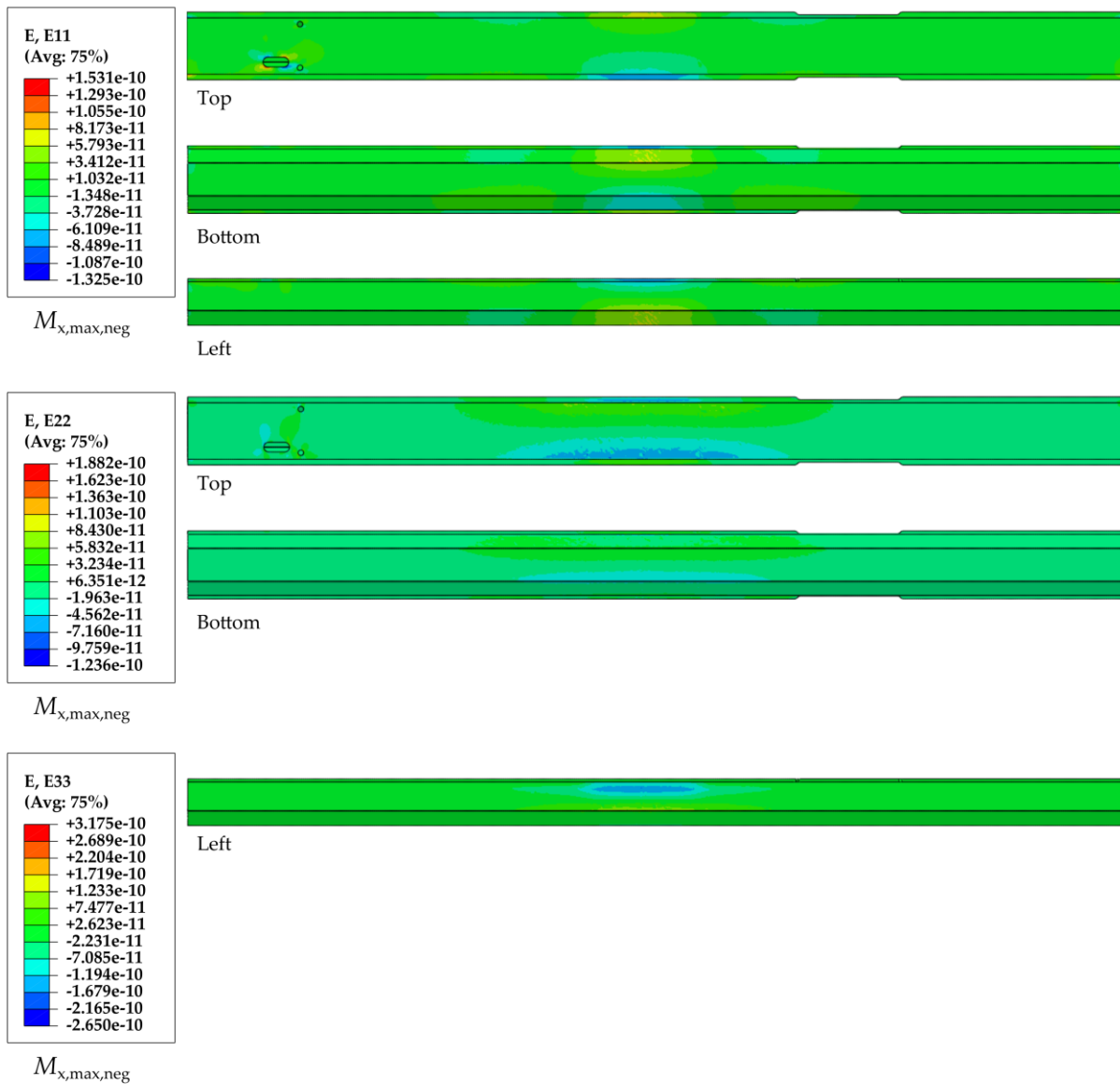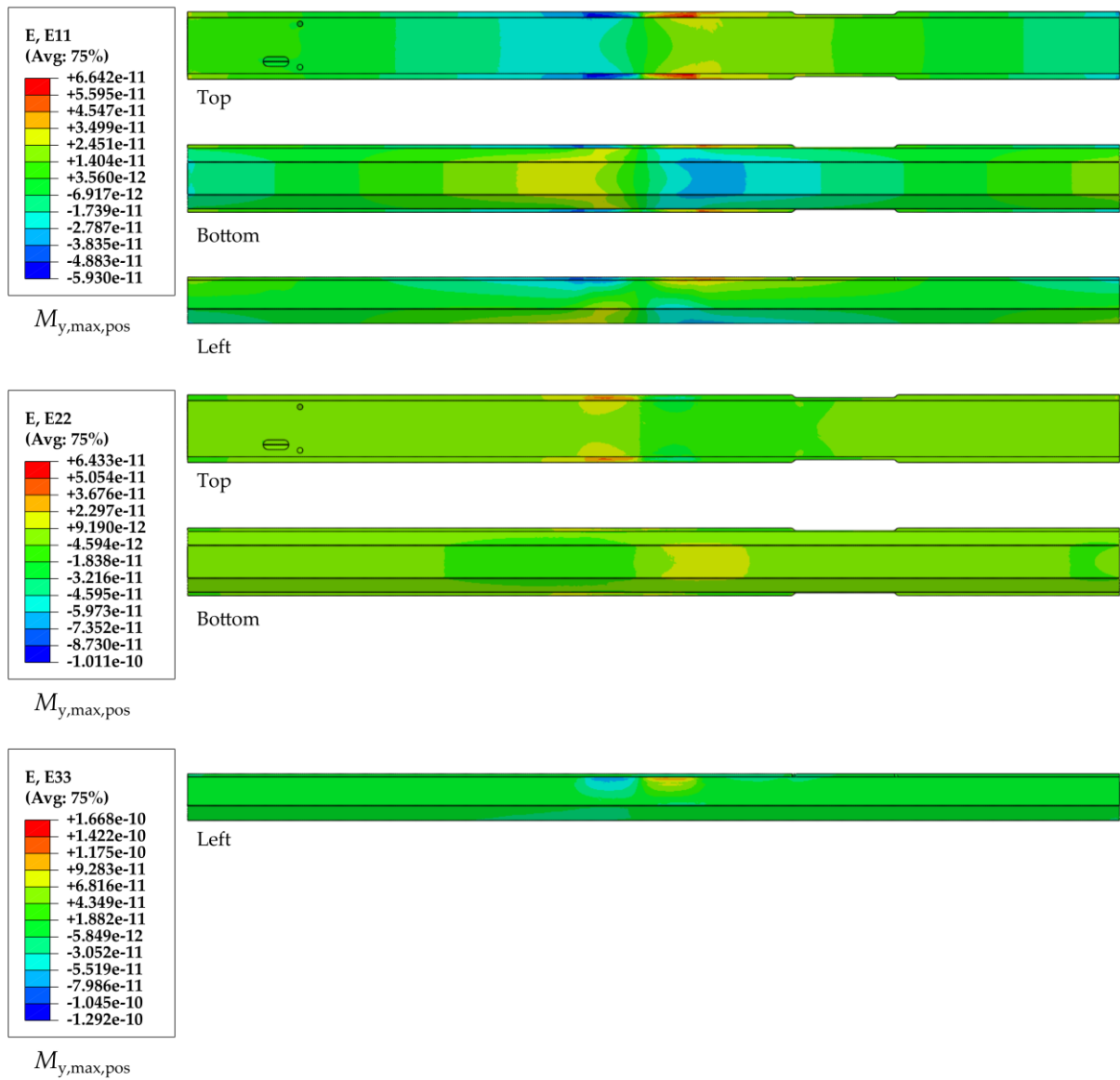
Figure A 22: FEM simulation of the strain for the maximal expected negative torque M_x

Figure A 23: FEM simulation of the strain for the maximal expected positive torque M_y
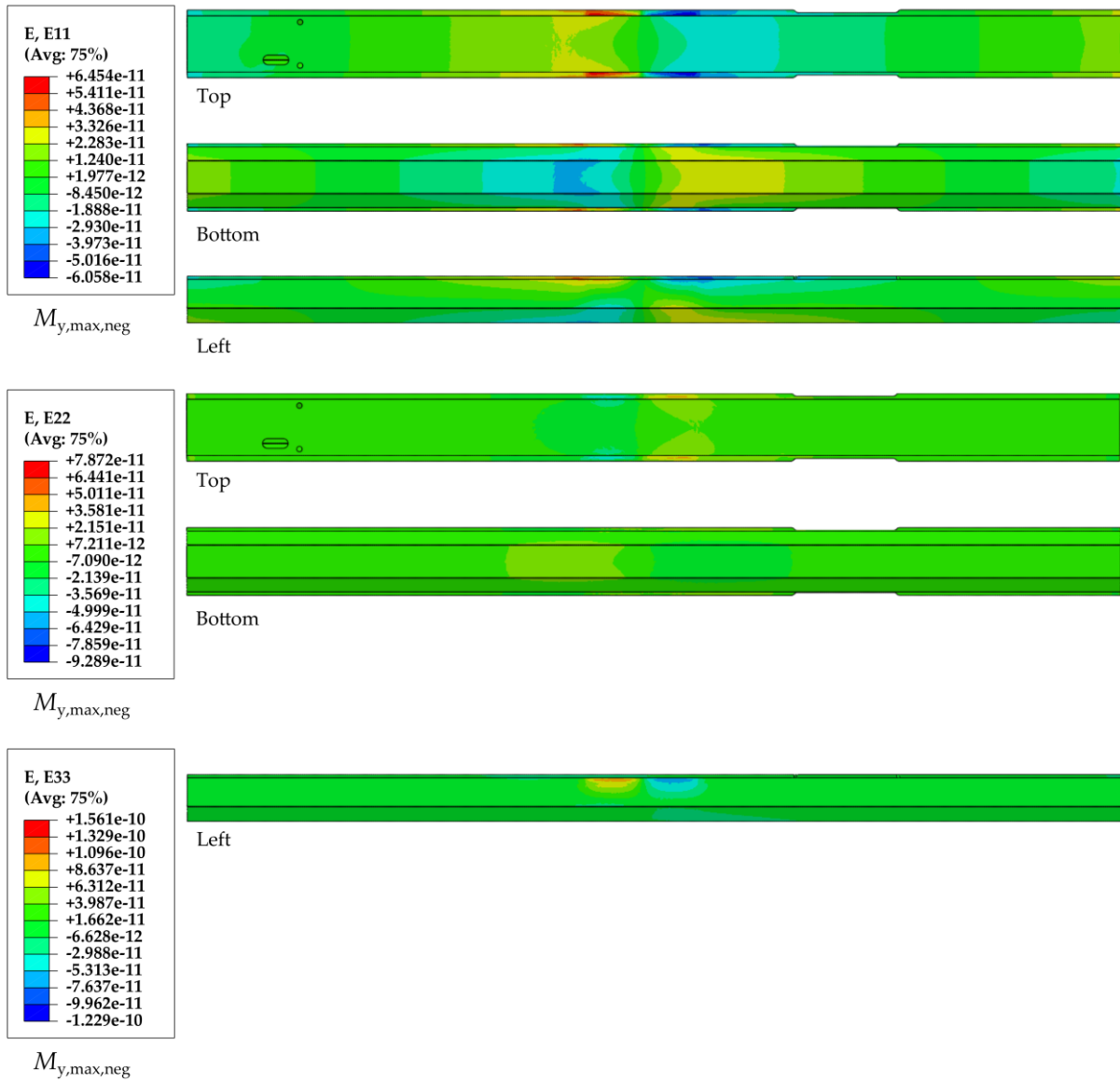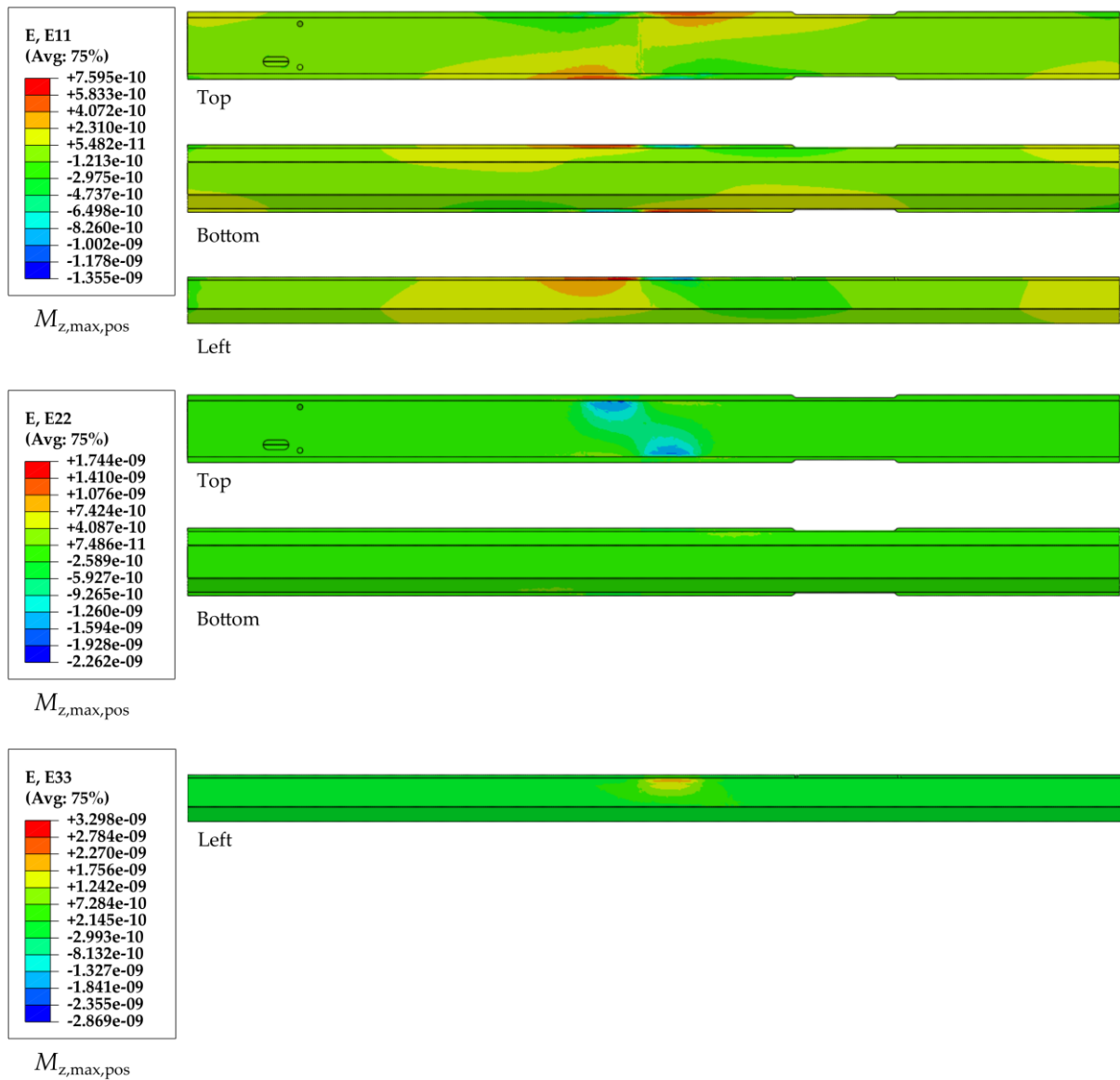
Figure A 24: FEM simulation of the strain for the maximal expected negative torque M_y

Figure A 25: FEM simulation of the strain for the maximal expected positive torque M_z
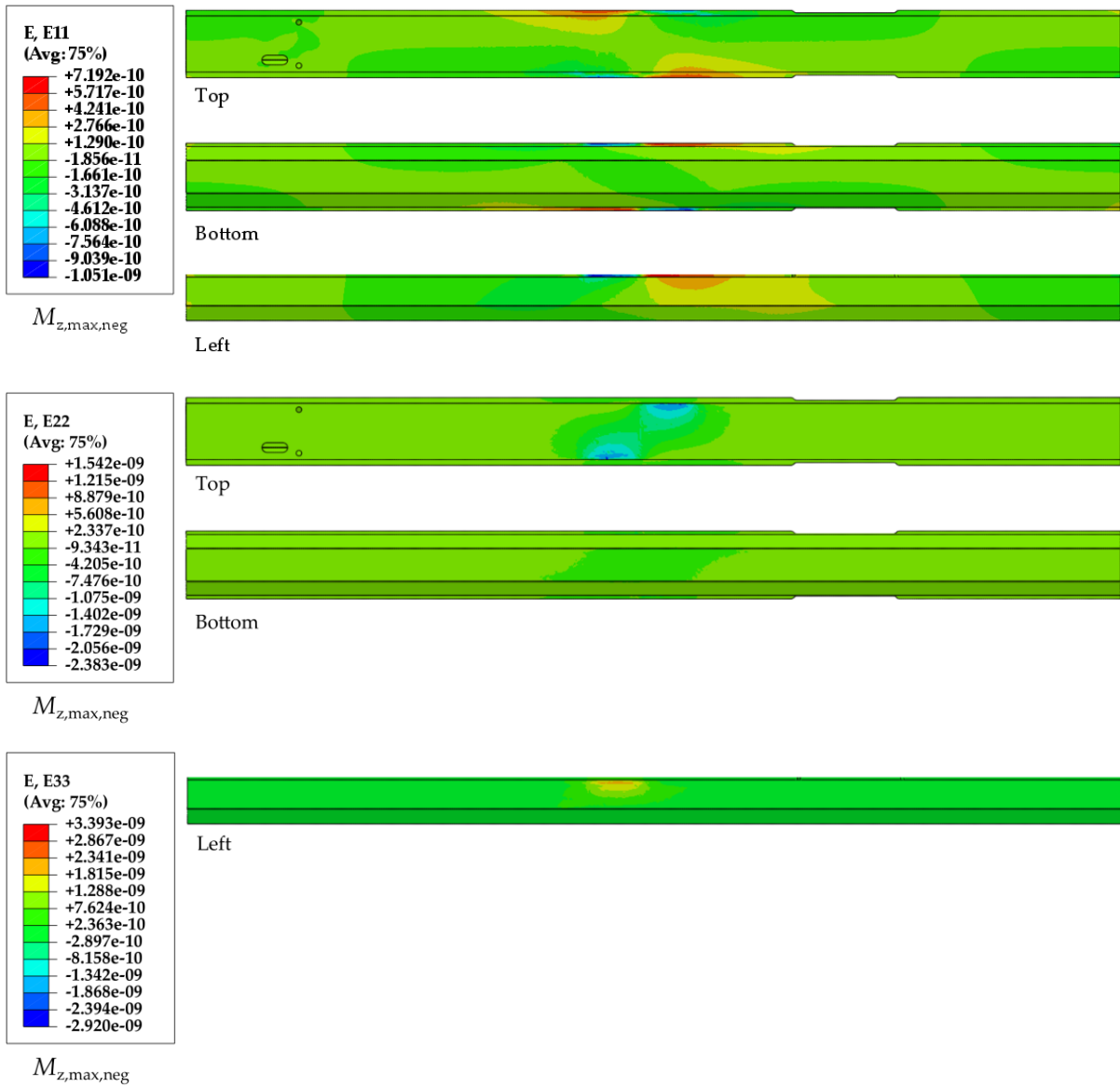
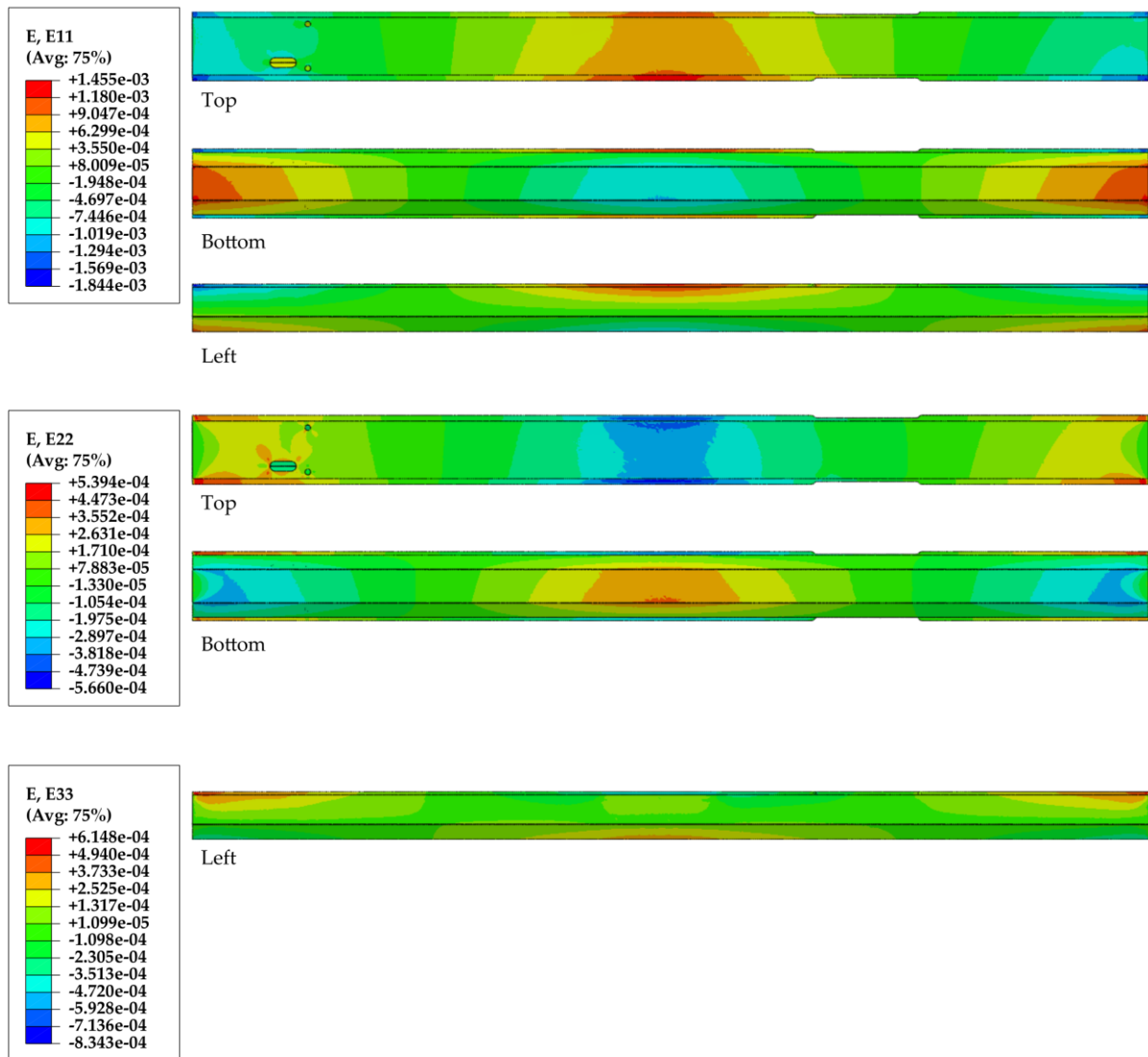Figure A 26: FEM simulation of the strain for the maximal expected negative torque M_z

Figure A 27: FEM simulation of the strain for the superposition of the positive loads which are maximal expected
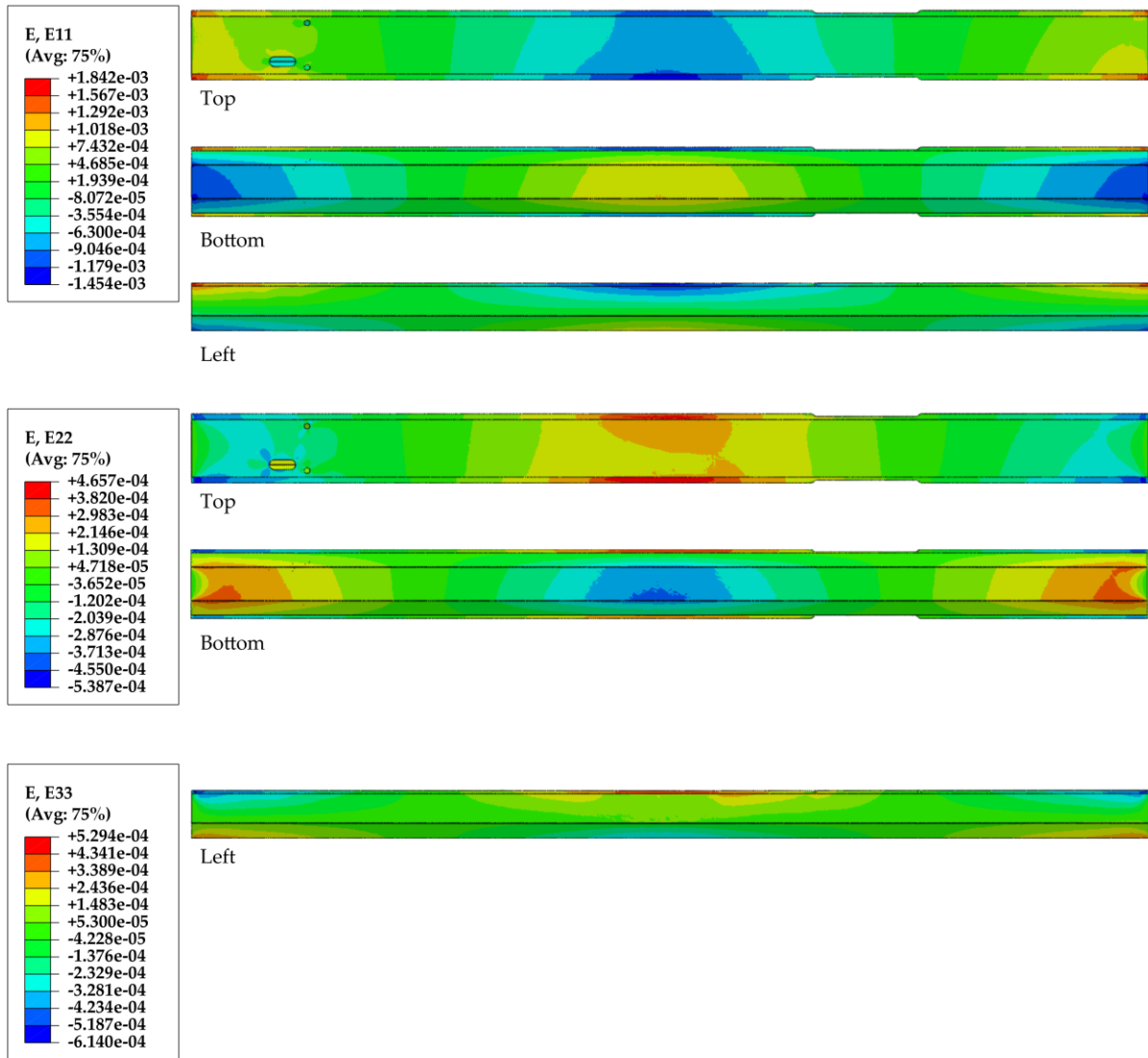
Figure A 28: FEM simulation of the strain for the superposition of the negative loads which are maximal expected

Appendix M: Risk Assessment

Due to NTNU regulations it is compulsory to conduct a risk assessment when starting with the master thesis. The form of the risk assessment has to be included into the thesis.

	Utarbeidet av	Nummer	Dato
	HMS-avd.	HMSRV2601	22.03.2011
	Godkjent av		Erstatter
	Rektor		01.12.2006

NTNU — HMS

Kartlegging av risikofylt aktivitet

Dato: 03.06.2016

Enhet: Department of Engineering Design and Materials

Linjeleder: Professor Torgeir Welo

Deltakere ved kartleggingen (m/ funksjon): Fabian Tobias Mayer
(Ansv. veileder, student, evt. medveiledere, evt. andre m. kompetanse)

Kort beskrivelse av hovedaktivitet/hovedprosess: Master Thesis of Fabian Tobias Mayer: Development of a Measuring System to Detect Loads Acting Between the Binding and the Roller Ski

Er oppgaven rent teoretisk? : No

«JA» betyr at veileder innestår for at oppgaven ikke inneholder noen aktiviteter som krever risikovurdering. Dersom «JA»: Beskriv kort aktiviteten i kartleggingsskjemaet under. Risikovurdering trenger ikke å fylles ut.

Signaturer: Ansvarlig veileder: _Torgeir Welo_   Student: _Fabian Mayer_

ID nr.	Aktivitet/prosess	Ansvarlig	Eksisterende dokumentasjon	Eksisterende sikringstiltak	Lov, forskrift o.l.	Kommentar
1	Construction of the measuring system	Fabian Mayer	-	-	-	-
1.1	Modification of the existing Roller Ski	Fabian Mayer	-	Security glasses	-	-
1.2	Assembly of the parts	Fabian Mayer	-	Security glasses	-	-
2	Testing of the measuring system	Fabian Mayer	-	-	-	-
2.1	Laboratory Tests	Fabian Mayer	-	Security glasses	-	-
2.2	Tests on the road	Fabian Mayer	-	Helmet, gloves	Vegtrafikkloven	-

NTNU (HMS)	Risikovurdering	Utarbeidet av	Nummer	Dato
		HMS-avd.	HMSRV2601	22.03.2011
		Godkjent av		Erstatter
		Rektor		01.12.2006

Dato: 03.06.2016

Enhet: Department of Engineering Design and Materials

Linjeleder: Professor Torgeir Welo

Deltakere ved kartleggingen (m/ funksjon): Fabian Tobias Mayer
(Ansv. Veileder, student, evt. medveiledere, evt. andre m. kompetanse)

Risikovurderingen gjelder hovedaktivitet: Master Thesis of Fabian Tobias Mayer: Development of a Measuring System to Detect Loads Acting Between the Binding and the Roller Ski

Signaturer: *Ansvarlig veileder:* [signature] *Student:* [signature]

ID nr	Aktivitet fra kartleggings-skjemaet	Mulig uønsket hendelse/ belastning	Vurdering av sannsyn-lighet (1-5)	Vurdering av konsekvens: Menneske (A-E)	Ytre miljø (A-E)	Øk/ materiell (A-E)	Om-dømme (A-E)	Risiko-Verdi (menn-eske)	Kommentarer/status Forslag til tiltak
1.1	Modification of the existing Roller Ski	Destruction of the roller ski	1	A	A	B	A	A1	-
1.2	Assembly of the parts	Destruction of sensors, other equipment, roller ski	1	A	A	B	A	A1	-
2.1	Laboratory Tests	Destruction of the measuring system and roller ski	2	A	A	C	A	A2	-
2.2	Tests on the road	Accident/fall: Injury, destruction of the measuring system and roller ski	2	C	A	C	A	C2	Test on roads with less traffic, wear a security vest, helmet and gloves

NTNU	Risikovurdering	Utarbeidet av	Nummer	Dato
		HMS-avd.	HMSRV2601	22.03.2011
HMS		Godkjent av		Erstatter
		Rektor		01.12.2006

Sannsynlighet vurderes etter følgende kriterier:

Svært liten 1	Liten 2	Middels 3	Stor 4	Svært stor 5
1 gang pr 50 år eller sjeldnere	1 gang pr 10 år eller sjeldnere	1 gang pr år eller sjeldnere	1 gang pr måned eller sjeldnere	Skjer ukentlig

Konsekvens vurderes etter følgende kriterier:

Gradering	Menneske	Ytre miljø Vann, jord og luft	Øk/materiell	Omdømme
E Svært Alvorlig	Død	Svært langvarig og ikke reversibel skade	Drifts- eller aktivitetsstans >1 år.	Troverdighet og respekt betydelig og varig svekket
D Alvorlig	Alvorlig personskade. Mulig uførhet.	Langvarig skade. Lang restitusjonstid	Driftsstans > ½ år Aktivitetsstans i opp til 1 år	Troverdighet og respekt betydelig svekket
C Moderat	Alvorlig personskade.	Mindre skade og lang restitusjonstid	Drifts- eller aktivitetsstans < 1 mnd	Troverdighet og respekt svekket
B Liten	Skade som krever medisinsk behandling	Mindre skade og kort restitusjonstid	Drifts- eller aktivitetsstans < 1 uke	Negativ påvirkning på troverdighet og respekt
A Svært liten	Skade som krever førstehjelp	Ubetydelig skade og kort restitusjonstid	Drifts- eller aktivitetsstans < 1 dag	Liten påvirkning på troverdighet og respekt

Risikoverdi = Sannsynlighet x Konsekvens
Beregn risikoverdi for Menneske. Enheten vurderer selv om de i tillegg vil beregne risikoverdi for Ytre miljø, Økonomi/materiell og Omdømme. I så fall beregnes disse hver for seg.

Til kolonnen "Kommentarer/status, forslag til forebyggende og korrigerende tiltak":
Tiltak kan påvirke både sannsynlighet og konsekvens. Prioriter tiltak som kan forhindre at hendelsen inntreffer, dvs. sannsynlighetsreduserende tiltak foran skjerpet beredskap, dvs. konsekvensreduserende tiltak.

NTNU		utarbeidet av	Nummer	Dato	
HMS/KS	Risikomatrise	HMS-avd.	HMSRV2604	08.03.2010	
		godkjent av		Erstatter	
		Rektor		09.02.2010	

MATRISE FOR RISIKOVURDERINGER ved NTNU

KONSEKVENS					
Svært alvorlig	E1	E2	E3	E4	E5
Alvorlig	D1	D2	D3	D4	D5
Moderat	C1	C2	C3	C4	C5
Liten	B1	B2	B3	B4	B5
Svært liten	A1	A2	A3	A4	A5
	Svært liten	Liten	Middels	Stor	Svært stor
	SANNSYNLIGHET				

Prinsipp over akseptkriterium. Forklaring av fargene som er brukt i risikomatrisen.

Farge		Beskrivelse
Rød		Uakseptabel risiko. Tiltak skal gjennomføres for å redusere risikoen.
Gul		Vurderingsområde. Tiltak skal vurderes.
Grønn		Akseptabel risiko. Tiltak kan vurderes ut fra andre hensyn.